TAE

September 18th, 2013

Physics with Jets (and Photons) at the LHC

J. Terrón (Universidad Autónoma de Madrid)

- **Outline**
  - $\longrightarrow$ Jets and Jet Algorithms
  - $\longrightarrow$ Jets with the ATLAS detector at the LHC
  - $\longrightarrow$ First measurements of jet production at $\sqrt{s} = 7$ TeV
  - $\longrightarrow$ More+better measurements of jet production
  - $\longrightarrow$ Multijet production and extraction of α_s
  - $\longrightarrow$ Measurements of jet production at $\sqrt{s} = 2.76$ TeV
  - $\longrightarrow$ Dijet azimuthal decorrelations
  - $\longrightarrow$ Looking inside jets
  - $\longrightarrow$ Inclusive photon, photon+jet and diphoton production

Jets

What is a jet?

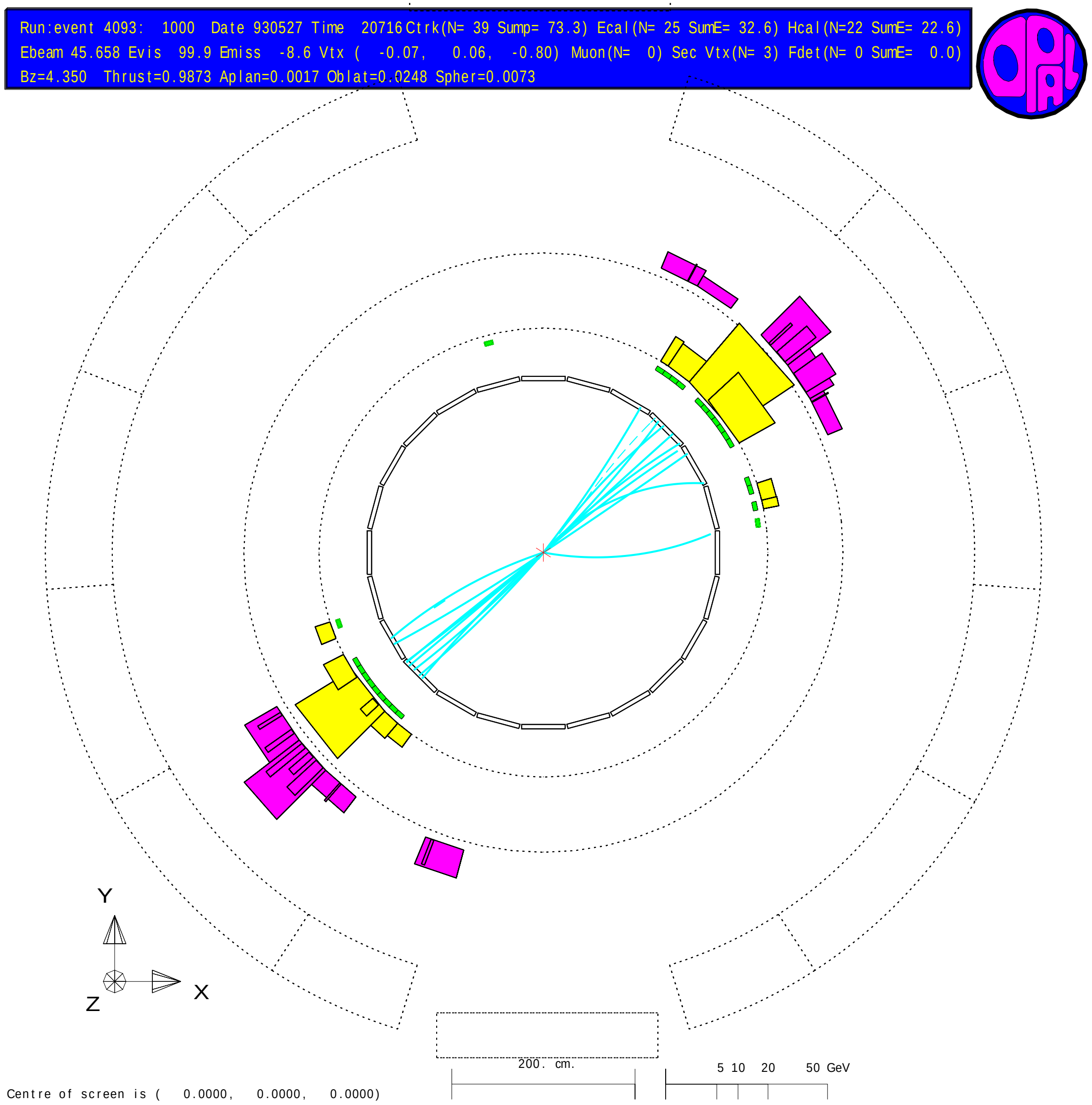

$e^+e^- \rightarrow \text{jet} + \text{jet}$ **(e^+e^- annihilation)**

What is a jet (II)?

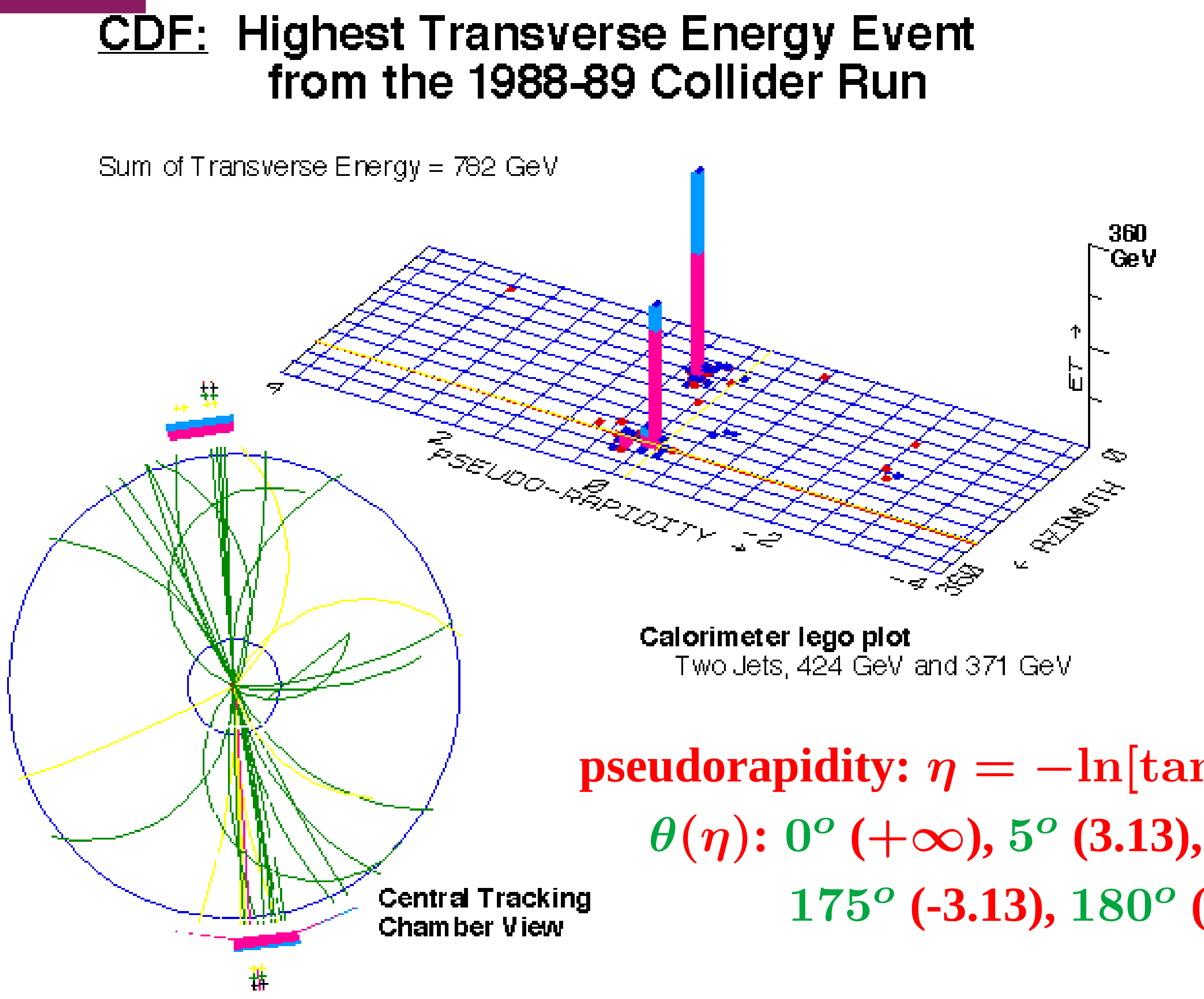

pseudorapidity: $\eta = -\ln[\tan(\theta/2)]$

$\theta(\eta)$: 0^o ($+\infty$), 5^o (3.13), 90^o (0)

175^o (-3.13), 180^o ($-\infty$)

$p\bar{p} \rightarrow \text{jet} + \text{jet} + \text{Anything}$ ($p\bar{p}$ collision)

What is a jet (III)?

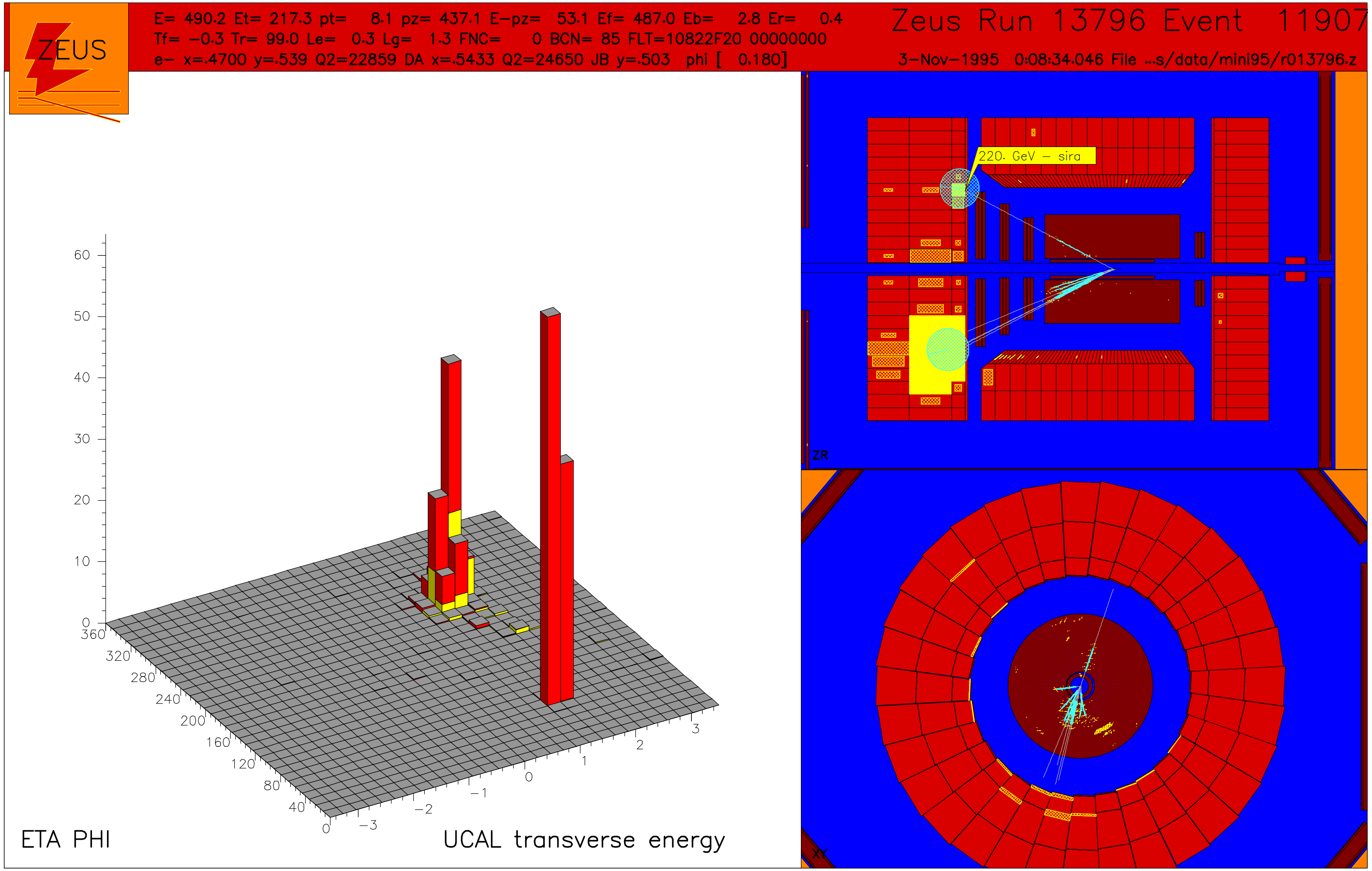

$ep \to e \; + \text{jet} \; + \text{Anything}$ **(NC DIS)**

What is a jet (IV)?

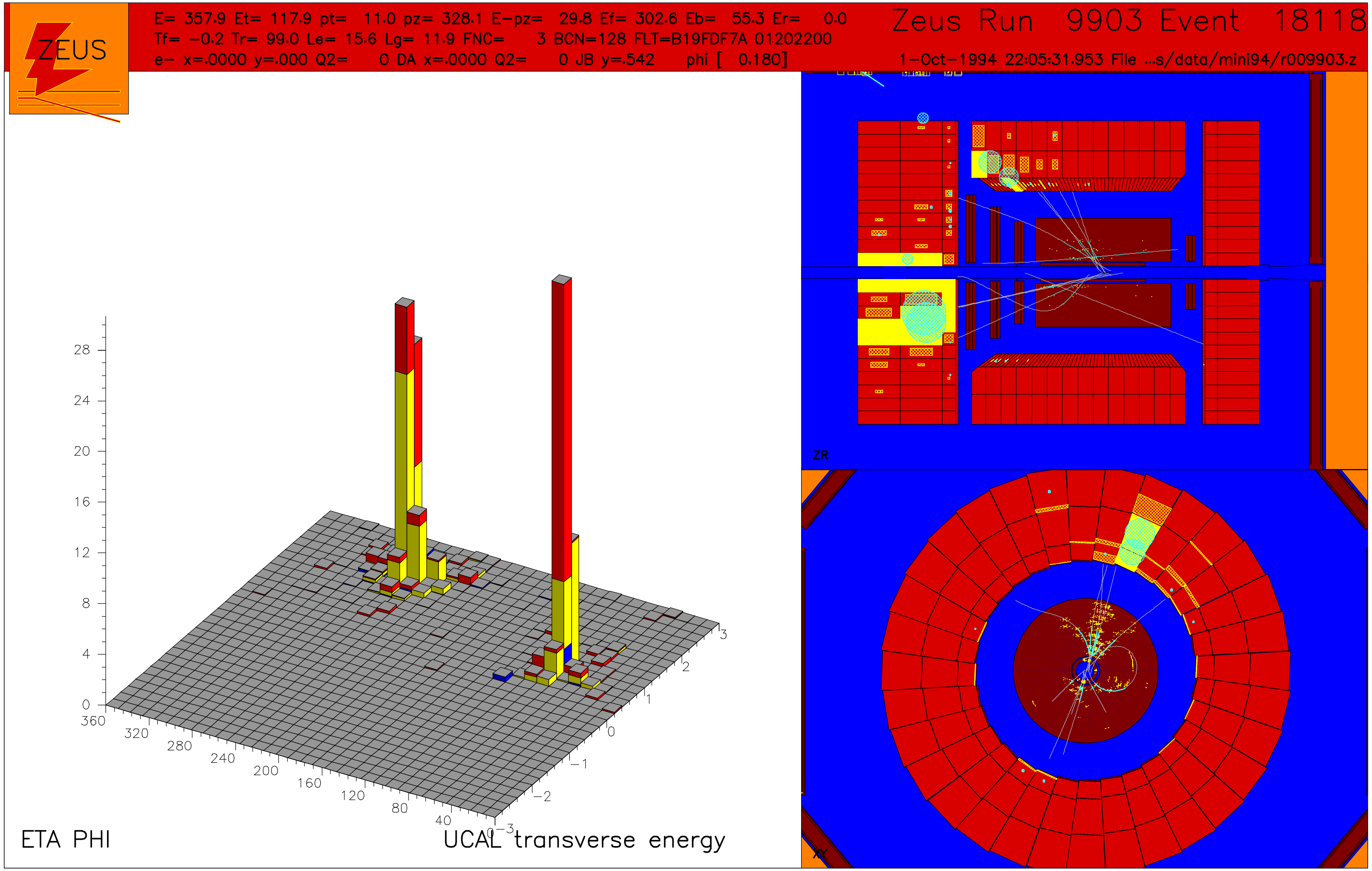

$ep \to \text{jet} + \text{jet} + \text{Anything}$ **(photoproduction)**

What is a jet (V)?

$$pp \to \text{jet} \ + \text{jet} \ + \text{Anything}$$

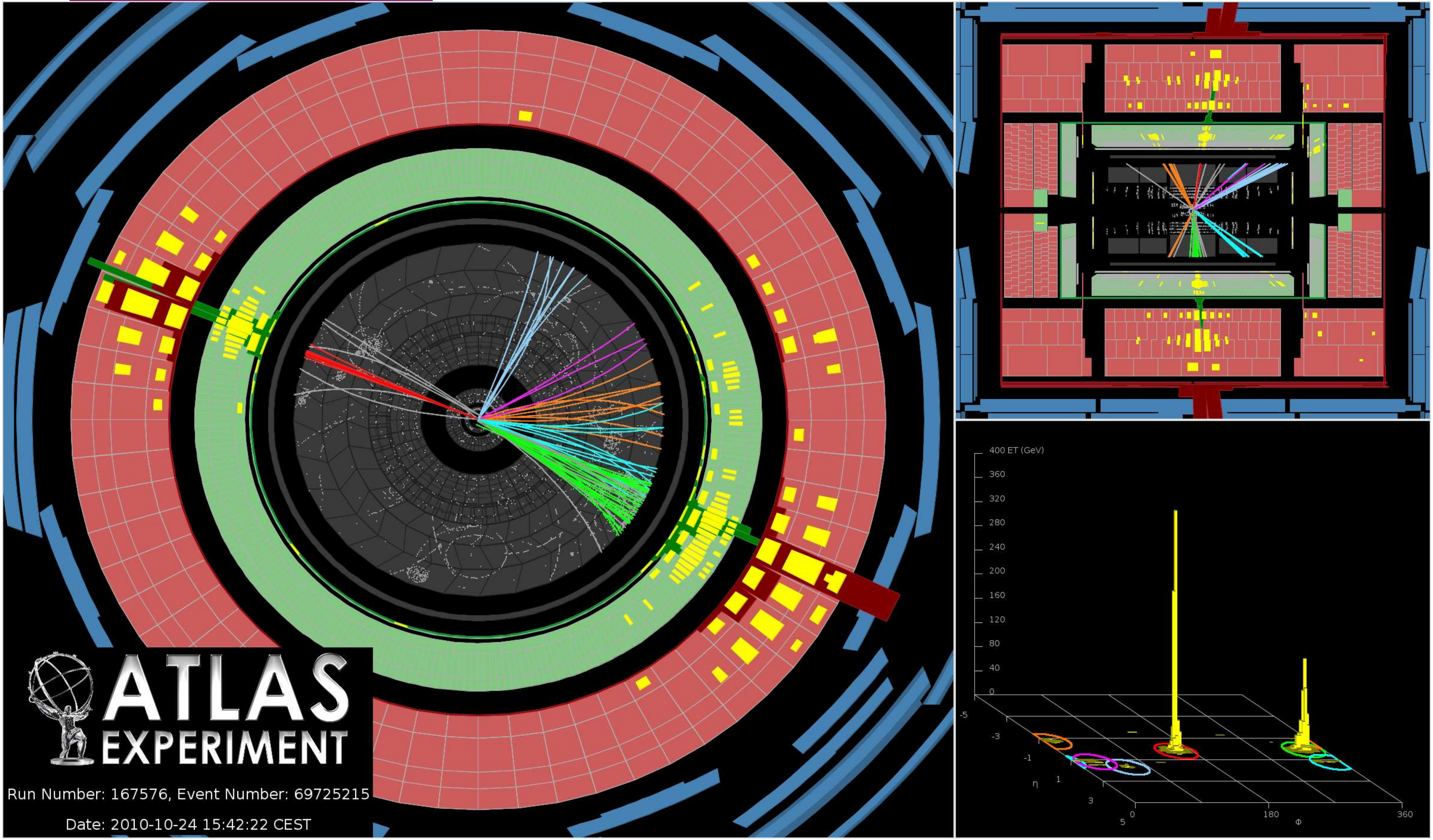

What is a jet (VI)?

$pp \rightarrow \text{jet} + \text{jet} + \text{Anything}$

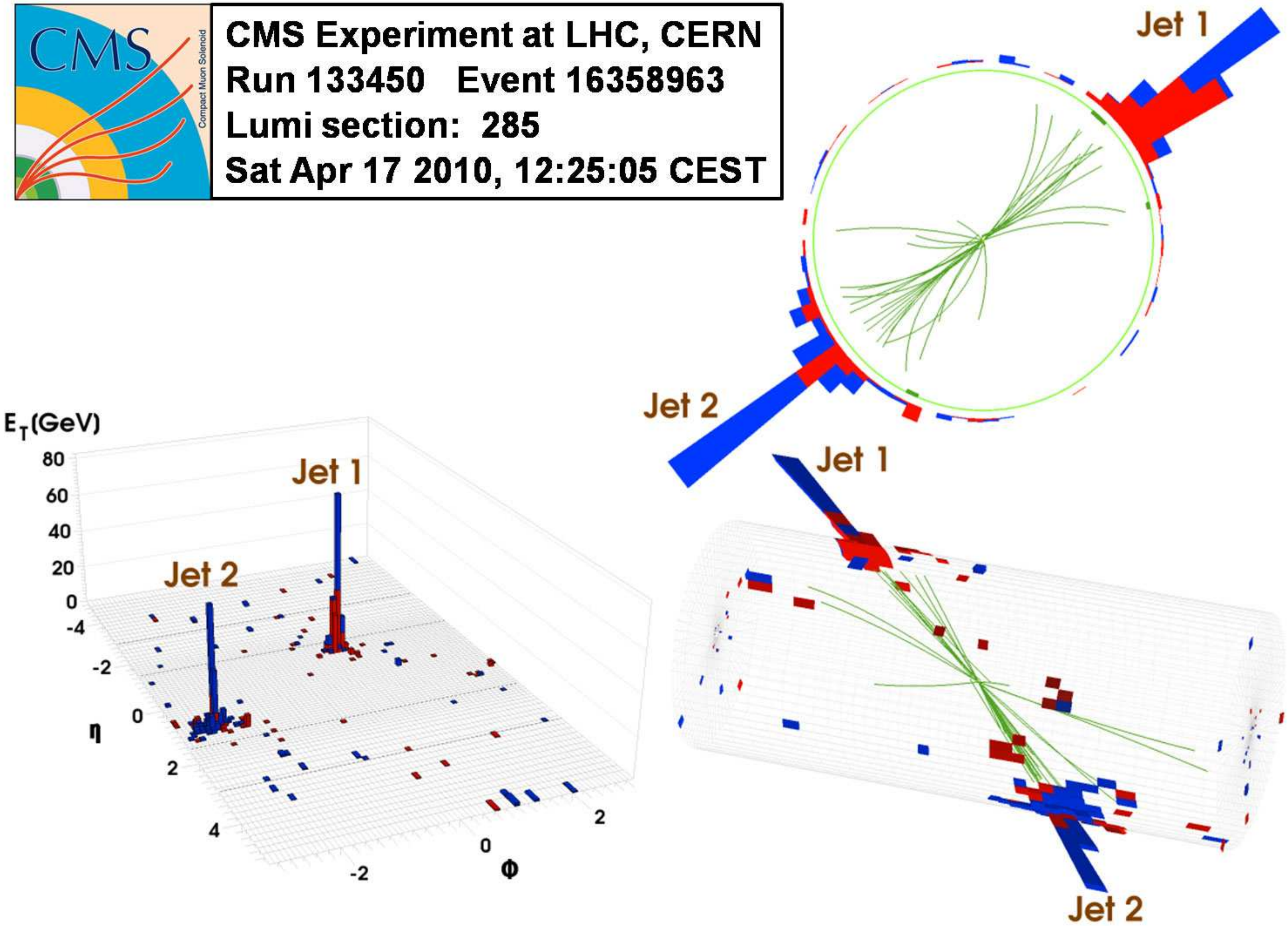

Some good reasons to study jets

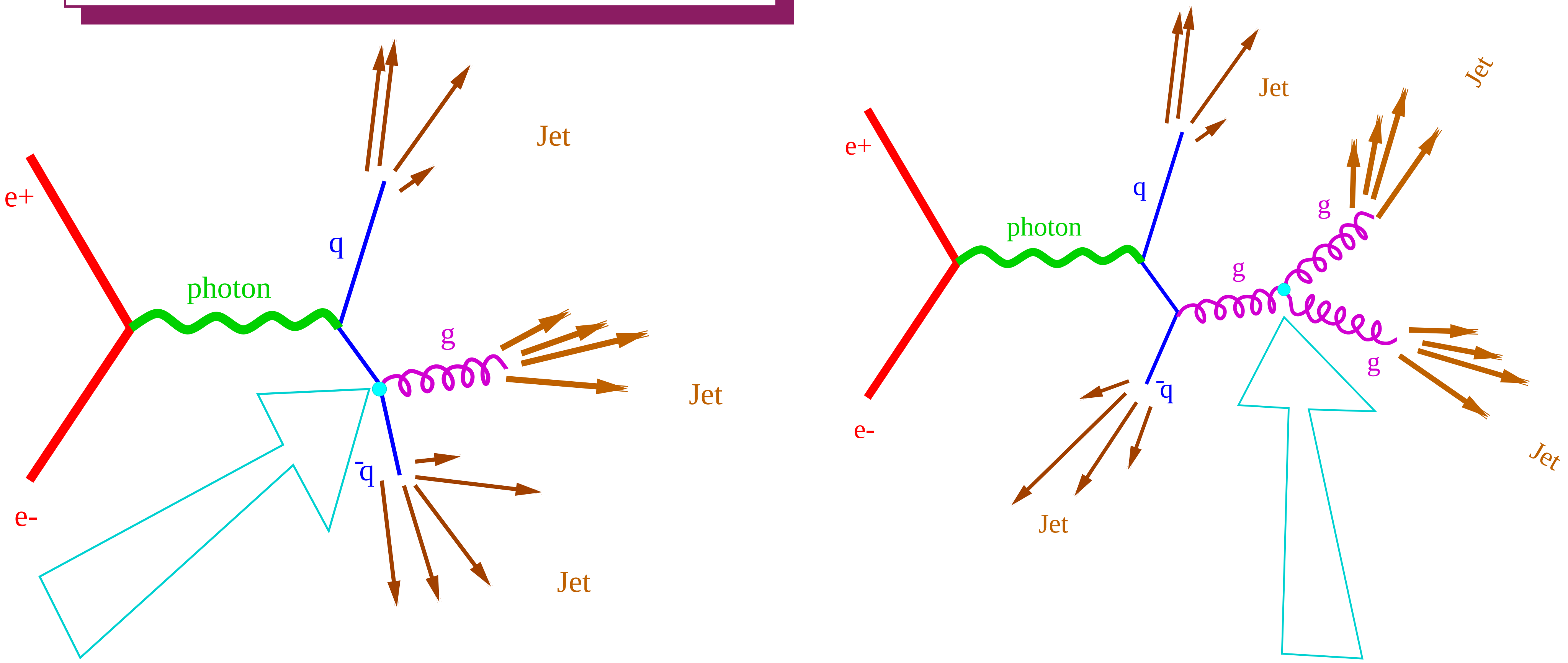

- **Studies of the strong interactions:**

$\longrightarrow$ **measurements of the strong coupling constant (α_S)**

$\longrightarrow$ **colour dynamics (e.g. the self-coupling of the gluon)**

Some good reasons to study jets (II)

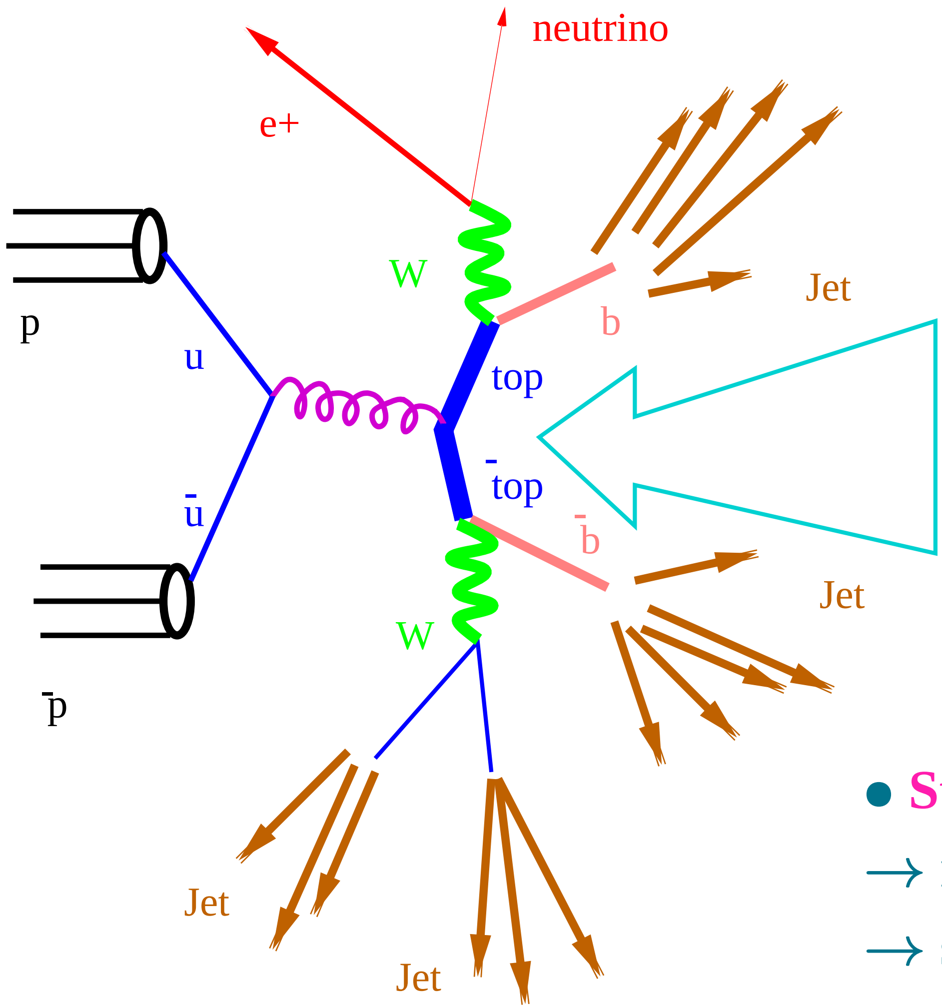

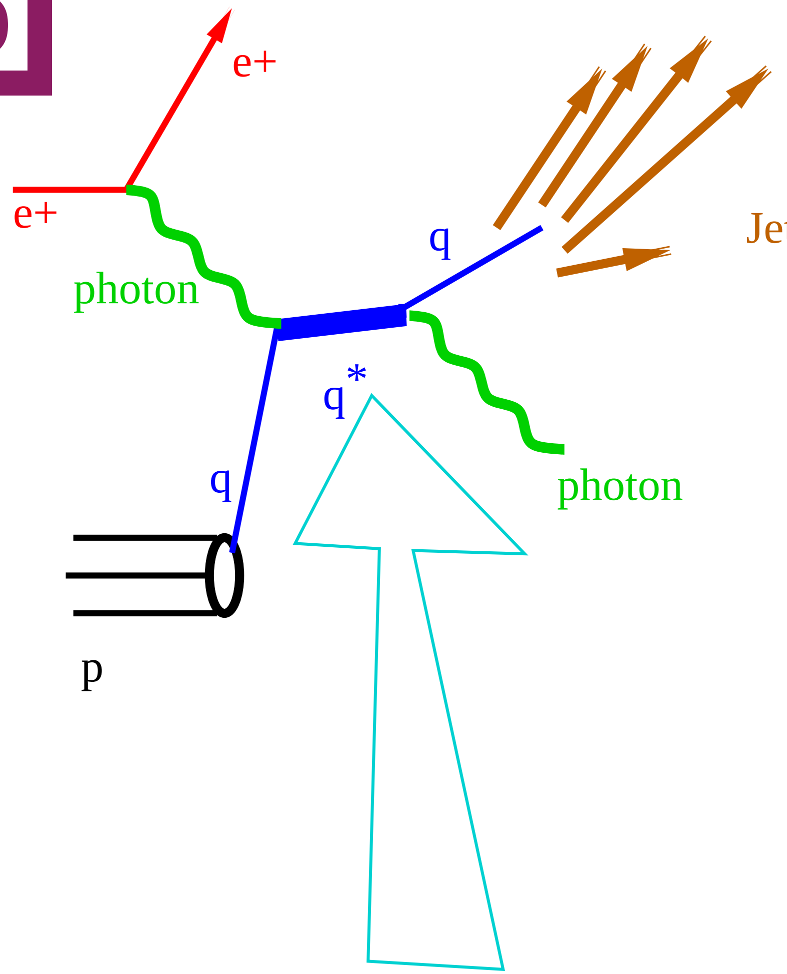

- **Study of and search for new heavy particles:**

→ measurements of top quark production

→ search for excited quarks

Some good reasons to study jets (III)

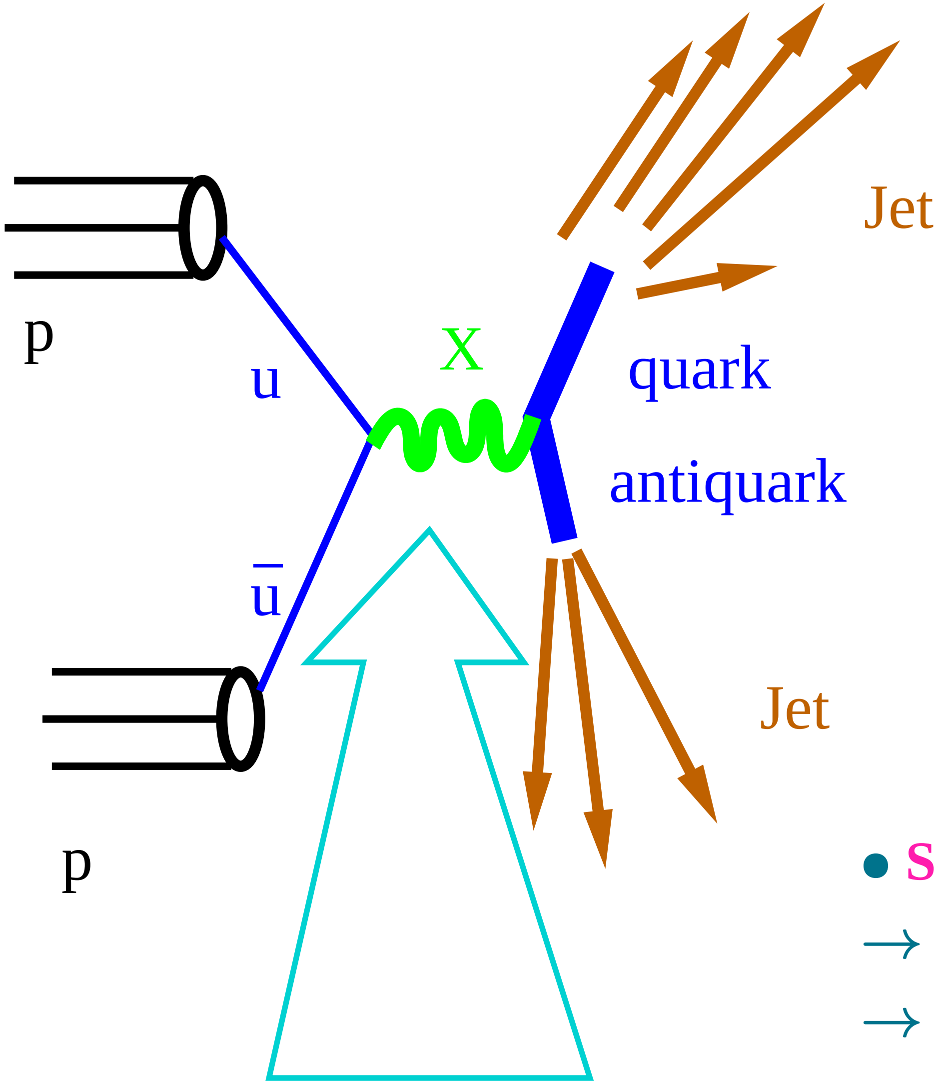

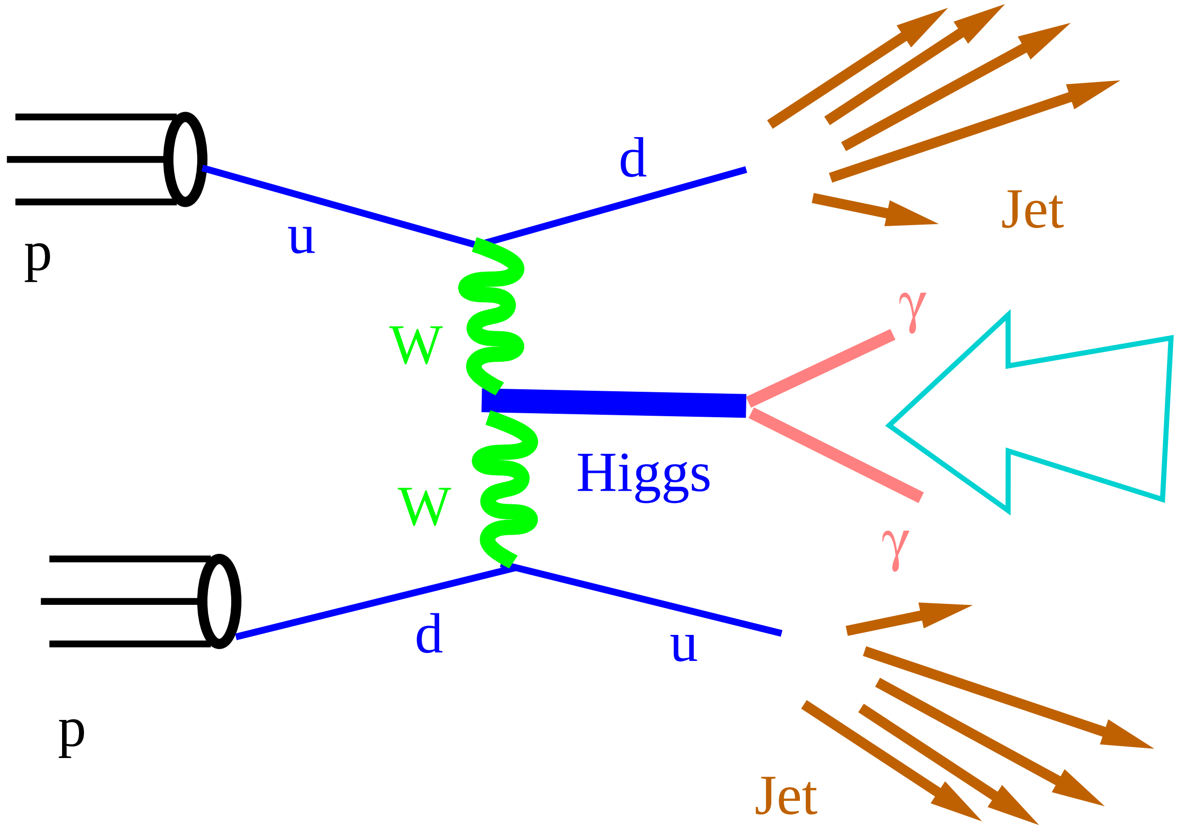

- **Search for new heavy particles:**

$\longrightarrow$ **new particles decaying to jets**

$\longrightarrow$ **Higgs Boson**

Jet Algorithms

How to find jets?

- **To reconstruct the final-state quarks and gluons**

  $\longrightarrow$ Something more sophisticated than a bucket is needed!

  $\Longrightarrow$ JET ALGORITHM

  $\longrightarrow$ MEASURABLE!

  $\longrightarrow$ CALCULABLE!

  $\longrightarrow$ ACCURATE!

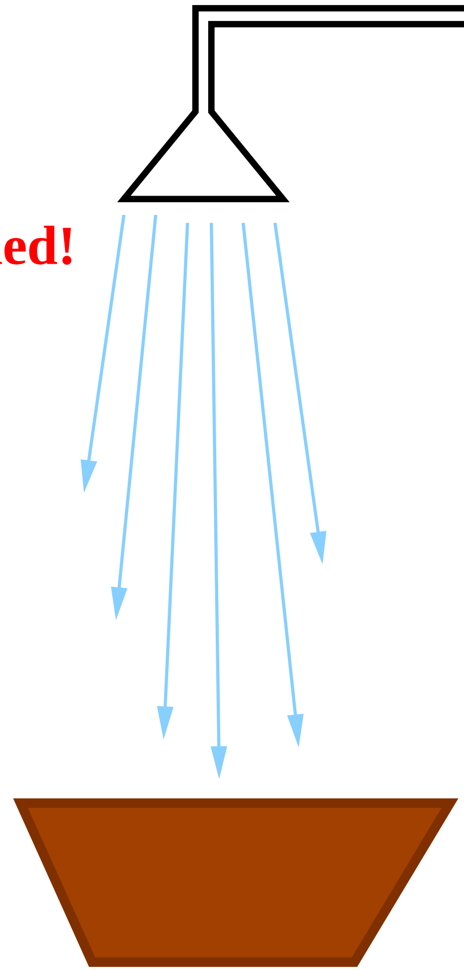

- **Jet algorithm:**

  $\longrightarrow$ Reference frame

  $\longrightarrow$ Variables of the hadron

  $\longrightarrow$ Combining hadrons

Variables for Jet Search in e^+e^- annihilations

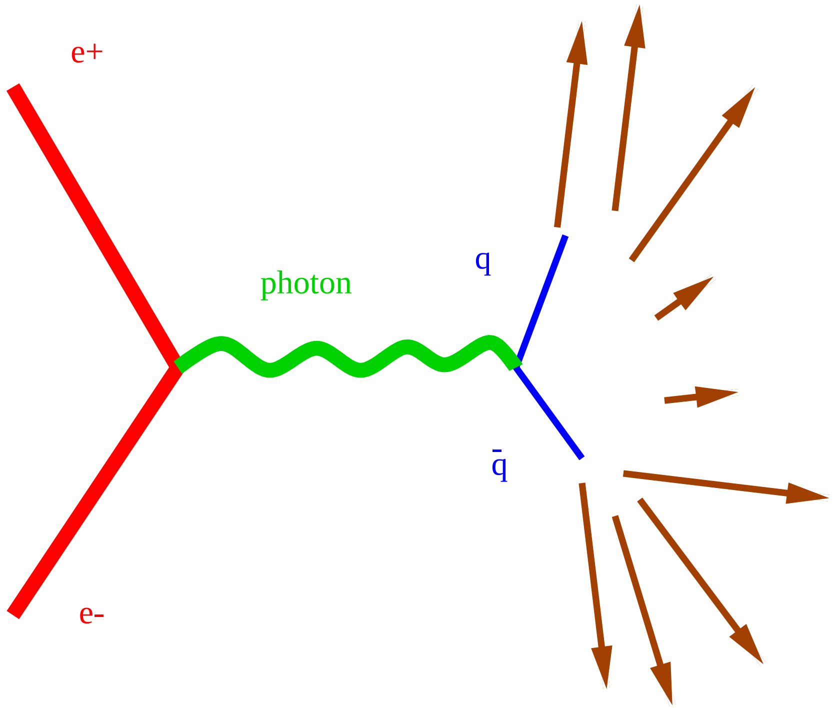

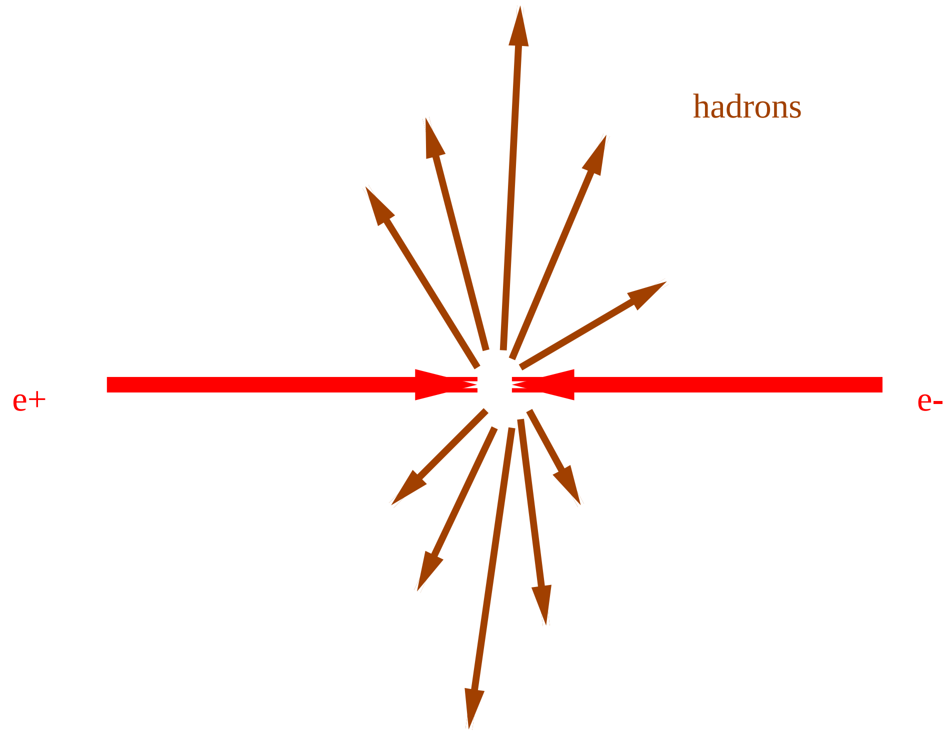

- e^+e^- **annihilations in the centre-of-mass system**
- **Invariance under rotations** ⇒ **Energies and angles**

⇒ Input to the jet algorithm: $\boldsymbol{E_i}$, $\boldsymbol{\theta_i}$ and $\boldsymbol{\phi_i}$ for every hadron $\boldsymbol{i}$

⇒ "distance" between hadrons $\boldsymbol{i}$ and $\boldsymbol{j}$: their angular separation $\boldsymbol{\theta_{ij}}$

Variables for Jet Search in pp collisions

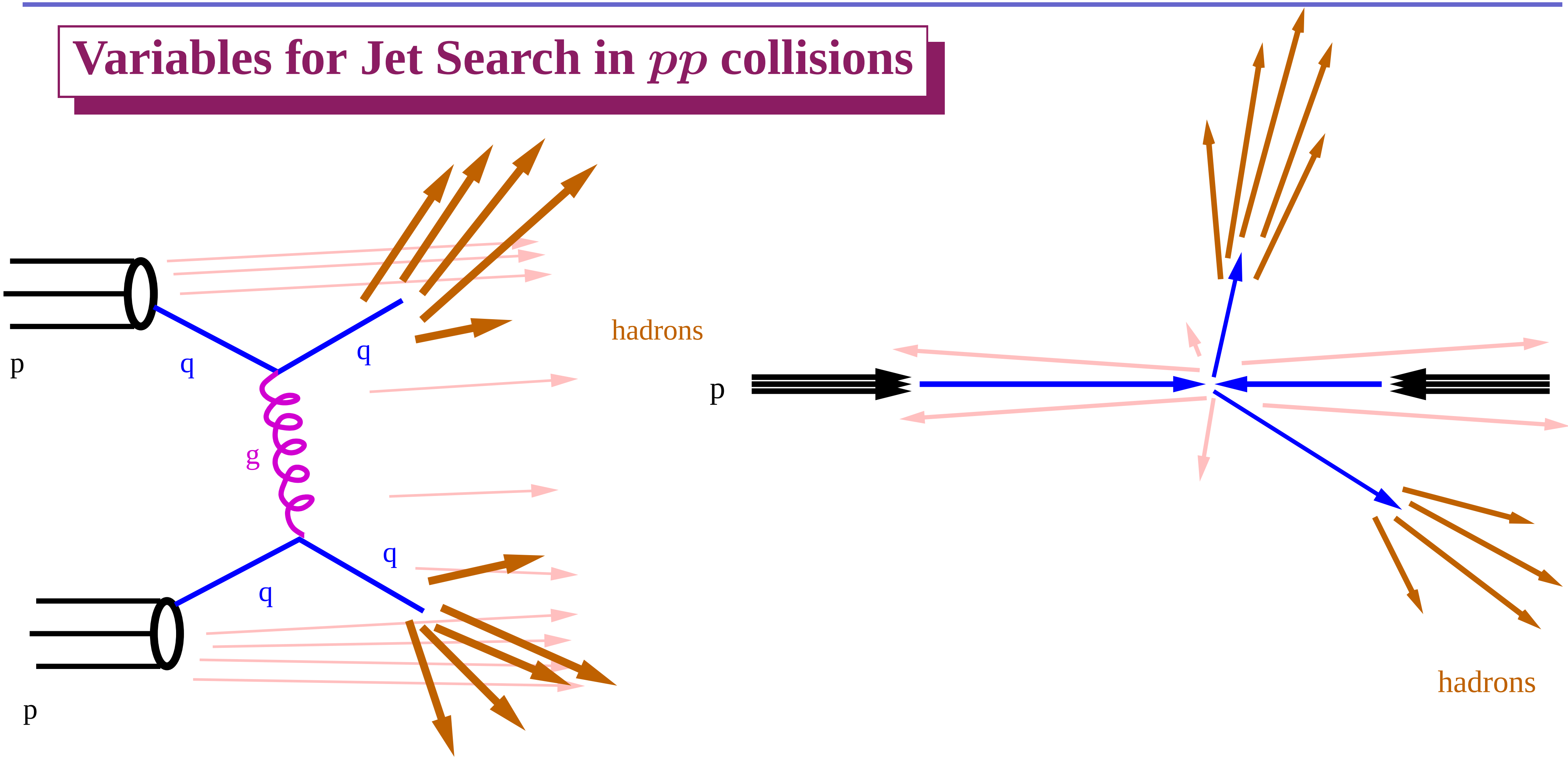

- pp collisions in the centre-of-mass system
- **However the initial-state parton-parton system is NOT at rest!**

depending upon the momentum fractions, x_{p1} and x_{p2}, wrt the parent hadrons

$\Rightarrow$ the final-state partonic system is BOOSTED along the beam axis

Variables for Jet Search in pp collisions (II)

- **Angular separations are NOT invariant under boosts!**

⇒ a given set of hadrons will appear more collimated depending upon the boost

- **To treat on equal footing all possible final-state hadronic systems**

invariance under longitudinal boosts ⇒ transverse momentum, rapidity* and azimuthal angle

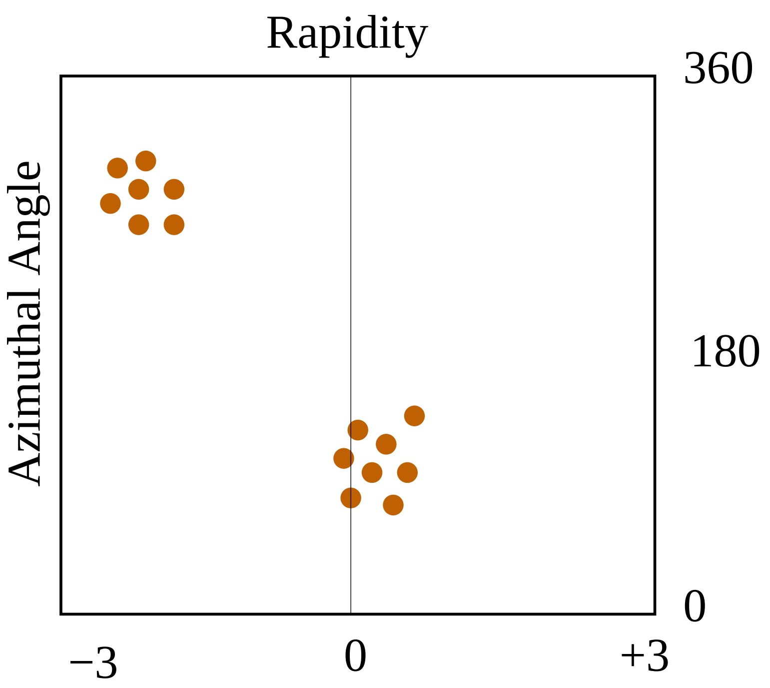

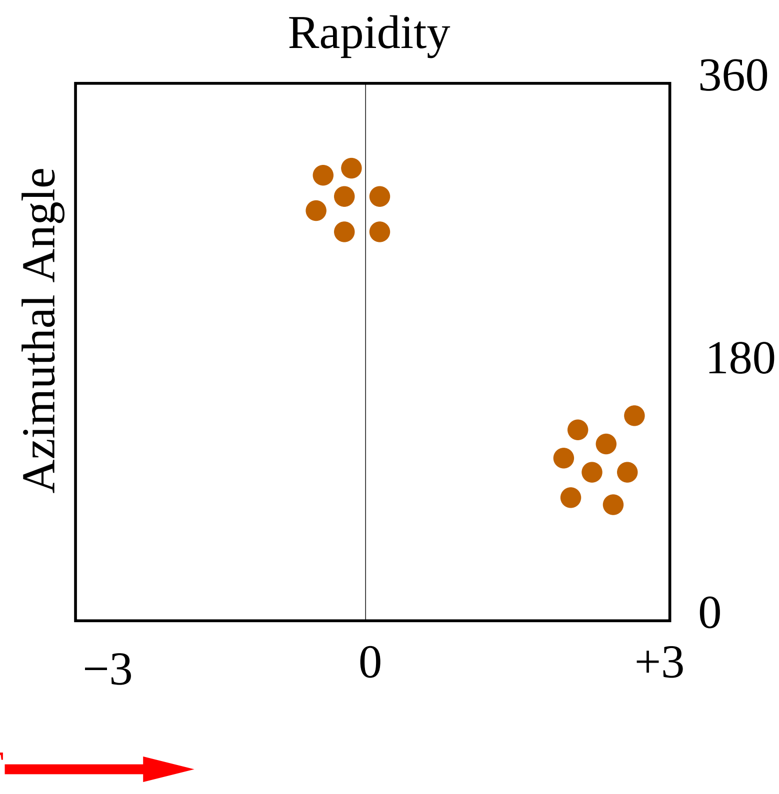

Under a boost:

$$y' = y + f(x_{p1}, x_{p2})$$

⇒ the difference in y between hadrons i and j

Δy_{ij} IS INVARIANT!

The "distance" defined as

$$r \equiv \sqrt{\Delta y_{ij}^2 + \Delta \phi_{ij}^2}$$

is INVARIANT!

Variables for Jet Search in pp collisions (III)

- **Advantage of using transverse momenta:**

Large energy $\neq$ small distance (hard scattering!)

The beam remnant jets have huge energies, but they HAVE NOT undergone a hard scattering!

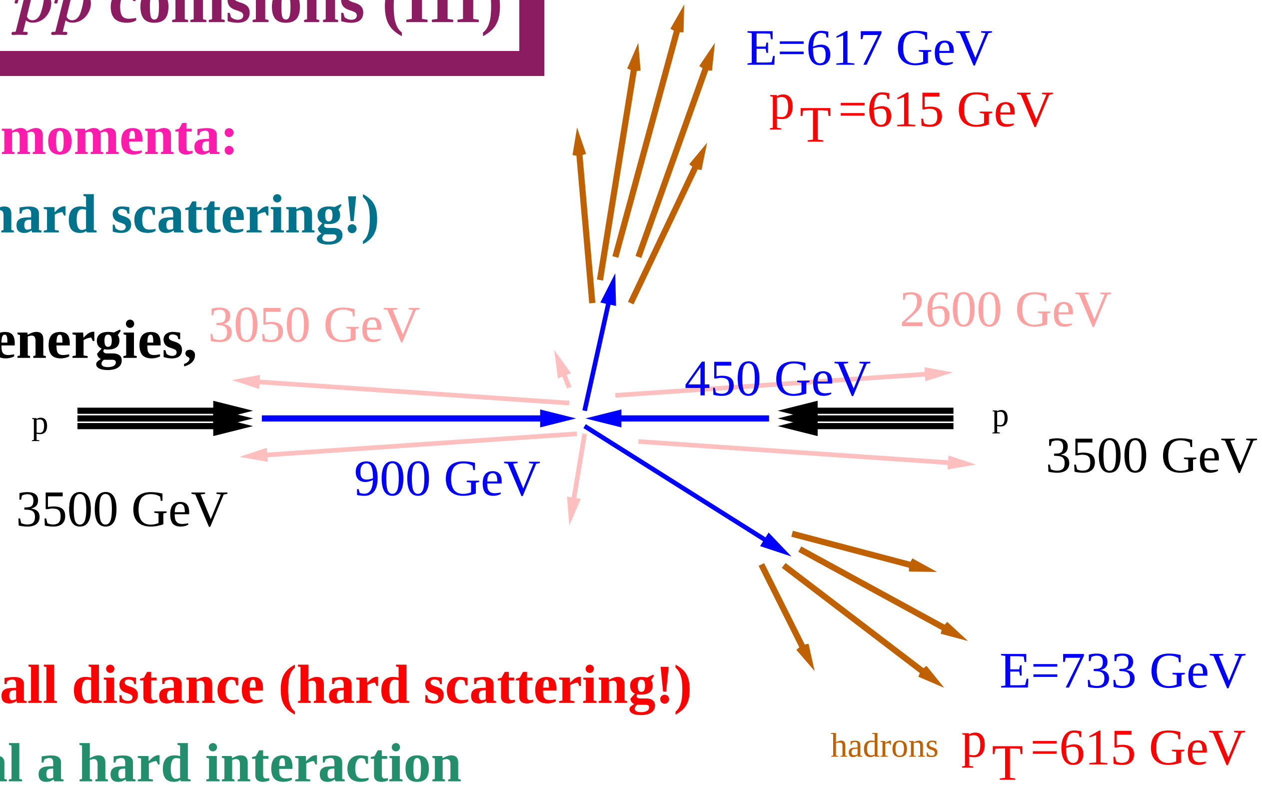

- **Large momentum transfer $\equiv$ small distance (hard scattering!)**

$\Rightarrow$ **large transverse momenta signal a hard interaction**

- **The use of transverse momenta helps to disentangle between the products of the hard interaction and the beam remnant jets/UE (absent in e^+e^- annihilations)**

$\Rightarrow$ Input to the jet algorithm: $p_{T,i}$, y_i and ϕ_i for every hadron i

$\Rightarrow$ "distance" between hadrons i and j: $\sqrt{\Delta y_{ij}^2 + \Delta \phi_{ij}^2}$

The best choice for jet algorithm in pp collisions

- There is no best choice since, at the end, it is a question of having the smallest uncertainty for the given observable:
  - $\rightarrow$ the smallest theoretical uncertainties (higher-order contributions)
  - $\rightarrow$ the smallest hadronisation/UE effects
  - $\rightarrow$ the smallest experimental uncertainties
- For most of the measurements, the longitudinally invariant anti-k_T algorithm (M. Cacciari, G. Salam and G. Soyez) has been used for comparisons between data and perturbative QCD at the LHC
  - $\rightarrow$ it is collinear and infrared safe to all orders in pQCD
  - $\rightarrow$ it provides $\approx$ circular jets

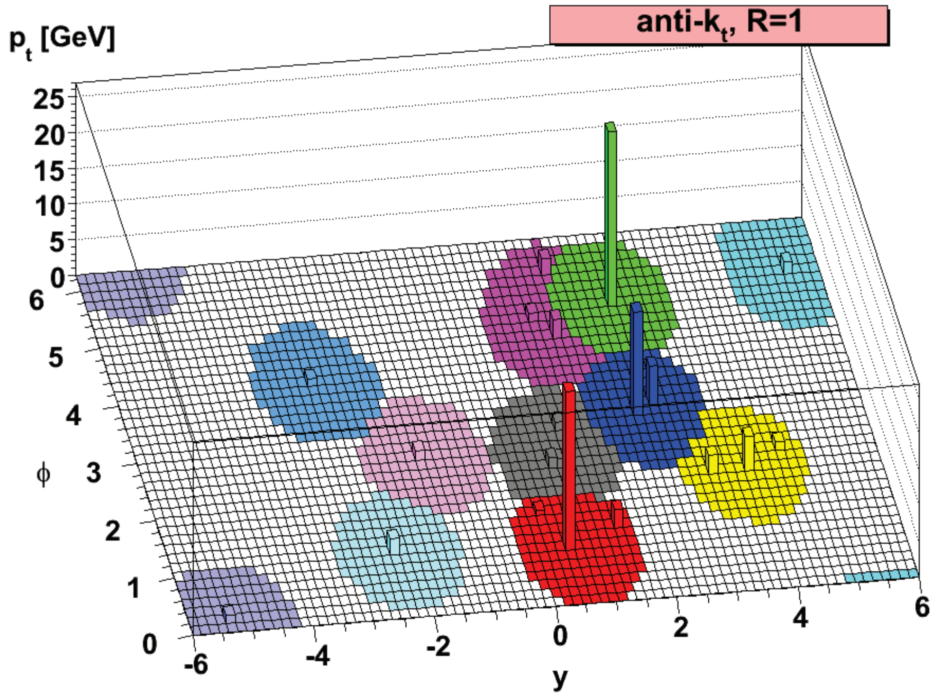

The longitudinally invariant anti-k_T algorithm for pp collisions

- **The clustering procedure is as follows:**
  - → List of particles (or calorimeter cells, clusters of calorimeter cells, partons, . . .)
  - → For every object k and for every pair of objects i, j the "distances" are evaluated

    $d_k^2 = 1/p_{T,k}^2$ (distance to the beam)

    $d_{ij}^2 = \min(1/p_{T,i}^2, 1/p_{T,j}^2) \cdot ((y_i - y_j)^2 + (\phi_i - \phi_j)^2)/R^2$
  - → If, of all the values $\{d_k^2, d_{ij}^2\}$, d_{mn}^2 is the smallest, then objects m and n are combined into a single new object according to (e.g.)

    $p_{ij} = p_i + p_j$
  - → If, however, d_k^2 is the smallest, then object k is considered a "protojet" and is removed from the list
  - → The procedure is iterated until the list of objects is empty
- **From the list of "protojets" the jets are selected by imposing certain criteria:**
  - → jet rapidity in the range $C_L < y_{\rm jet} < C_U$
  - → jet transverse momentum in the range $p_{T,\rm jet} > p_{T,0}$

⇒ **the lower the $p_{T,0}$, the larger the theoretical and experimental uncertainties!**

Benefits of the anti-k_T algorithm

- The anti-k_T jet algorithm provides jets with better control on the shape (≈ circular) and area (dictated by the jet radius R) than other jet algorithms

- Essential to control and suppress the energy contributions from particles that fall into the jet but originate from

→ the "underlying event" (hadrons from the same proton-proton collision but unrelated to the hard interaction (a proton is an extended object)

→ additional soft proton-proton interactions overlaid with the interesting one (pile-up)

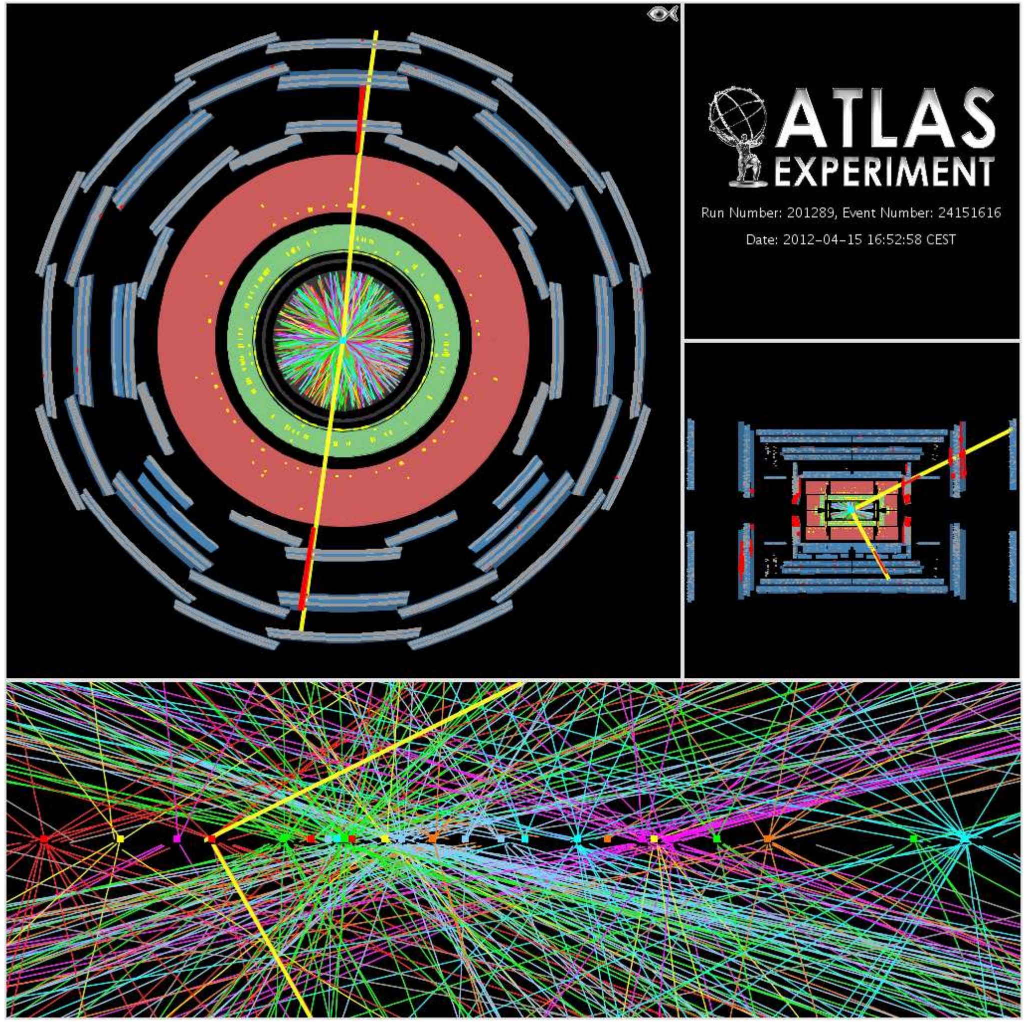

$Z \to \mu^+\mu^-$ event candidate with 25 (!!) reconstructed vertices
High pile-up environment in 2012

Jets with the ATLAS detector

The ATLAS detector

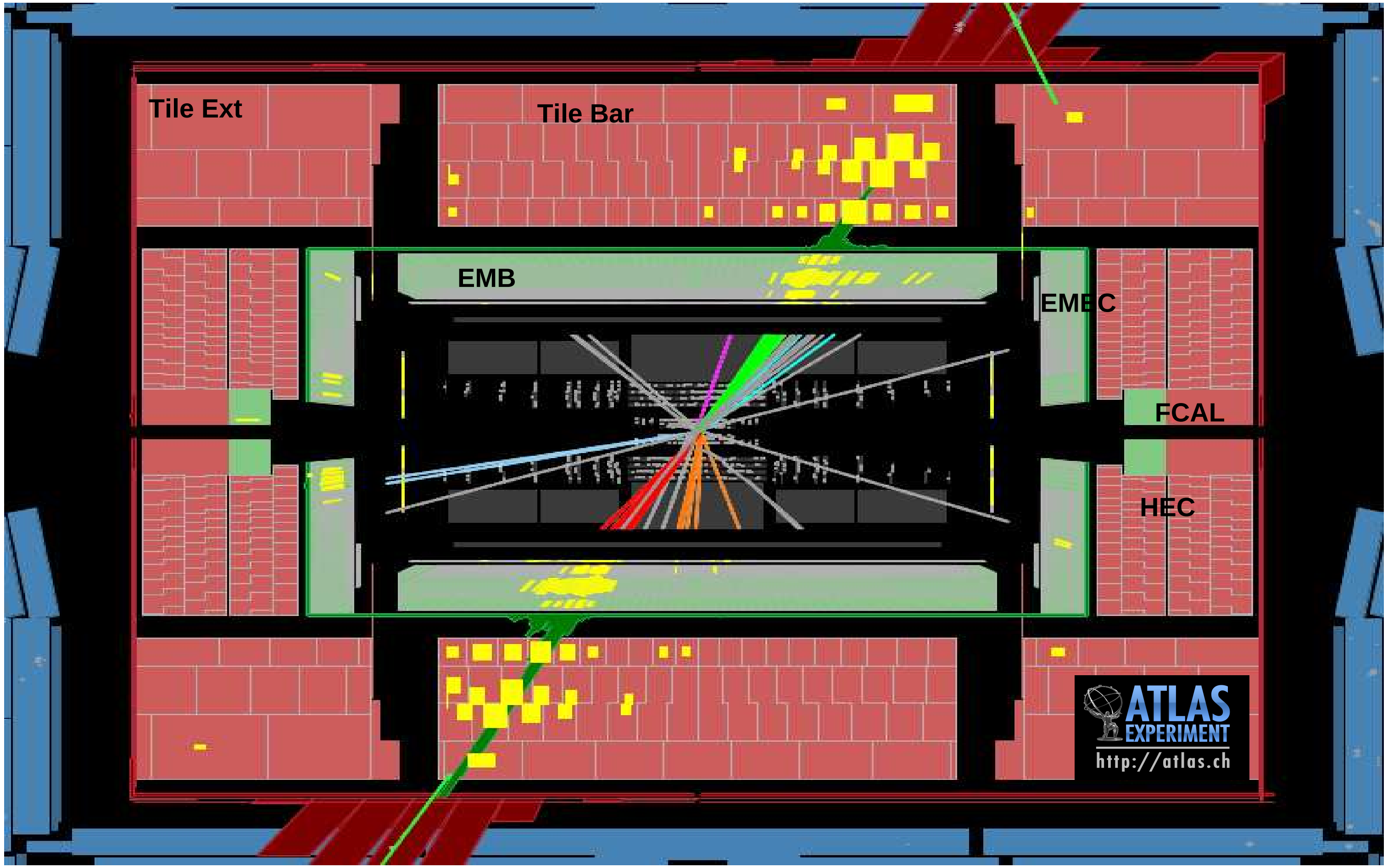

- Inner detector (ID): tracking and particle identification in $|\eta| < 2.5$
- Calorimeters: electromagnetic (LAr) $\rightarrow$ barrel $|\eta| < 1.475$, endcap $1.375 < |\eta| < 3.2$, forward $3.1 < |\eta| < 4.9$; hadronic (scintillator/steel, LAr/Cu, LAr/W) $\rightarrow$ barrel $|\eta| < 0.7$ extended barrel $0.8 < |\eta| < 1.7$, endcap $1.5 < |\eta| < 3.2$ and forward $3.1 < |\eta| < 4.9$

Jet reconstruction in pp collisions with ATLAS

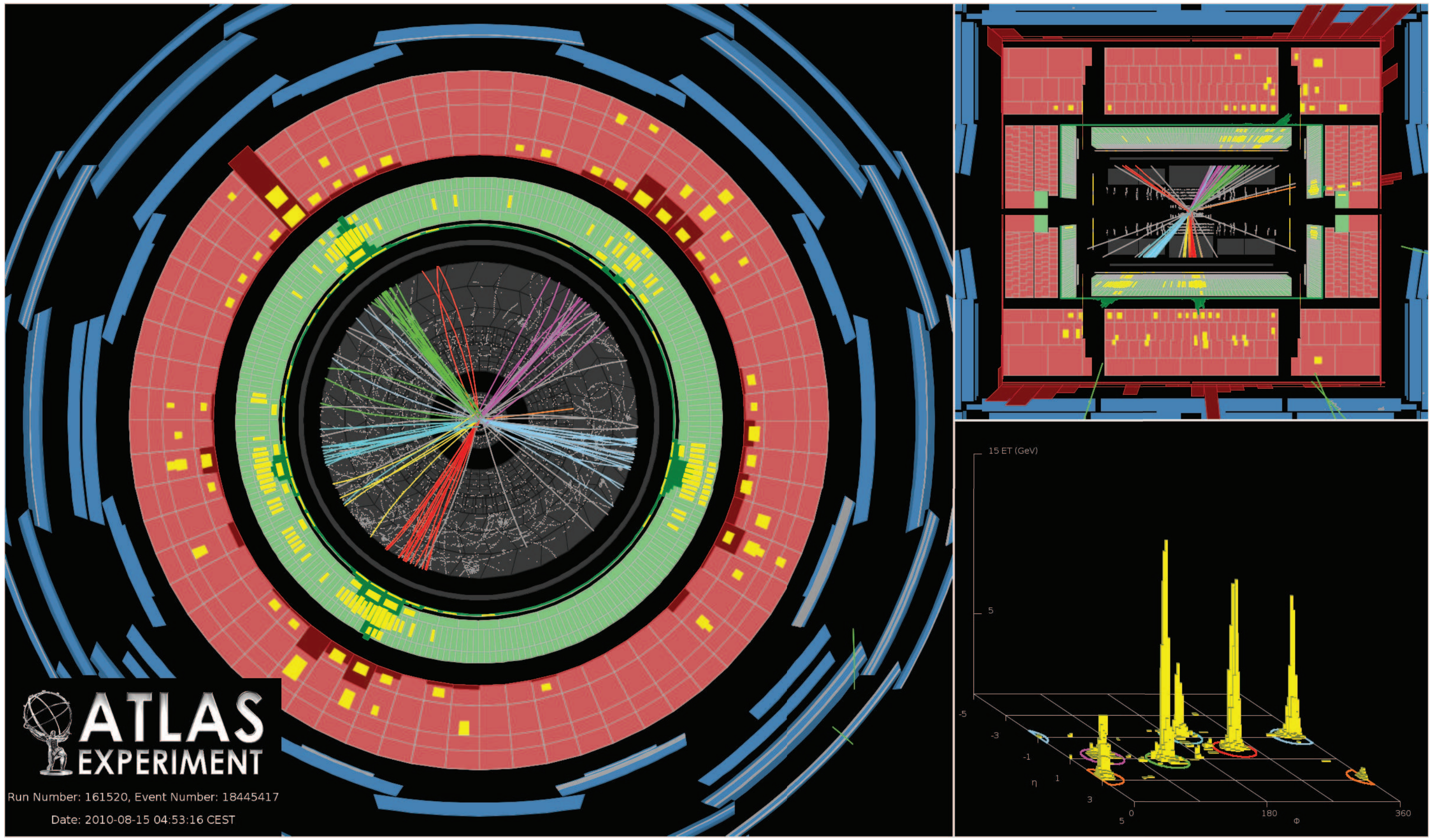

- Jet reconstruction using the anti-k_T algorithm with $R = 0.4$ or $R = 0.6$ (FASTJET) in $y - \phi$ space; four-momentum recombination scheme
- Calorimeter jets: the inputs are topological calorimeter clusters (topoclusters)

Topological calorimeter clusters

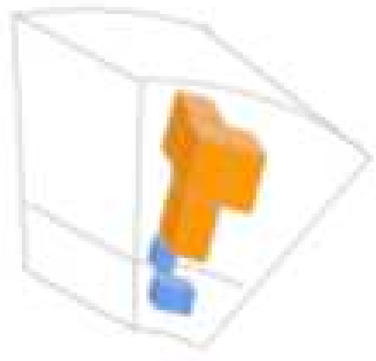

Topological clusters

- Topoclusters: groups of calorimeter cells designed to follow the shower development (using the fine segmentation of the ATLAS calorimeters) of a particle
- Algorithm:
  - ⋆ starting with seeds, cells with $|E_{cell}| > 4\sigma$ (σ = RMS of the noise)
  - ⋆ adding neighbouring cells with $|E_{cell}| > 2\sigma$
  - ⋆ all further immediate neighbours are also added
  - ⋆ clusters are split/merged according to the positions of local maxima and minima $\rightarrow$ to separate showers from close-by particles

$\Rightarrow$ $E_{topo} = \sum E_{cell}$; topocluster direction from energy-weighted averages of η_{cell} and ϕ_{cell}

$\Rightarrow$ Topocluster 4-momentum (assumed massless)

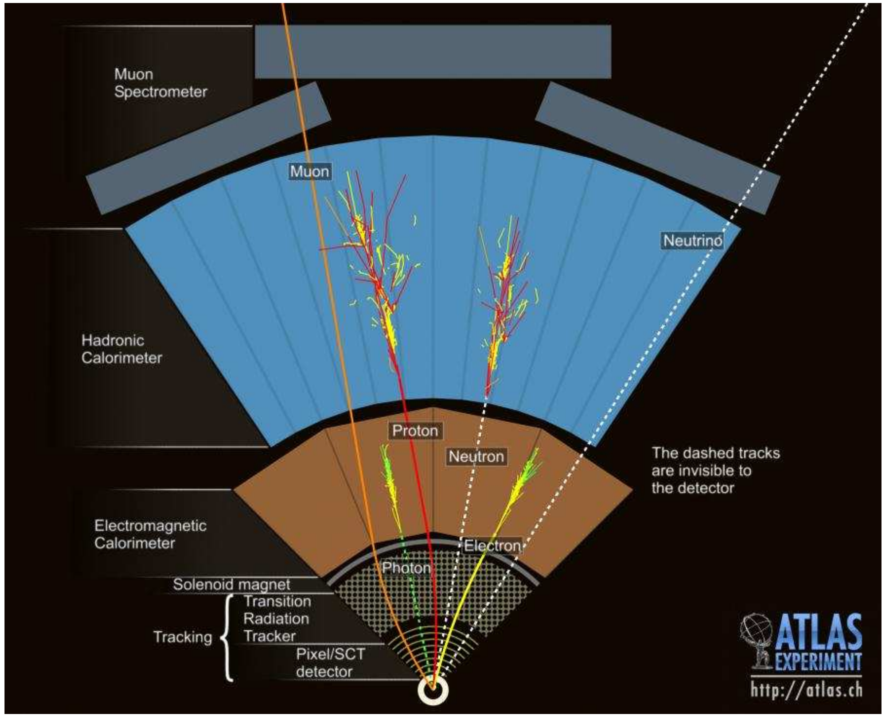

Monte Carlo simulations

Monte Carlo simulations

⇒ **To study the detector response for physics processes**

- **Event generators: from the hard subprocess to the final-state particles (hadrons and leptons)**
  → PYTHIA, HERWIG, SHERPA, ALPGEN+PYTHIA, MC@NLO + HERWIG, ...
- **Simulation of the response of the subdetectors**
- **Output of the simulation chain: in identical format to the output of the ATLAS data acquisition system**

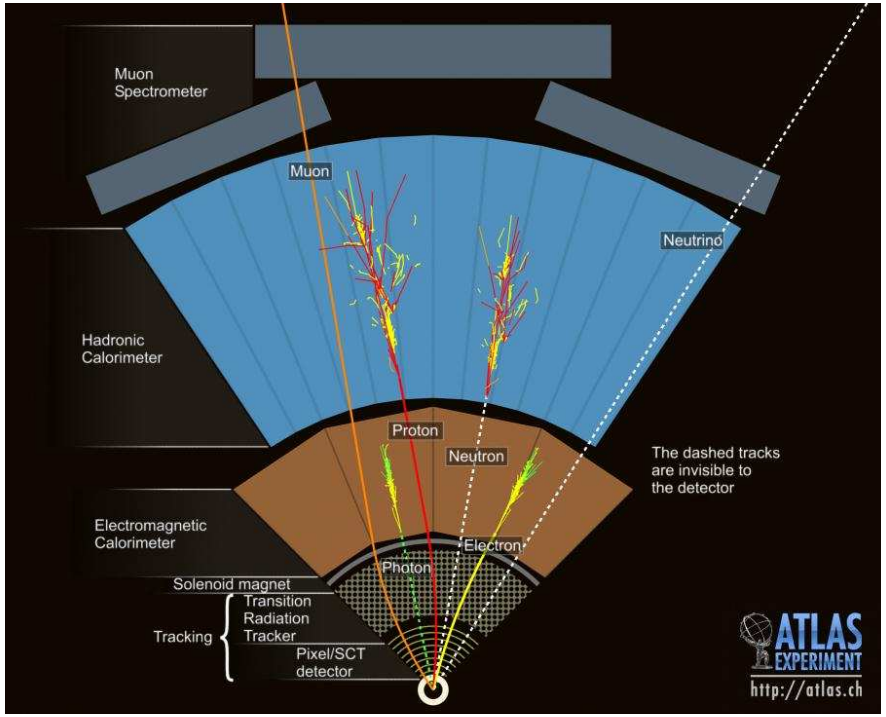

- **Very important tool for jet measurements**

→ jet reconstruction from topoclusters in a MC event

→ jet reconstruction from final-state particles in a MC event

→ jet reconstruction from final-state partons in a MC event

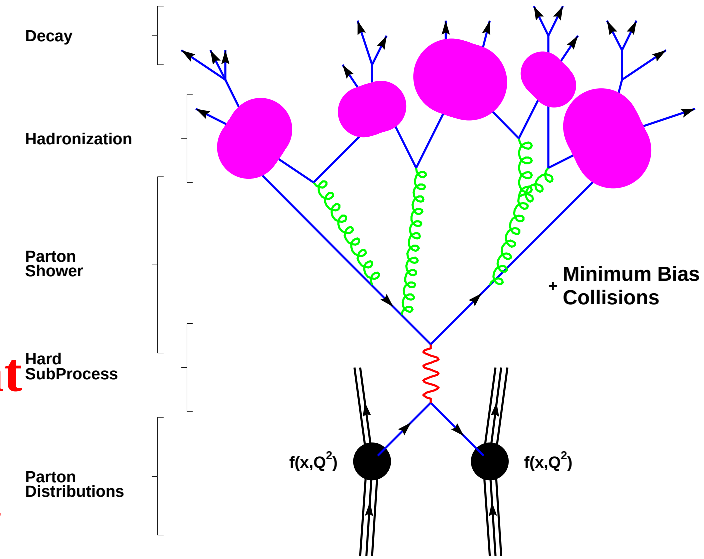

Event generators: How to go from here ...

(Torbjörn Sjöstrand's talk at YETI'06-SM, IPPP, Durham, UK, March 06)

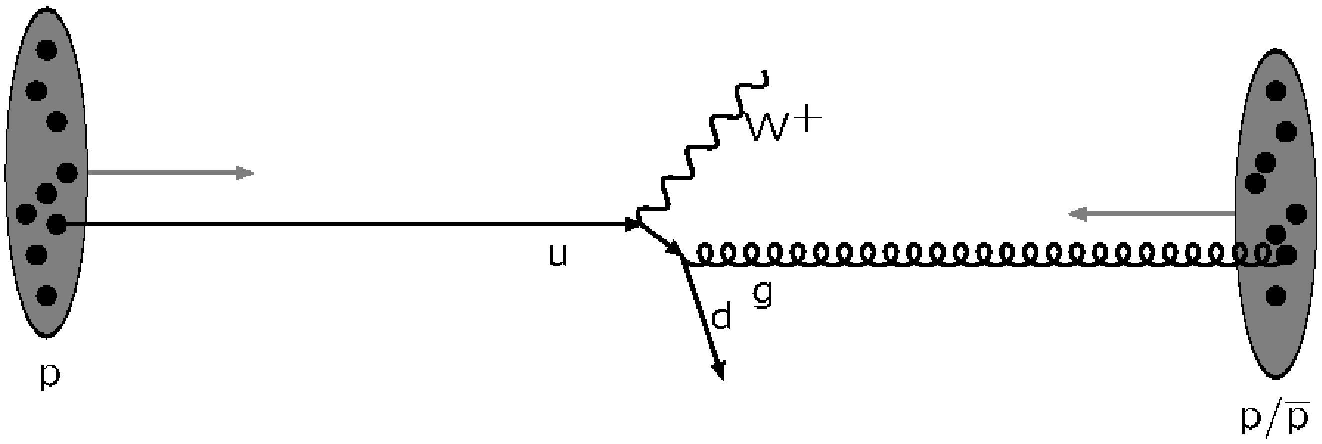

Hard subprocess: described by matrix elements

Event generators: through here ...

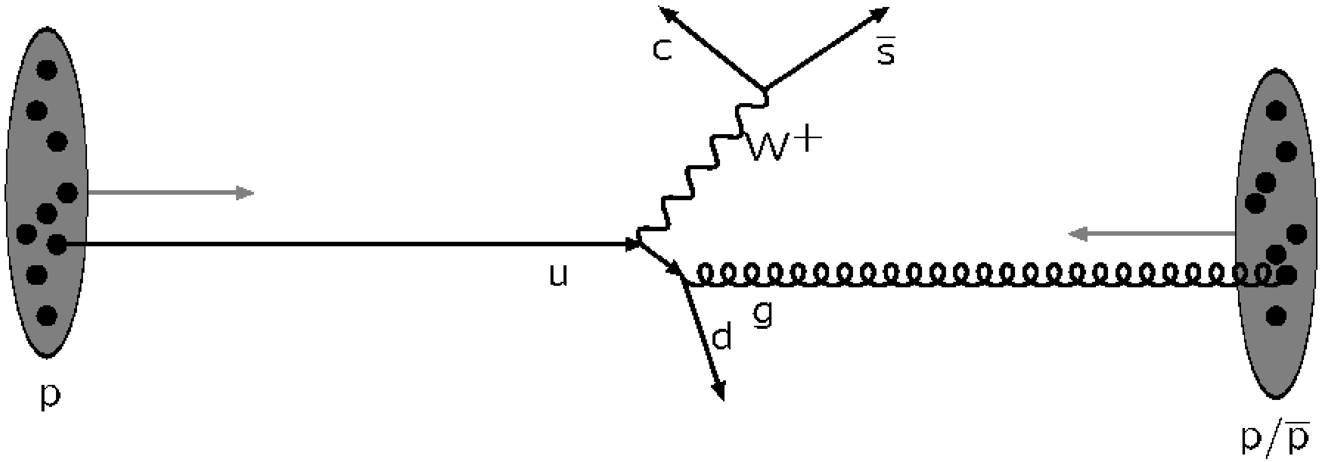

Resonance decays: correlated with hard subprocess

Event generators: through here ...

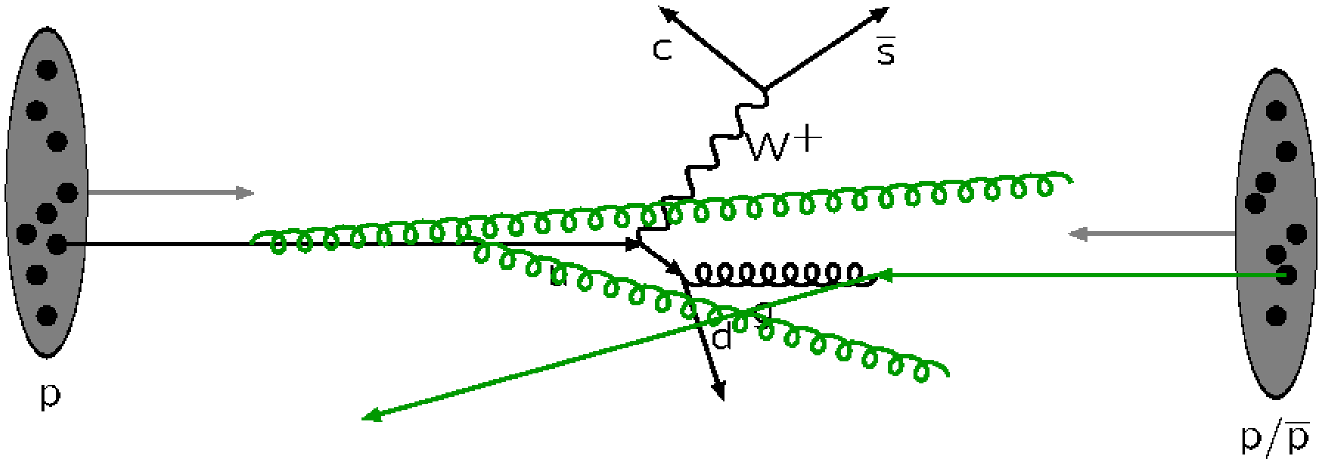

Initial-state radiation: spacelike parton showers

Event generators: through here ...

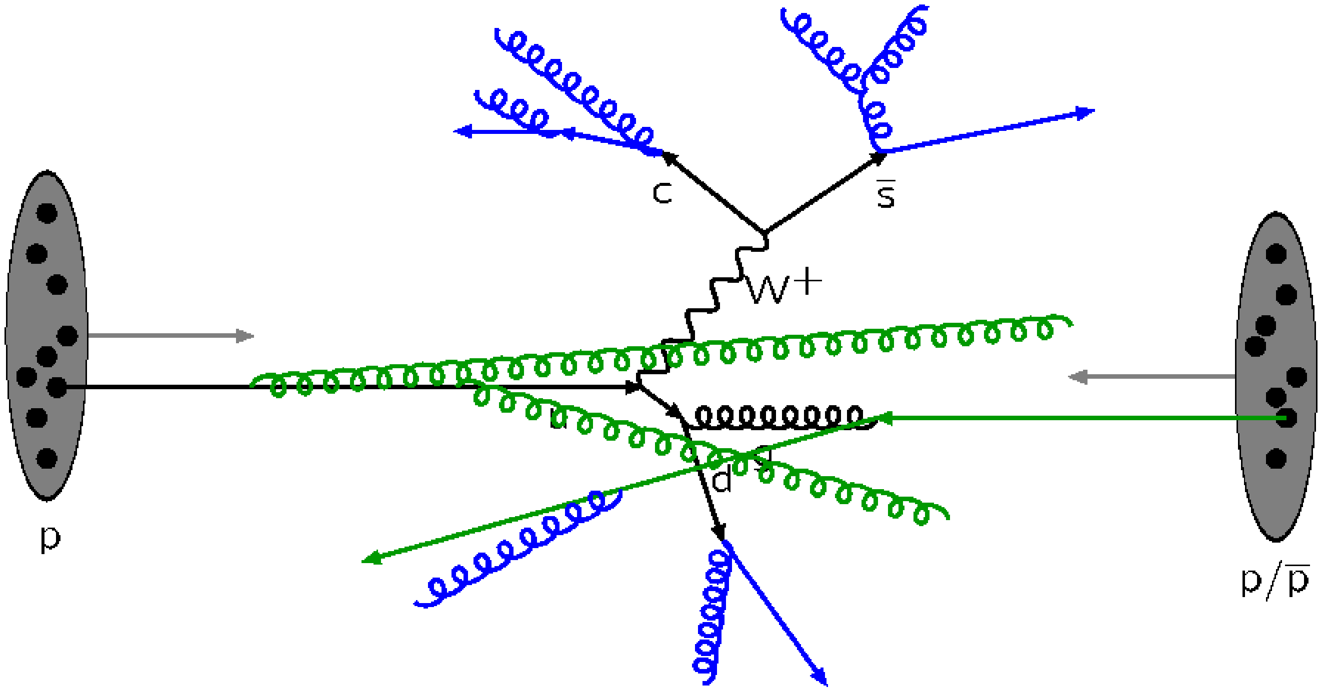

Final-state radiation: timelike parton showers

Event generators: through here ...

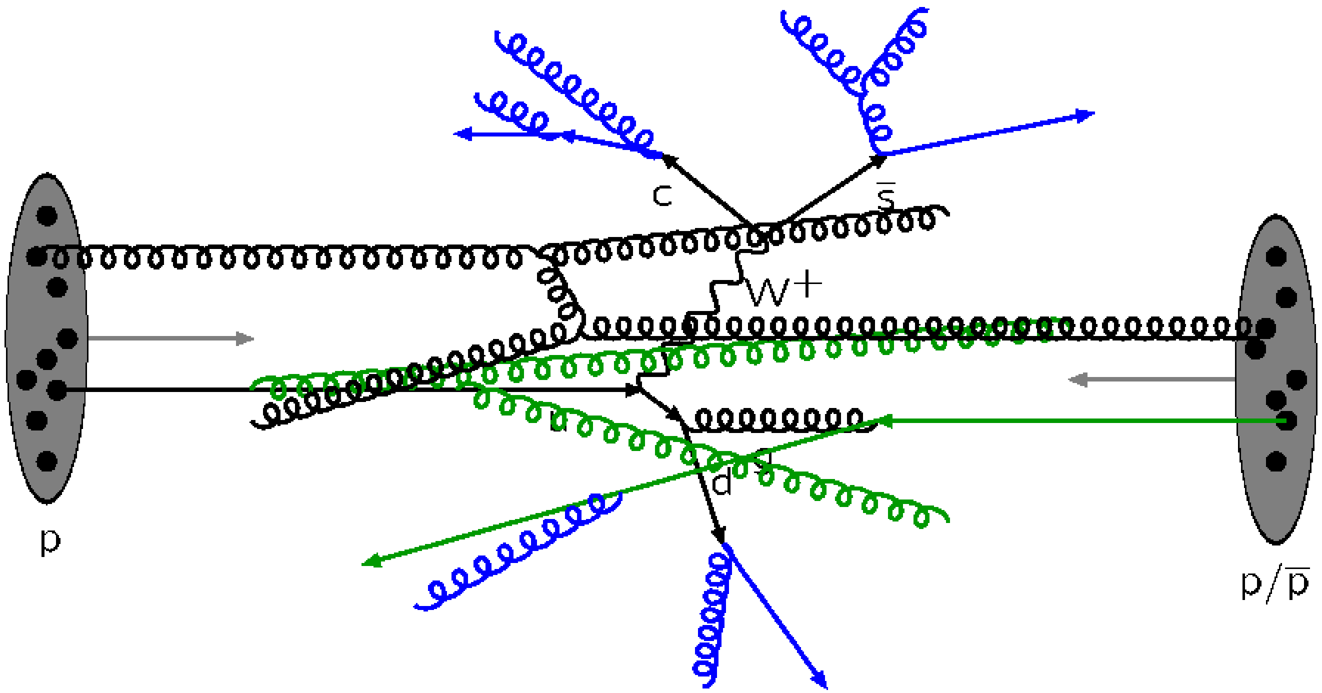

Multiple parton–parton interactions . . .

Event generators: through here ...

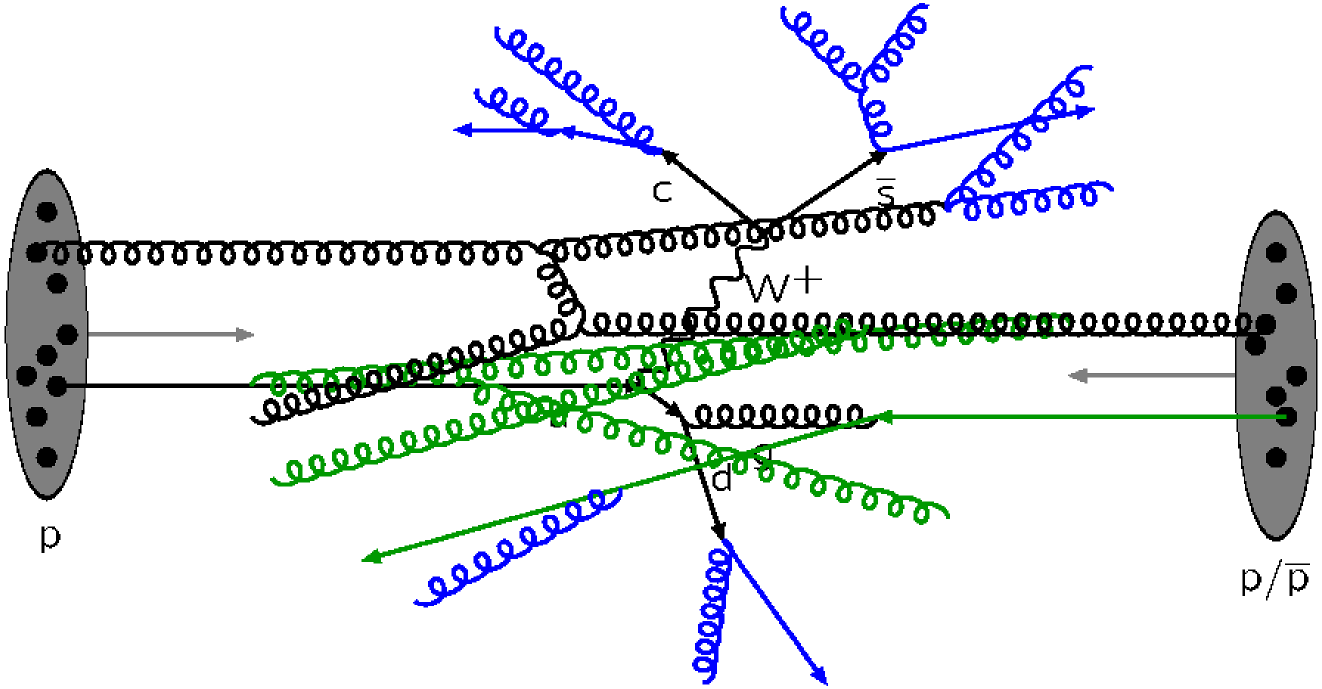

. . . with its initial- and final-state radiation

Event generators: through here ...

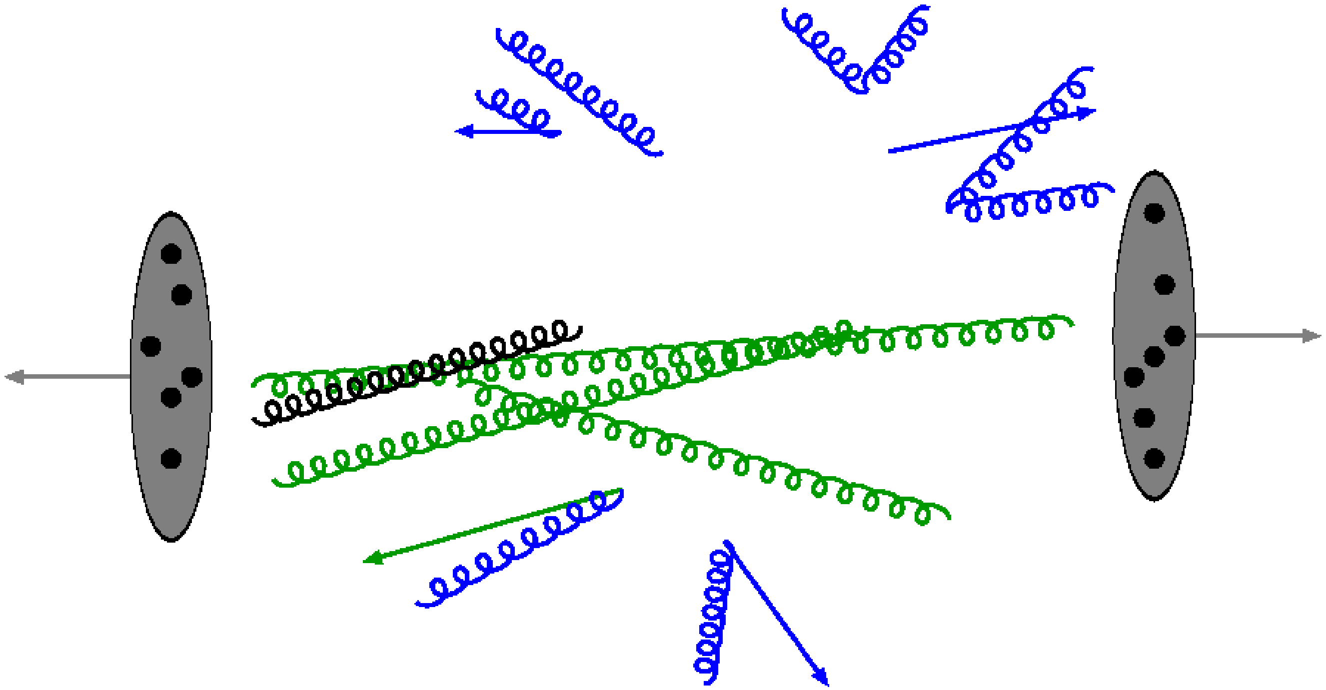

Beam remnants and other outgoing partons

Event generators: through here ...

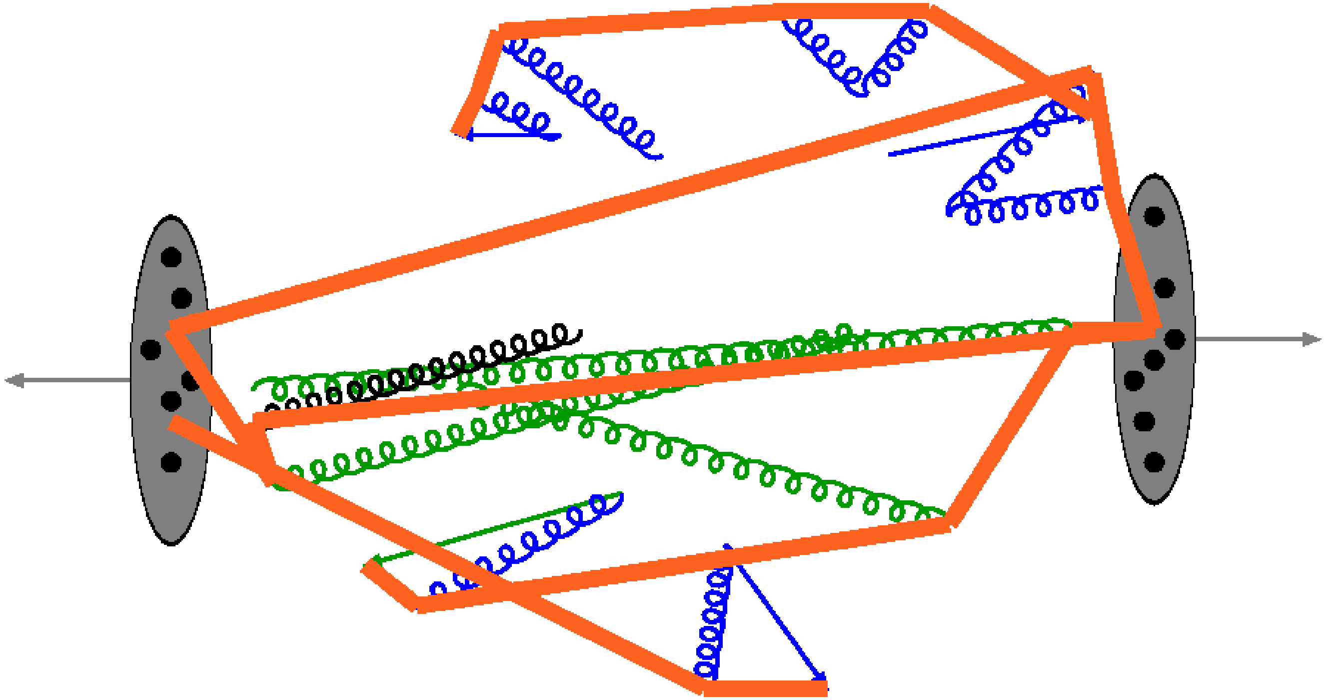

Everything is connected by colour confinement strings

Recall! Not to scale: strings are of hadronic widths

Event generators: through here ...

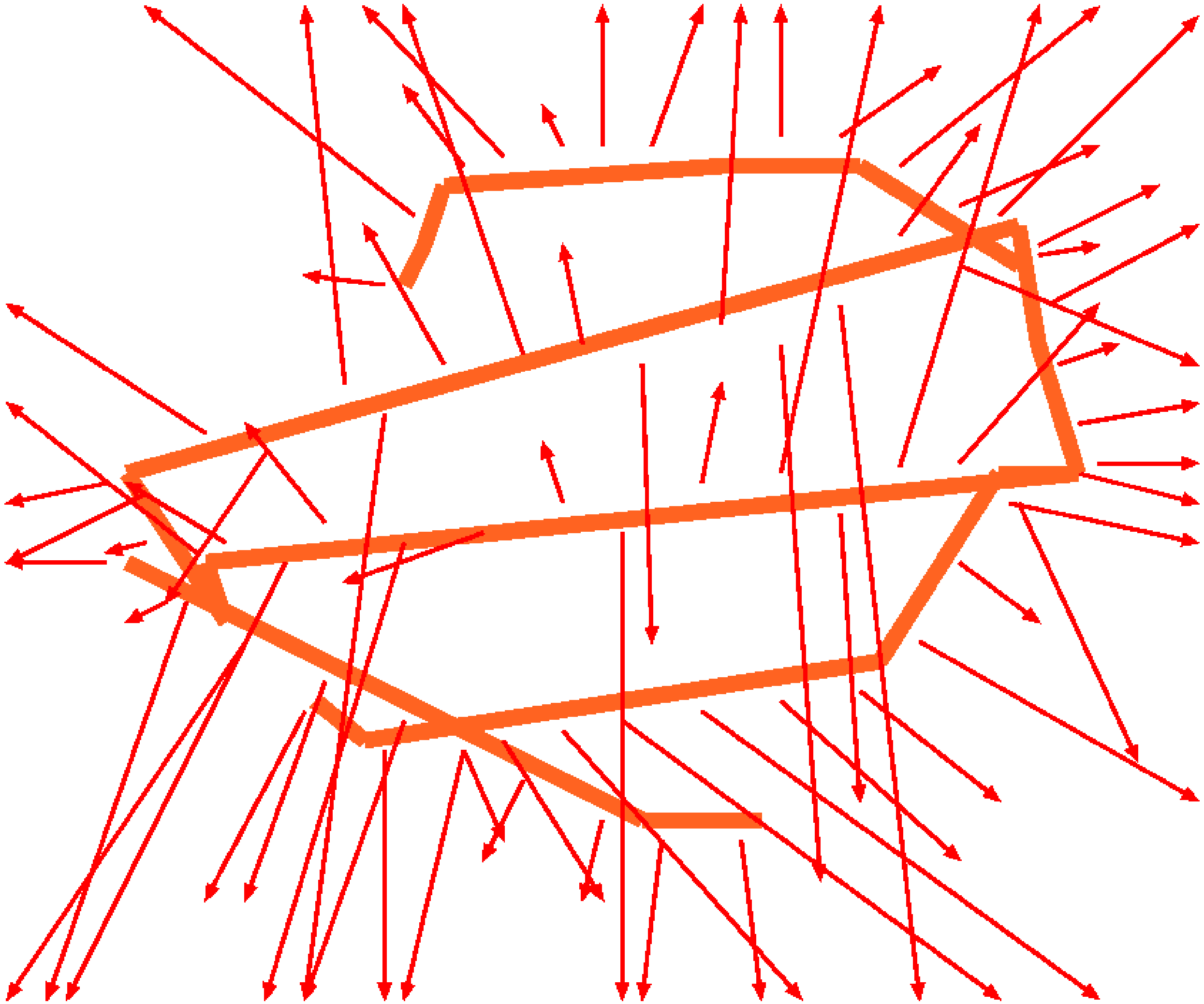

The strings fragment to produce primary hadrons

Event generators: up to here!

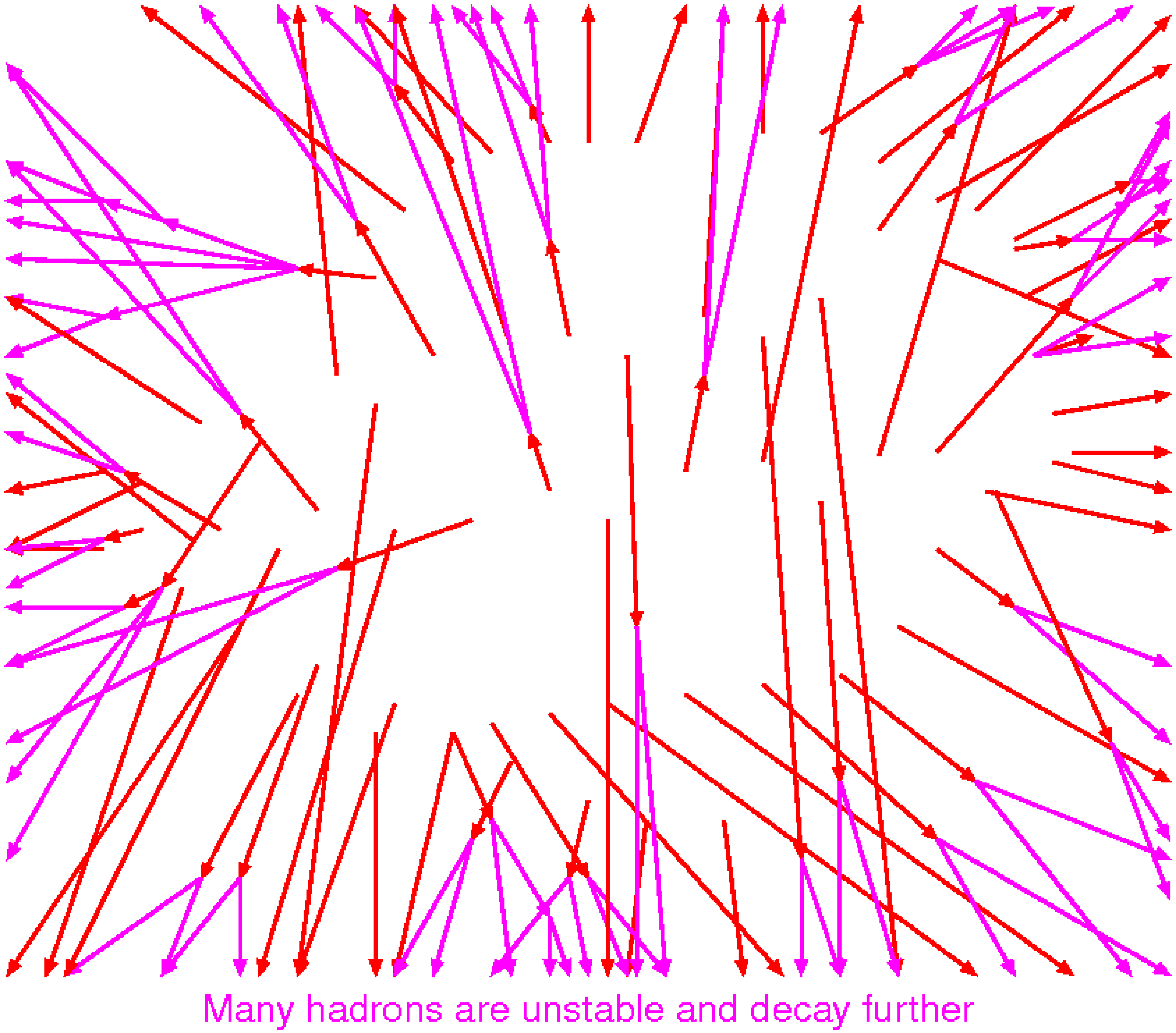

Detector simulation

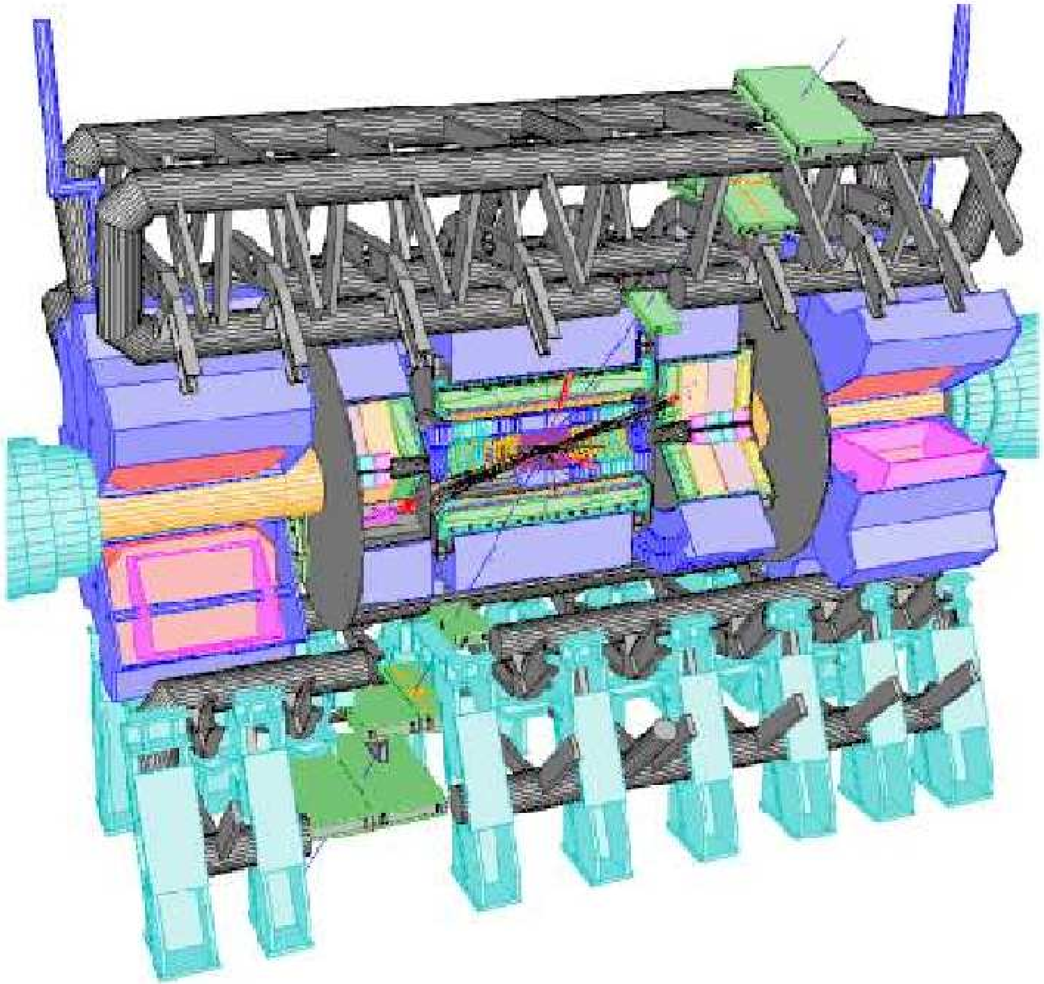

These are the particles that hit the detector

The role of event generators in the game

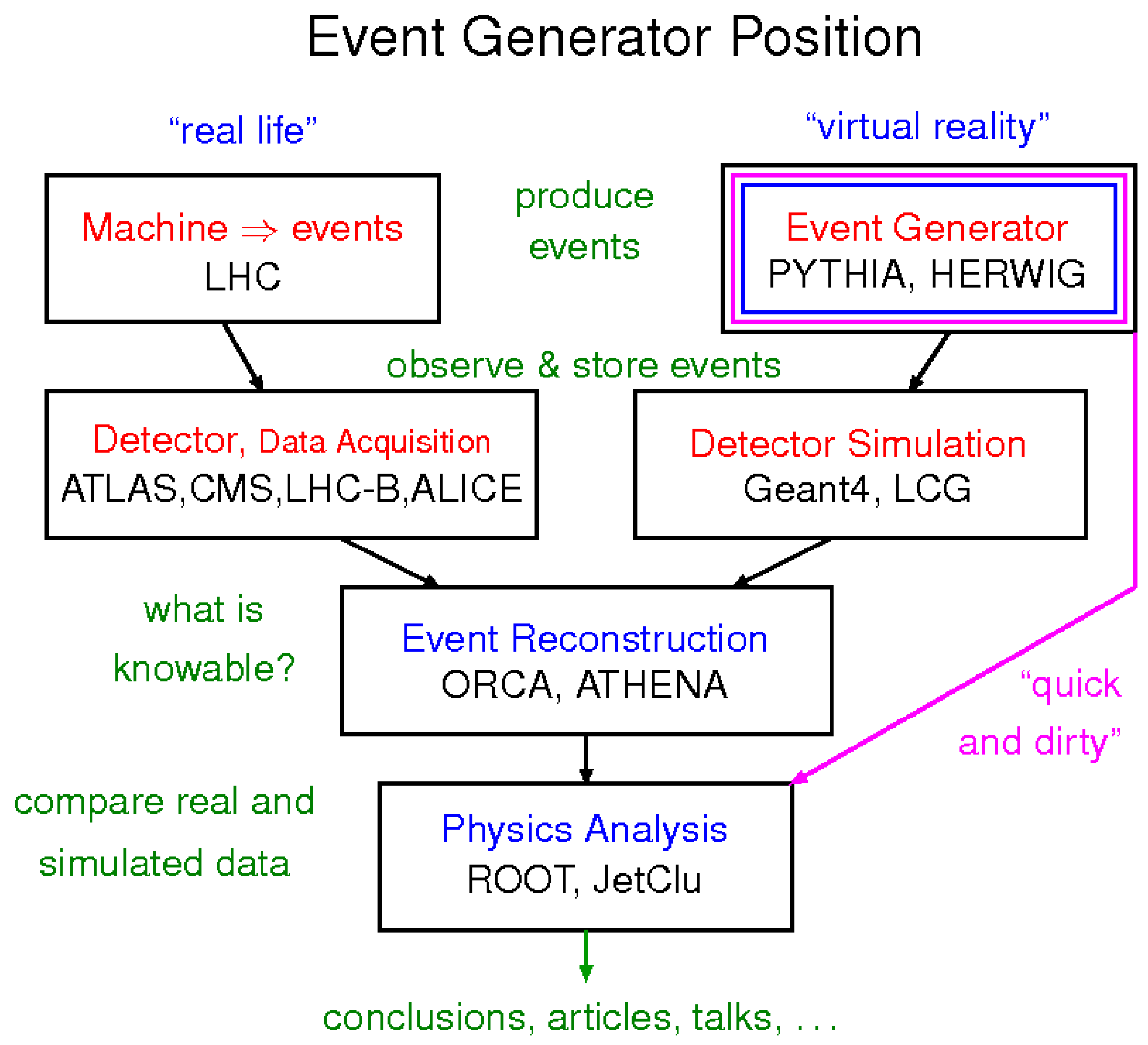

Jets of particles and partons in MC simulated events

- **Jets of particles ("truth jets"):**

→ **jet algorithm applied to the final-state particles with lifetime > 10 ps**

→ **particles from overlaid pp interactions (pile-up) excluded!**

⇒ **Used to obtain jet energy and direction corrections to topocluster-based jets; jet properties restored to "particle" level**

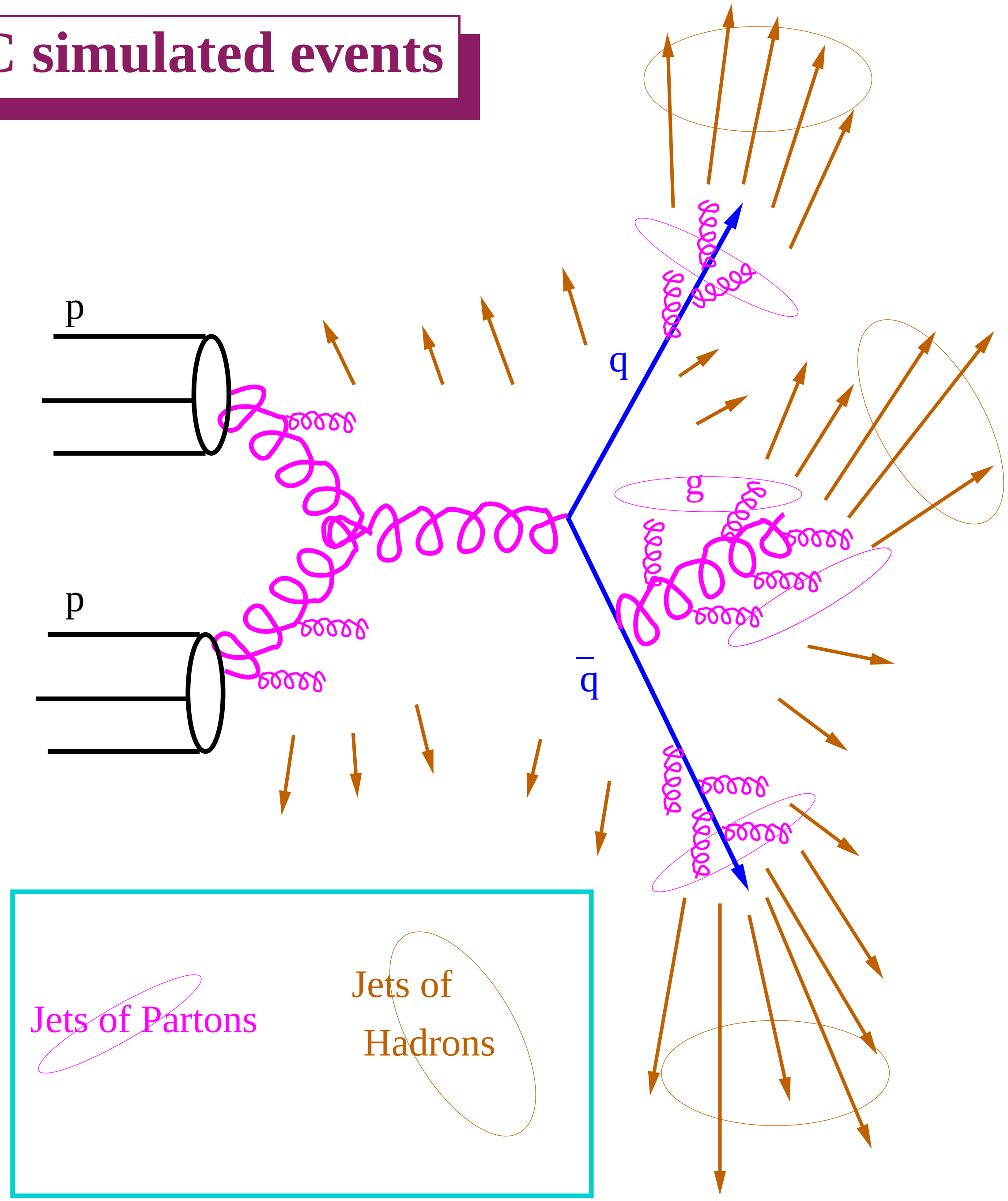

Jets of particles and partons in MC simulated events

- Jets of partons ("partonic jets"):

→ jet algorithm applied to the final-state partons (after the parton shower)

- Parton-to-hadron (hadronisation) and underlying event effects are **non-perturbative**

→ estimated with MC simulations

- Non-perturbative (NP) corrections:

$$C_{NP} = \frac{\sigma_{\rm jet}({\rm MC, particle-level, UE})}{\sigma_{\rm jet}({\rm MC, parton-level, no\ UE})}$$

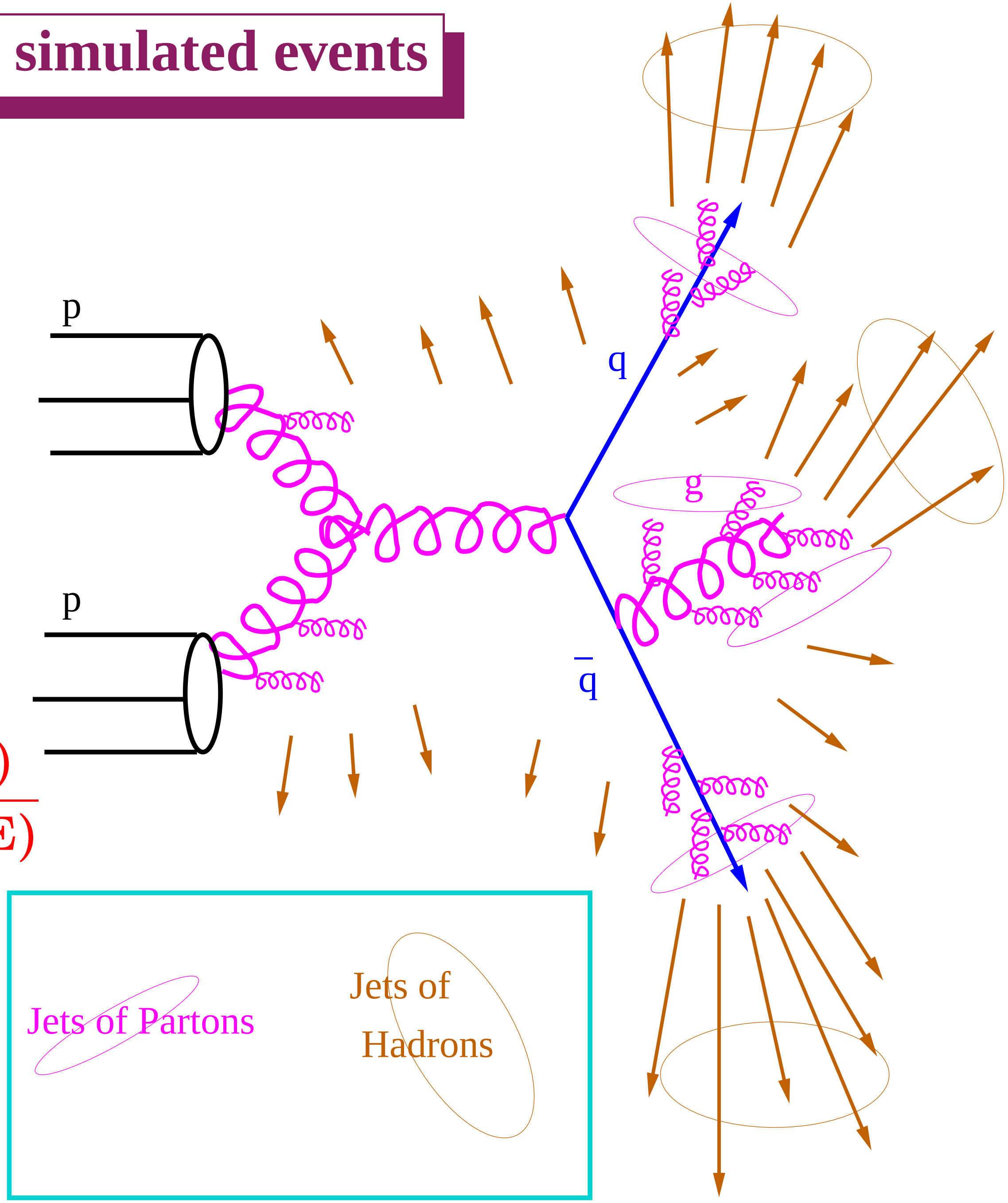

- NP corrections applied to theoretical calculations for jets of partons → so as to close the bridge between the measurements (jets of particles) and the pQCD calculations

Jet calibration in ATLAS

Jet calibration: from EM scale to "truth"

- **Topoclusters calibrated at electromagnetic (EM) scale: the EM scale correctly reconstructs the energy deposited by particles in an electromagnetic shower in the calorimeter**
  - **→ established using test-beam measurements**
  - **→ corrected in situ using $Z \to e^+e^-$ events**
- **Corrections are needed to account for:**
  - **→ calorimeter non-compensation (lower response to hadrons)**
  - **→ energy losses in inactive regions ("dead" material)**
  - **→ particles with showers not contained**
  - **→ particles clustered in the "truth" jet, but not in the topocluster-based jet**
  - **→ inefficiencies in jet clustering and jet reconstruction**
  - **→ subtraction of the contribution from pile-up**
- **Estimation of the uncertainties on the jet energy and validation with measurements in situ!**

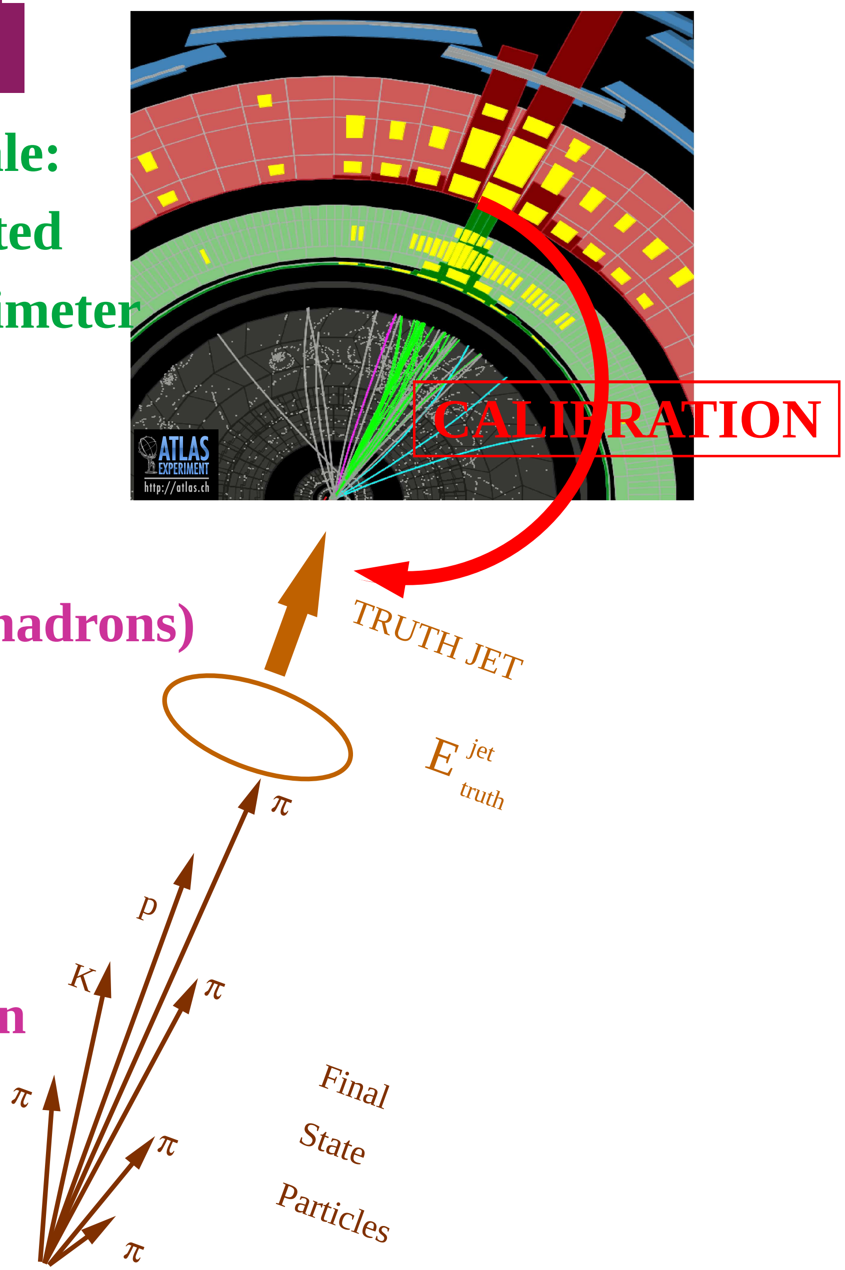

Jet calibration (EM+JES scheme)

- The (simple) EM+JES calibration scheme applies corrections as a function of the jet energy and η to jets reconstructed at the electromagnetic scale

- Three steps:

→ Pile-up correction: subtraction of energy due to overlaid proton-proton interactions

→ Vertex correction: jet direction corrected such that it originates from the primary vertex

→ Jet energy and direction correction: jet energy and direction corrected back to the jet of hadrons

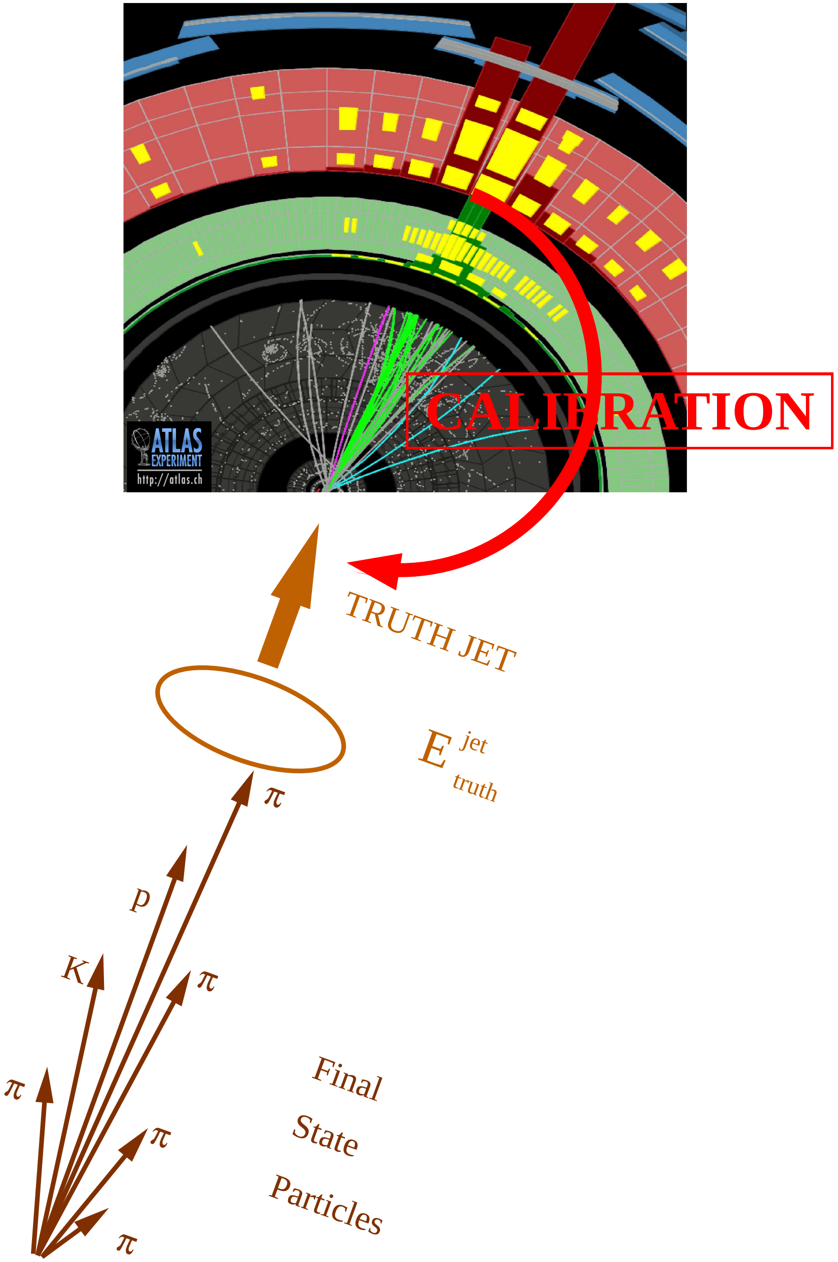

Pileup correction

- The average additional energy due to additional pp interactions is subtracted from the measured energy using correction constants obtained in situ
- Offset correction derived from minimum bias data as a function of N_{PV}, jet η and bunch spacing: $\mathcal{O}(\eta, N_{PV}, \tau_{bunch})$
  $\rightarrow$ applied to jet E_T at EM scale
  $E_T^{corr} = E_T^{uncorr} - \mathcal{O}(\eta, N_{PV}, \tau_{bunch})$

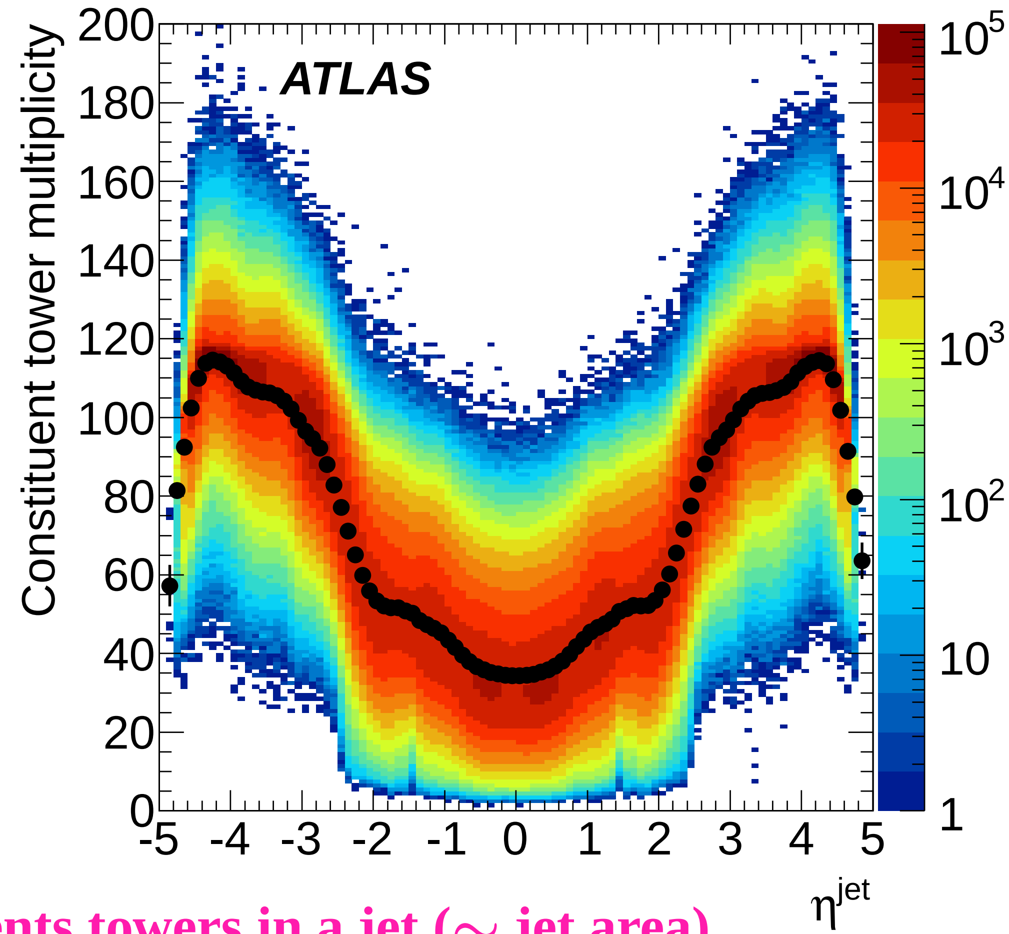

- Jet offset correction $\propto$ number of constituents towers in a jet ($\sim$ jet area)
  $\rightarrow$ equivalent number of constituent towers for jets built from topoclusters
- The multiplicity of calorimeter towers in jets depends on the internal jet composition and pileup; the average can be measured in situ $\rightarrow$ distribution of constituent tower multiplicity for jets based on towers with $p_T > 7$ GeV as a function of jet η

Pileup correction

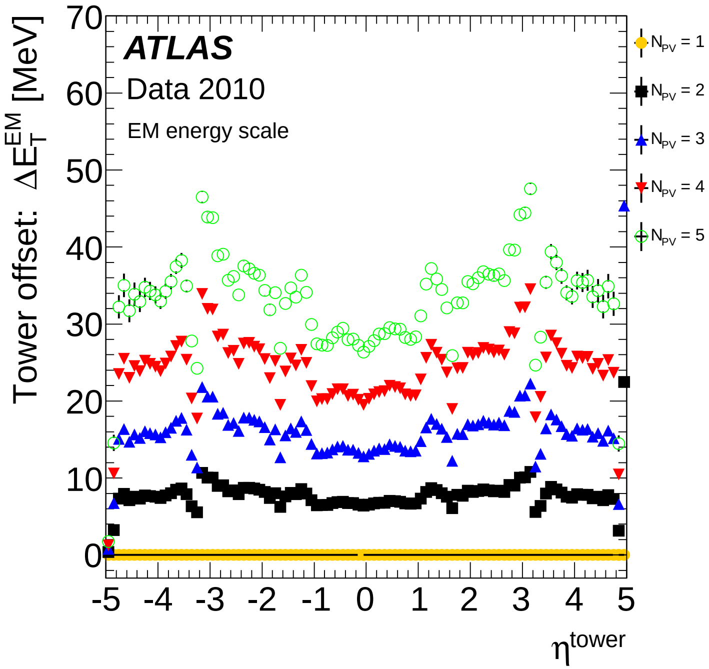

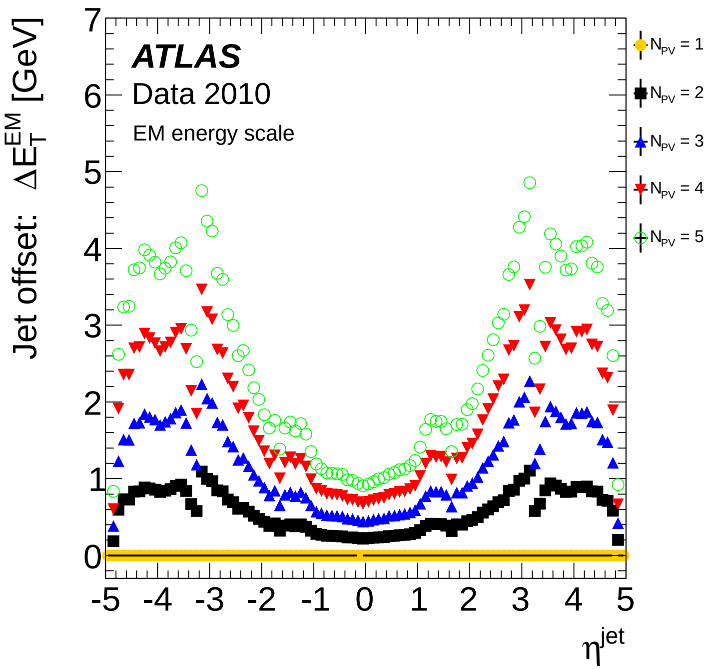

- **Calorimeter tower offset at EM scale derived by measuring the average tower E_T for all towers (non-noise suppressed) in events with $N_{PV} = 1, 2, \ldots$ and comparing with N_{PV}=1**

$$\mathcal{O}_{tower}(\eta, N_{PV}) = \langle E_T^{tower}(\eta, N_{PV})\rangle - \langle E_T^{tower}(\eta, 1)\rangle \quad \text{for each } N_{PV}$$

- **Tower off set extrapolated to an EM-scale jet offset:**

$$\mathcal{O}_{jet|tower}(\eta, N_{PV}) = \mathcal{O}_{tower}(\eta, N_{PV}) \cdot A^{jet} \quad \text{where } A^{jet}\text{=jet area}$$

→ for jets built from towers ⇒ $A^{jet} = N^{jet}_{towers}$

→ for jets built from topoclusters ⇒ A^{jet} = mean equivalent constituent tower multiplicity

Final jet energy correction

- Final step of the calibration: from the reconstructed jet energy (E^{jet}_{EM}) to the truth jet energy (E^{jet}_{EM})
  $\rightarrow$ MC simulations without pileup
- Matching reconstructed jets and truth jets ($\Delta R = 0.3$)
  $\rightarrow$ jets must be isolated; no other jet with $p_T > 7$ GeV within $\Delta R = 2.5R$
- Calibration parametrised as a function of
  $\rightarrow$ E^{jet}_{EM} and detector η
- EM-scale jet energy response: $\mathcal{R}^{jet}_{EM} = \frac{E^{jet}_{EM}}{E^{jet}_{truth}}$
  for each matched pair of calorimeter and truth jets
  $\rightarrow$ calibration $\mathcal{F}_{calib,k}(E^{jet}_{EM})$ in bin k of η_{det}
- Final JES correction:

$$E^{jet}_{EM+JES} = \frac{E^{jet}_{EM}}{\mathcal{F}_{calib,k}(E^{jet}_{EM})}$$

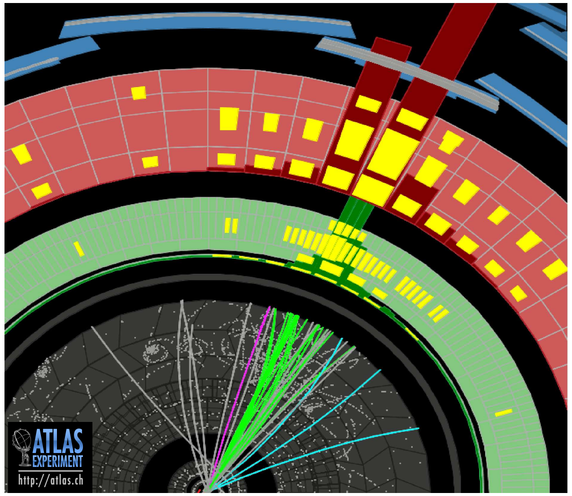

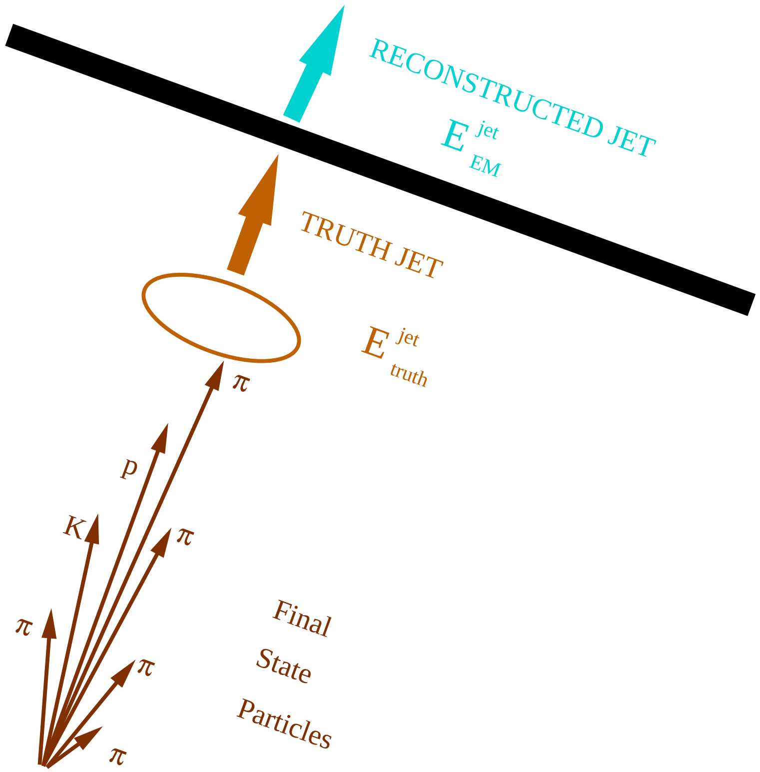

Final jet energy correction

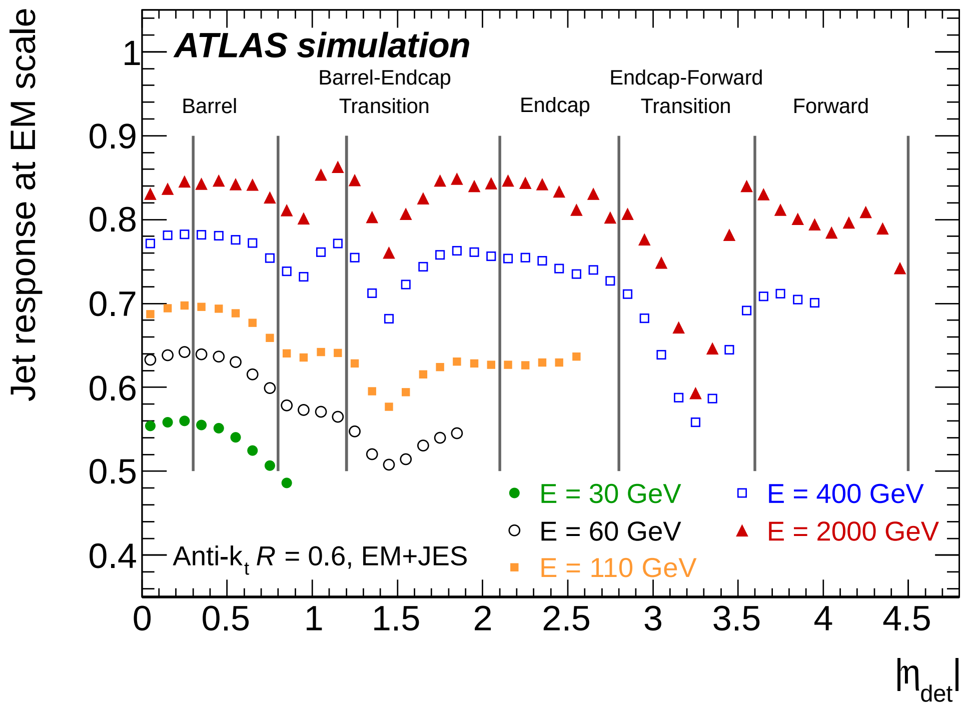

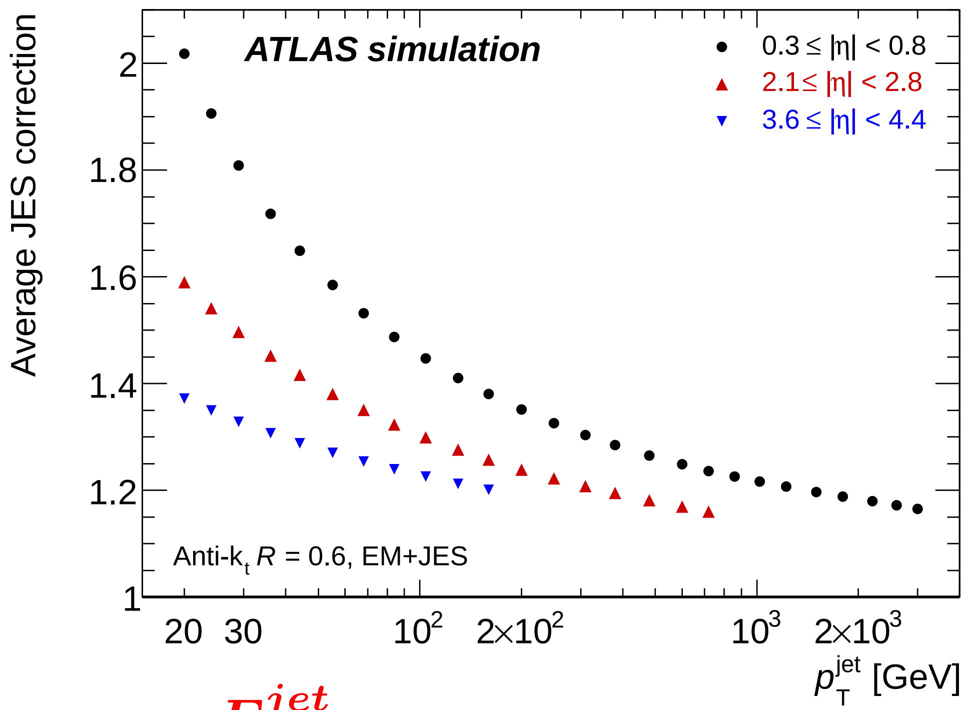

- Average EM-scale jet energy response, $\langle \mathcal{R}_{EM}^{jet} \rangle = \langle \frac{E_{EM}^{jet}}{E_{truth}^{jet}} \rangle$, as a function of η_{det}
- Average final JES correction, $\langle \frac{1}{\mathcal{F}_{calib,k}(E_{EM}^{jet})} \rangle$, as a function of calibrated jet p_T^{jet};

from about 2.1 at low jet energies in the central region

$\rightarrow$ less than 1.2 for high energy jets in the most forward region

Final jet pseudorapidity correction

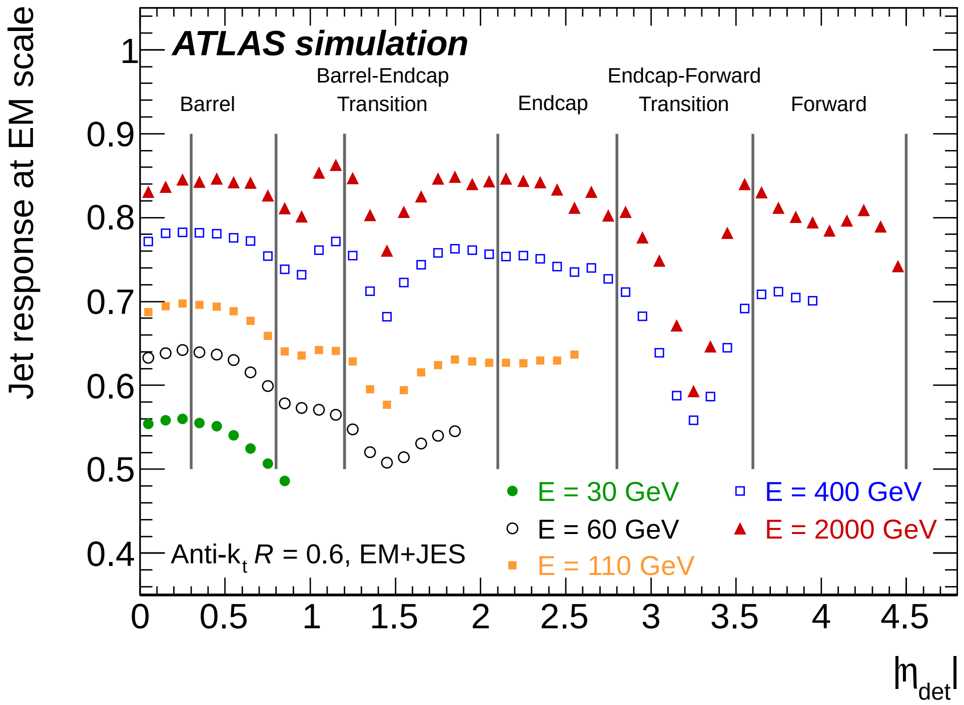

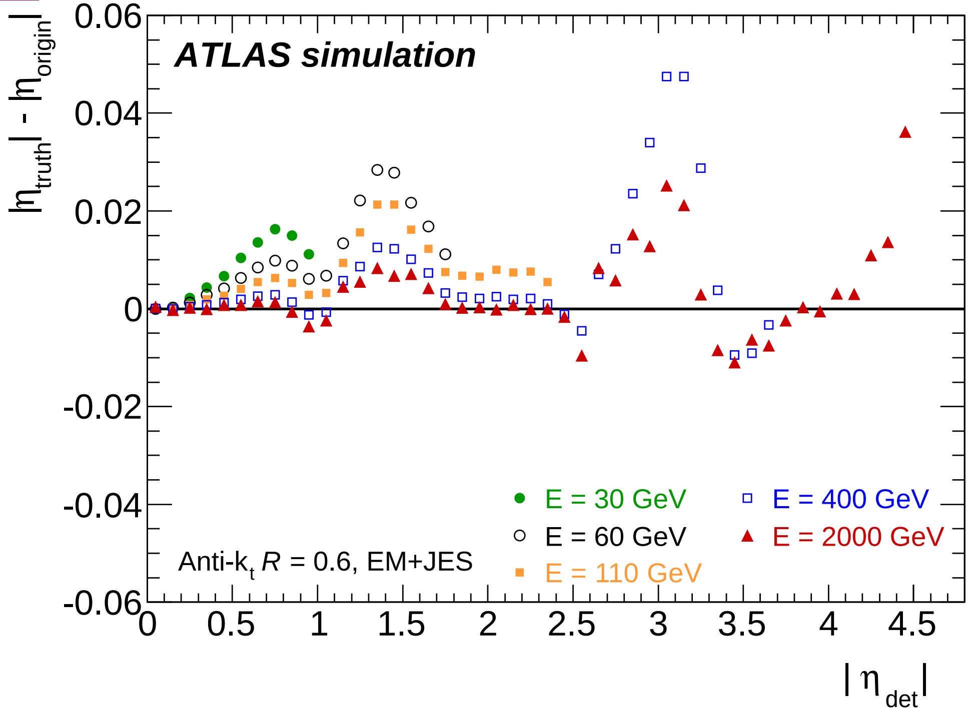

- **The origin-corrected jet η is further corrected for bias due to poorly instrumented regions $\rightarrow$ lower energy topoclusters $\rightarrow$ jet direction biased towards better instrumented regions**

- **Derivation of the η-correction from the average difference $\Delta\eta = \eta_{truth} - \eta_{origin}$ in bins of E^{jet}_{truth} and η_{det} and parametrised as a function of E^{jet}_{EM+JES} and η_{det} $\Rightarrow$ very small correction ($\Delta\eta < 0.01$) except in transition regions**

Jet energy scale uncertainty

Uncertainty on the Jet Energy Scale

$\Rightarrow$ **Dominant systematic uncertainty for jets!**

- Estimated by combining information from data and MC simulations

$\rightarrow$ single-hadron response measured in situ

$\rightarrow$ single-pion test-beam measurements

$\rightarrow$ uncertainties on amount of detector material

$\rightarrow$ description of electronic noise

$\rightarrow$ MC model used in the event generation

- JES uncertainty for all jets with $|\eta| > 0.8$ determined relative to the central barrel region $0.3 < |\eta| < 0.8$ (very well known!) plus a contribution from intercalibration
  - $\rightarrow$ by using dijet balance between a non-central jet and a central jet (in the same event)

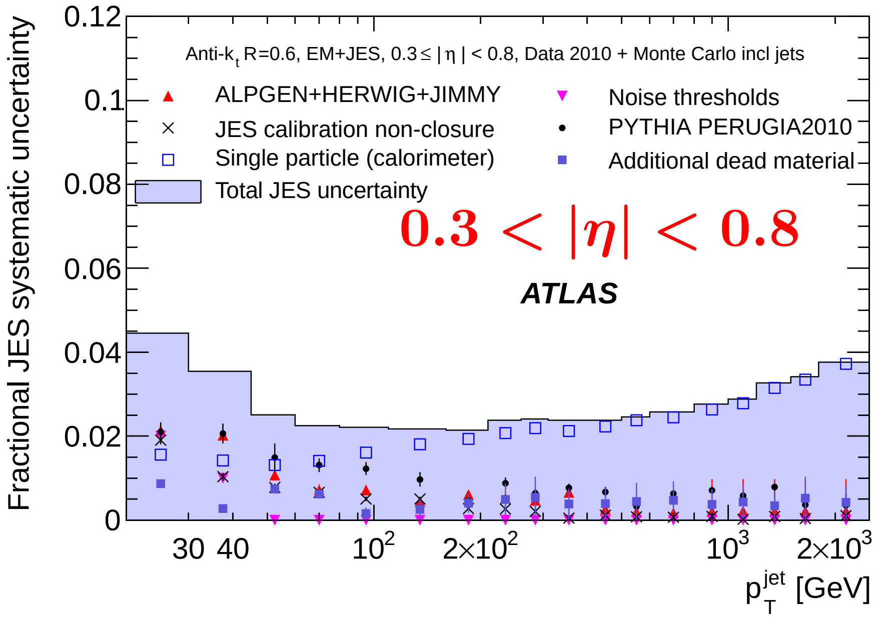

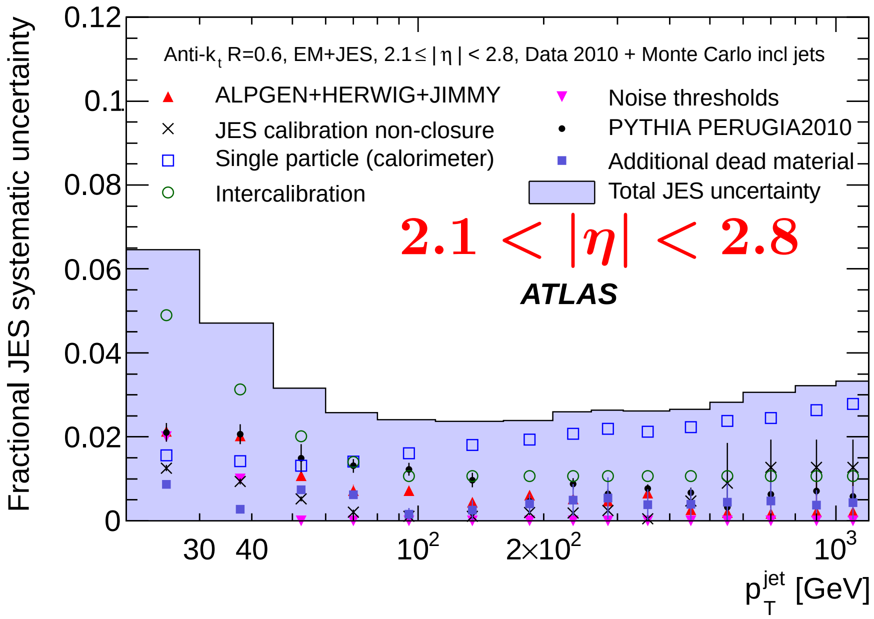

Single hadron response

- The response (+uncertainties) for single particles interacting in the ATLAS calorimeters is used to derive the jet energy scale uncertainty (central region)

$\rightarrow$ in-situ measurements of E/p for single particles

$\rightarrow$ pion response measurements in combined test-beam (pion beams between 20 and 350 GeV)

$\Rightarrow$ Significant reduction of the uncertainty

- Additional uncertainties:

$\rightarrow$ Calorimeter acceptance for low p_T particles

$\rightarrow$ Calorimeter response to particles $p_T > 400$ GeV

$\rightarrow$ Baseline absolute EM scale for particles in the kinematic range not measured in situ

$\rightarrow$ Calorimeter response to neutral hadrons

$\Rightarrow$ In the central region ($|\eta| < 0.8$), the JES uncertainty due to that on hadron response is 1.5-4%

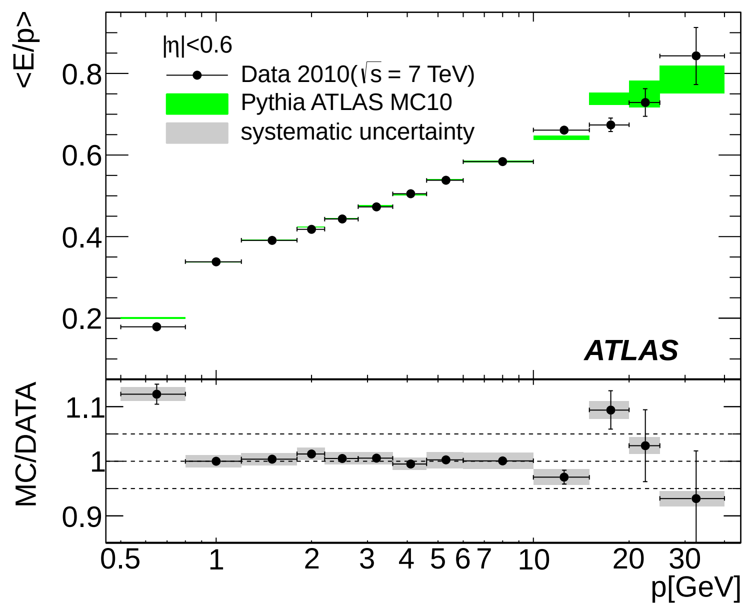

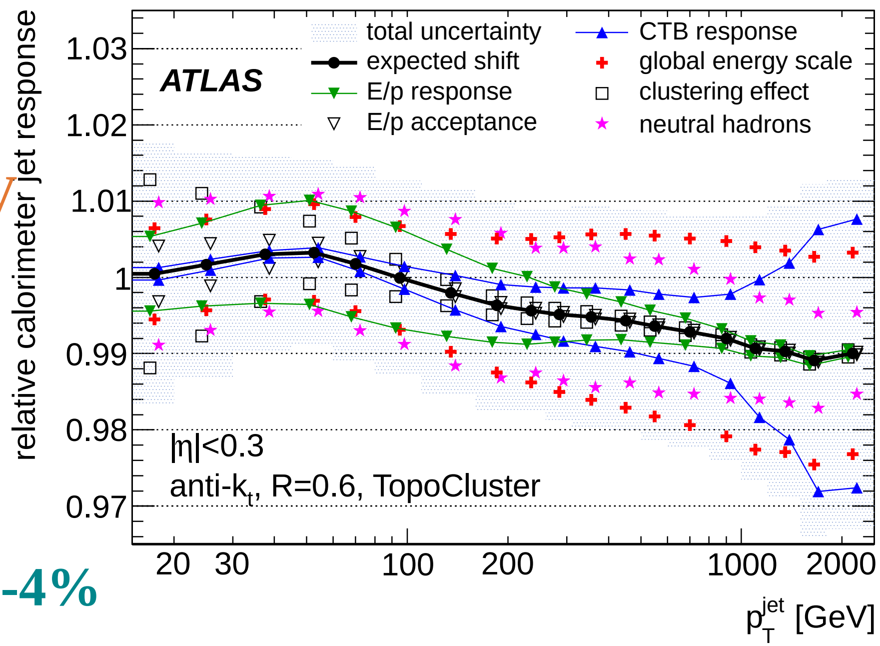

Uncertainty on the Jet Energy Scale

- Uncertainty on jet calibration method:

→ deviations from unity (non-closure) after application of the calibration to the jets in MC

→ due to approximations, same correction applied to E and p_T (jet mass!), jet resolution, etc

⇒ 2% at low p_T and $< 1\%$ for $p_T > 30$ GeV in the central region

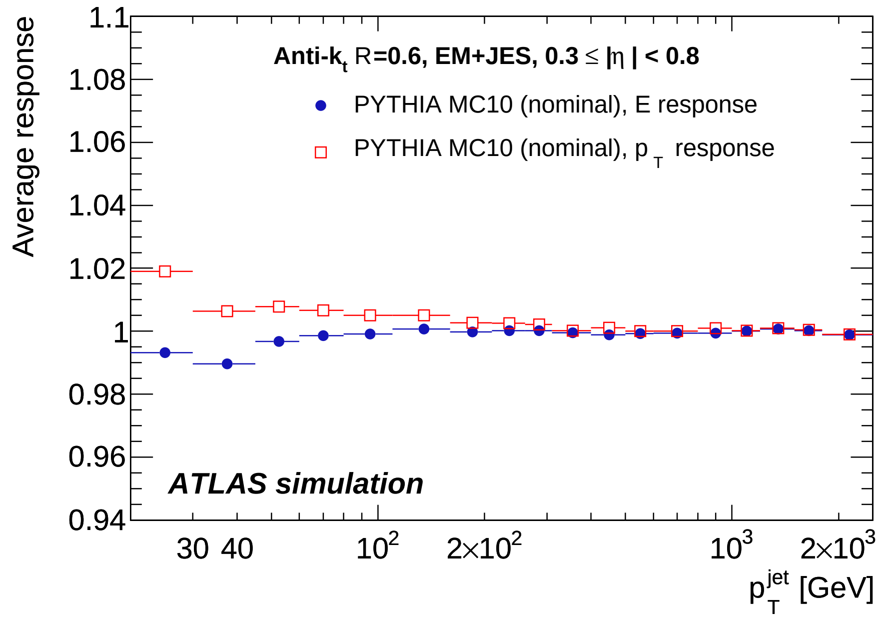

- Uncertainties due to MC models: hadronisation, underlying event and other approximations in event modelling

→ comparison with PYTHIA Perugia2010 tune to account for soft-physics modelling

→ comparison with ALPGEN+HERWIG+JIMMY, which uses different models for all steps

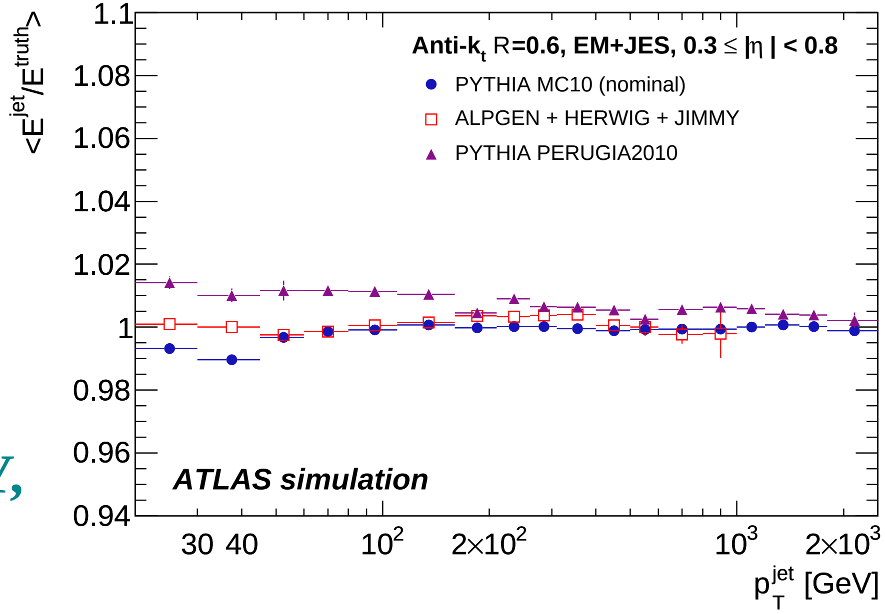

In situ η-intercalibration with dijets

- Response of ATLAS calorimeters to jets depends on jet direction (different technologies, amount of dead material)

$\rightarrow$ η-intercalibration needed to ensure a uniform calorimeter response to jets

$\rightarrow$ achieved by applying corrections derived from MC simulations to be validated with data

- Relative jet calorimeter response and its uncertainty studied by comparing the transverse momenta of a well calibrated central jet and a jet in the forward region in events with only two jets at high p_T (dijets) $\Rightarrow$ p_T balance
- Asymmetry: $\mathcal{A} = (p_T^{probe} - p_T^{ref})/p_T^{avg}$ in bins of η^{probe} and p_T^{avg} ($|\eta^{ref}| < 0.8$)

Intercalib. factors $c_{ik} = (2 - \langle A_{ik} \rangle)/(2 + \langle A_{ik} \rangle)$

Relative response $p_T^{probe}/p_T^{ref} = 1/c$

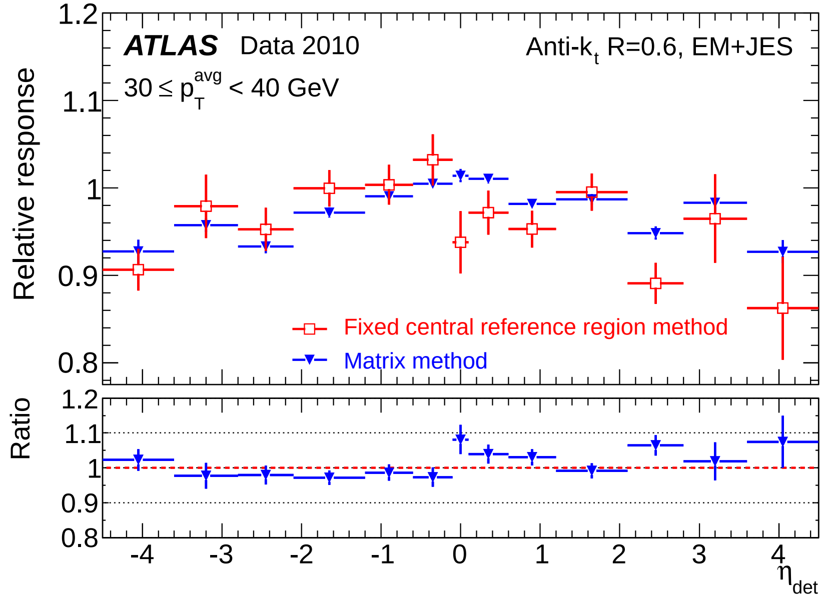

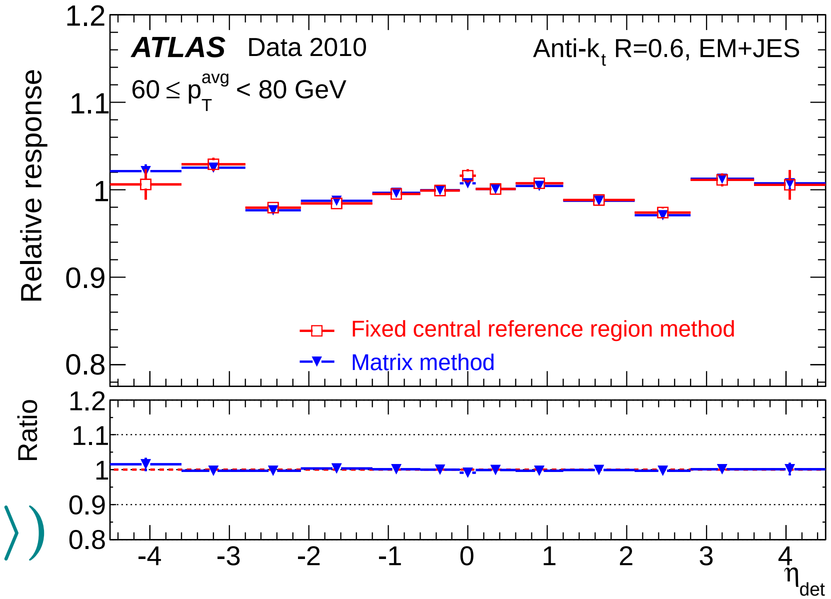

In situ η-intercalibration with dijets

- Selection of dijet events

$\rightarrow$ at least two jets with $p_T^{jet} > 7$ GeV

$\rightarrow p_T^{avg} > 20$ GeV and $\Delta\phi(j_1, j_2) > 2.6$ rad

$\rightarrow p_T(j_3) < \max(0.15 p_T^{avg}, 7\text{ GeV})$

- Lowest p_T^{avg}-bins expected to be biased

$\rightarrow$ failure of assumption of dijet balance due to residual low-p_T jet effects

- Comparison of relative jet responses using this method and a matrix method (higher statistics)

$\rightarrow$ compatible results

[matrix method used to obtain final uncertainty on the in situ η-intercalibration due to its higher statistical precision]

Relative response $p_T^{probe}/p_T^{ref} = 1/c$

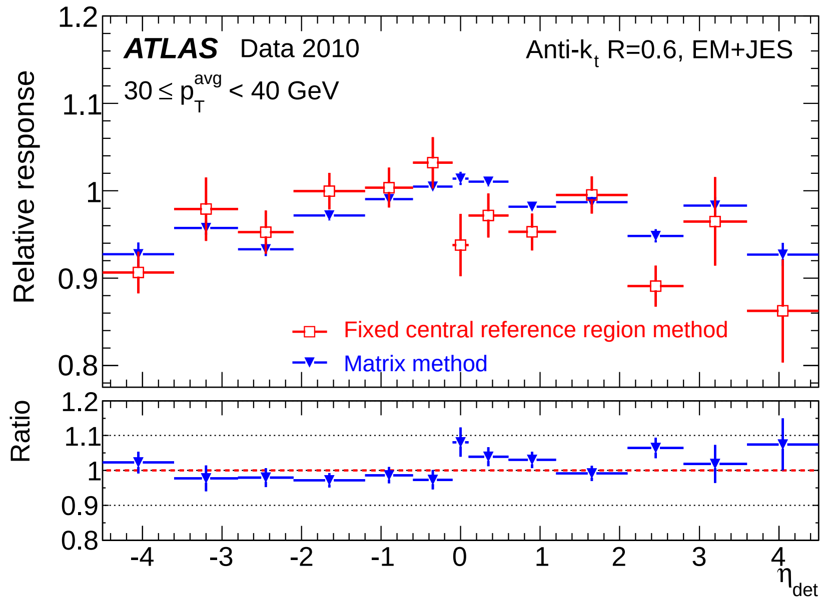

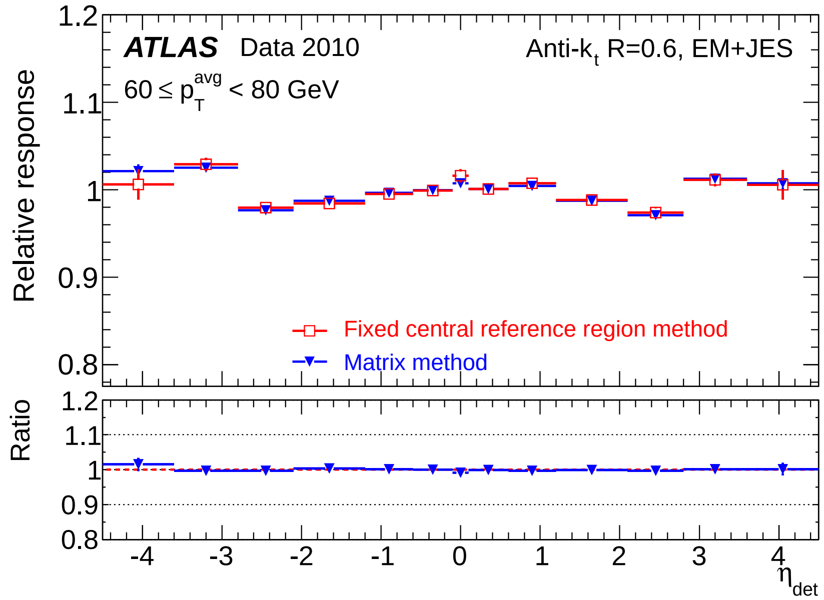

η-intercalibration with dijets: data vs MC

- Comparison of relative response between data and several MCs (PYTHIA MC10 and Perugia2010, HERWIG++, ALPGEN)

$\rightarrow$ normalization: average relative response in $|\eta| < 0.8$ equals unity (for data and MC)

- Good description of the data by MC for $p_T > 60$ GeV; at lower $p_T \rightarrow$ differences between data and MC, and different MCs (large spread)

- Uncertainty on relative response: RMS deviation of the MC predictions from the data

$\rightarrow$ at high p_T, small spread, reflection of the true difference between the response in data and sim.

$\rightarrow$ at low p_T and large η, physics modelling

Relative response $p_T^{probe}/p_T^{ref} = 1/c$

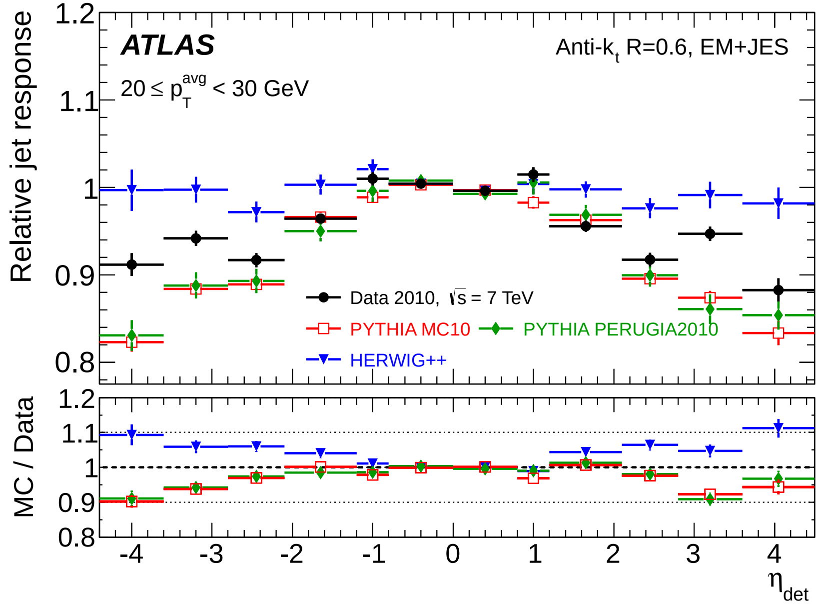

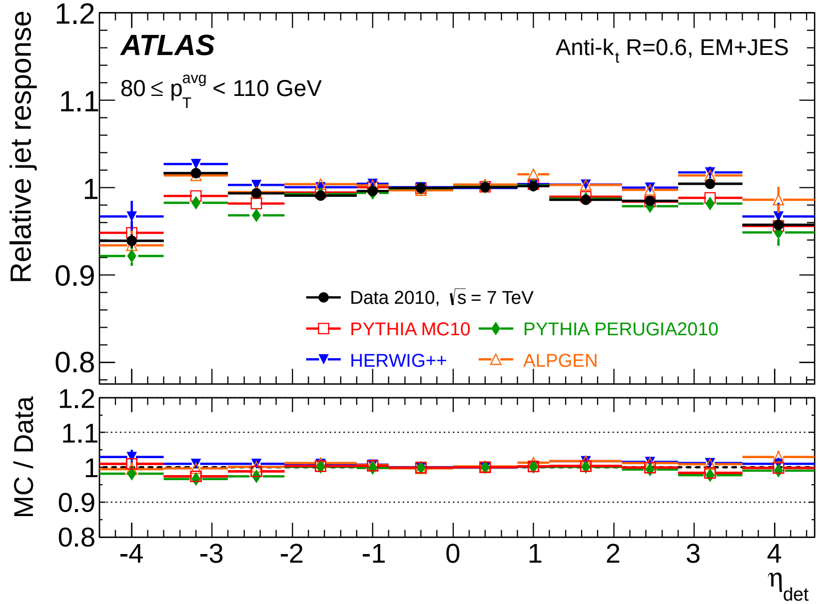

Jet Energy Scale uncertainty for non-central jets

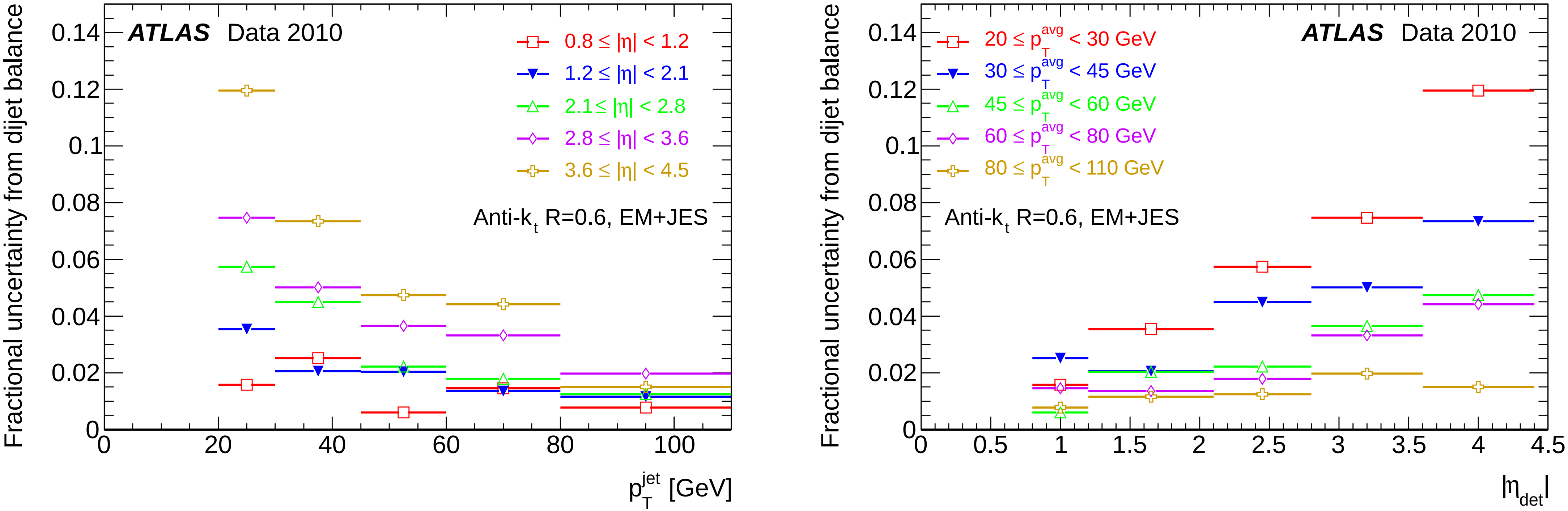

- **Uncertainty in the jet response relative to jets in the central region $|\eta| < 0.8$ as a function of p_T and $|\eta|$**
- **Final uncertainty: total JES uncertainty in the central region $0.3 < |\eta| < 0.8$ as a baseline plus uncertainty from the relative intercalibration (RMS deviation of MC from data)**

Summary of Jet Energy Scale systematic uncertainties

$0.3 < |\eta| < 0.8$

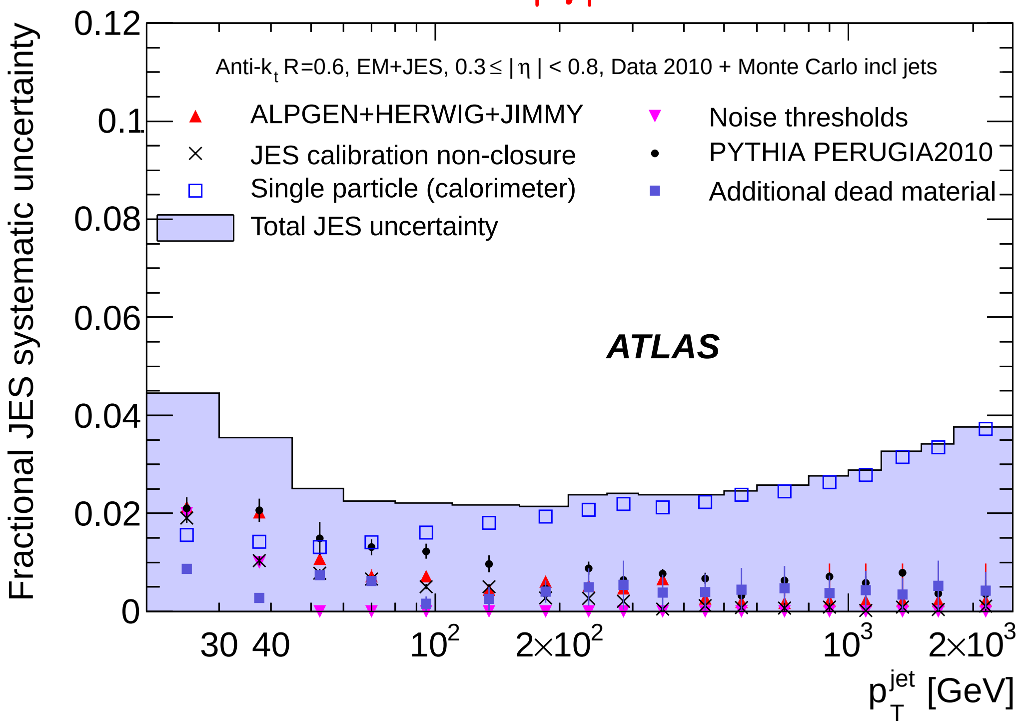

$2.1 < |\eta| < 2.8$

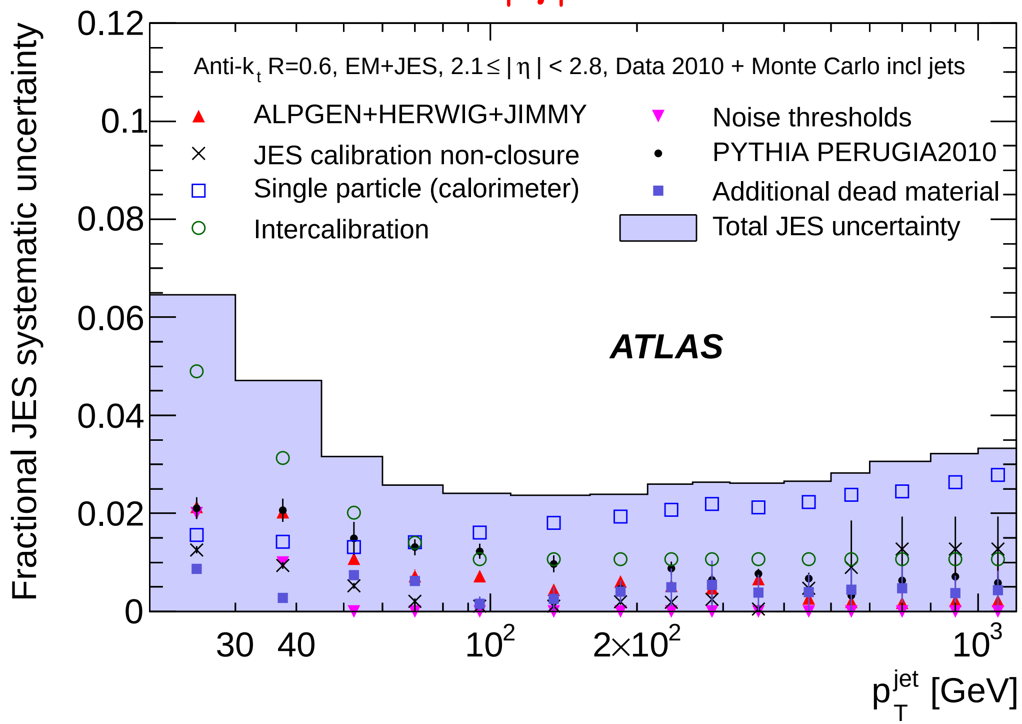

- **Fractional JES uncertainty in the central region: 2-4% for $p_T < 60$ GeV and 2-2.5% for $60 < p_T < 800$ GeV; 2.5-4% for $p_T > 800$ GeV**
- **Fractional JES uncertainty in the endcap region: up to 7% for $p_T < 60$ GeV and up to 3% for $p_T > 60$ GeV**
- **Study repeated with $R = 0.4$, leading to similar results**

In situ validation of Jet Energy Scale uncertainties

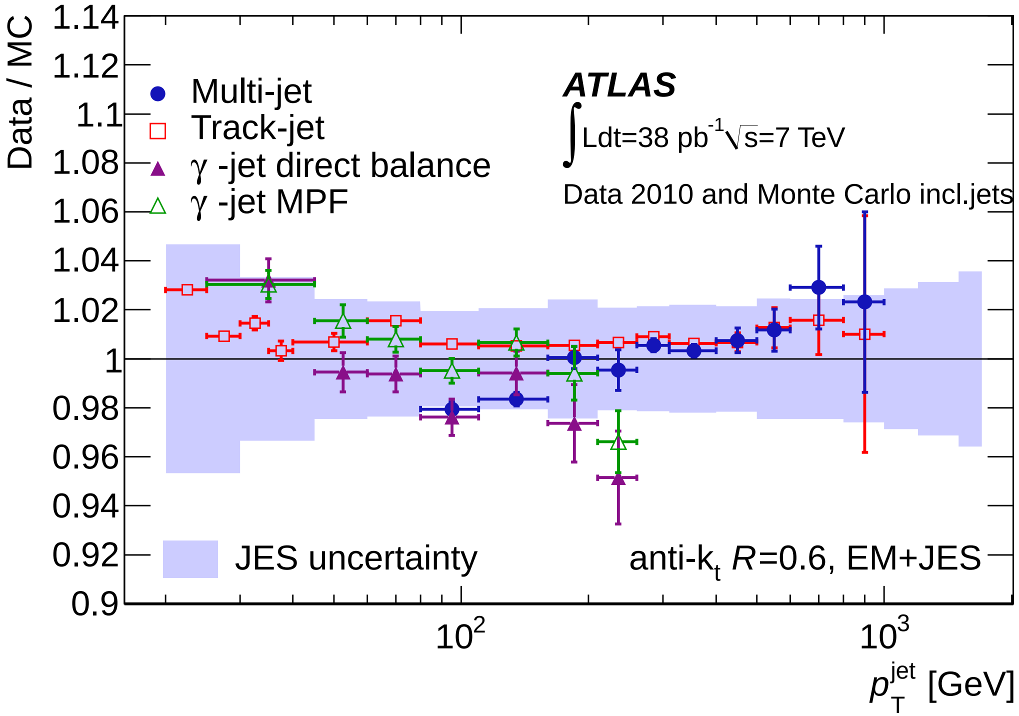

- Test of the jet energy calibration using a well-calibrated object
  - → comparison to the momentum carried by tracks associated to a jet
  - → direct p_T balance between a photon and a jet
  - → photon p_T balance to hadronic recoil
  - → balance between a high-p_T jet and a system of low-p_T jets

- All methods applied to data and MC simulations ⇒ double ratios!
- The techniques rely on assumptions that are only approx. fulfilled: e.g. perfect balance → affected by the presence of additional high-p_T particles → need to disentangle physics and detector effects → variations of the event selection criteria → systematic uncertainties
- Double Ratio of p_T^{jet} over reference p_T in data and MC

  ⇒ support the estimate of the Jet Energy Scale uncertainty

Example: multijet balance technique

- Useful to assess the jet calibration in the TeV region
- Study of $MJB = |\vec{p}_T^{\,leading}|/|\vec{p}_T^{\,recoil}|$
  MJB expected to be 1; close-by jets, soft-gluon emission, pile-up, selection criteria $\rightarrow$ bias
- Double ratio $r = [MJB]_{data}/[MJB]_{MC}$
- Event selection: at least three jets with $p_T > 20$ GeV and $|y| < 2.8$
  $\rightarrow \beta > 1$ rad (no jets within $|\Delta\phi| = 1$ rad around leading jet
  $\rightarrow \alpha = |\Delta\phi - \pi| < 0.3$ rad
  $\rightarrow p_T^{recoil} > 80$ GeV
  $\rightarrow p_T^{Jet2}/p_T^{recoil} < 0.6$ to ensure leading jet at a higher scale than the non-leading jets

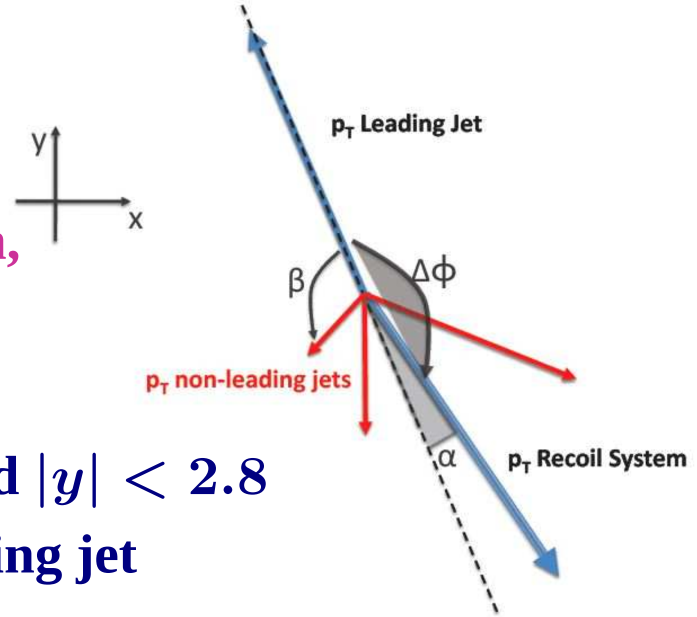

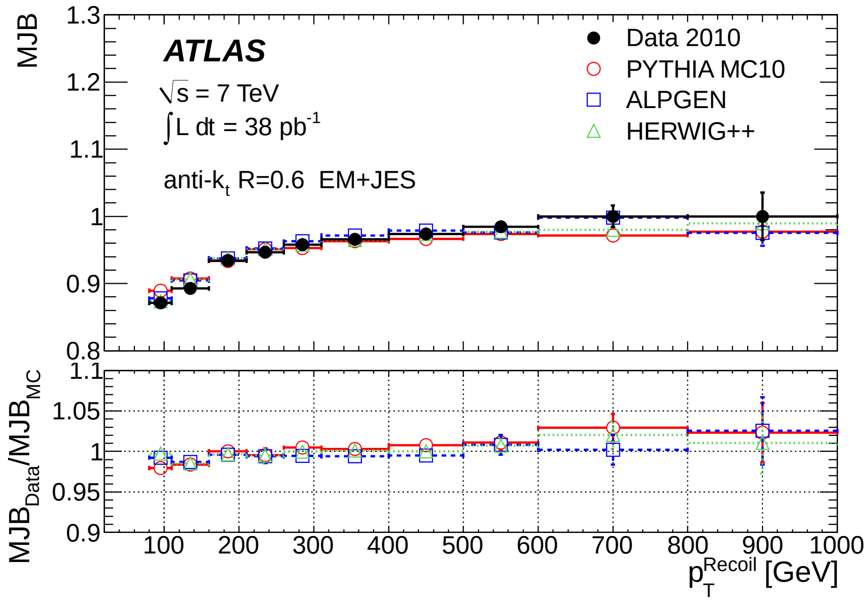

- MJB study from 80 GeV up to 1 TeV

$\Rightarrow$ the average value of data to MC ratio is within 3%

Example: multijet balance technique

- Useful to assess the jet calibration in the TeV region
- Study of $MJB = |\vec{p}_T^{\,leading}|/|\vec{p}_T^{\,recoil}|$
  MJB expected to be 1; close-by jets, soft-gluon emission, pile-up, selection criteria $\rightarrow$ bias
- Double ratio $r = [MJB]_{data}/[MJB]_{MC}$
- Event selection: at least three jets with $p_T > 20$ GeV and $|y| < 2.8$
  $\rightarrow \beta > 1$ rad (no jets within $|\Delta\phi| = 1$ rad around leading jet
  $\rightarrow \alpha = |\Delta\phi - \pi| < 0.3$ rad
  $\rightarrow p_T^{recoil} > 80$ GeV
  $\rightarrow p_T^{Jet2}/p_T^{recoil} < 0.6$ to ensure leading jet at a higher scale than the non-leading jets

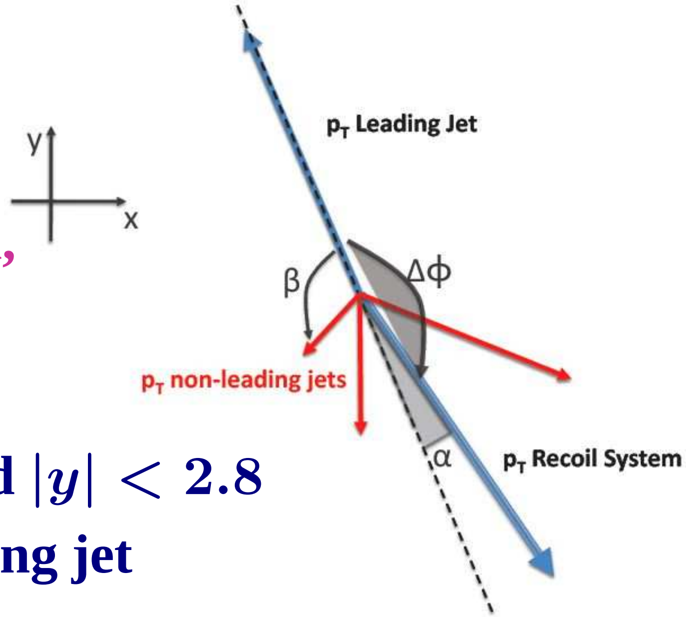

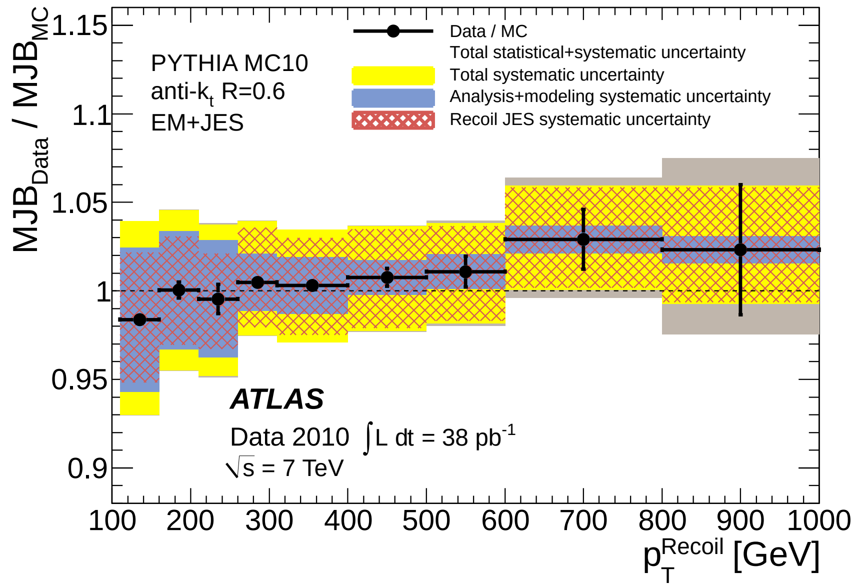

- Taking into account systematic uncertainties

$\Rightarrow$ validation of the high-p_T jet energy scale to within 5% up to 1 TeV

First measurements of jet production at the LHC

Jet production in pp collisions

- In pp collisions, jet production is the dominant high-p_T process

- First glimpse at the TeV scale

- Measuremens of jet production allow

$\rightarrow$ tests of perturbative QCD

$\rightarrow$ determination of α_s

$\rightarrow$ experimental information on PDFs

- Understanding jet production for the benefit of other measurements and searches for new particles or interactions

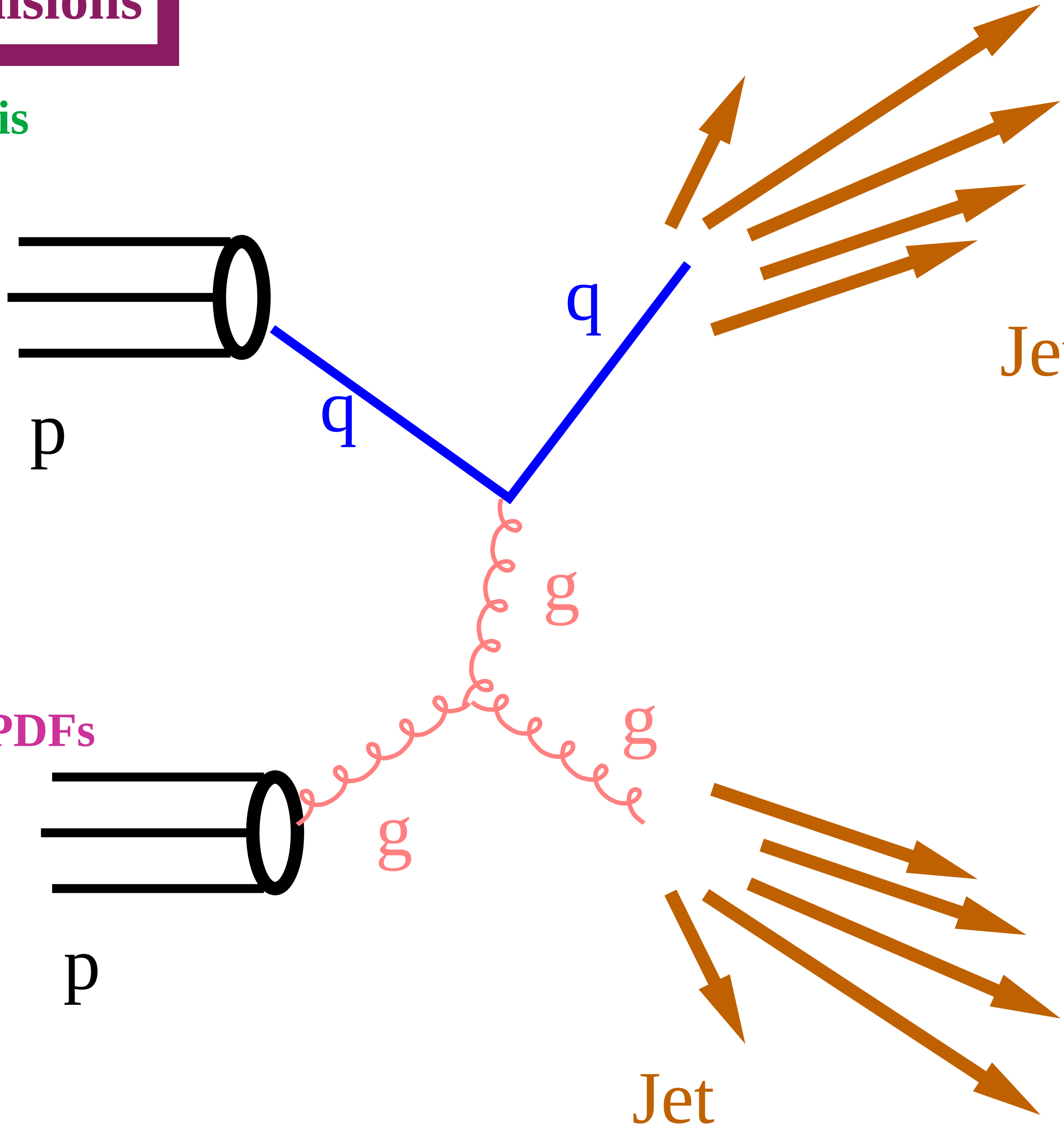

NLO pQCD calculations of jet production in pp collisions

• Comparison of measurements of jet production (corrected to the "particle level") and

→ QCD predictions at fixed-order in perturbation theory corrected for NP effects

→ model predictions of Monte Carlo models (at particle level) with different levels of sophistication: 2 → 2 LO matrix elements (ME) plus parton showers (PS) as PYTHIA and HERWIG, 2 → n LO ME + PS as SHERPA and ALPGEN, NLO ME+PS as POWHEG, ...

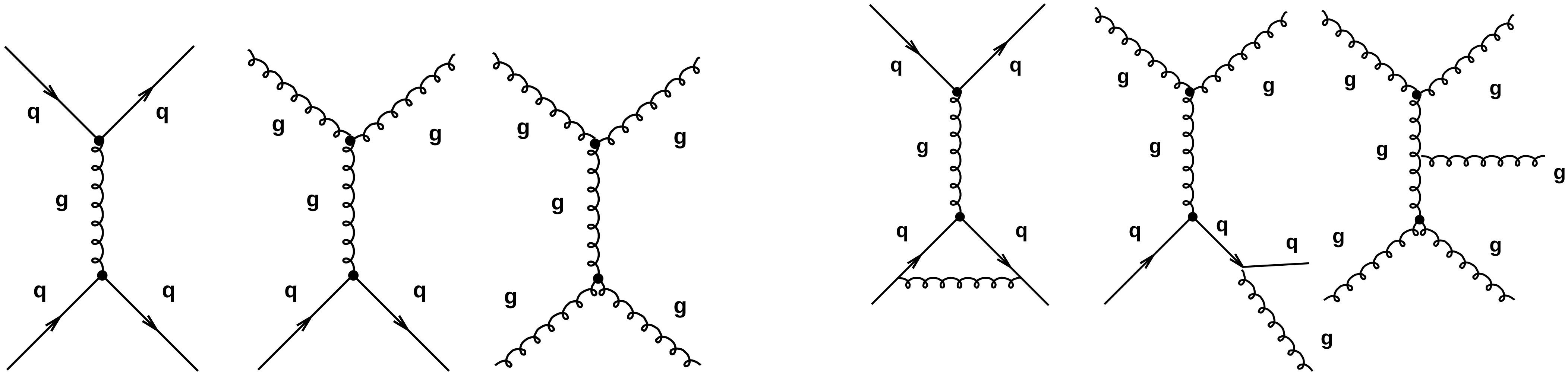

$$\sigma_{pp\to jet+X} = \sum_{i,j,a,b} \int_0^1 dx_1\, f_{i/p}(x_1,\mu_F^2) \int_0^1 dx_2\, f_{j/p}(x_2,\mu_F^2)\ \hat{\sigma}_{ij\to ab}$$

First measurements of jet production in pp collisions at $\sqrt{s} = 7$ TeV

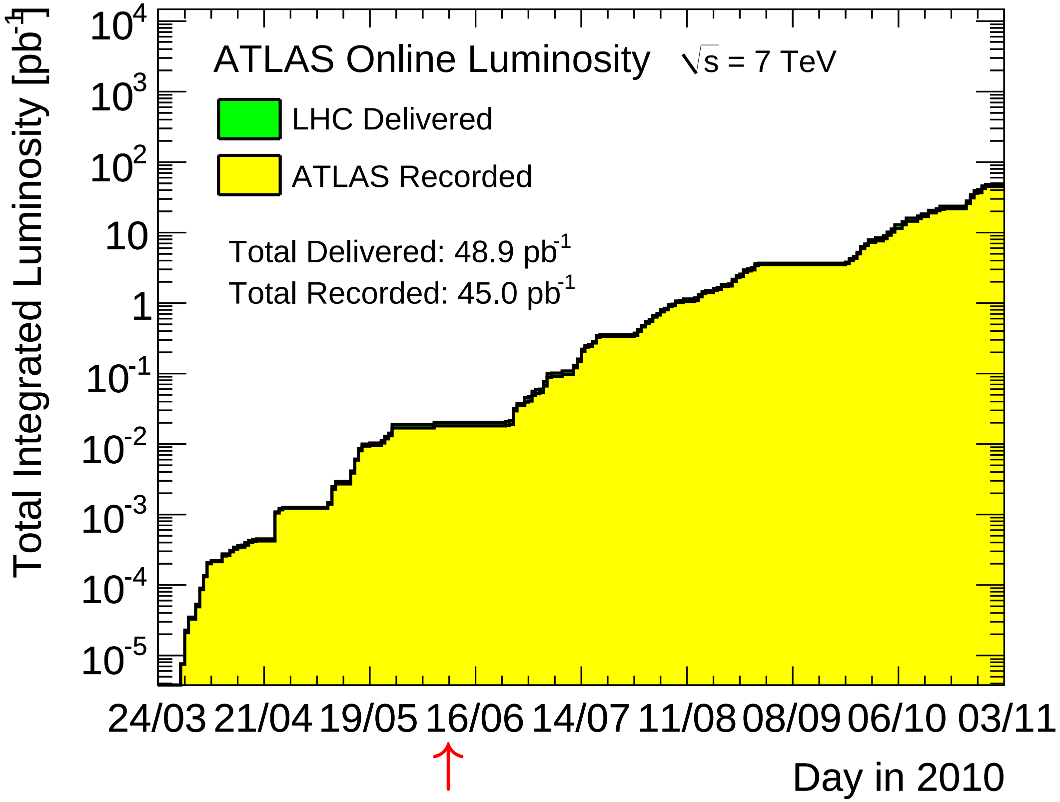

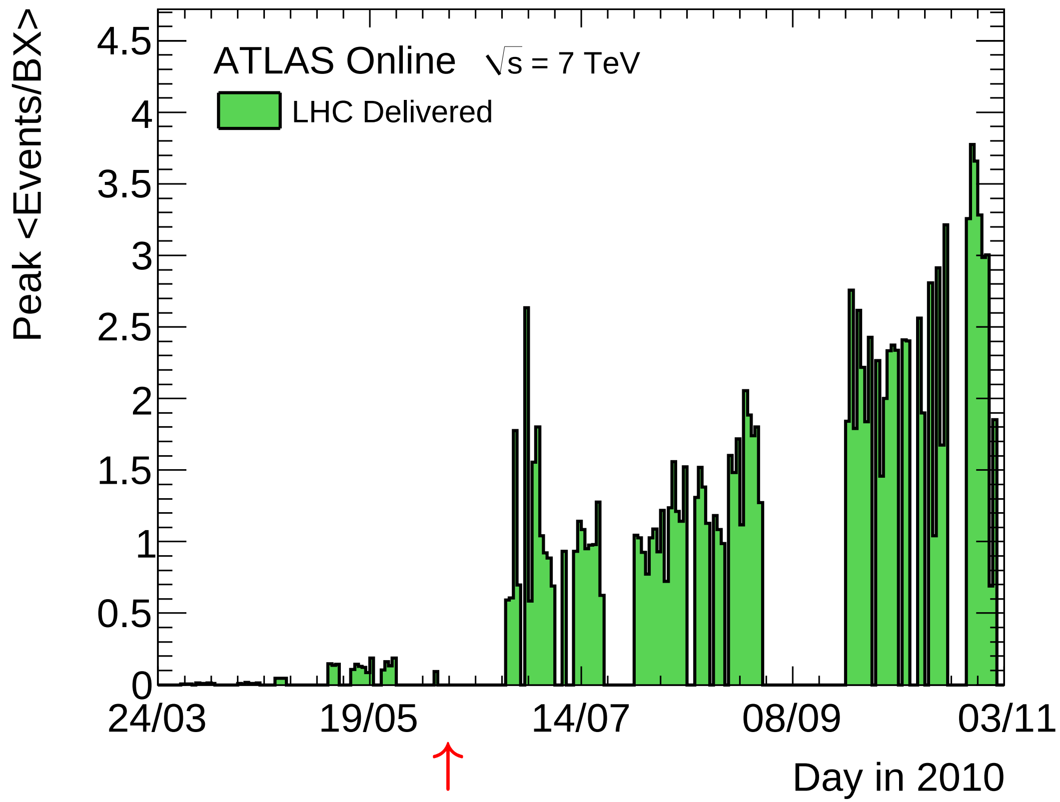

- First measurements with an integrated luminosity of $\mathcal{L} = 17$ nb^{-1}

$\rightarrow$ data taken from March 30th to June 5th 2010

$\rightarrow$ first determination of the calorimeter jet energy response

$\rightarrow$ effects of pile-up $\rightarrow$ small

Reminder:

$$N_{events} = \sigma \times \mathcal{L}$$

First measurements of jet production in pp collisions at $\sqrt{s} = 7$ TeV

- Measurement of the inclusive jet cross section $d\sigma/dp_T$ as a function of p_T for $|y| < 2.8$

→ Every jet in $|y| < 2.8$ with $p_T > 60$ GeV defined using the anti-k_T algorithm with $R = 0.6$ ($R = 0.4$) using $\mathcal{L} = 17$ nb^{-1}

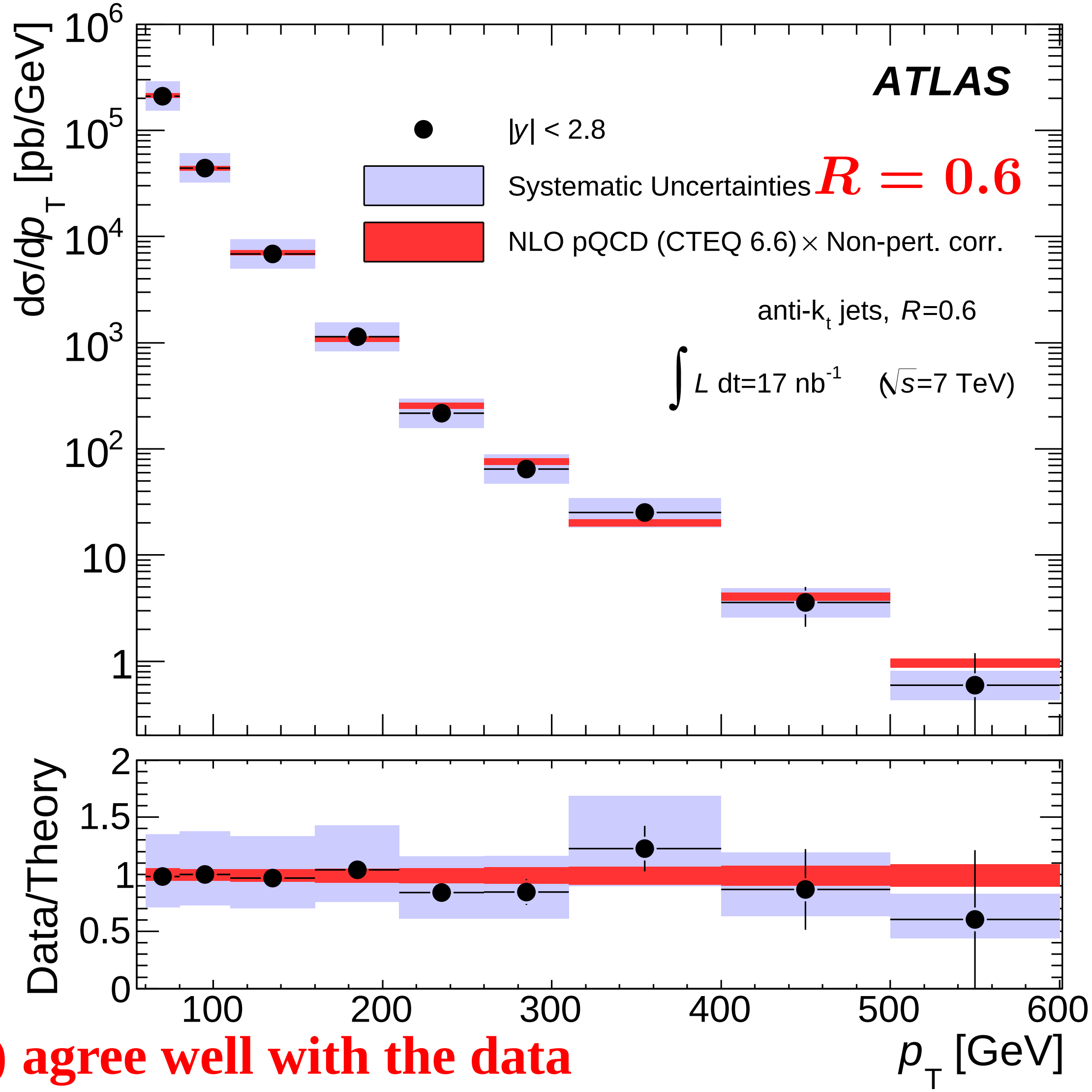

- The measurements cover the range $60 < p_T < 600$ GeV and 5 orders of magnitude in the cross section

⇒ Exploration of new kinematic regimes

- Systematic uncertainties (due mostly to JES) of about 40%

→ NLO QCD calculations (NP corrected) agree well with the data

⇒ validation of the perturbative QCD description of jet production at $\sqrt{s} = 7$ TeV

First measurements of jet production in pp collisions at $\sqrt{s} = 7$ TeV

- Measurement of the inclusive jet cross section $d\sigma/dp_T$ as a function of p_T for $|y| < 2.8$

→ Every jet in $|y| < 2.8$ with $p_T > 60$ GeV defined using the anti-k_T algorithm with $R = 0.4$ ($R = 0.6$) using $\mathcal{L} = 17$ nb^{-1}

- The measurements cover the range $60 < p_T < 600$ GeV and 5 orders of magnitude in the cross section

⇒ Exploration of new kinematic regimes

- Systematic uncertainties (due mostly to JES) of about 40%

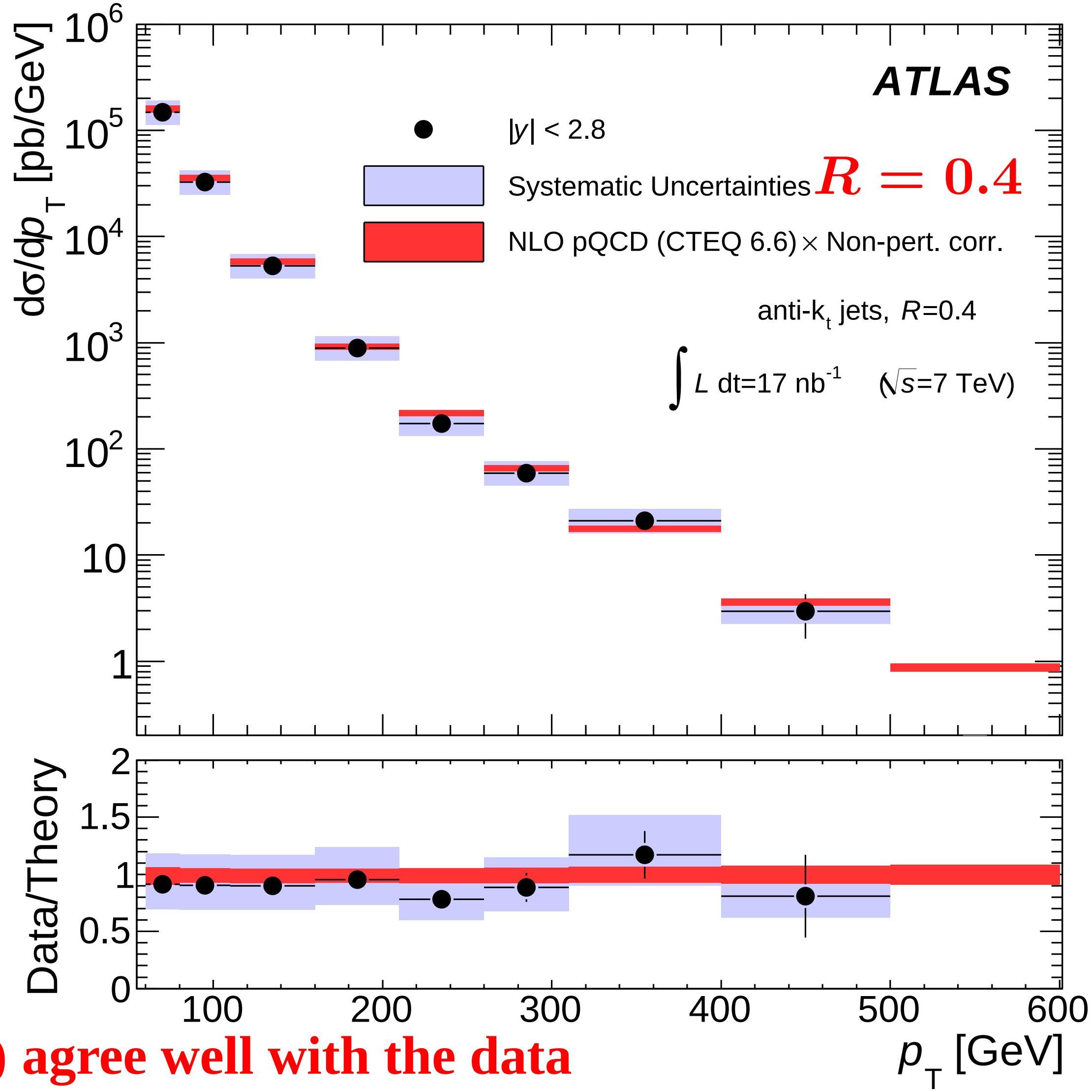

→ NLO QCD calculations (NP corrected) agree well with the data

⇒ validation of the perturbative QCD description of jet production at $\sqrt{s} = 7$ TeV

First measurements of jet production in pp collisions at $\sqrt{s} = 7$ TeV

- **Measurement of the dijet cross section $d^2\sigma/dm_{12}d|y|_{max}$ as a function of m_{12} for different ranges of $|y|_{max}$, where $|y|_{max} = \max(|y_1|, |y_2|)$ using $\mathcal{L} = 17$ nb^{-1}**

→ **Two leading jets in $|y| < 2.8$, $p_T^{1,2} > 60(30)$ GeV defined using the anti-k_T algorithm with $R = 0.6$**

- **The measurements extend up to dijet masses ~ 2 TeV**

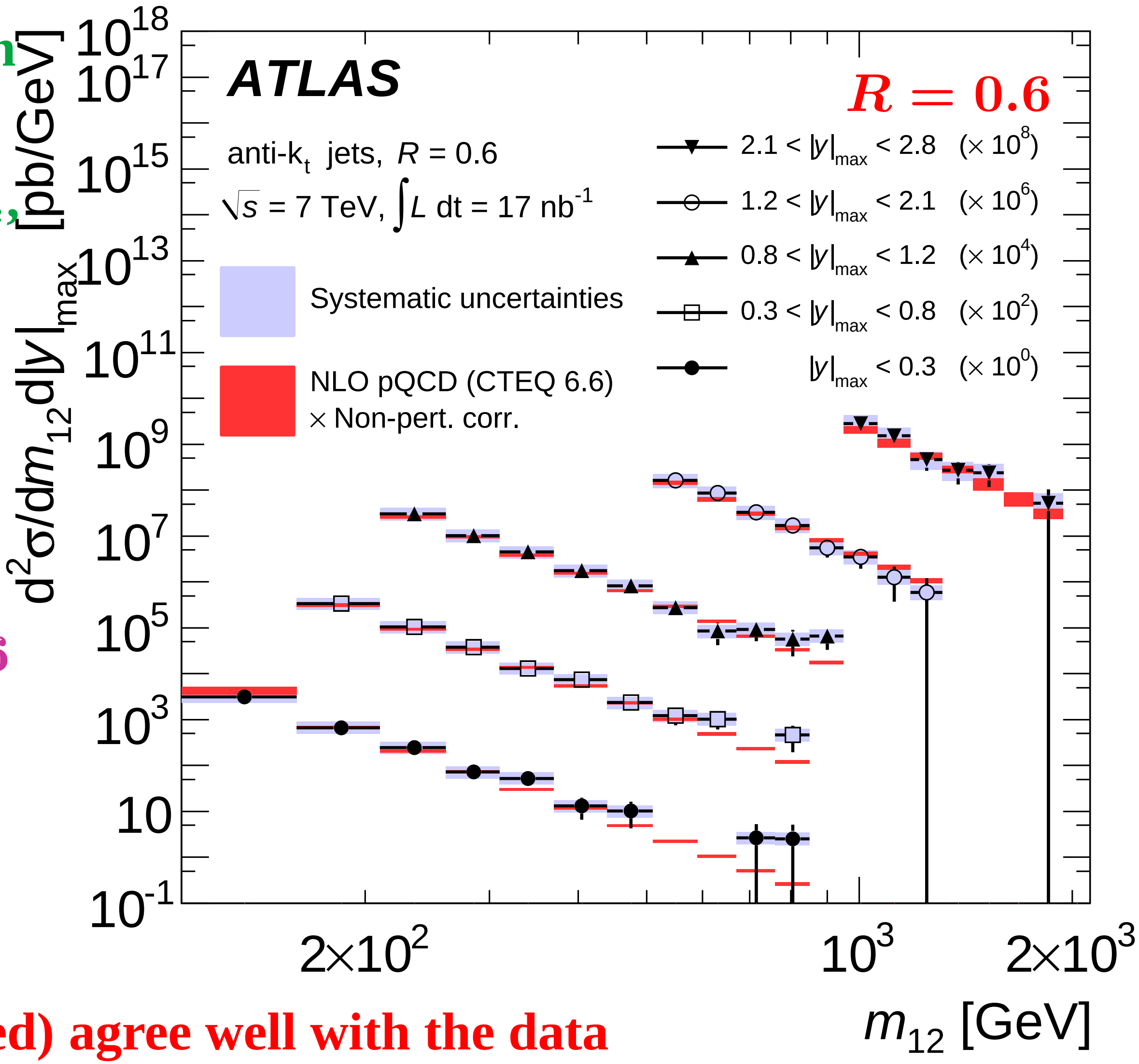

→ **NLO QCD calculations (NP corrected) agree well with the data**

⇒ **validation of the perturbative QCD description of dijet production at $\sqrt{s} = 7$ TeV**

Dijet production

- Measurement of the dijet cross section $d^2\sigma/dm_{12}d|y|_{max}$ as a function of m_{12} for different ranges of $|y|_{max}$, where $|y|_{max} = \max(|y_1|, |y_2|)$ using $\mathcal{L} = 17$ nb^{-1}

→ Two leading jets in $|y| < 2.8$, $p_T^{1,2} > 60(30)$ GeV defined using the anti-k_T algorithm with $R = 0.6$

- The measurements extend up to dijet masses ~ 2 TeV

→ NLO QCD calculations (NP corrected) agree well with the data

⇒ validation of the perturbative QCD description of dijet production at $\sqrt{s} = 7$ TeV

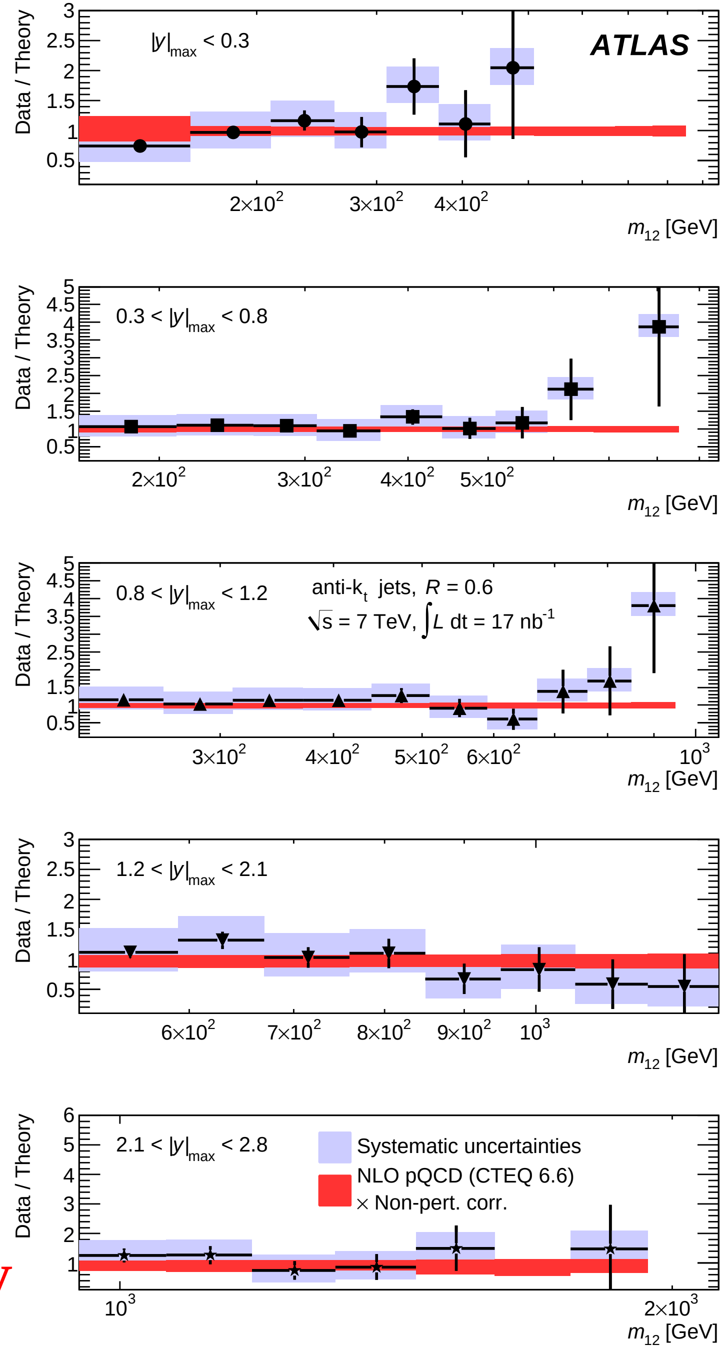

Dijet angular distribution

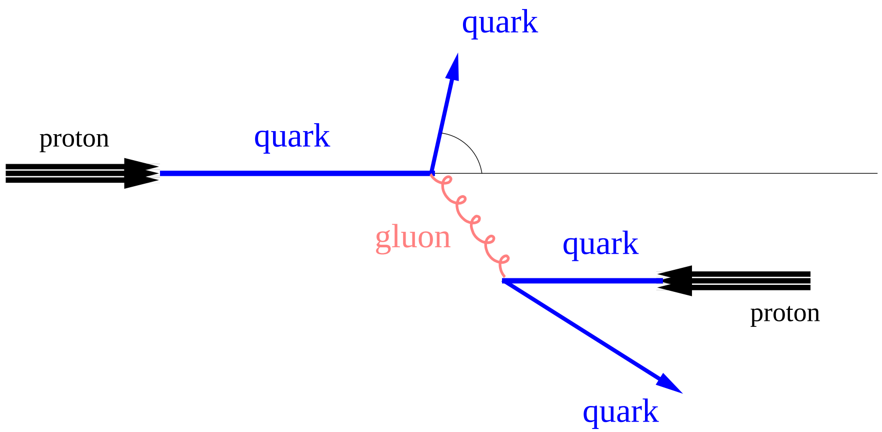

- Dijet angular distribution $d\sigma/d\cos\theta^*$ in the parton-parton centre-of-mass system **sensitive to the spin of the exchanged particle**

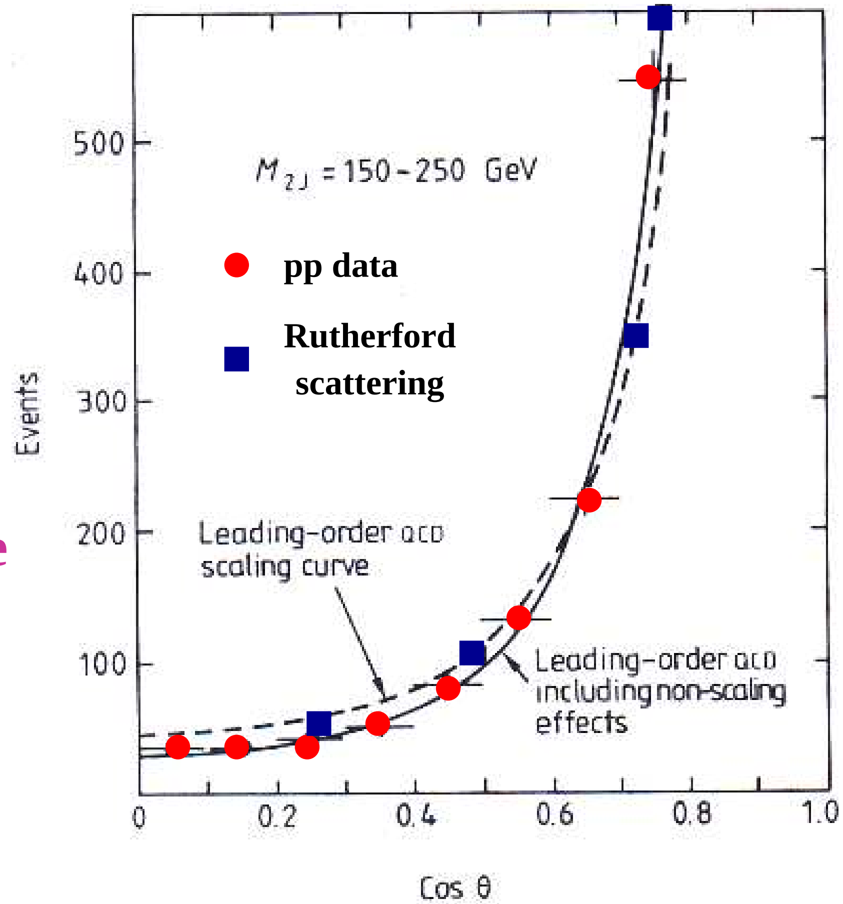

- Dijet production dominated by gluon-exchange in t or u channels

$$\frac{d\sigma}{d\cos\theta^*} \sim \frac{1}{(1-\cos\theta^*)^2} \quad \text{as } \cos\theta^* \to 1$$

$\to$ very steep increase due to massless-gluon exchange

- For $2 \to 2$ hard collinear scattering

$$\cos\theta^* = \tanh\left|\frac{y_1 - y_2}{2}\right|$$

- Transformation to variable $\chi \equiv \frac{1+\cos\theta^*}{1-\cos\theta^*}$
Rutherford scattering $\Rightarrow d\sigma/d\chi$ distribution is flat

Dijet angular distribution

- Measurement of the dijet cross section $d^2\sigma/d\chi dm_{12}$ as a function of χ for different ranges in m_{12} in the region defined by $y^* \equiv \frac{|y_1 - y_2|}{2} < \frac{1}{2}\ln(30)$ and $|y_{boost}| \equiv |\frac{y_1+y_2}{2}| < 1.1$ using $\mathcal{L} = 17$ nb^{-1}

→ Two leading jets in $|y| < 2.8$, $p_T^{1,2} > 60(30)$ GeV defined using the anti-k_T algorithm with $R = 0.6$

- Measurements of the dijet angular distribution for dijet masses from 340 GeV up to ∼ 1.2 TeV
- NLO pQCD calculations consistent with the data

⇒ Rutherford scattering between quarks and gluons up to the TeV scale

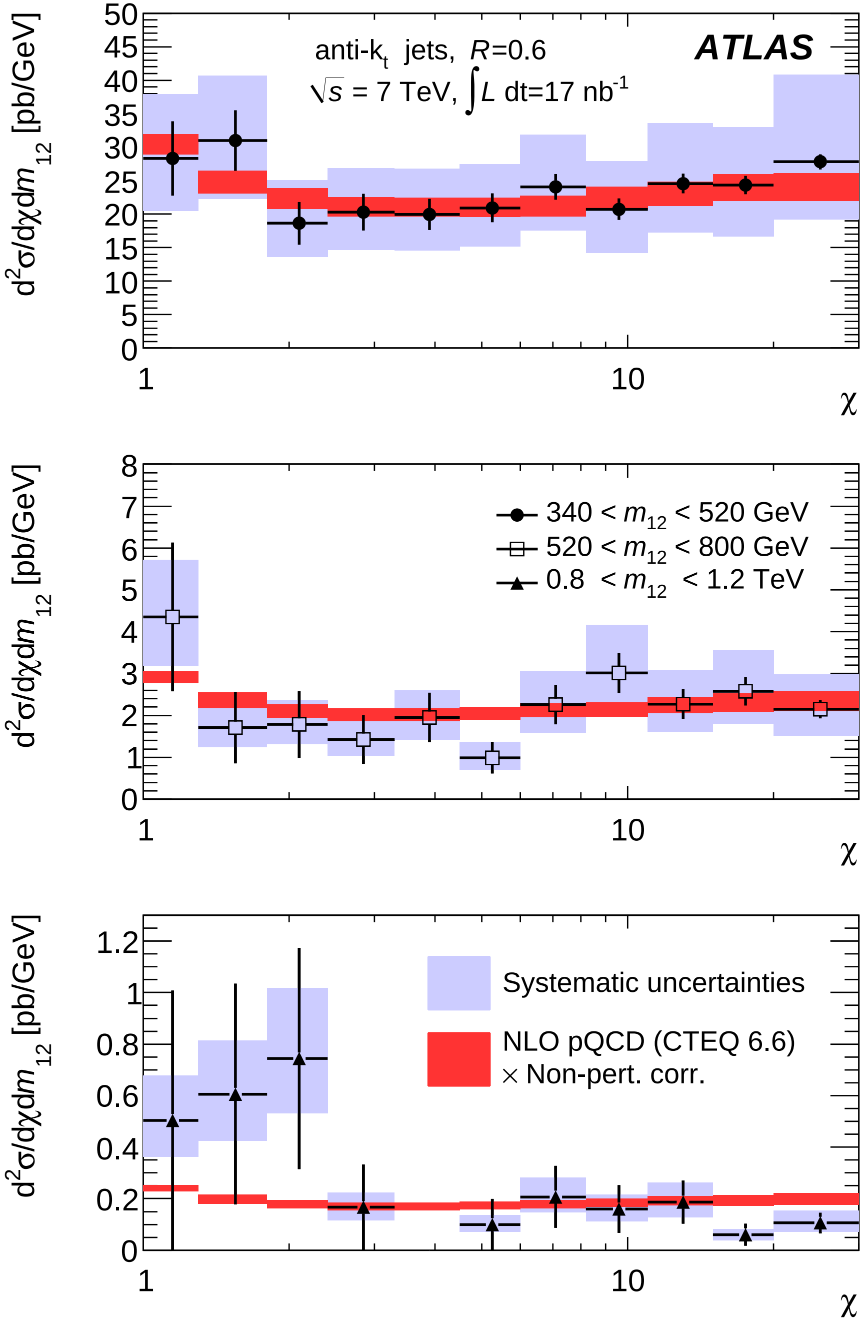

More+better measurements of jet production at the LHC

More data...

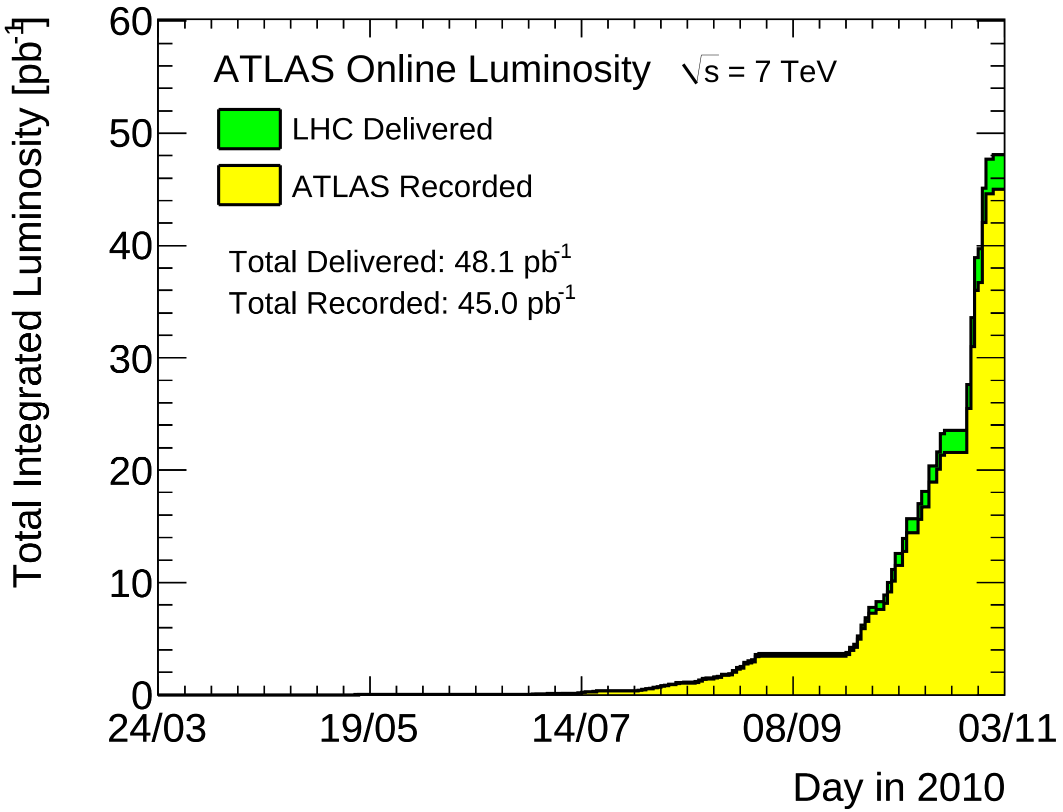

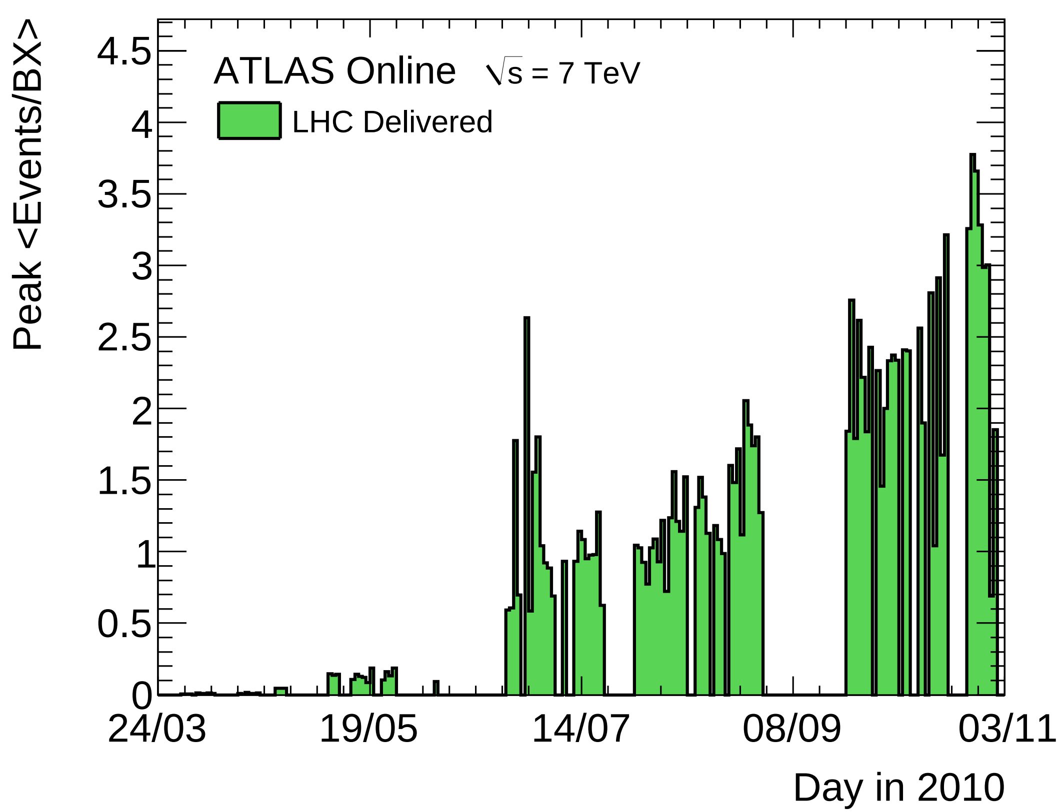

- Measurements with an integrated luminosity 2000 times larger (!) than first analyses

→ Extension of the measurements to higher jet p_T and dijet mass

→ Improved understanding of the jet energy scale uncertainty

⇒ Exploration of new regimes with improved precision

Inclusive jet and dijet production with the full 2010 data sample

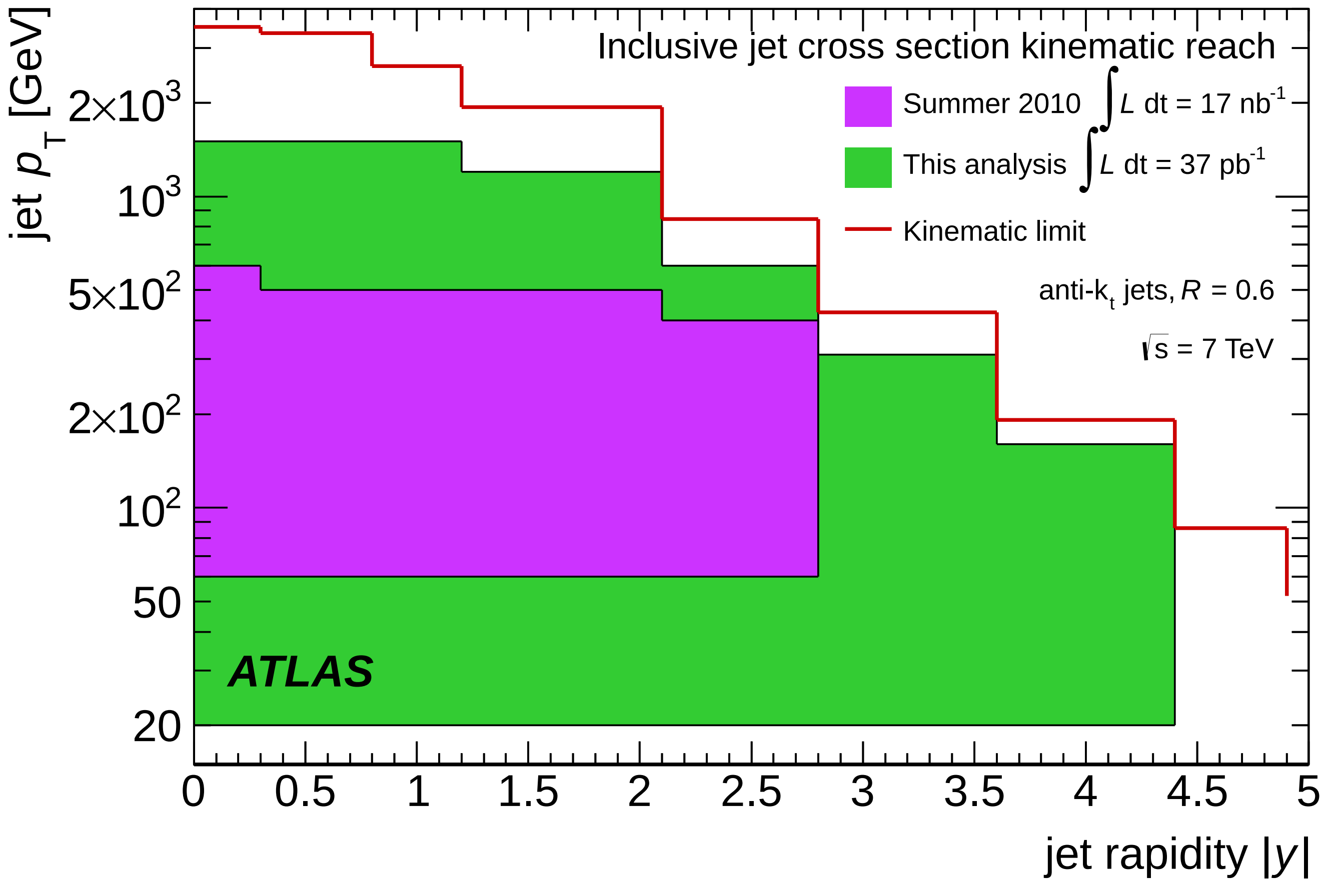

- Extension in jet p_T from (60 GeV, 700 GeV) to (20 GeV, 1500 GeV)
- Extension in jet $|y|$ from (0, 2.8) to (0, 4.4)
- Extension in dijet mass from 1.8 TeV to 5 TeV

Inclusive jet production in pp collisions at $\sqrt{s} = 7$ TeV ($R = 0.4$)

- Measurement of the inclusive jet cross section $d^2\sigma/dp_T dy$ as a function of p_T for different ranges in y (from $|y| < 0.3$ to $3.6 < |y| < 4.4$)

→ Every jet in $|y| < 4.4$ with $p_T > 20$ GeV defined using the anti-k_T algorithm with $R = 0.4$ ($R = 0.6$) using $\mathcal{L} = 37$ pb^{-1}

- The measurements cover two orders of magnitude in jet p_T, from 20 GeV to ~ 1.5 TeV and 10 orders of magnitude in the cross section

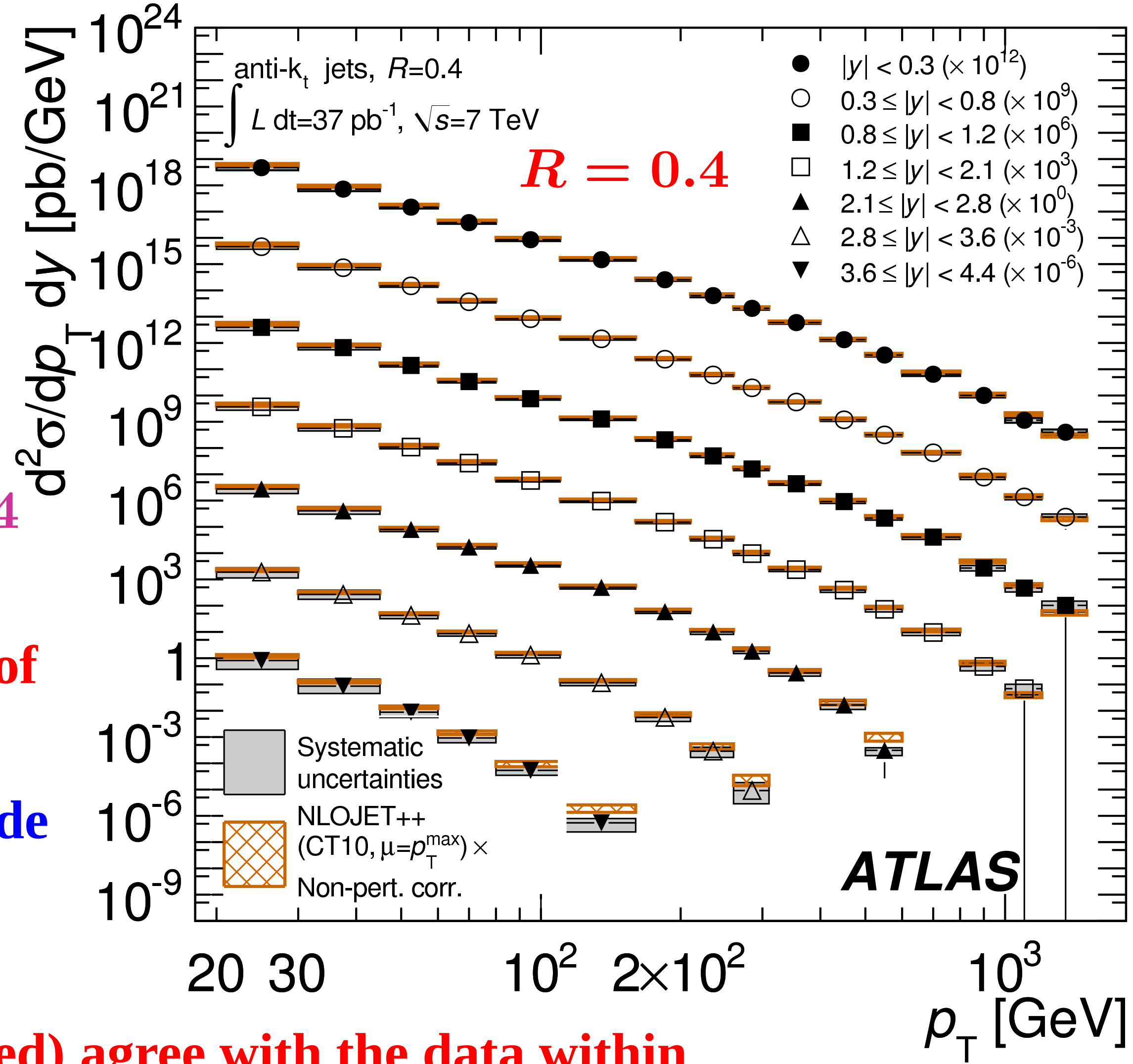

→ NLO QCD calculations (NP corrected) agree with the data within the experimental and theoretical uncertainties

Inclusive jet production in pp collisions at $\sqrt{s} = 7$ TeV ($R = 0.6$)

- Measurement of the inclusive jet cross section $d^2\sigma/dp_T dy$ as a function of p_T for different ranges in y (from $|y| < 0.3$ to $3.6 < |y| < 4.4$)

→ Every jet in $|y| < 4.4$ with $p_T > 20$ GeV defined using the anti-k_T algorithm with $R = 0.4$ ($R = 0.6$) using $\mathcal{L} = 37$ pb^{-1}

- The measurements cover two orders of magnitude in jet p_T, from 20 GeV to $\sim$ 1.5 TeV and 10 orders of magnitude in the cross section

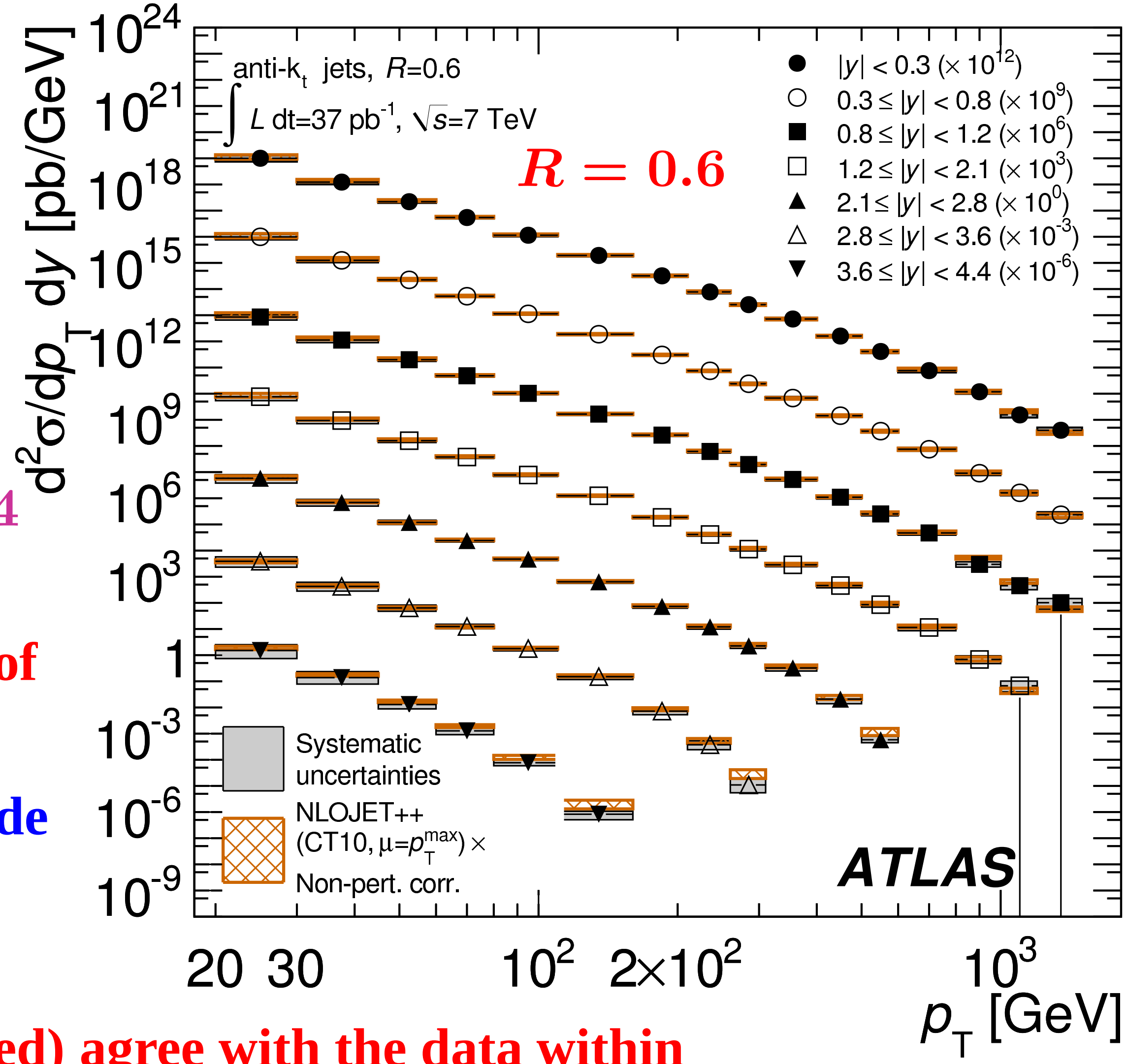

→ NLO QCD calculations (NP corrected) agree with the data within the experimental and theoretical uncertainties

Non-perturbative corrections to NLO QCD calculations

- Non-perturbative (NP) corrections: $C_{NP} = \frac{\sigma_{\rm jet}(\rm MC, particle-level, UE)}{\sigma_{\rm jet}(\rm MC, parton-level, no\ UE)}$
- The NP corrections depend strongly on R
- The size of the correction and its uncertainty depend on the interplay of hadronisation and underlying event
  $\rightarrow$ significant influence at low p_T

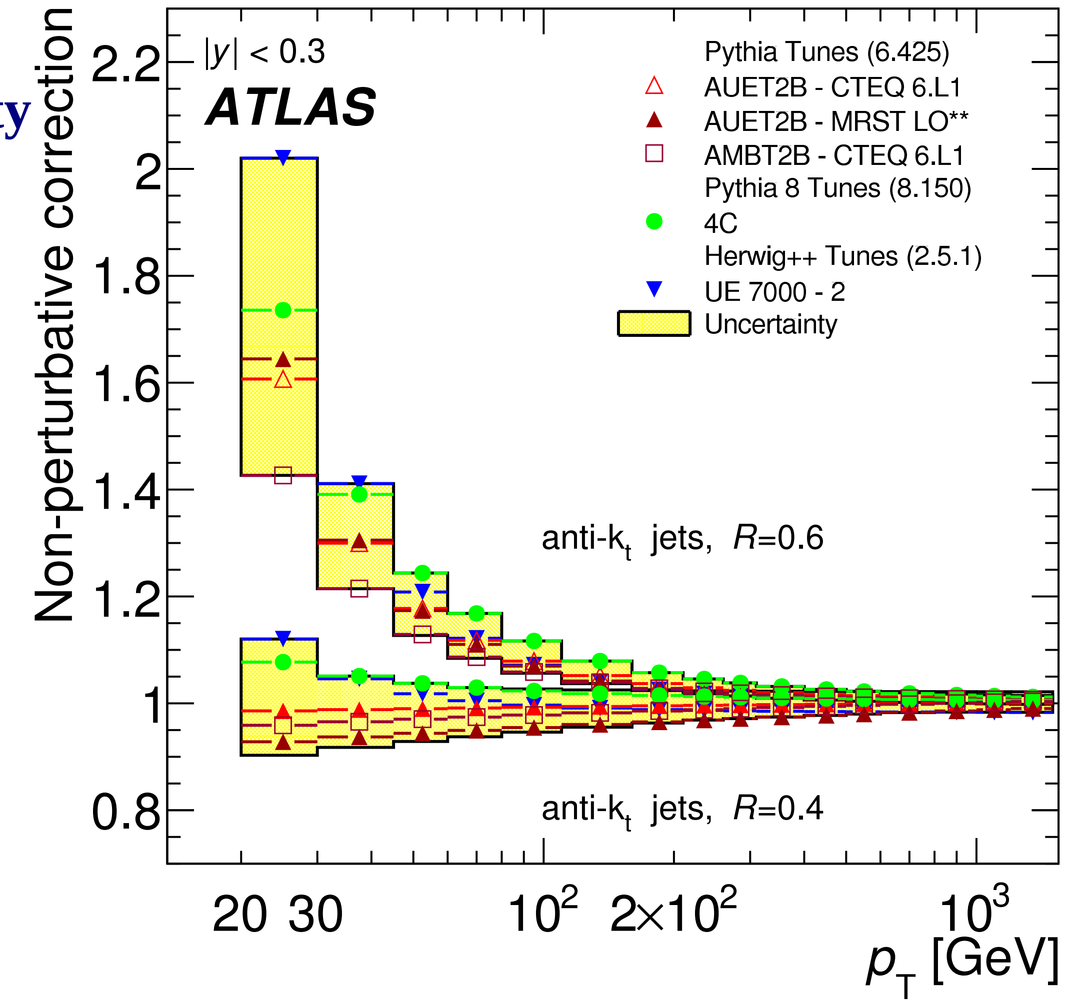

- Corrections for $R = 0.4$: dominated by hadronisation; 0.95 at $p_T \sim 20$ GeV; closer to 1 at higher p_T
- Corrections for $R = 0.6$: dominated by underlying event; 1.6 at $p_T \sim 20$ GeV; between 1.0 and 1.1 for $p_T > 100$ GeV

Improving the jet energy scale (JES) uncertainty

- JES uncertainty is dominant!
- Reduced by up to a factor 2 (previous analyses)

→ improved calibration of EM energy scale obtained from $Z \to ee$ events

→ improved determination of the single particle energy measurement uncertainties from in situ and test-beam measurements

- Improvement confirmed by independent measurements: tracks associated to jets, momentum balance in $\gamma + $jet, dijet and multijet events

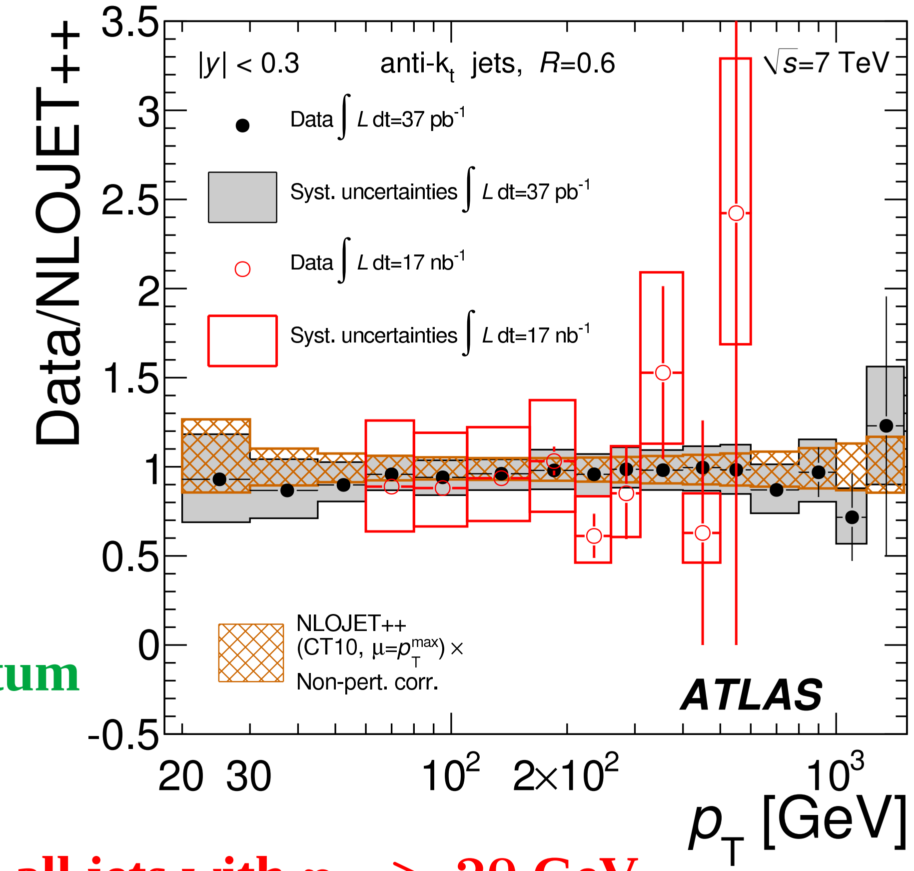

- Central region ($|\eta| < 0.8$): lower than 4.6% for all jets with $p_T > 20$ GeV and decreases to $< 2.5\%$ for $60 < p_T < 800$ GeV; JES uncertainty largest for low-p_T (~ 20 GeV) jets in most forward region ($|\eta| > 3.6$) → 11-12%
- Comparison to previous measurements: good agreement with much reduced uncertainties

Experimental uncertainties

$2.1 < |y| < 2.8$ $3.6 < |y| < 4.4$

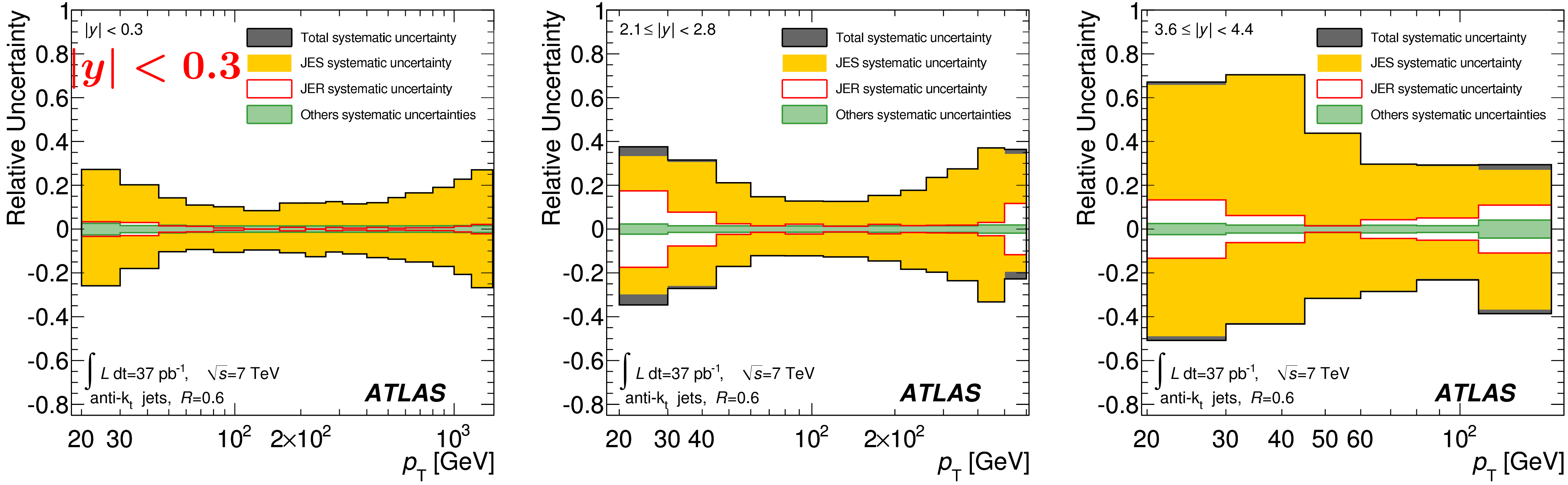

p_T [GeV]	$|y|$	JES	JER	Trigger	Jet rec.
20–30	2.1–2.8	$^{+35\%}_{-30\%}$	17%	1%	2%
20–30	3.6–4.4	$^{+65\%}_{-50\%}$	13%	1%	2%
80–110	<0.3	10%	1%	1%	1%

- **Dominant systematics**

→ JES (jet energy scale)

→ JER (jet energy resolution)

→ Trigger

→ Jet reconstruction

→ Luminosity uncertainty (3.4%)

Correlations of cross section measurements

$|y| < 0.3$ $\quad$ $2.1 < |y| < 2.8$

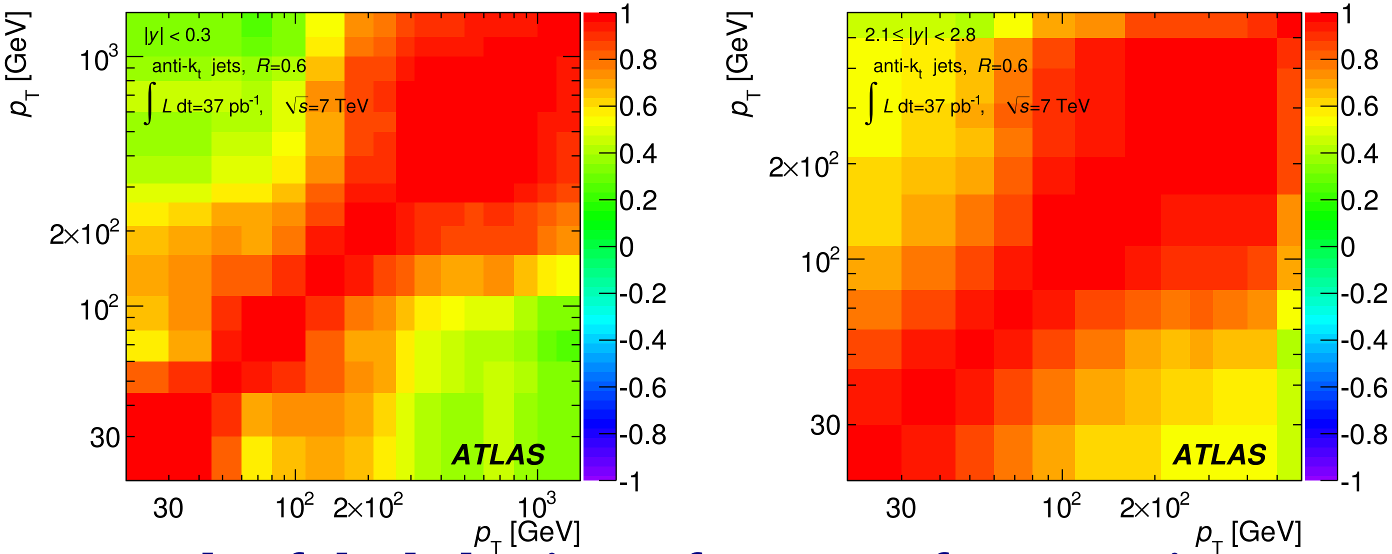

- **Study of the behaviour of sources of systematic uncertainty in different parts of the detector**
  → their correlations across bins in p_T and y
- **22 independent sources of systematic uncertainty identified; upon study of y dependence → 87 nuisance parameters to describe the correlations over the whole phase space**

⇒ Important information for PDF fits!

Uncertainty Source
JES 1: Noise threshold
JES 2: Theory UE
JES 3: Theory showering
JES 4: Nonclosure
JES 5: Dead material
JES 6: Forward JES
JES 7: E/p response
JES 8: E/p selection
JES 9: EM + neutrals
JES 10: HAD E-scale
JES 11: High p_T
JES 12: E/p bias
JES 13: Test-beam bias
Unfolding
Jet matching
Jet energy resolution
y-resolution
Jet reconstruction eff.
Luminosity
JES 14: Pileup (u_1)
Trigger (u_2)
Jet identification (u_3)

Inclusive jet cross section ($R = 0.6$)

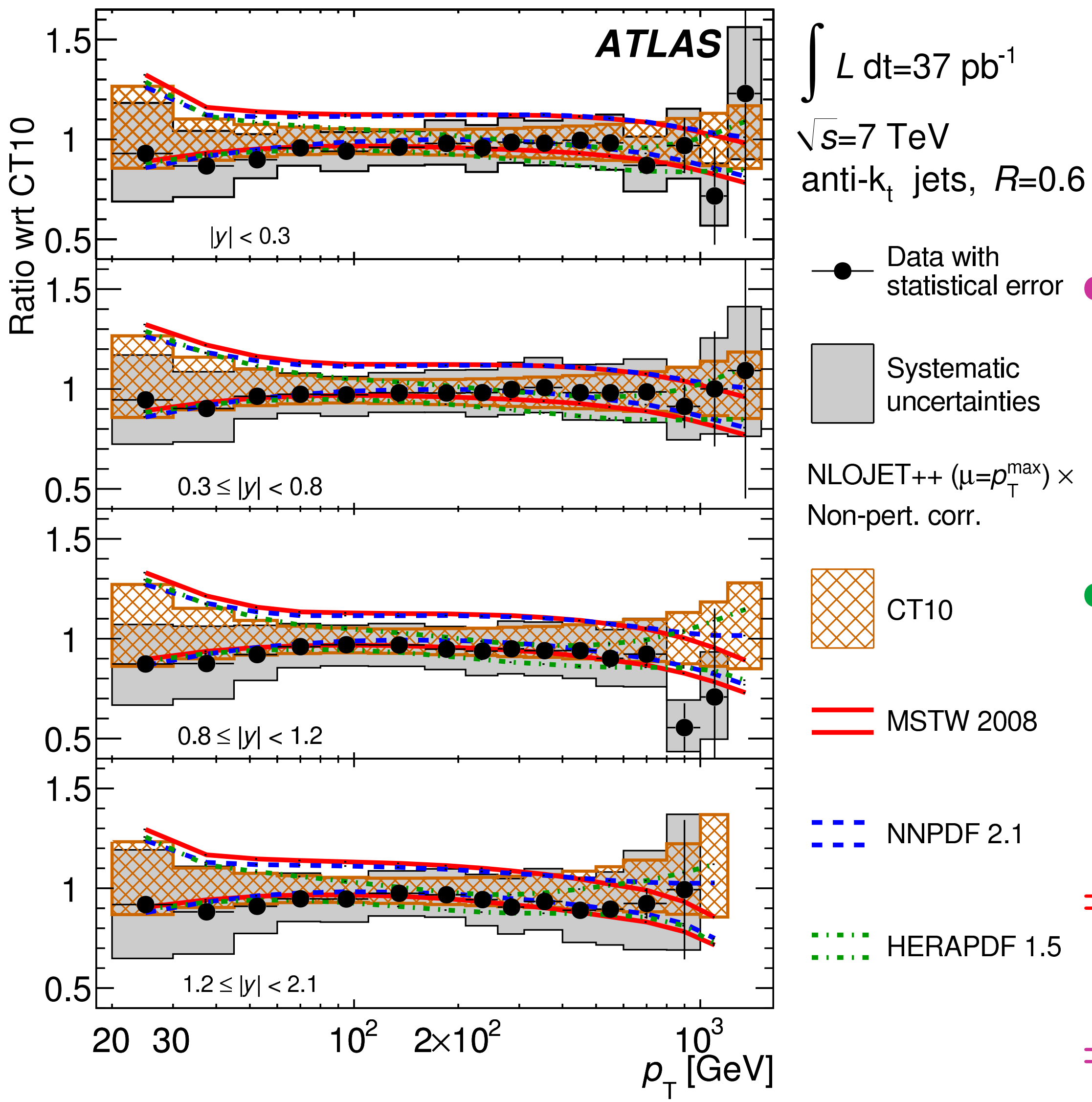

- Comparison to NLO QCD calculations using different parametrisations of PDFs: CT10, MSTW2008, NNPDF 2.1, ...
- The description of the data by NLO worsens for very large p_T and $|y|$; MSTW2008 follows the measured trend better
- Differences between data and calculations lie within the experimental and theoretical uncertainties

⇒ Test of QCD at high momentum transfers $\sim$ 1 TeV

⇒ Potential to constrain the PDFs at large x

Inclusive jet cross section ($R = 0.6$)

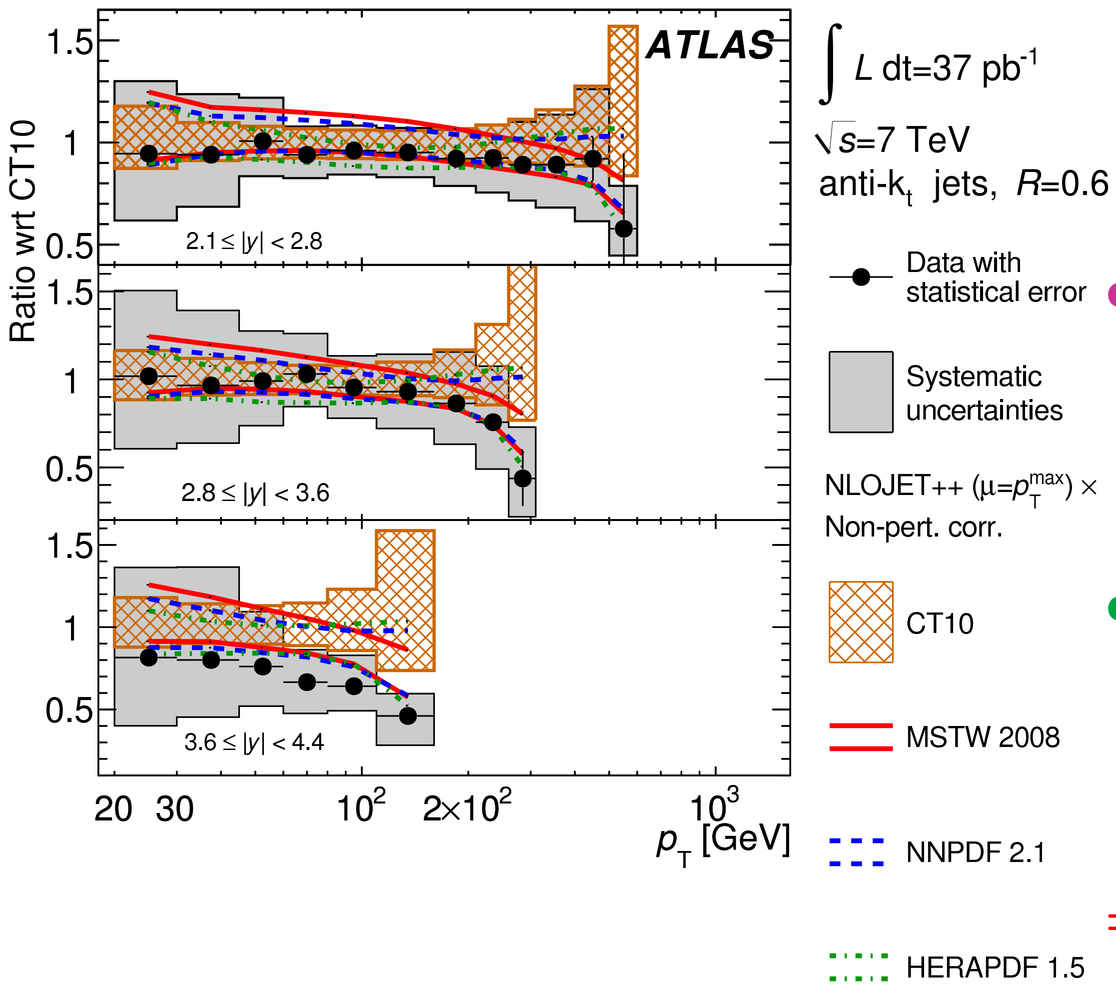

- Comparison to NLO QCD calculations using different parametrisations of PDFs: CT10, MSTW2008, NNPDF 2.1, ...
- The description of the data by NLO worsens for very large p_T and $|y|$; MSTW2008 follows the measured trend better
- Differences between data and calculations lie within the experimental and theoretical uncertainties

$\Rightarrow$ Test of QCD at high momentum transfers $\sim$ 1 TeV

$\Rightarrow$ Potential to constrain the PDFs at large x

Dijet production in pp collisions at $\sqrt{s} = 7$ TeV ($R = 0.4$)

- Measurement of the dijet cross section $d^2\sigma/dm_{12}dy^*$ as a function of the dijet invariant mass m_{12} for different ranges in y^* (from $y^* < 0.5$ to $4.0 < y^* < 4.4$)

→ Two leading jets in $|y^{jet}| < 4.4$
$p_T^{jet1(2)} > 30$ GeV (20 GeV)
defined using the anti-k_T algorithm with $R = 0.4$ ($R = 0.6$) using $\mathcal{L} = 37$ pb^{-1}

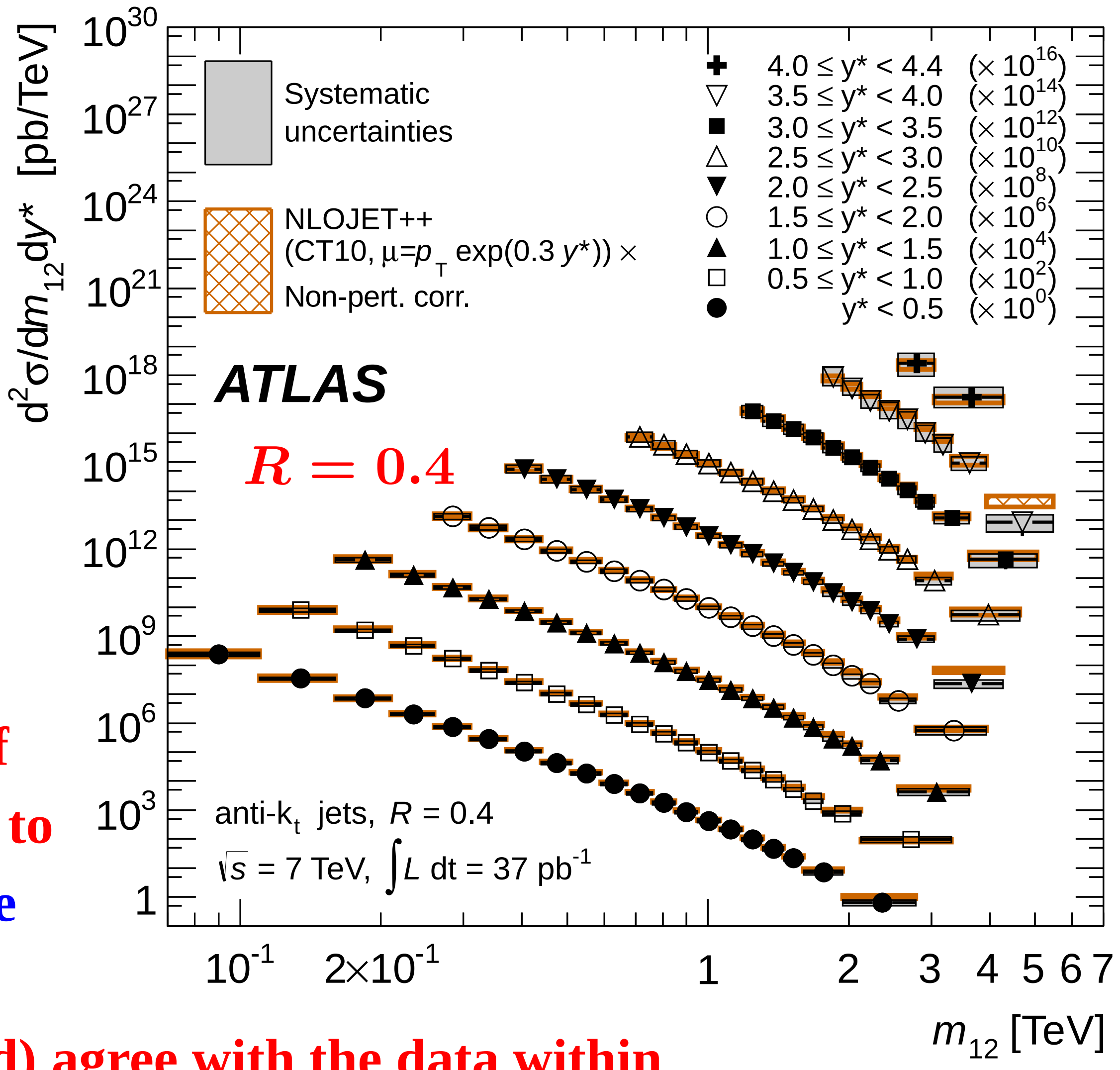

- The measurements cover two orders of magnitude in dijet mass, from 70 GeV to $\sim$ 5 TeV and nine orders of magnitude in the cross section

→ NLO QCD calculations (NP corrected) agree with the data within the experimental and theoretical uncertainties (particularly at low y^*)

Dijet production in pp collisions at $\sqrt{s} = 7$ TeV ($R = 0.6$)

- **Measurement of the dijet cross section $d^2\sigma/dm_{12}dy^*$ as a function of the dijet invariant mass m_{12} for different ranges in y^*** (from $y^* < 0.5$ to $4.0 < y^* < 4.4$)

→ **Two leading jets in $|y^{jet}| < 4.4$ $p_T^{jet1(2)} > 30$ GeV (20 GeV) defined using the anti-k_T algorithm with $R = 0.4$ ($R = 0.6$) using $\mathcal{L} = 37$ pb^{-1}**

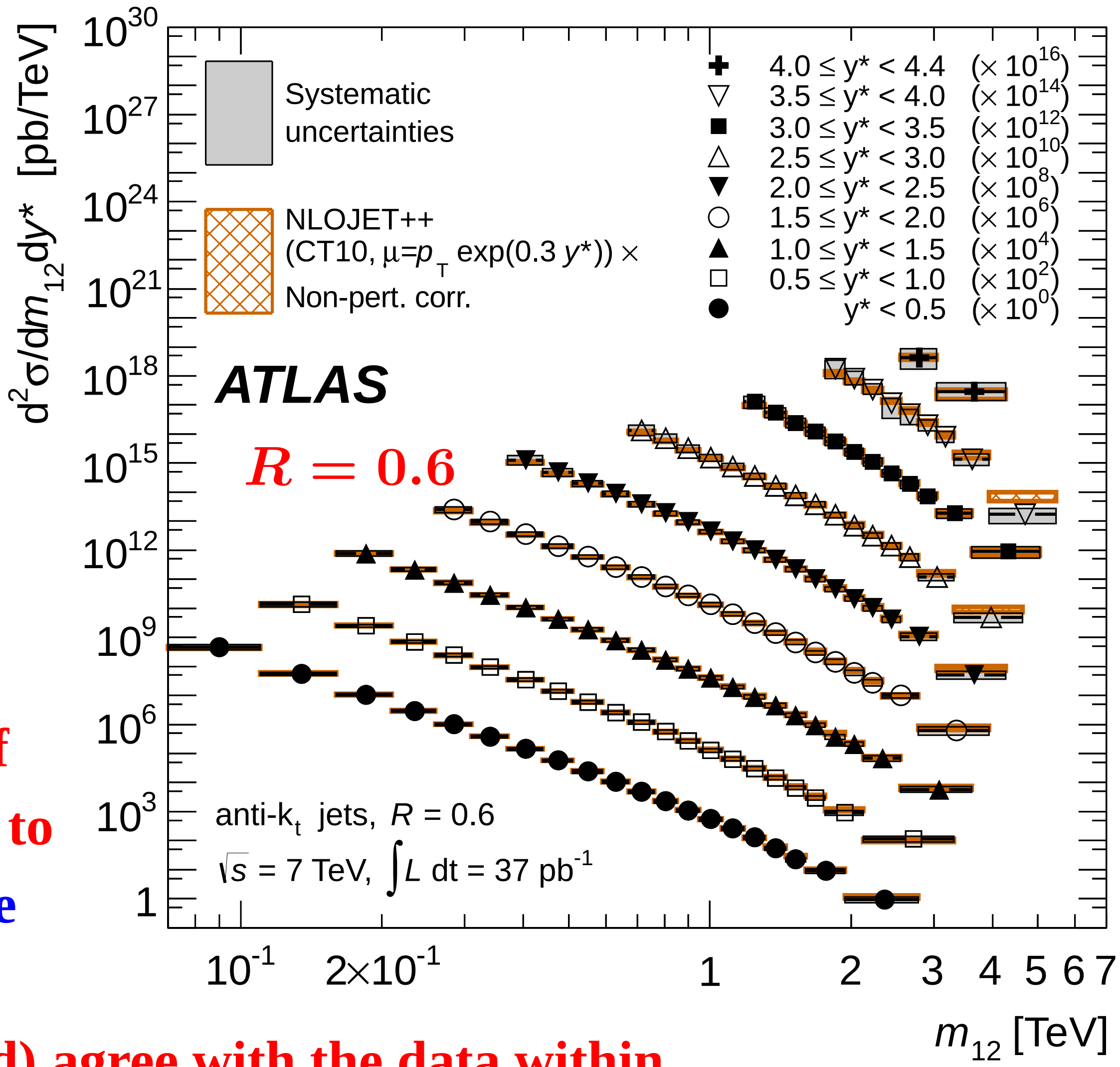

- **The measurements cover two orders of magnitude in dijet mass, from 70 GeV to $\sim$ 5 TeV and nine orders of magnitude in the cross section**

→ **NLO QCD calculations (NP corrected) agree with the data within the experimental and theoretical uncertainties (particularly at low y^*)**

Dijet mass cross section ($R = 0.6$)

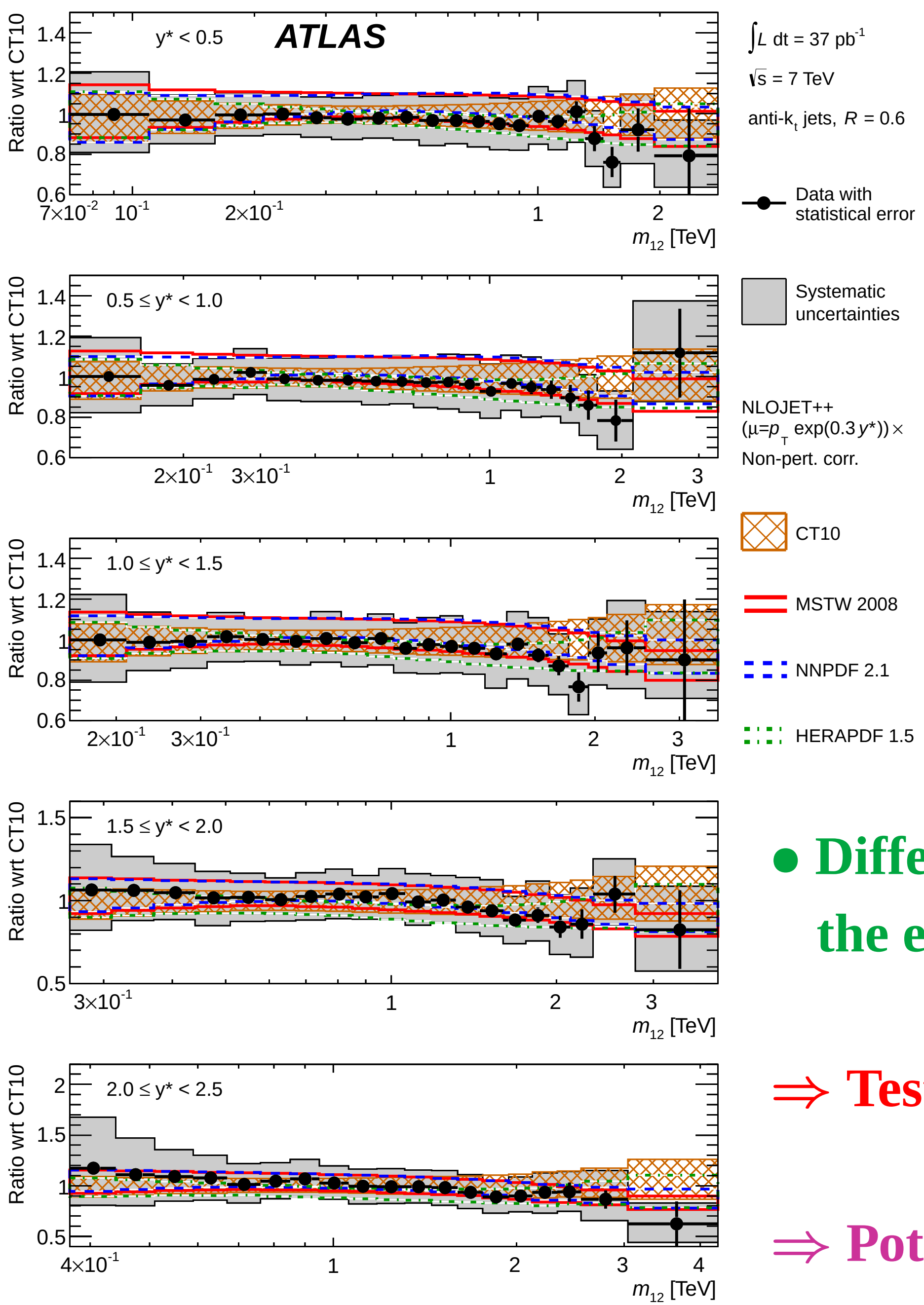

- Comparison to NLO QCD calculations using different parametrisations of the proton PDFs: CT10, MSTW2008, NNPDF 2.1, HERAPDF1.5
- Tendency in the data to be below the calculations at high dijet mass, specially for CT10 → better described by the other PDF sets
- Differences between data and calculations lie within the experimental and theoretical uncertainties

⇒ Test of QCD at high dijet masses ∼ 5 TeV

⇒ Potential to constrain the PDFs at large x

Dijet mass cross section ($R = 0.6$)

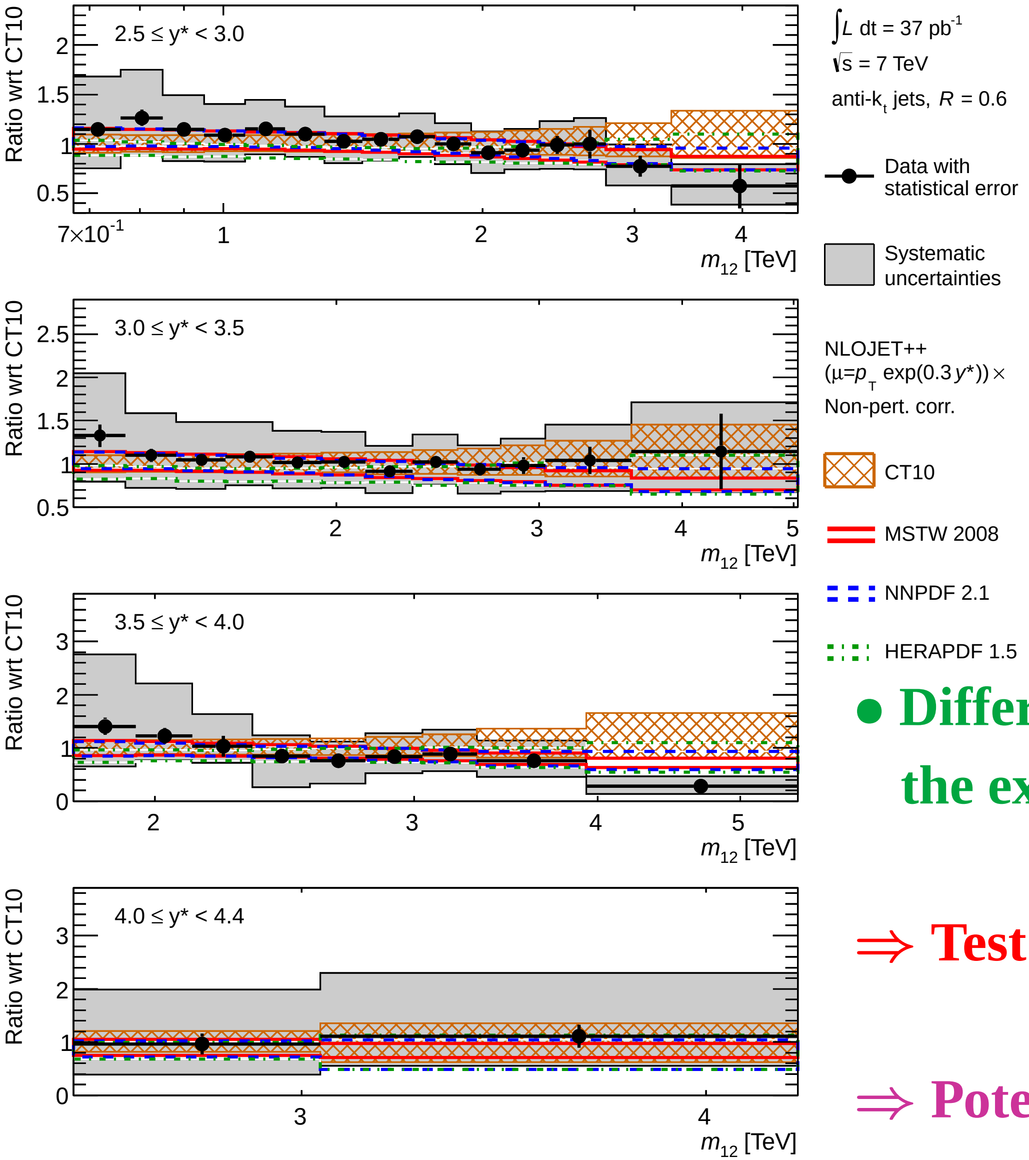

- Comparison to NLO QCD calculations using different parametrisations of the proton PDFs: CT10, MSTW2008, NNPDF 2.1, HERAPDF1.5
- Tendency in the data to be below the calculations at high dijet mass, specially for CT10 $\to$ better described by the other PDF sets
- Differences between data and calculations lie within the experimental and theoretical uncertainties

$\Rightarrow$ Test of QCD at high dijet masses $\sim$ 5 TeV

$\Rightarrow$ Potential to constrain the PDFs at large x

Measurements of multijet production at the LHC

Multijet production in *pp* collisions

- **Multijetproduction in *pp* collisions allows**

→ **tests of perturbative QCD**

→ **robustness of the predictions of model predictions for high jet multiplicities**

→ **determination of α_s at much higher energies than explored so far**

→ **understanding multijet production for the benefit of other measurements and searches for new particles or interactions**

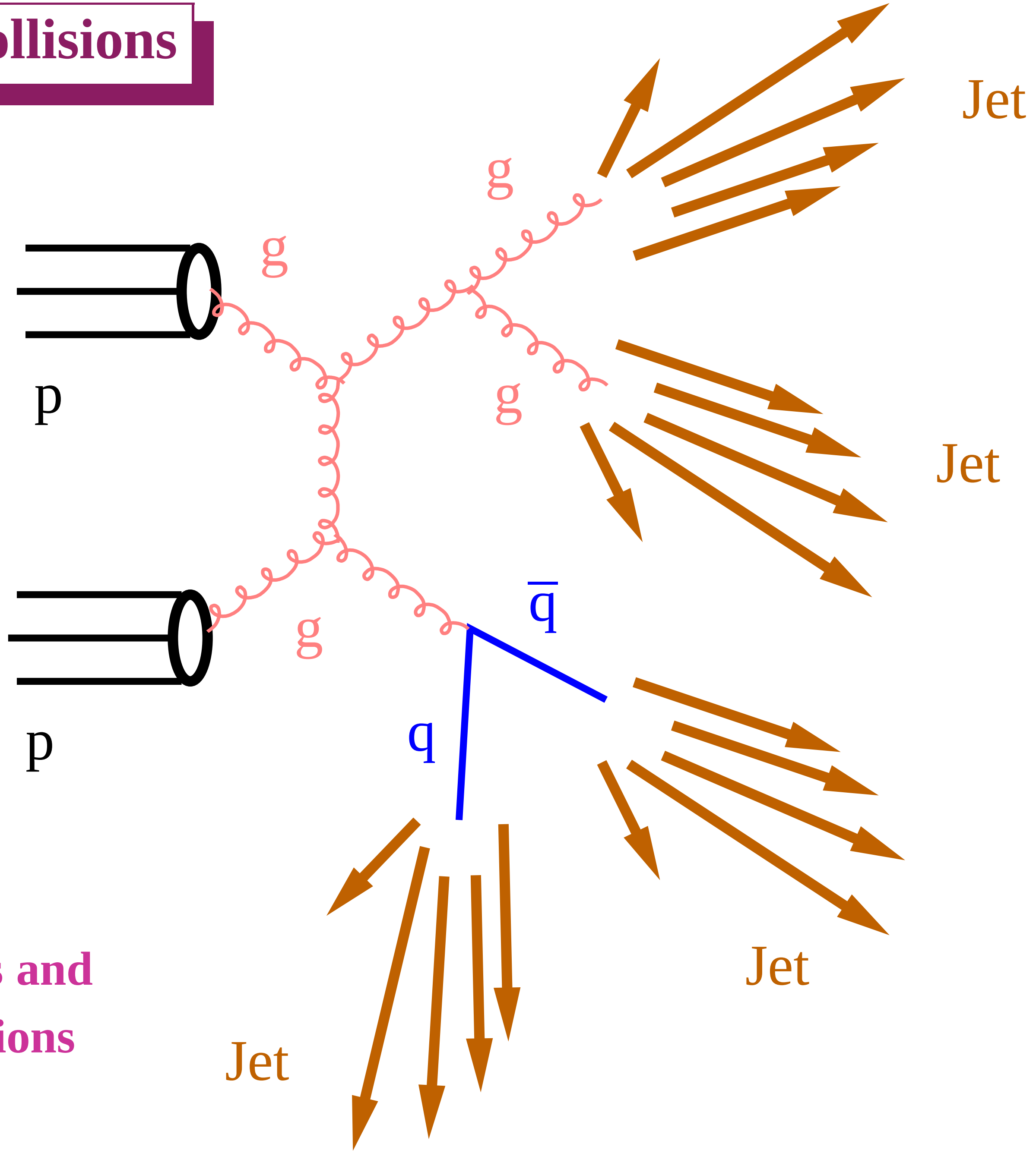

Multijet production in pp collisions at $\sqrt{s} = 7$ TeV

- **Measurement of cross sections for multijet production**
  $p_T^{jet} > 60$ **GeV and** $|y^{jet}| < 2.8$
  $p_T^{lead\ jet} > 80$ **GeV**
  defined using the anti-k_T algorithm with $R = 0.4$ ($R = 0.6$) using $\mathcal{L} = 2.4$ pb^{-1}

Events with up to 6 jets are observed $\Rightarrow$

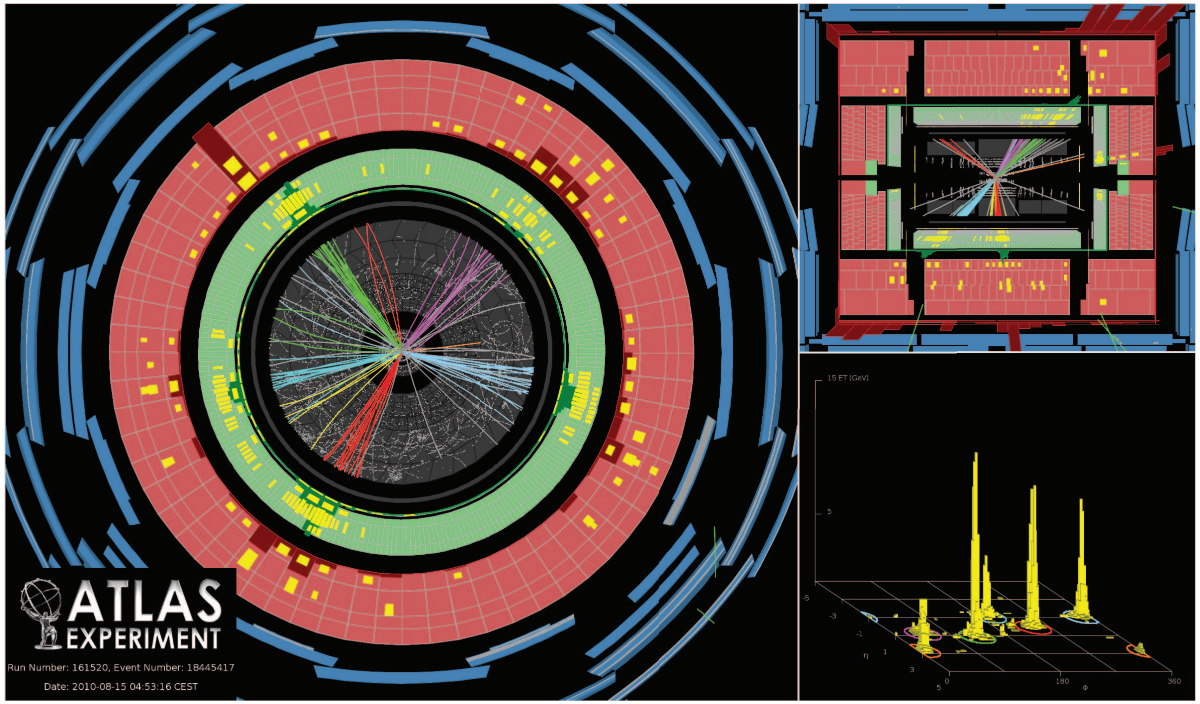

- **The measurements are compared to**

$\rightarrow$ **predictions of MC models based on $2 \rightarrow 2$ matrix elements + parton shower (PYTHIA)**

$\rightarrow$ **predictions of MC models based on $2 \rightarrow n$ matrix elements + parton shower with n up to 6 (ALPGEN and SHERPA)**

$\rightarrow$ **NLO QCD calculations (NLOJET++) for the ratio of the inclusive three-jet to two-jet cross sections; corrections for non-perturbative effects applied**

Multijet production in pp collisions at $\sqrt{s} = 7$ TeV

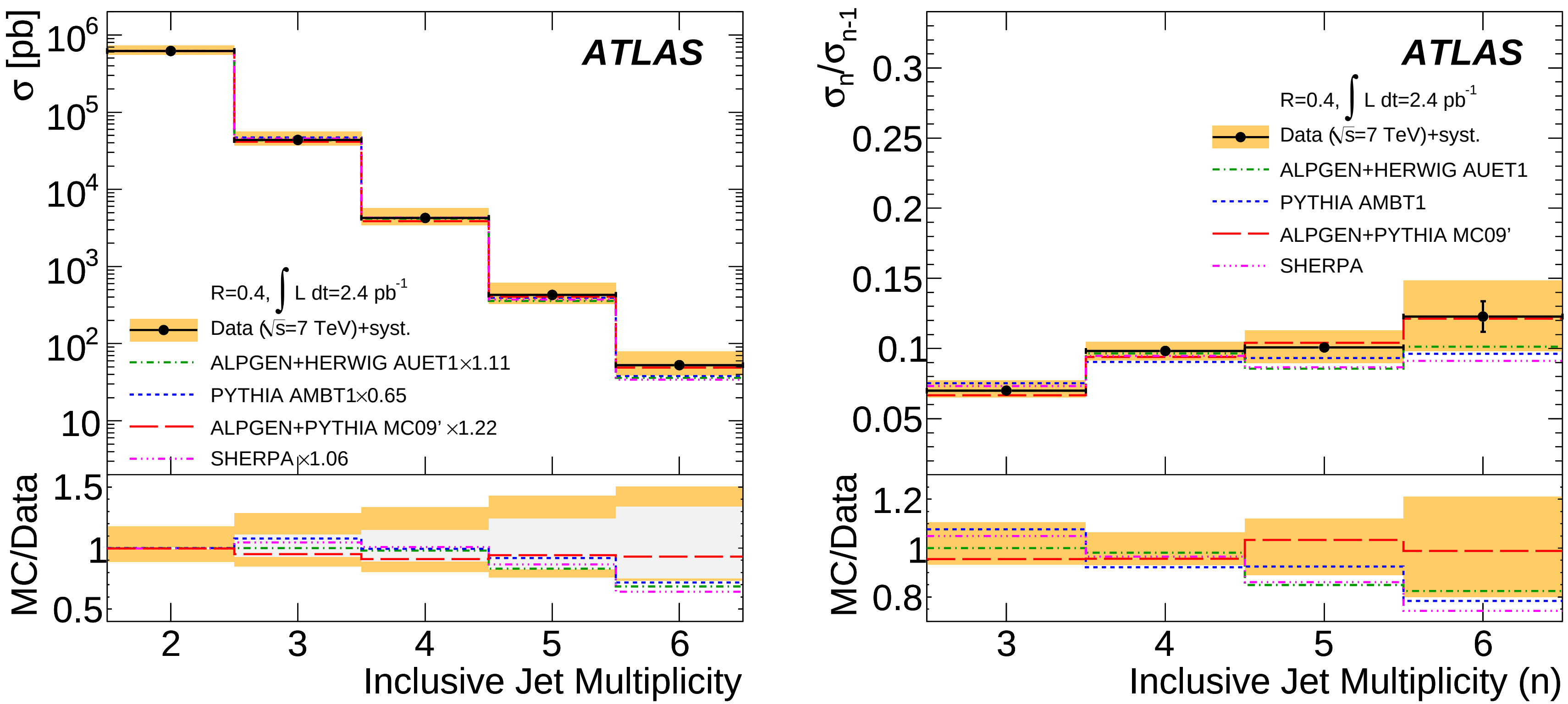

- Measurement of cross section for inclusive jet multiplicity up to $N_{jets} \geq 6$ (MC predictions normalised to the measured inclusive two-jet cross section)
- Data described by PYTHIA ($2 \to 2$+PS) and SHERPA and ALPGEN ($2 \to n$+PS)
- Measurements of ratios σ_n / σ_{n-1} have reduced uncertainties:

$\to$ the predictions of the MC models are consistent with the data within uncertainties

Multijet production in pp collisions at $\sqrt{s} = 7$ TeV

p_T Leading Jet / p_T Second Leading Jet

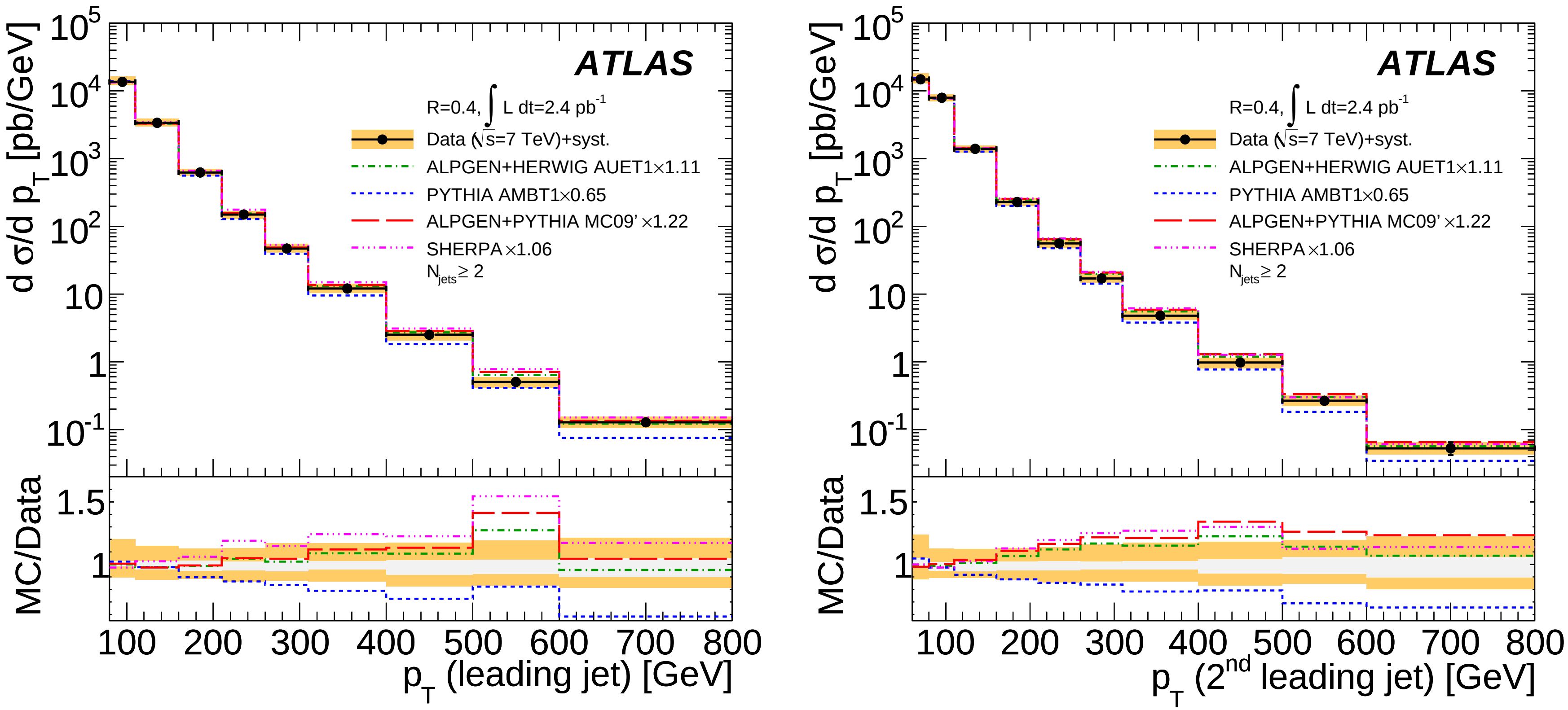

- Measurement of $d\sigma/dp_T^{\rm jet}$ for leading and 2nd leading jet in events with $N_{jets} \geq 2$ (MC predictions normalised to the measured inclusive two-jet cross section)
- Reasonable description: → PYTHIA (2 → 2+PS) predicts softer spectra

→ SHERPA and ALPGEN (2→ n+PS), tendency to predict harder spectra

Multijet production in pp collisions at $\sqrt{s} = 7$ TeV

p_T Third Leading Jet / p_T Fourth Leading Jet

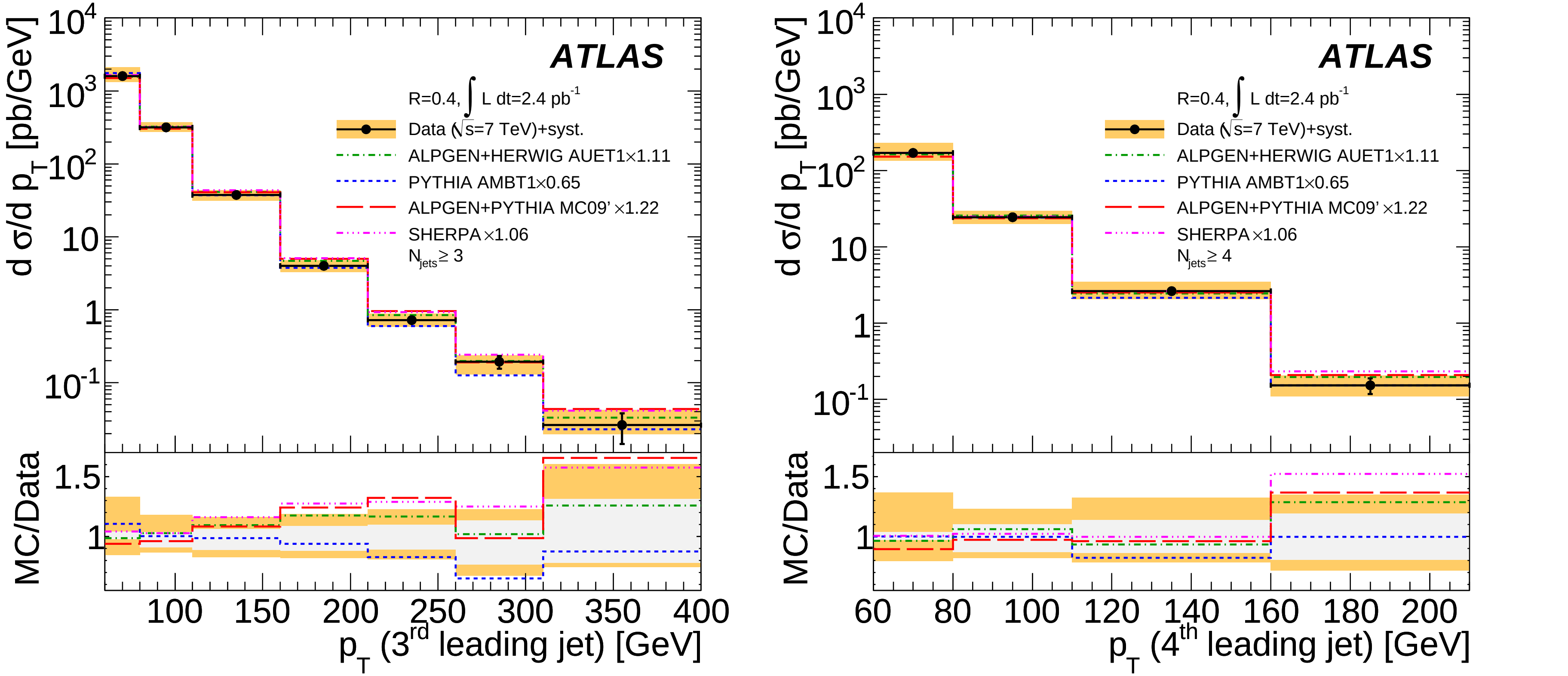

- Measurement of $d\sigma/dp_T^{\rm jet}$ for 3rd leading ($N_{jets} \geq 3$) and 4th leading jet ($N_{jets} \geq 4$) (MC predictions normalised to the measured inclusive two-jet cross section)
- Reasonable description of the data by PYTHIA, ALPGEN and SHERPA

$\Rightarrow$ Exploration of multijet production up to p_T(4th jet)$\sim$ 200 GeV

Multijet production in pp collisions at $\sqrt{s} = 7$ TeV

$N_{jets} \geq 2$ $N_{jets} \geq 3$ $N_{jets} \geq 4$

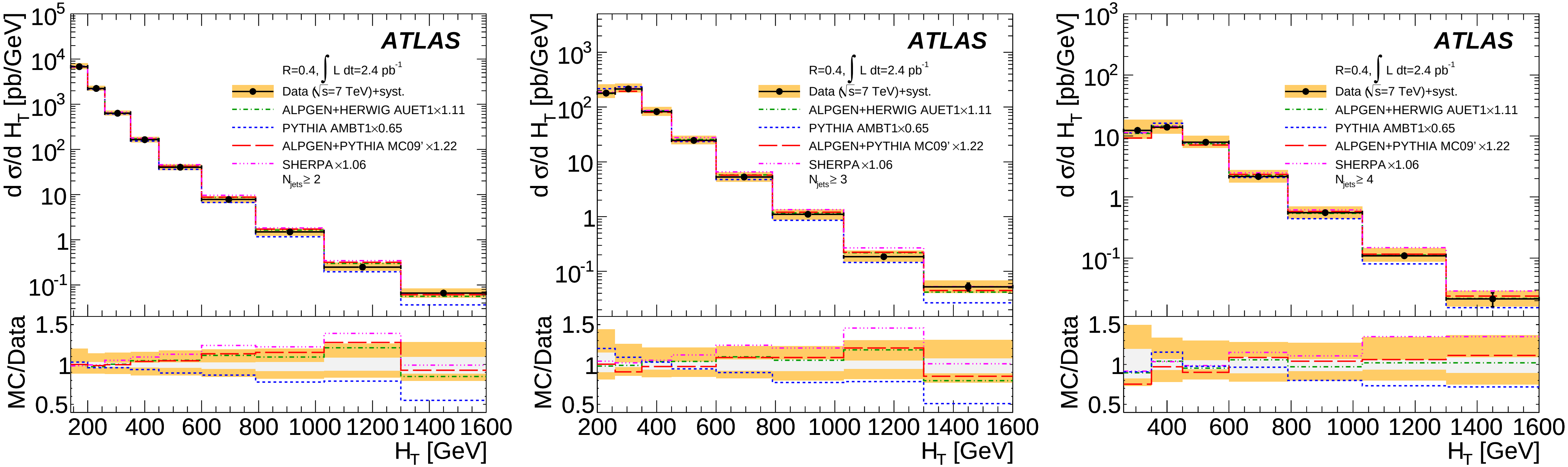

- **The variable H_T (top, searches, ...):**

$$H_T = \sum_i p_T^{jet,i}$$

- **Measurement of $d\sigma/dH_T$ for $N_{jets} \geq 2, 3, 4$**
  (MC predictions normalised to the measured inclusive two-jet cross section)
- **Reasonable description (with caveats) of the data up to $H_T \sim 1.6$ TeV**

Multijet production in pp collisions at $\sqrt{s} = 7$ TeV ($R = 0.6$)

$p_T^{min} > 60$ GeV, $p_T^{lead} > 80$ GeV $p_T^{min} > 80$ GeV, $p_T^{lead} > 110$ GeV $p_T^{min} > 110$ GeV, $p_T^{lead} > 160$ GeV

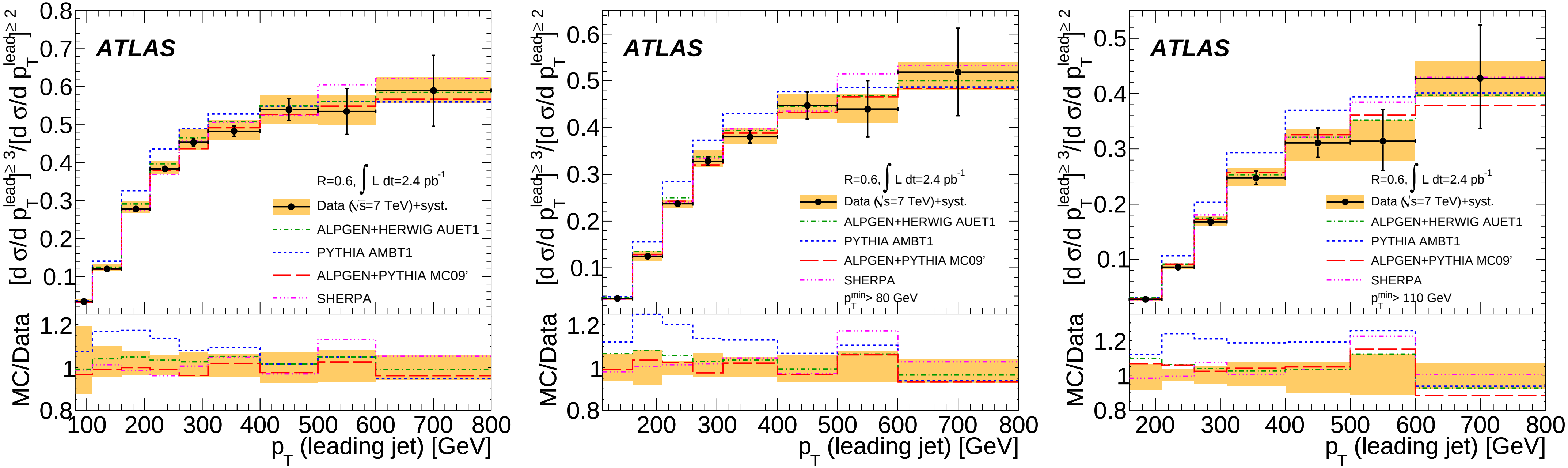

- The ratio $R_{3/2}(p_T^{lead})$ of the inclusive three-jet to two-jet cross section

$\rightarrow$ reduced experimental (sys. unc. $\sim 5\%$) and theoretical uncertainties

$\rightarrow$ sensitive probe of modelling of high order contributions and α_s

- ALPGEN and SHERPA describe the data well up to $p_T^{lead} \sim 800$ GeV while PYTHIA fails (also in the case of using other PDFs and tunes)

Multijet production in pp collisions at $\sqrt{s} = 7$ TeV ($R = 0.6$)

$p_T^{min} > 60$ GeV, $p_T^{lead} > 80$ GeV | $p_T^{min} > 80$ GeV, $p_T^{lead} > 110$ GeV | $p_T^{min} > 110$ GeV, $p_T^{lead} > 160$ GeV

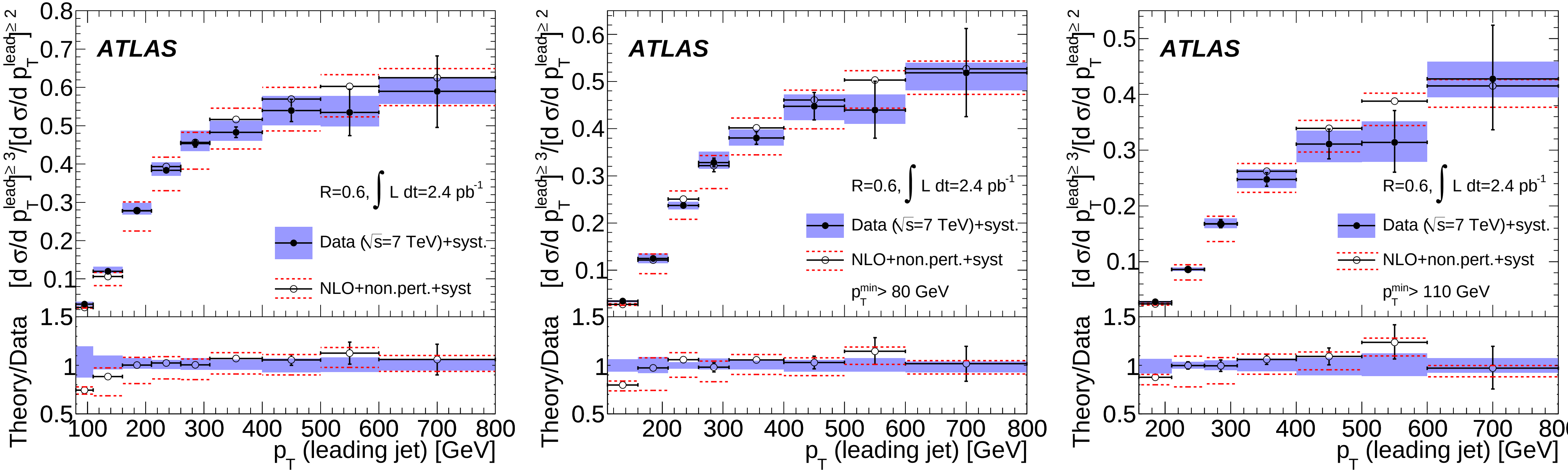

- **The ratio $R_{3/2}(p_T^{lead})$ of the inclusive three-jet to two-jet cross section**

→ reduced experimental (sys. unc. $\sim 5\%$) and theoretical uncertainties

→ sensitive probe of modelling of high order contributions and α_s

- **NLO QCD (NP corrected) describe the data well up to $p_T^{lead} \sim 800$ GeV except first bin (the description improves upon increase of cut on p_T^{lead})**

Multijet production in pp collisions at $\sqrt{s} = 7$ TeV ($R = 0.6$)

- **The comparison with the NLO QCD calculations can be more stringent by measuring $R_{3/2}$ as a function of $H_T^{(2)}$**

$$H_T^{(2)} = p_T^{lead} + p_T^{2nd\ lead}$$

→ similar experimental uncertainties

→ reduced theoretical uncertainties

- **Good description of the data by the NLO QCD calculations up to $H_T^{(2)} \sim 1.2$ TeV except for first bin due to limitations in the region $H_T^{(2)} < 160$ GeV, where NLO is effectively LO**

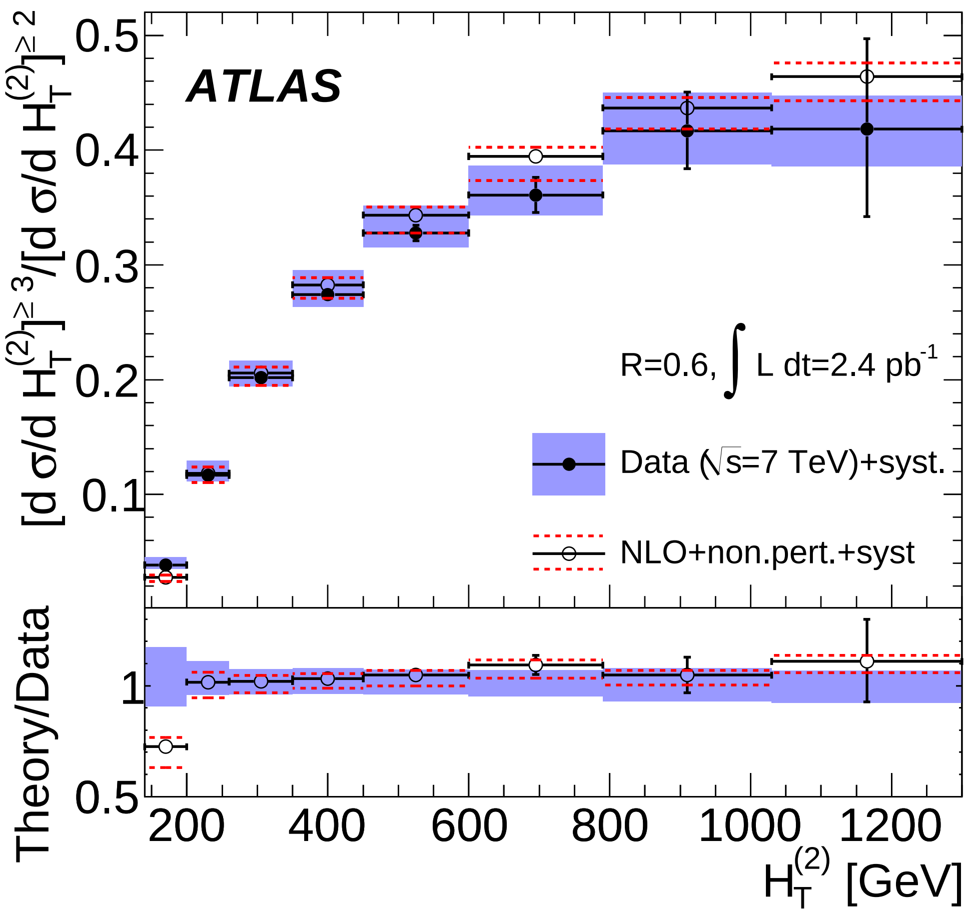

⇒ A compelling test of perturbative QCD in multijet production at LHC energies

Measurement of R_{32} and determination of α_s

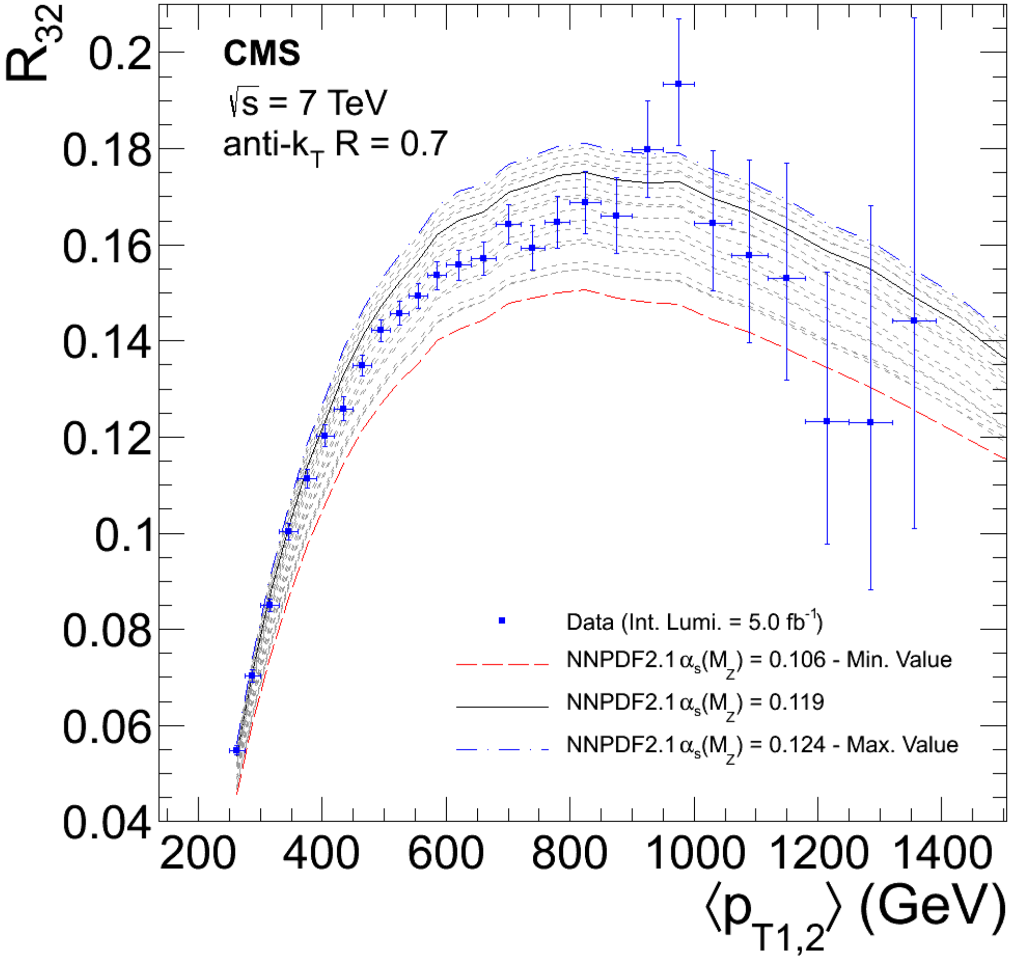

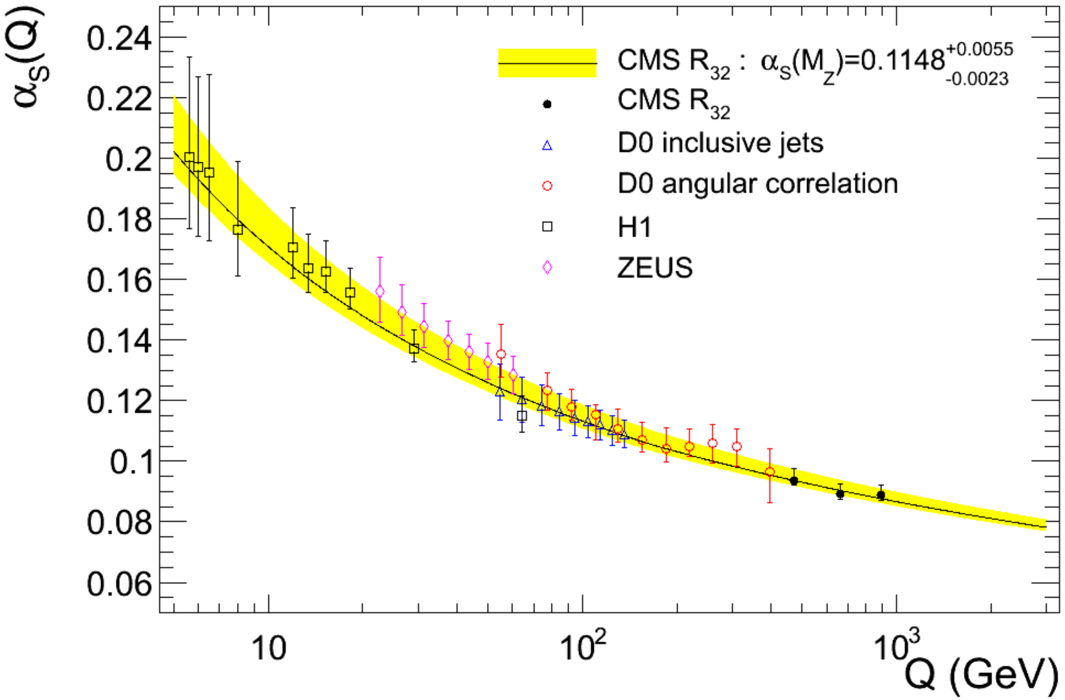

$\Rightarrow \alpha_s(M_Z) = 0.1148 \pm 0.0014(\text{exp}) \pm 0.0018(\text{PDF})^{+0.0050}_{-0.0000}(\text{scale})$

$\rightarrow$ **First determination from measurements at energy scales beyond 0.6 TeV**

$\rightarrow$ **Test of the evolution of $\alpha_s(Q)$ beyond 0.42 TeV**

Measurement of three-jet mass cross section and determination of α_s

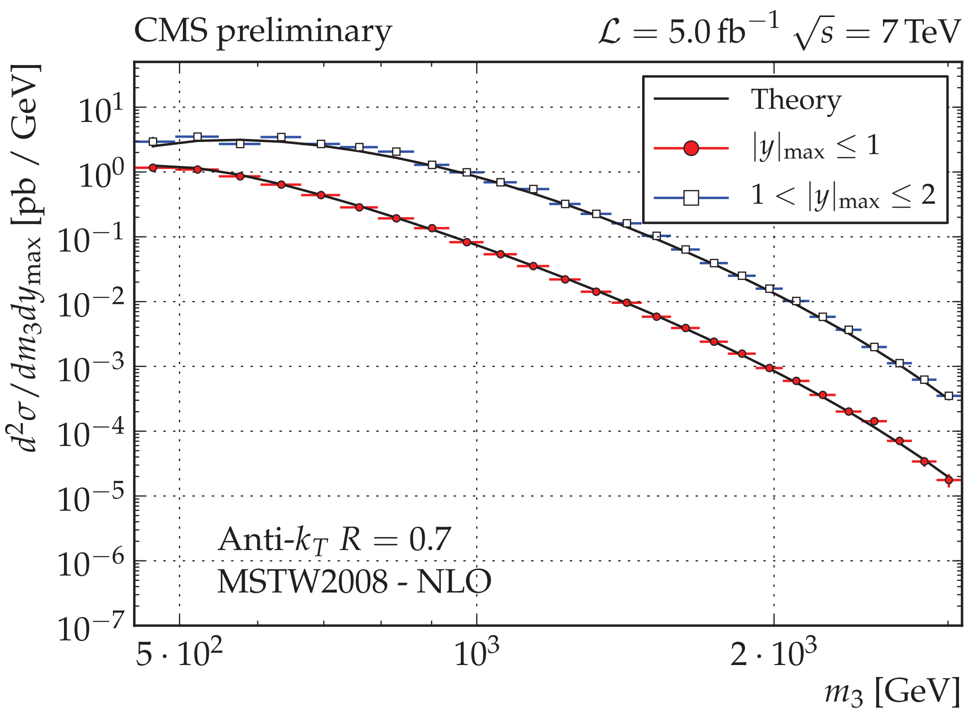

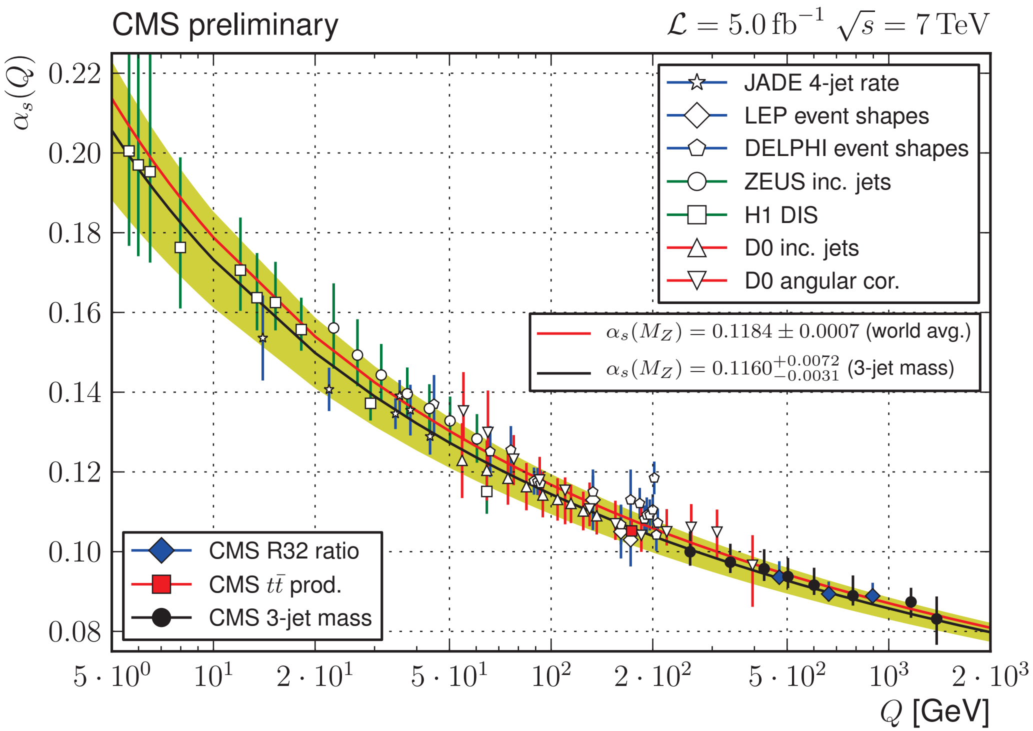

- **Measurement of the 3-jet cross section $d^2\sigma/dm_3dy_{max}$**

$\rightarrow$ at least three jets with $p_T > 100$ GeV and $|y| < 3$ using anti-k_T algorithm $R = 0.7$

$\rightarrow$ the measurements cover $450 < m_3 < 3.1$ TeV

- **NLO QCD calculations describe well the measurements**

$$\Rightarrow \alpha_s(M_Z) = 0.1160^{+0.0025}_{-0.0023}(\mathrm{exp, PDF, NP})^{+0.0068}_{-0.0021}(\mathrm{scale})$$

$\rightarrow$ Test of the evolution of $\alpha_s(Q)$ up to 1.4 TeV

Measurements of jet production at $\sqrt{s} = 2.76$ TeV

Inclusive jet cross sections in pp collisions at $\sqrt{s} = 2.76$ TeV

- Measurement of the inclusive jet cross section $d^2\sigma/dp_T dy$ as a function of p_T for different ranges in y (from $|y| < 0.3$ to $3.6 < |y| < 4.4$)

→ Every jet with $p_T > 20$ GeV and $|y| < 4.4$ defined using the anti-k_T algorithm with $R = 0.4$ ($R = 0.6$) in pp collisions at $\sqrt{s} = 2.76$ TeV using $\mathcal{L} = 0.2$ pb^{-1}

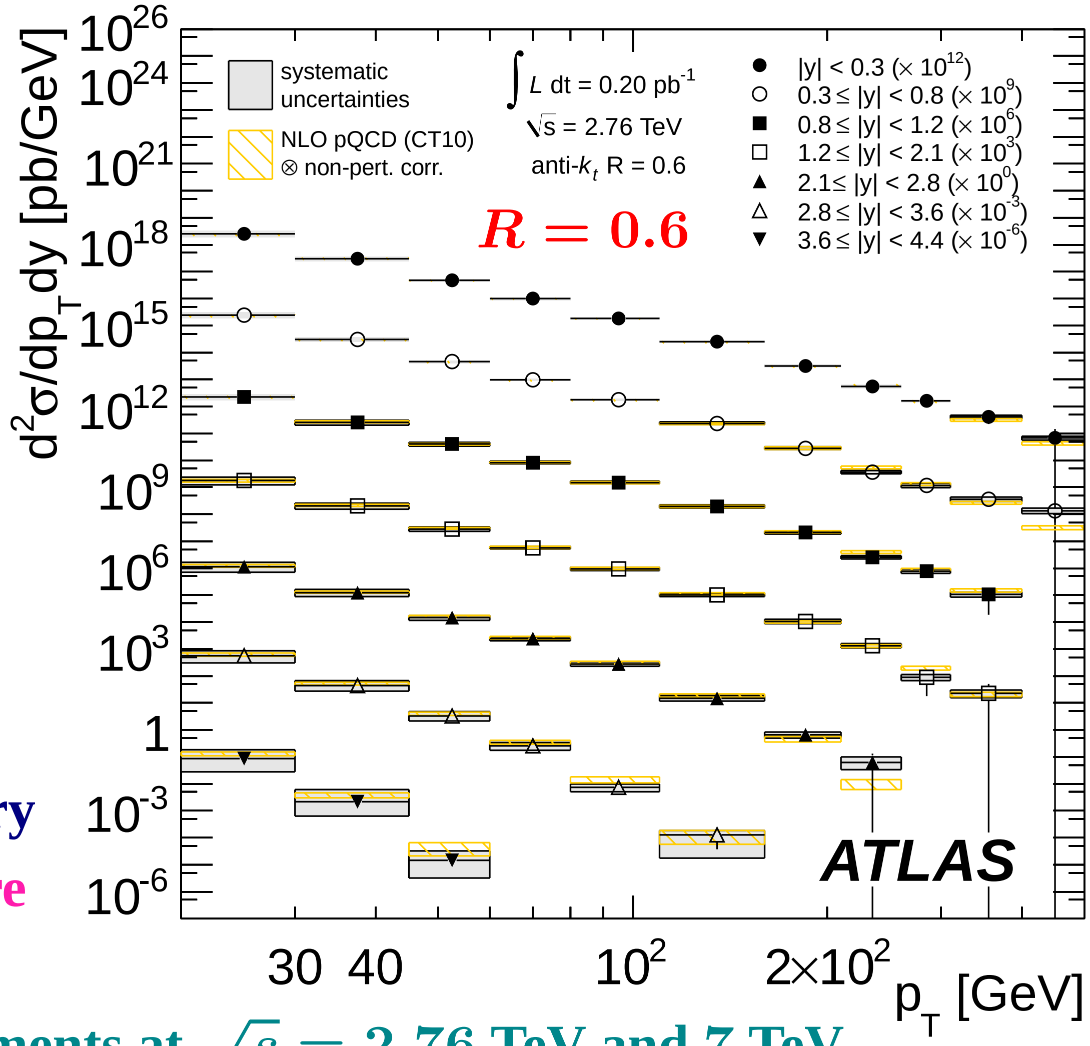

- Measurements with the same detector at different $\sqrt{s}$ → stringent tests of the theory since dominant systematic uncertainties are correlated

⇒ Simultaneous fit (or ratios) of measurements at $\sqrt{s} = 2.76$ TeV and 7 TeV benefit from reduced uncertainties

Inclusive jet cross sections in pp collisions at $\sqrt{s} = 2.76$ TeV

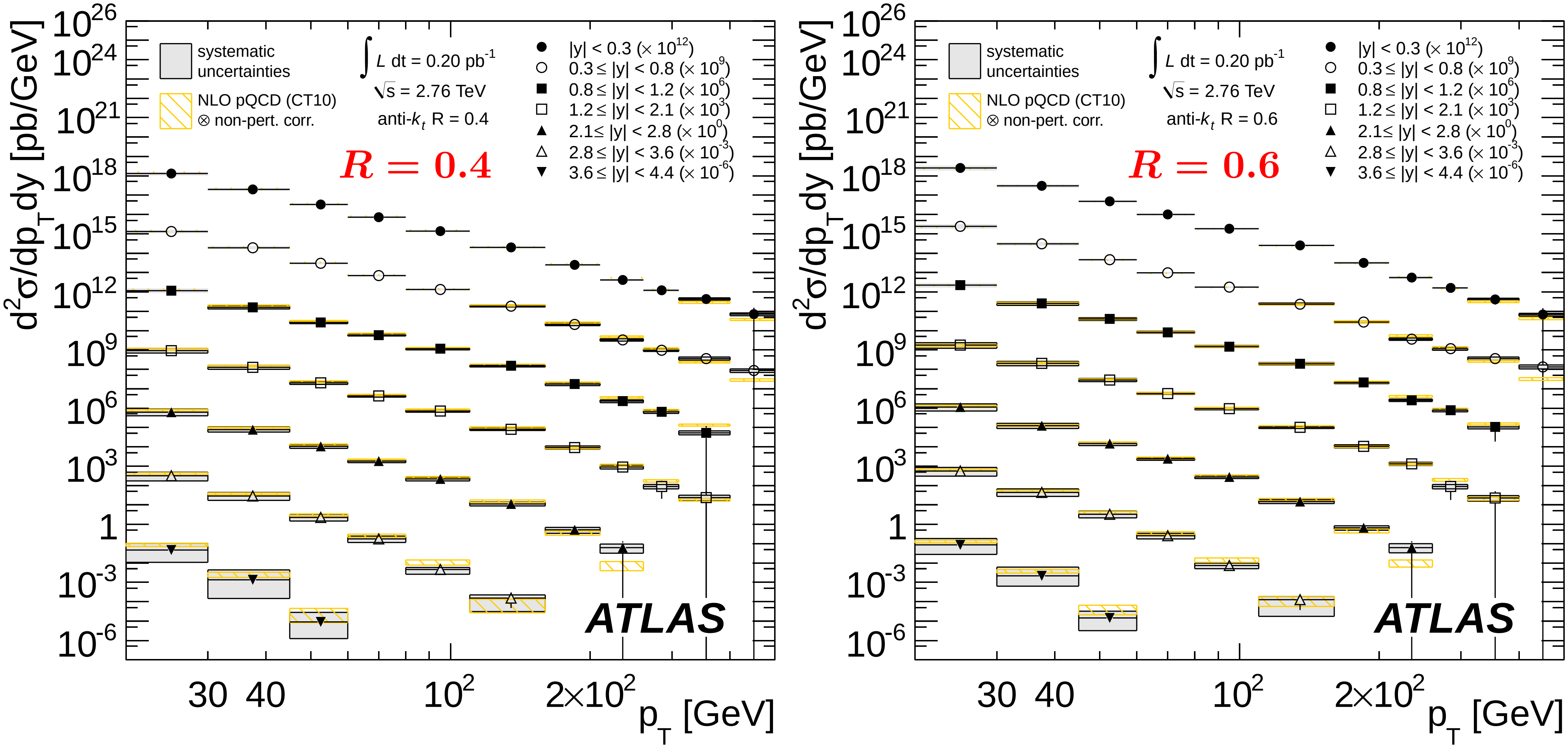

- **The measurements span jet p_T from 20 GeV to 430 GeV in the region $|y| < 4.4$ and cover seven orders of magnitude in cross section $\rightarrow$ comparison with NLO QCD**

Inclusive jet cross sections in pp collisions at $\sqrt{s} = 2.76$ TeV ($R = 0.6$)

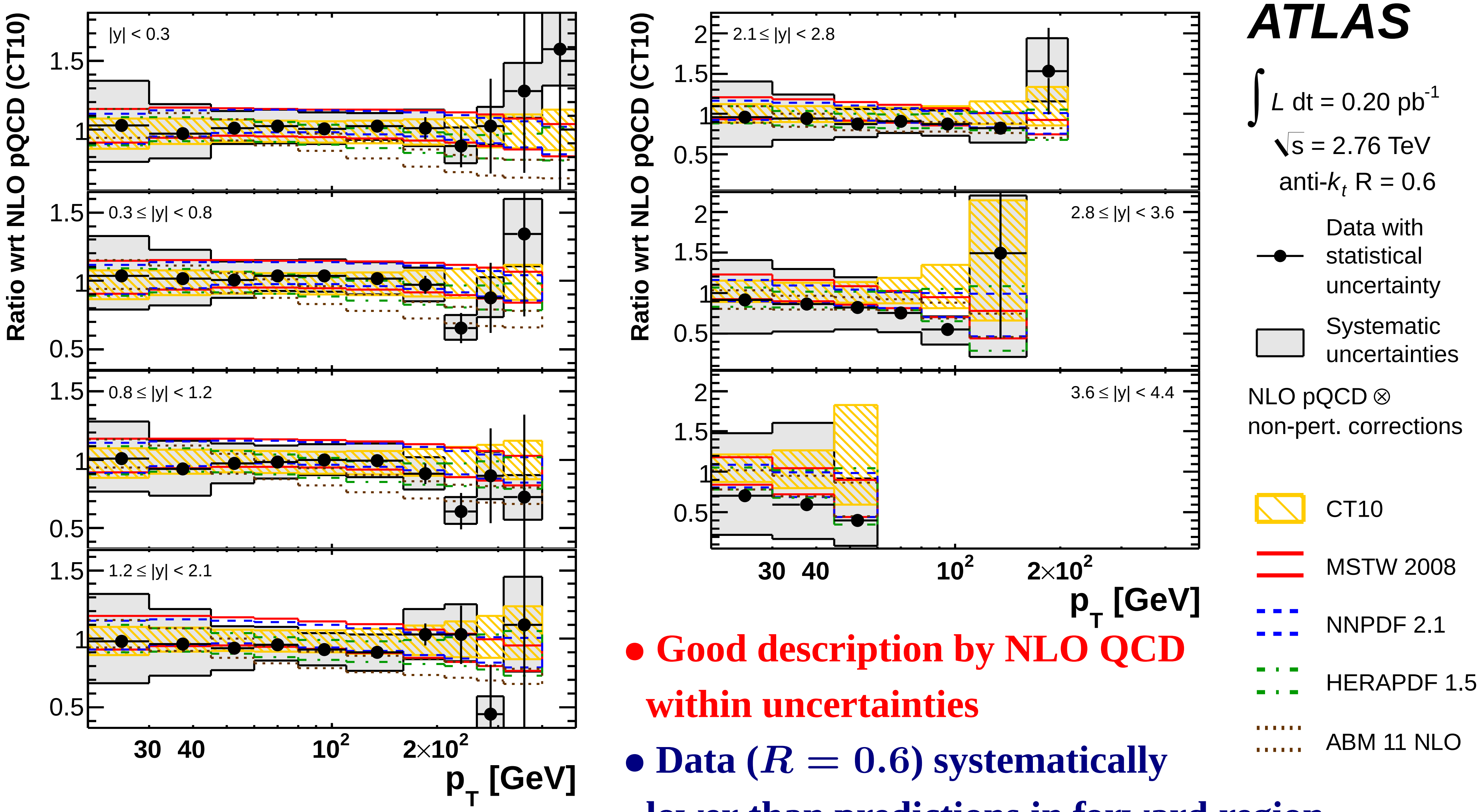

- **Good description by NLO QCD within uncertainties**
- **Data ($R = 0.6$) systematically lower than predictions in forward region**

Inclusive jet cross sections in pp collisions at $\sqrt{s} = 2.76$ TeV ($R = 0.4$)

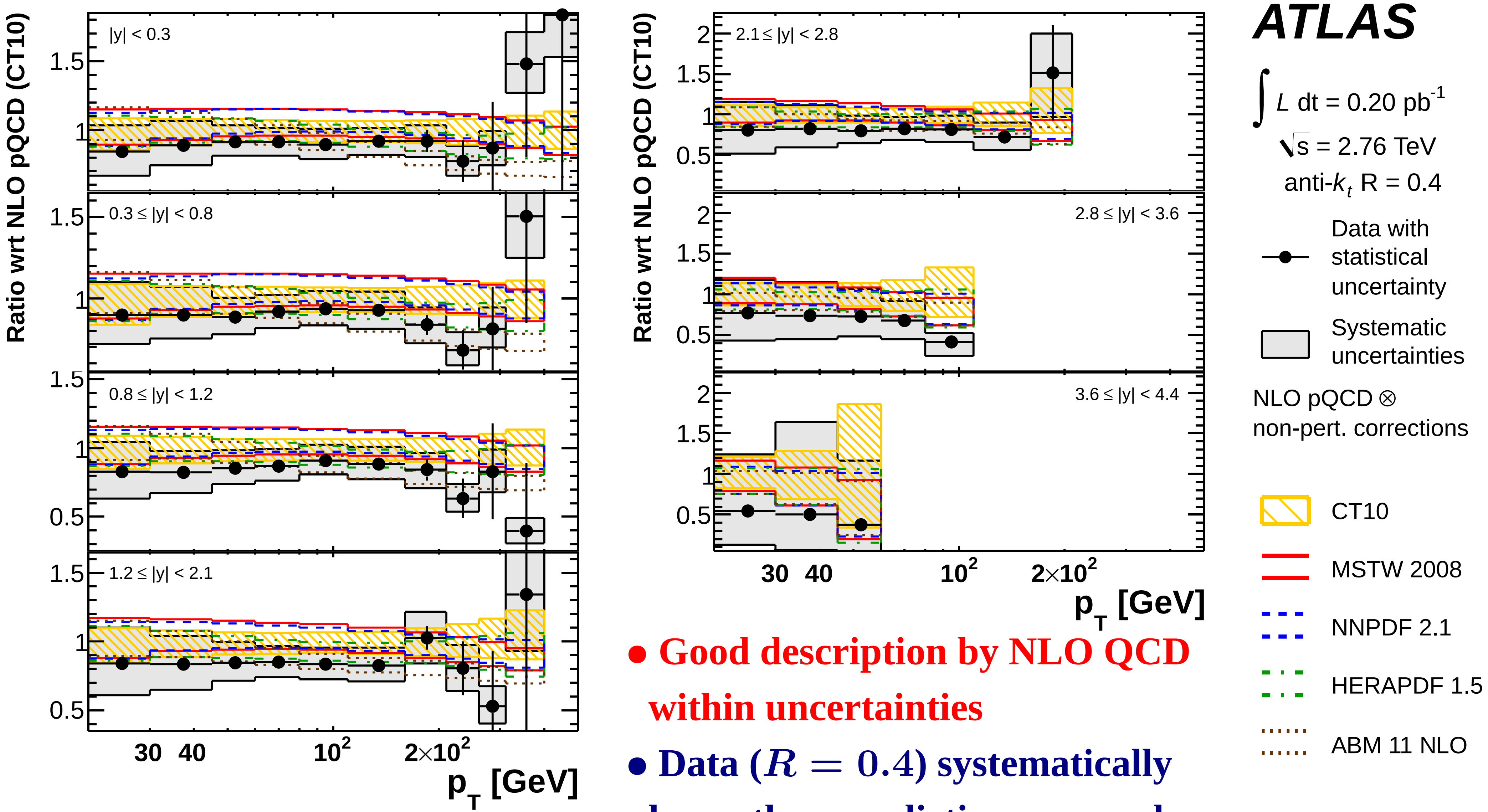

- **Good description by NLO QCD within uncertainties**
- **Data ($R = 0.4$) systematically lower than predictions everywhere**

Ratios of jet cross sections at different $\sqrt{s}$

- Invariant cross section $\leftrightarrow$ inclusive jet double differential cross section

$$E\frac{d^3\sigma}{dp^3} = \frac{1}{2\pi p_T}\frac{d^2\sigma}{dp_T dy}$$

- Dimensionless scale-invariant cross section:

$$F(y, x_T, \sqrt{s}) = p_T^4 E\frac{d^3\sigma}{dp^3} = \frac{p_T^3}{2\pi}\frac{d^2\sigma}{dp_T dy} = \frac{s}{8\pi}x_T^3\frac{d^2\sigma}{dx_t dy}$$

$$x_T \equiv 2p_T/\sqrt{s}$$

in the quark parton model $F(y, x_T, \sqrt{s})$ does not depend on s

QCD $\rightarrow$ scaling violations; main effects: scale dependence of PDFs and α_s

- Cross section ratio $\rho(y, x_T) = \frac{F(y, x_T, 2.76\ \mathrm{TeV})}{F(y, x_T, 7\ \mathrm{TeV})}$

scaling violations $\rightarrow$ deviations of $\rho(y, x_T)$ from unity!

- Cross section ratio $\rho(y, P_T) = \frac{\sigma(y, p_T, 2.76\ \mathrm{TeV})}{\sigma(y, p_T, 7\ \mathrm{TeV})}$

since JES uncert. dominant $\rightarrow$ systematic uncert. significantly reduced in ratio (same p_T)

Theoretical uncertainties on the ratios $\rho(y, x_T)$ and $\rho(y, p_T)$

cross section at 2.76 TeV

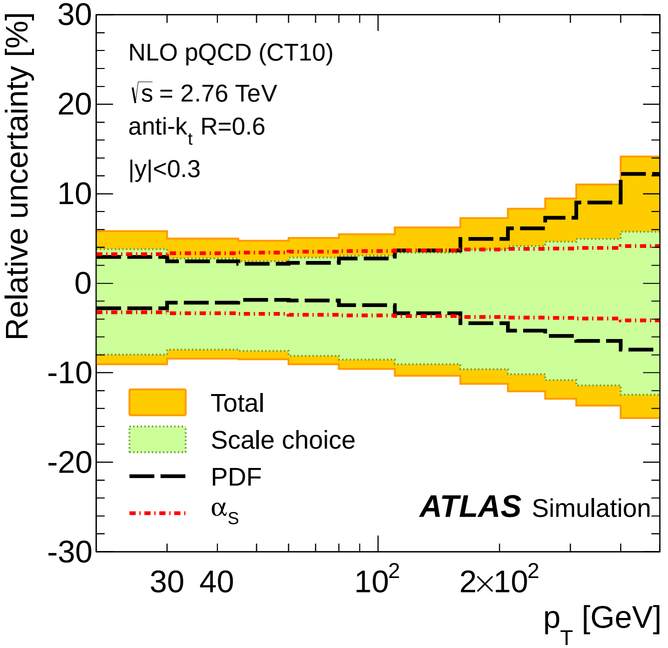

$\rho(y, x_T)$

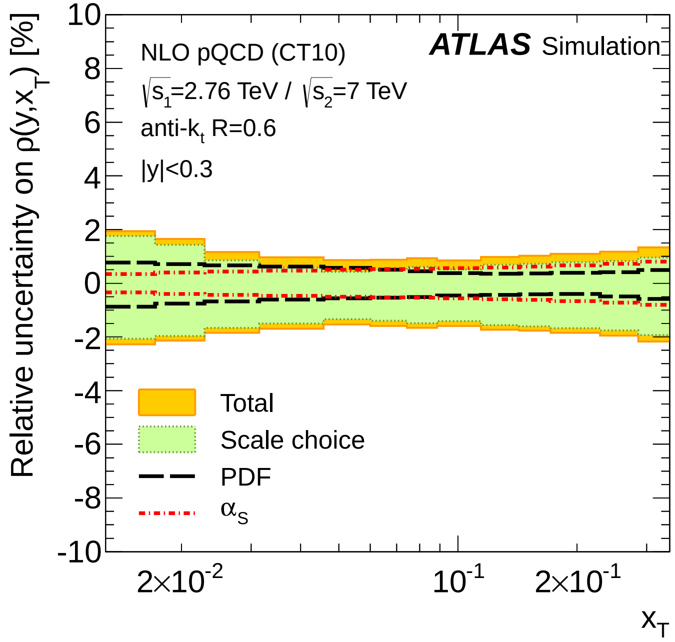

$\rho(y, p_T)$

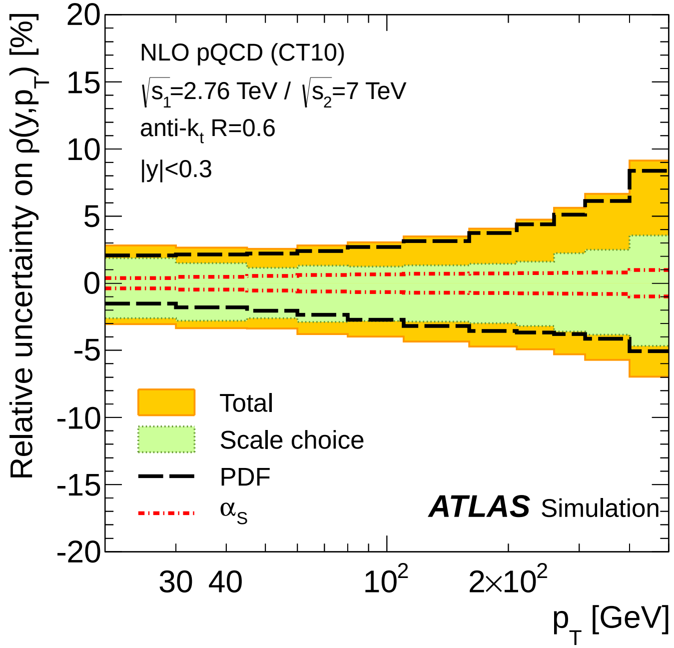

- **Theoretical uncertainties: terms beyond NLO (scales), PDFs and α_s**

- **Theoretical uncertainties on ratios estimated by simultaneous variations:**

→ significantly reduced (few %!) for $\rho(y, x_T)$

→ uncertainty on $\rho(y, p_T)$ below 5% for p_T up to 200 GeV in central region

Non-perturbative corrections to the ratios $\rho(y, x_T)$ and $\rho(y, p_T)$

- NP corrections for $\rho(y, p_T)$

$\rightarrow$ similar p_T dependence for R=0.4 and 0.6

$\rightarrow$ below 1 since the corrections are bigger for 7 TeV than for 2.76 TeV

- NP corrections for $\rho(y, x_T)$

$\rightarrow$ different x_T dependence for R=0.4 and 0.6; for same x_T

$$x_T \equiv 2p_T/\sqrt{s} \Rightarrow$$

p_T(7 TeV) = (7/2.76) p_T(2.76 TeV)

and NP correction at high p_T is flat

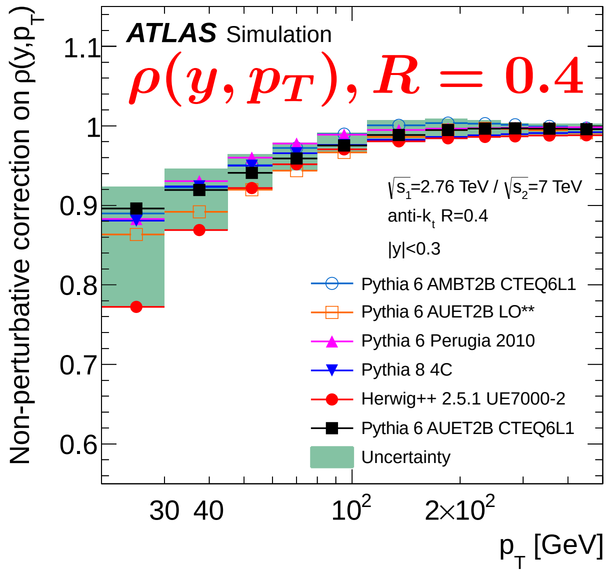

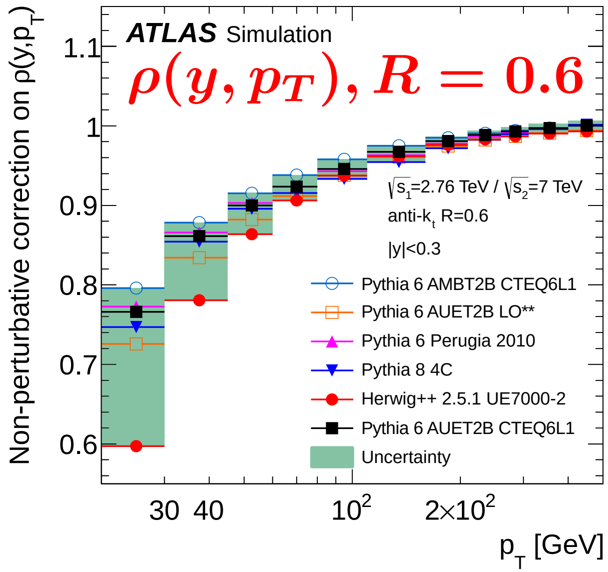

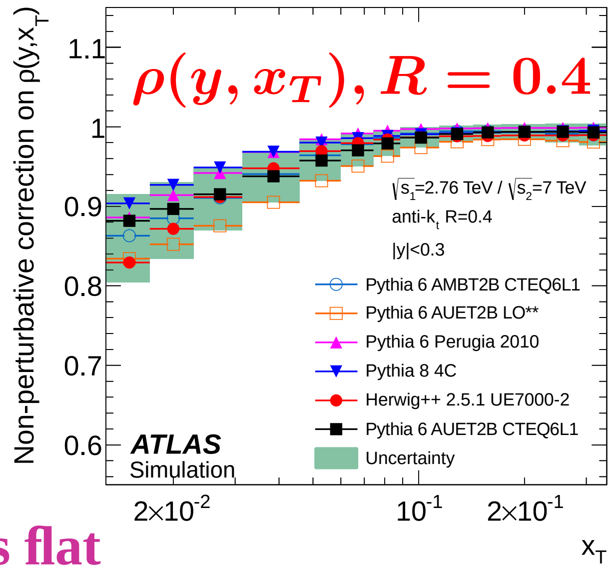

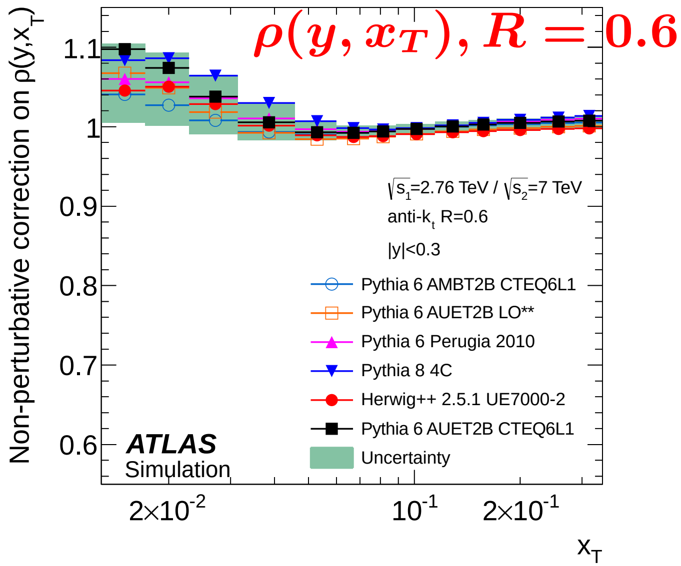

Ratio $\rho(y, x_T)$ of $\sqrt{s} = 2.76$ TeV and 7 TeV inclusive jet data

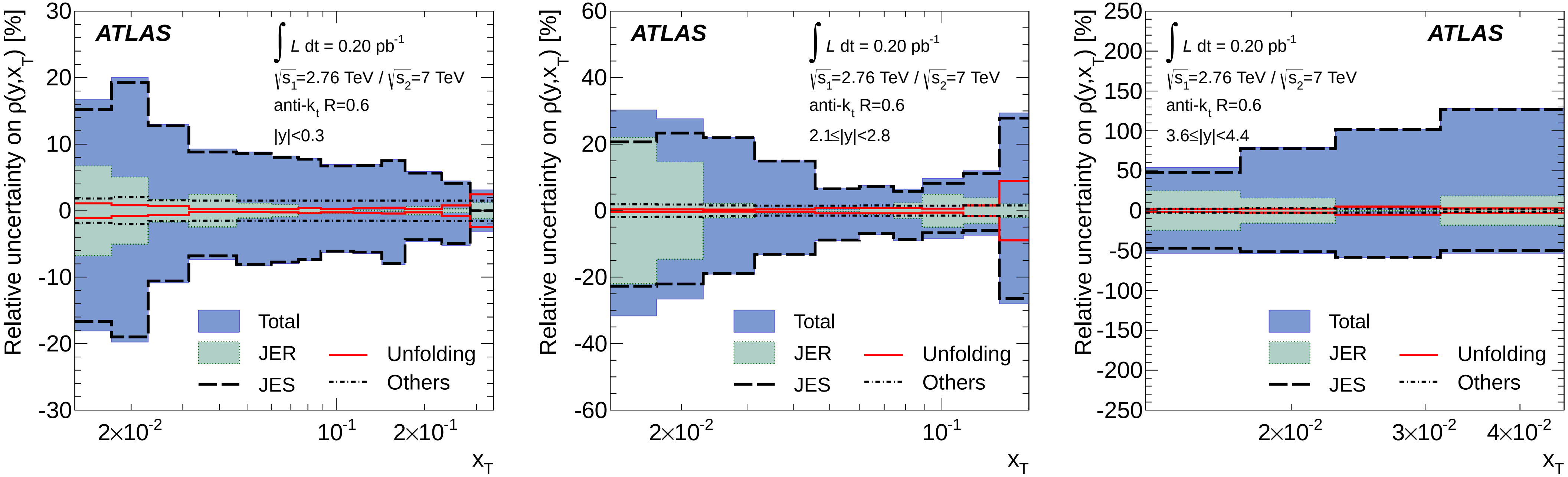

- Systematic uncertainties due to jet reconstruction and calibration are considered as fully correlated

$\longrightarrow$ others are treated as uncorrelated (added in quadrature)

- Uncertainty for $\rho(y, x_t)$ with $R = 0.6$

$\longrightarrow$ 5-20% in the central region

$\longrightarrow$ $^{+160}_{-60}\%$ in forward region

- Similar for $R = 0.4$, except $\rightarrow \pm 15\%$ for central jets at low p_T

Ratio $\rho(y, x_T)$ of $\sqrt{s} = 2.76$ TeV and 7 TeV inclusive jet data

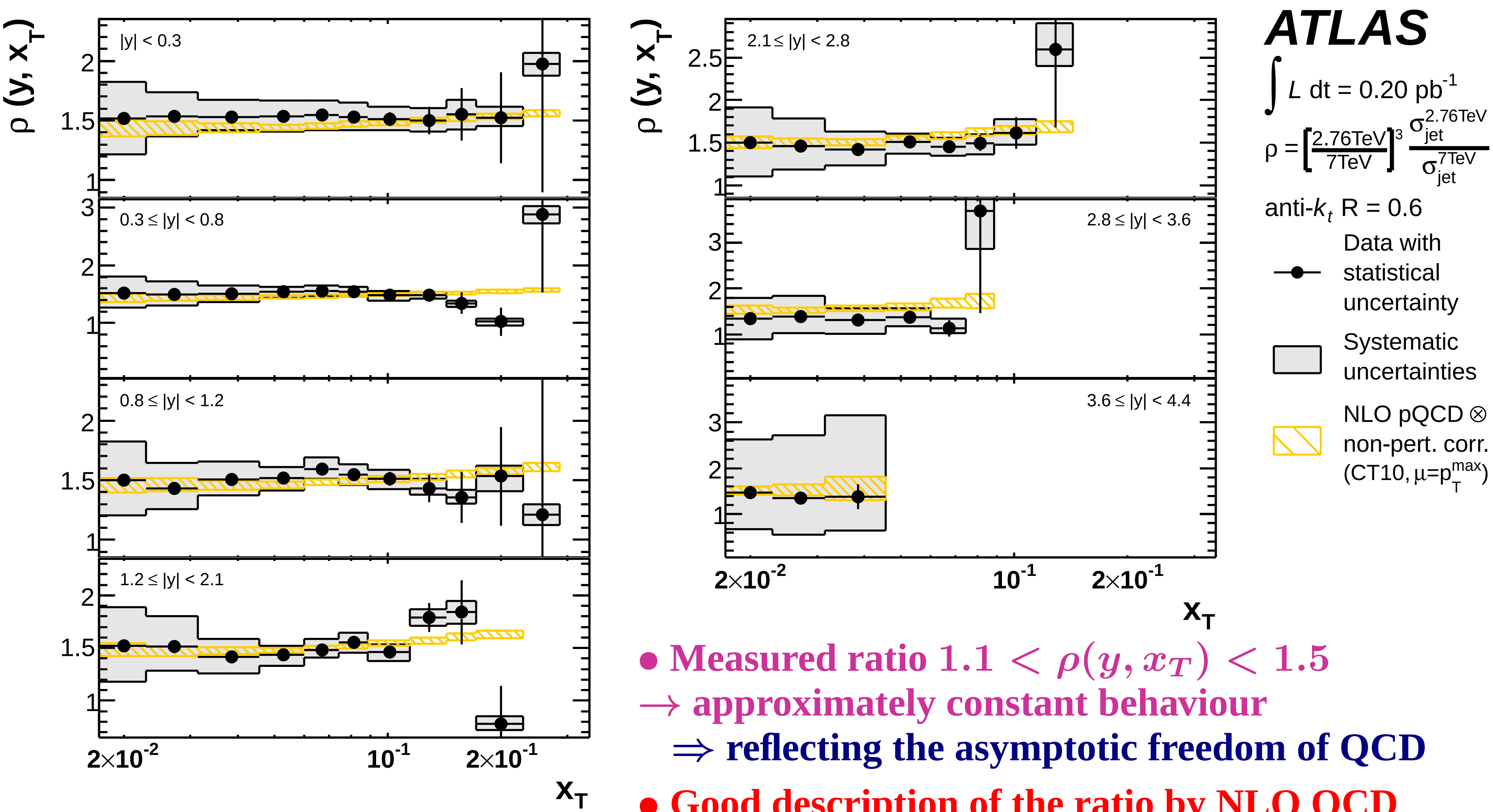

- Measured ratio $1.1 < \rho(y, x_T) < 1.5$

$\rightarrow$ approximately constant behaviour

$\Rightarrow$ **reflecting the asymptotic freedom of QCD**

- Good description of the ratio by NLO QCD

Ratio $\rho(y, p_T)$ of $\sqrt{s} = 2.76$ TeV and 7 TeV inclusive jet data

- **Systematic uncertainties due to jet reconstruction and calibration are considered as fully correlated**

$\longrightarrow$ others are treated as uncorrelated (added in quadrature)

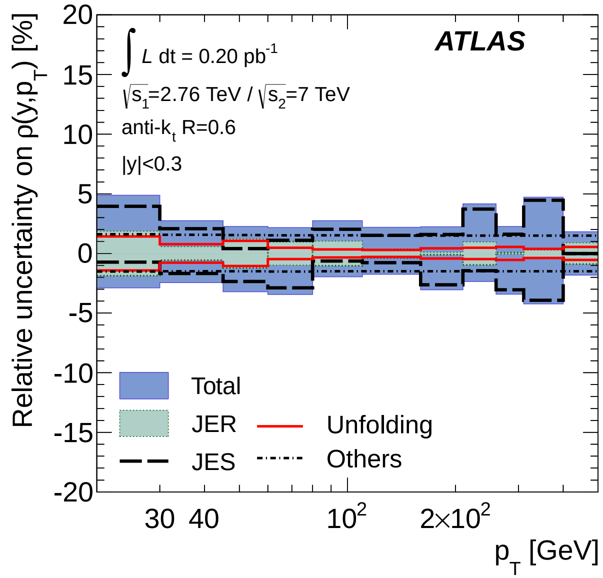

- **Significant reduction of uncertainty for $\rho(y, p_t)$**

$\longrightarrow$ well below 5% in the central region

$\longrightarrow$ forward region: $\pm 70\%$ for $R = 0.6$, $^{+100}_{-70}\%$ for $R = 0.4$

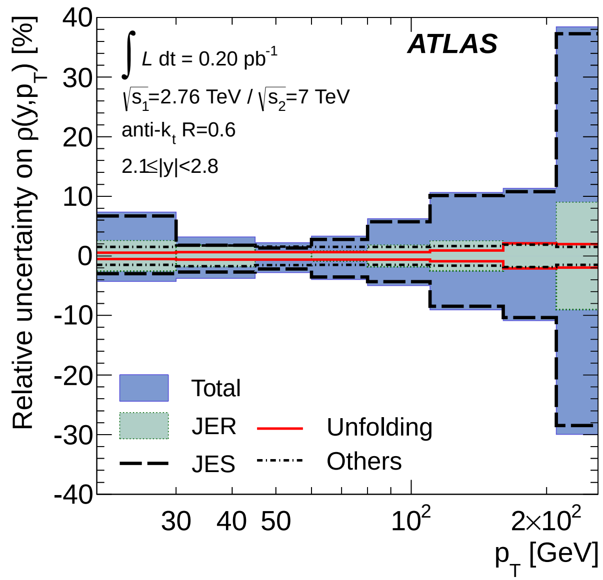

- **Comparison of the measured ratio $\rho(y, p_t)$ with NLO QCD**

$\longrightarrow$ experimental uncertainty generally smaller than theoretical

$\longrightarrow$ measurements slightly higher than theory in central region

$\longrightarrow$ measurements lower than theory in forward region

$\longrightarrow$ sensitivity to PDFs

$\Longrightarrow$ the measurements may contribute to constrain PDFs in a global NLO QCD fit

Ratio $\rho(y, p_T)$ of $\sqrt{s} = 2.76$ TeV and 7 TeV inclusive jet data

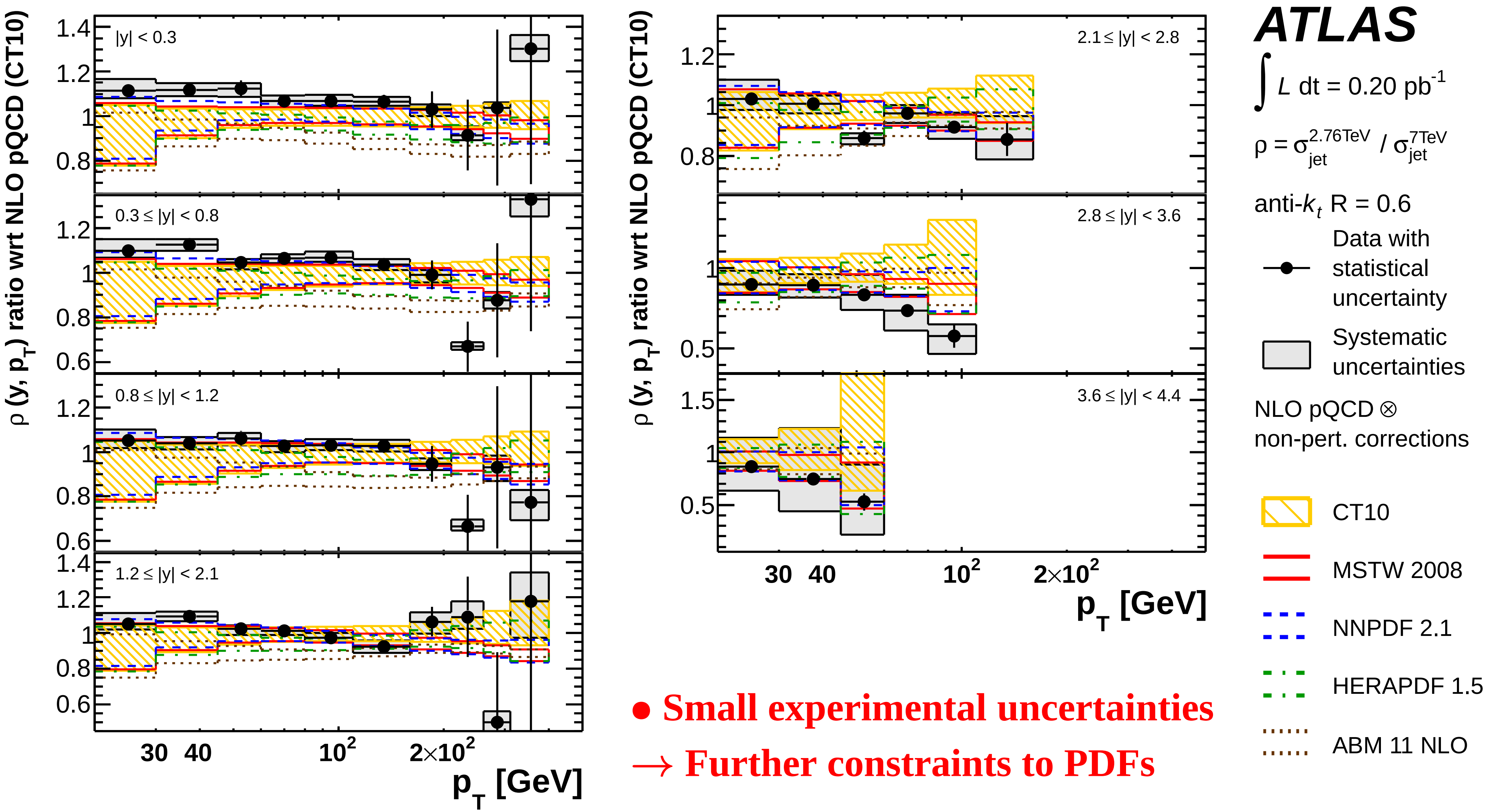

- **Small experimental uncertainties**

→ **Further constraints to PDFs**

NLO QCD analysis of HERA and ATLAS jet data

- Inclusive jet production at low/moderate p_T
  $\rightarrow$ sensitive to the gluon distribution function
- Strong correlation of systematic uncertainties between inclusive jet measurements at $\sqrt{s} = 2.76$ and 7 TeV
  $\rightarrow$ increased sensitivity when both are included
  in a NLO QCD fit of the PDFs
  $\rightarrow$ proper treatment of correlations (specially JES)!
- NLO QCD combined fit of HERA I ($Q^2 > 3.5$ GeV^2) and ATLAS jet data ($p_T > 45$ GeV)
  $\rightarrow$ independent fits for $R = 0.4$ and 0.6
  $\Rightarrow$ Very good fit quality
  $\Rightarrow$ harder gluon distribution and smaller uncertainty
  when including ATLAS data $\rightarrow$ softer sea distribution
  - Including only one ATLAS data set, 2.76 or 7 TeV,
    $\rightarrow$ the impact on xg is largely reduced

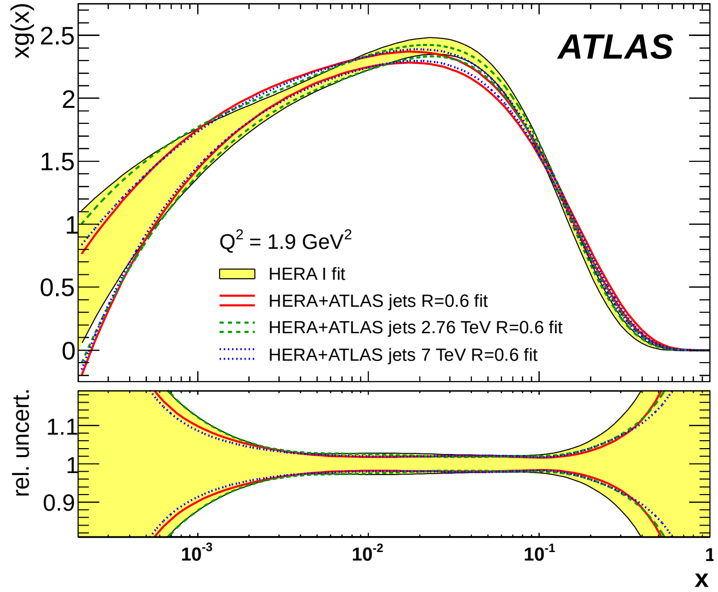

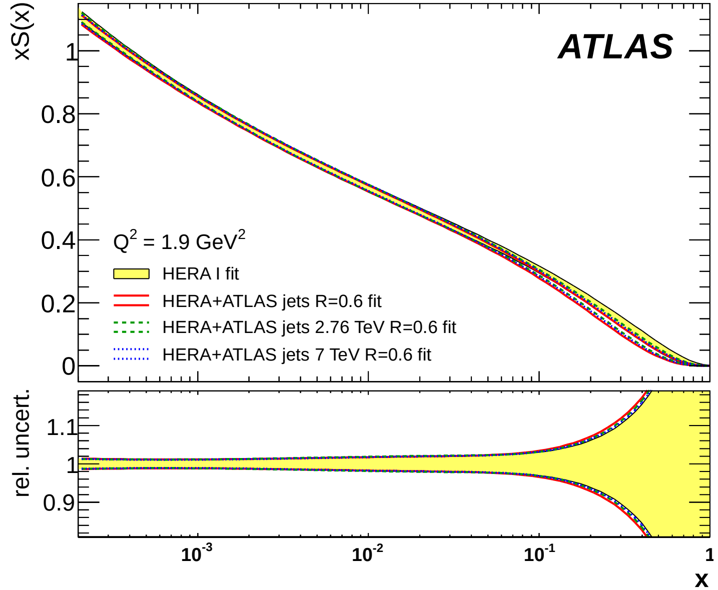

NLO QCD analysis of HERA and ATLAS jet data

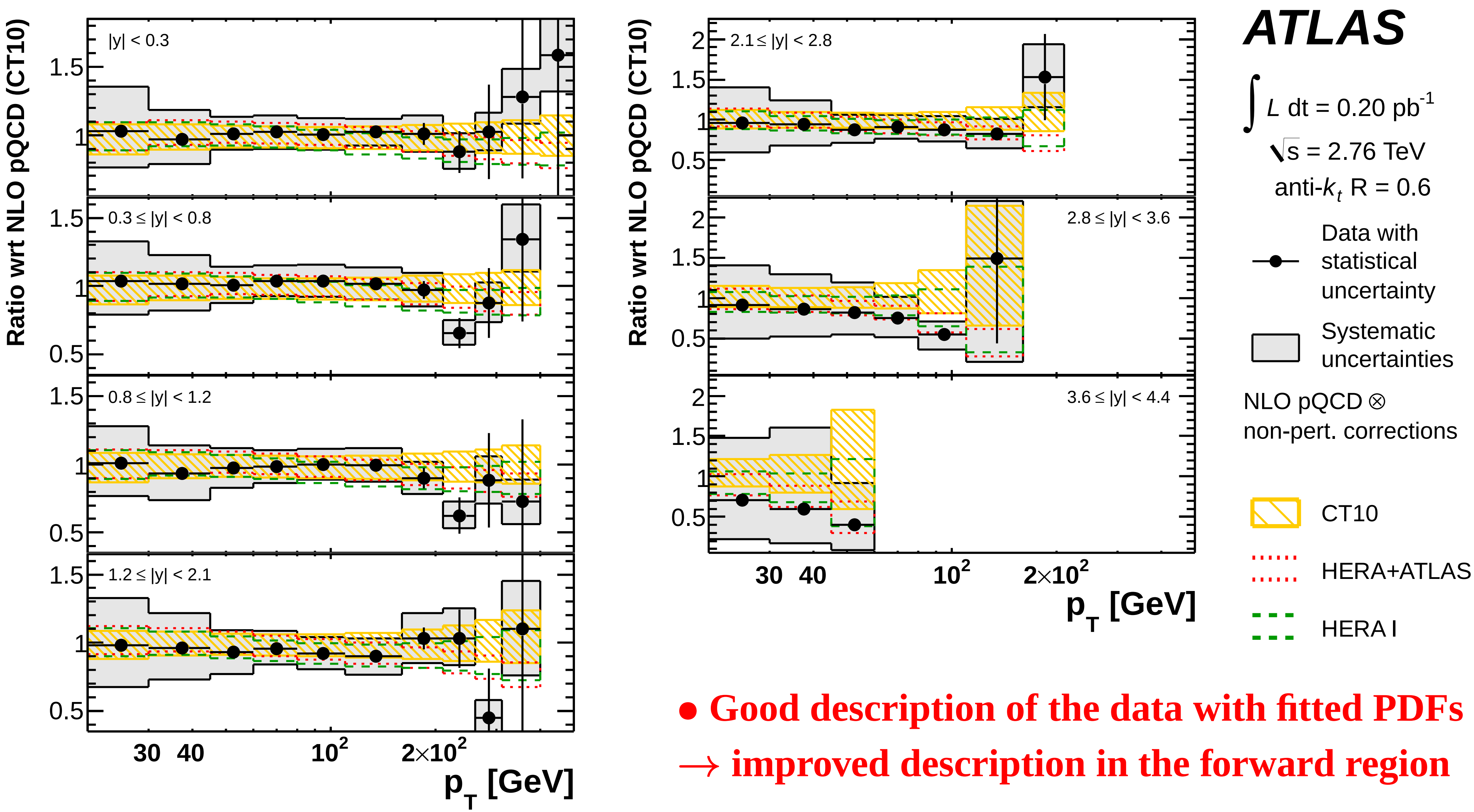

- Good description of the data with fitted PDFs
→ improved description in the forward region

NLO QCD analysis of HERA and ATLAS jet data

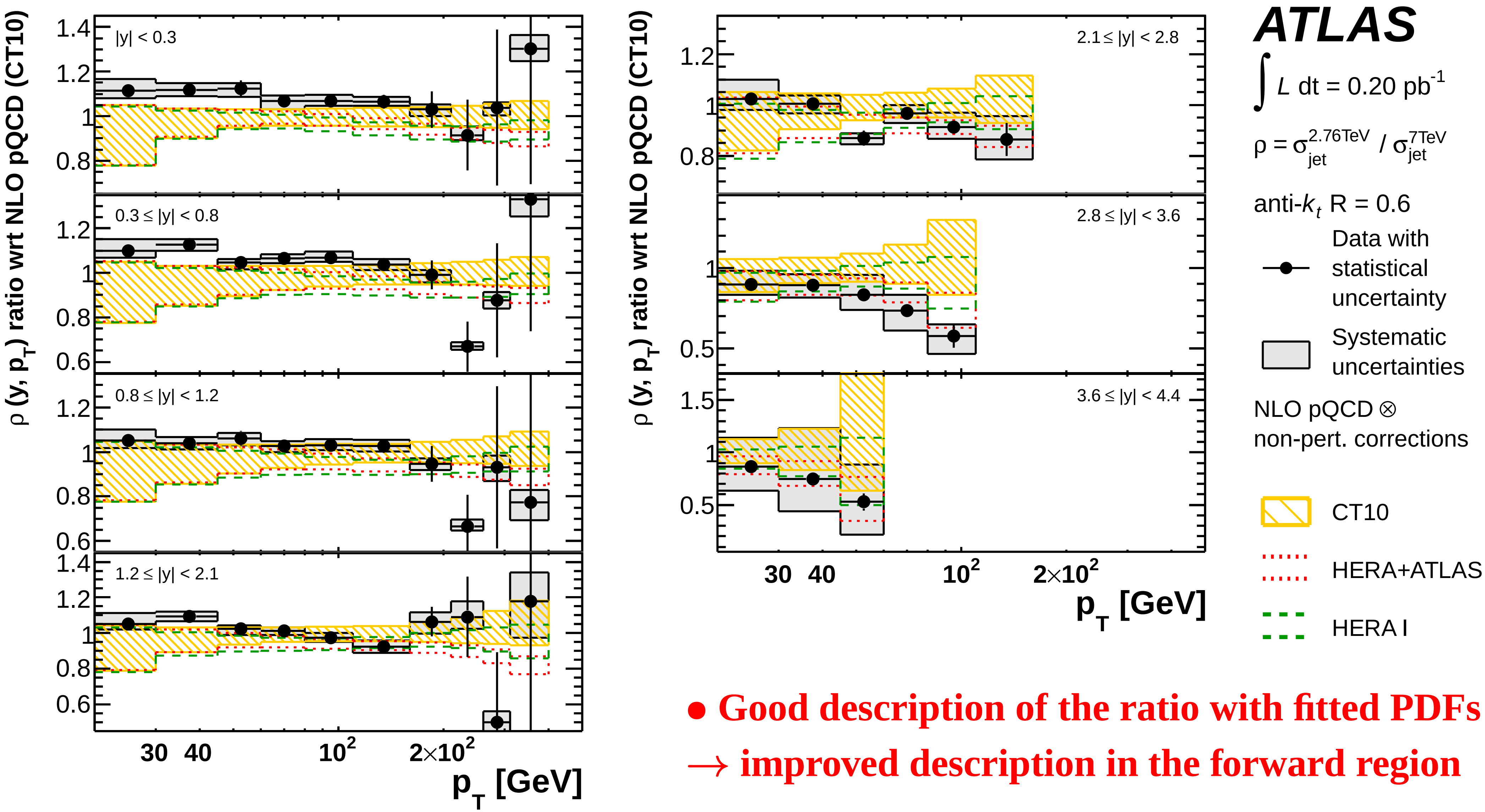

- Good description of the ratio with fitted PDFs

→ improved description in the forward region

Dijet azimuthal decorrelations

Dijet azimuthal decorrelations in pp collisions at $\sqrt{s} = 7$ TeV

- Azimuthal decorrelations between the two central jets with highest p_T are sensitive to the dynamics of multiple jets

$\rightarrow$ Events with only two high-p_T jets: $\Delta\phi \sim \pi$

$\rightarrow$ Events with $\Delta\phi \ll \pi$: evidence of multiple jets

- QCD prediction: $\Delta\phi$ distribution narrows with increasing jet p_T

- Test of QCD for multijet production <u>without</u> requiring the measurement of additional jets

- A detailed understanding of dijet production with $\Delta\phi \ll \pi$ is relevant for searches for new physical phenomena

$\phi_1 = -2.8, \phi_2 = 0.3 \rightarrow \Delta\phi = 3.1$

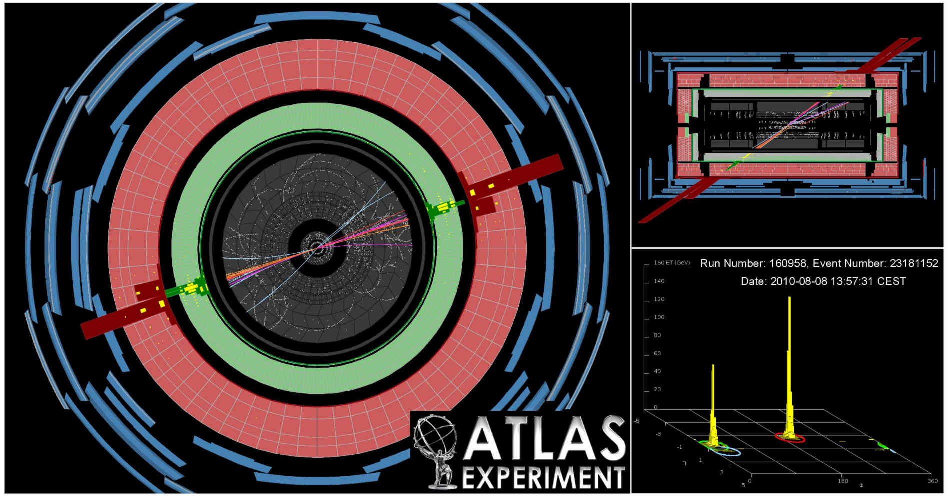

$\phi_1 = -2.8, \phi_2 = -0.3 \rightarrow \Delta\phi = 2.5$

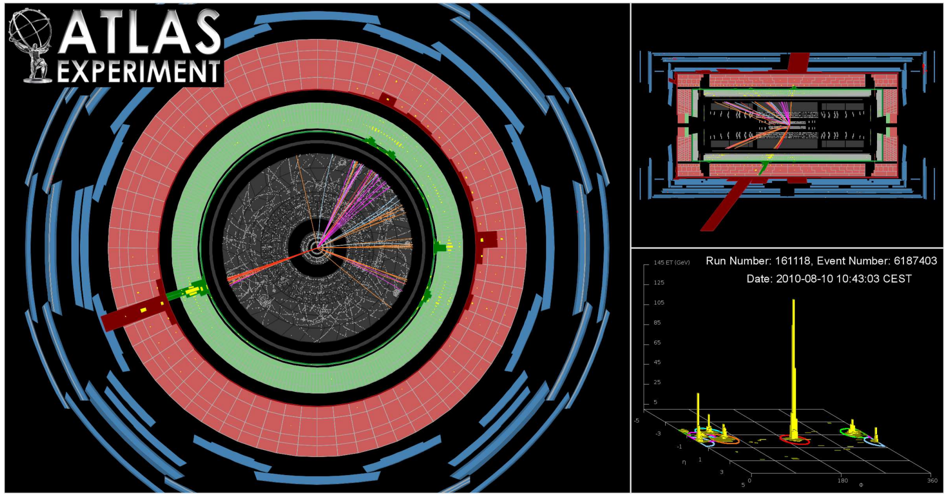

Dijet azimuthal decorrelations in pp collisions at $\sqrt{s} = 7$ TeV

- **Measurement of normalised differential cross section $(1/\sigma)d\sigma/d\Delta\phi$ with $\Delta\phi$ computed from the two leading jets in the region $\pi/2 \leq \Delta\phi \leq \pi$**
  Anti-k_T algorithm with $R = 0.6$

$\rightarrow$ **Requirements on all jets:**
$p_T > 100$ GeV and $|y| < 2.8$

$\rightarrow$ **Further requirements on leading jets:**
both $|y| < 0.8$ and $p_T^{jet1} > p_T^{max}$

- **Measurement in nine regions of p_T^{max} starting at 110 GeV and up to 800 GeV**
- **The azimuthal decorrelation increases when a third high-p_T jet is required; additional jets lead to a wider distribution**

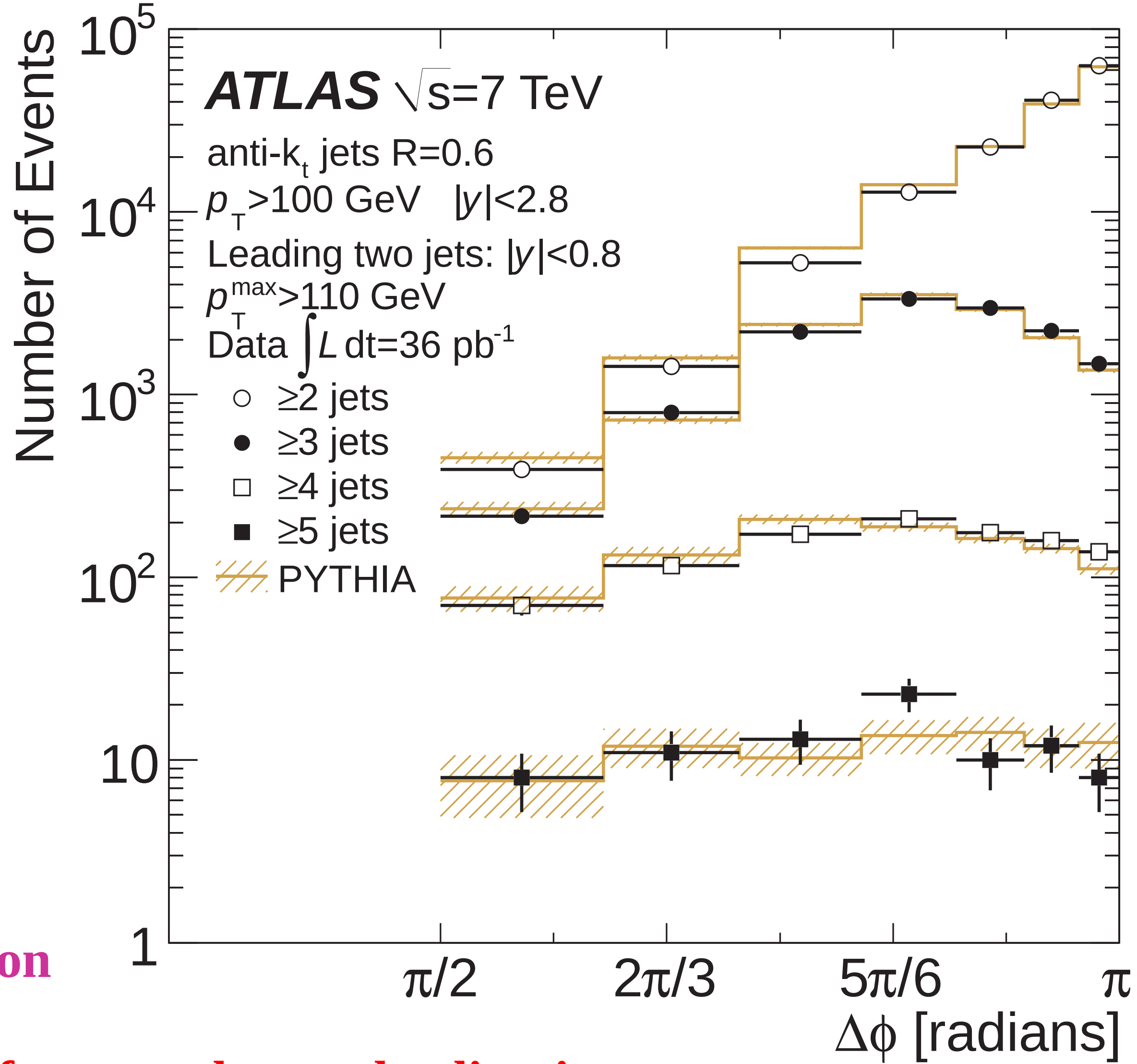

- **Now, let's forget the additional jets and focus on the two leading jets...**

Dijet azimuthal decorrelations

- **Measurement of normalised differential cross section $(1/\sigma)d\sigma/d\Delta\phi$ with $\Delta\phi$ computed from the two leading jets in the region $\pi/2 \leq \Delta\phi \leq \pi$**
- **Leading sources of systematic uncertainty: JES 2-17%, unfolding 1-19%, JER and JAR 0.5-5% (range $\Delta\phi \sim \pi, \pi/2$)**
- **Increase slope of the $\Delta\phi$ distribution as p_T^{max} is observed**
- **Comparison to NLO QCD calculations corrected for non-perturbative effects (smaller than 3%):**
  $\Rightarrow$ they describe the general characteristics, in particular the increasing slope with p_T^{max} and the shape near $\Delta\phi \sim \pi/2$ (where multijet events make a considerable contribution)

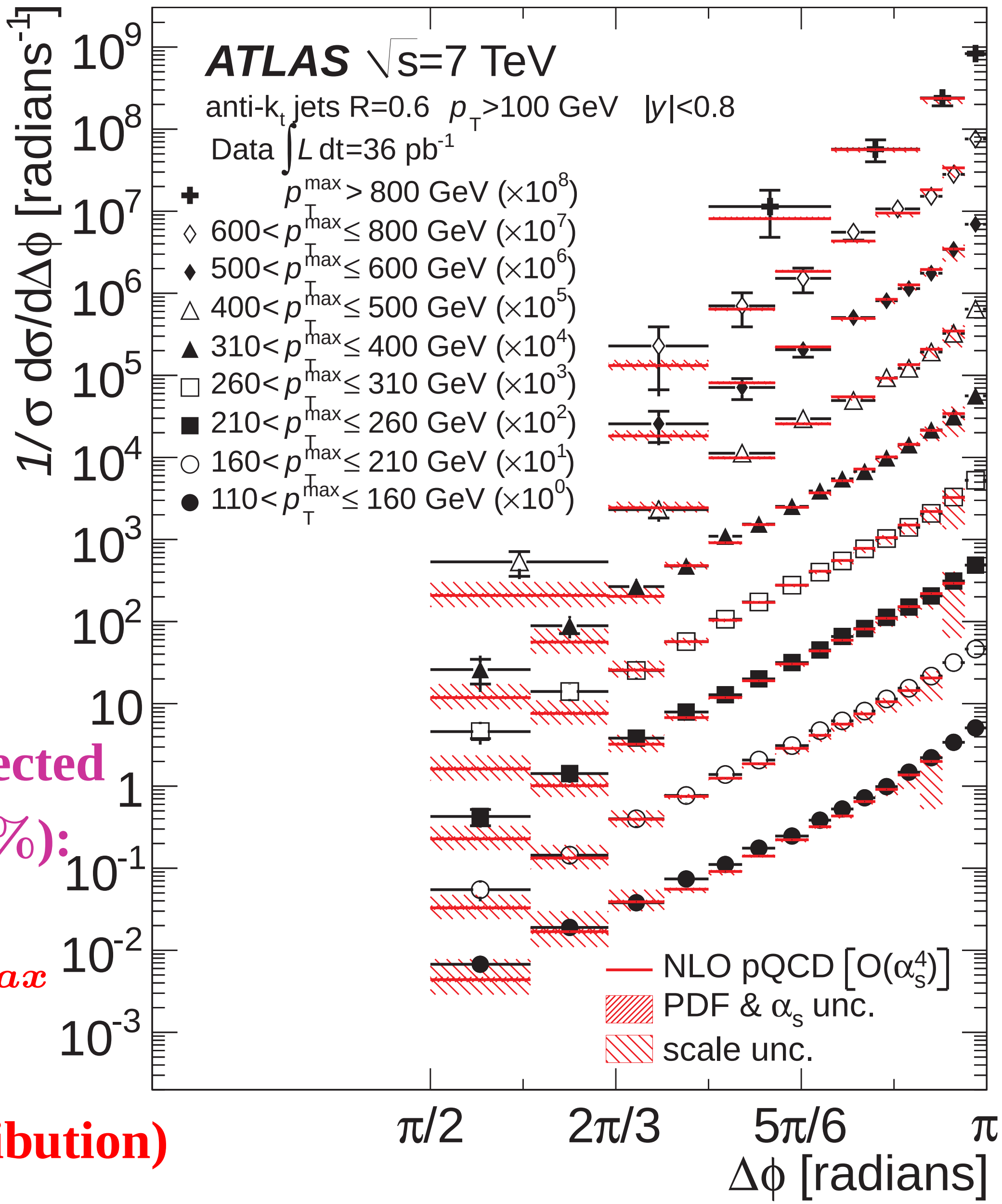

Dijet azimuthal decorrelations

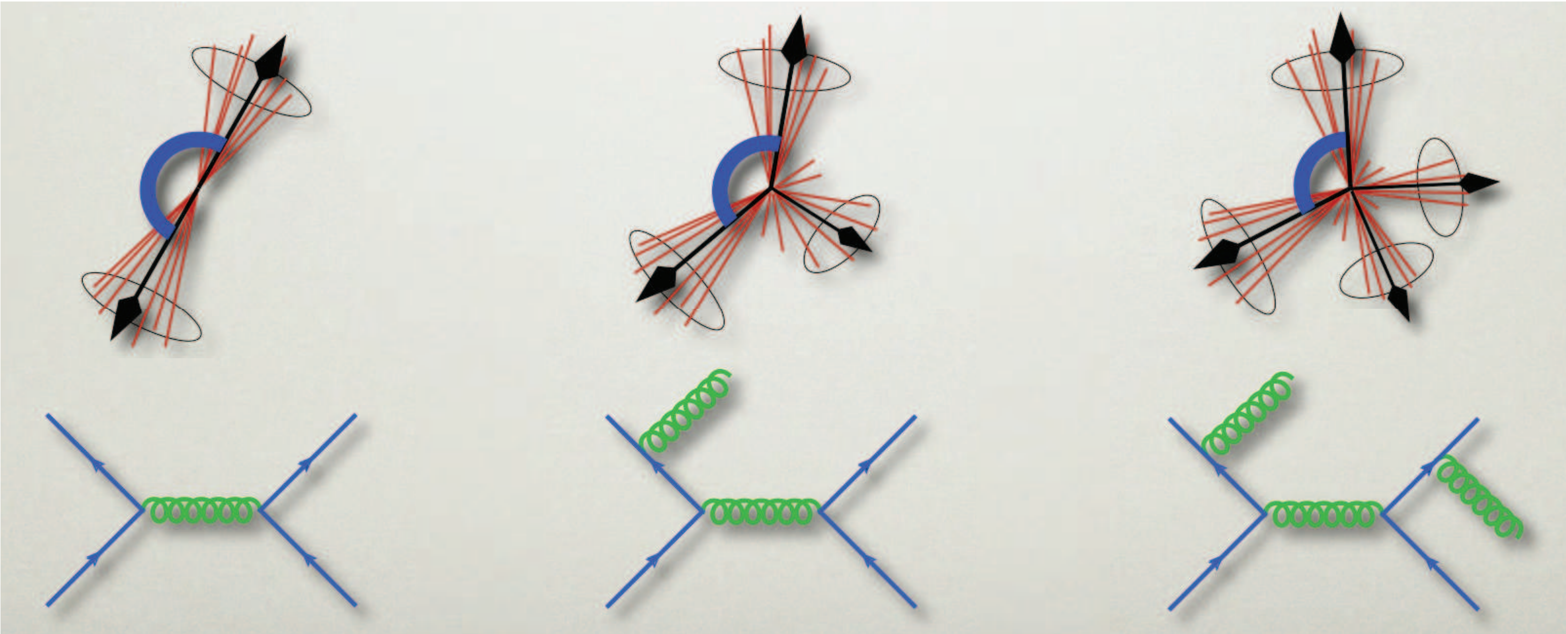

$\mathcal{O}(\alpha_s^2)$ $\mathcal{O}(\alpha_s^3)$ $\mathcal{O}(\alpha_s^4)$

- $\mathcal{O}(\alpha_s^2)$ $(2 \to 2) \Rightarrow \Delta\phi = \pi$ (Dirac's delta)
- $\mathcal{O}(\alpha_s^3)$ $(2 \to 3) \Rightarrow 2\pi/3 < \Delta\phi < \pi$, 1st non-zero contribution in this region
- $\mathcal{O}(\alpha_s^4)$ $(2 \to 4) \Rightarrow \pi/2 < \Delta\phi < \pi$

$\Rightarrow$ 1st QCD correction in the region $2\pi/3 < \Delta\phi < \pi \Rightarrow$ NLO QCD calculation

$\Rightarrow$ 1st non-zero contribution in the region $\pi/2 < \Delta\phi < 2\pi/3 \Rightarrow$ an effective LO QCD calc.

Dijet azimuthal decorrelations

- **Comparison to NLO QCD $\mathcal{O}(\alpha_s^4)$ calculations (NP corrected)**

$\rightarrow$ **calculation fails for $\Delta\phi \sim \pi$, which is sensitive to multiple soft collinear emissions**

$\rightarrow$ **scale uncertainties larger in the region $\pi/2 < \Delta\phi < 2\pi/3$**

- **In most regions, NLO QCD is consistent with the data**

$\rightarrow$ **the prediction is relatively low in the range $110 < p_T^{max} < 160$ GeV for the central region in $\Delta\phi$, where the scale uncertainties are small**

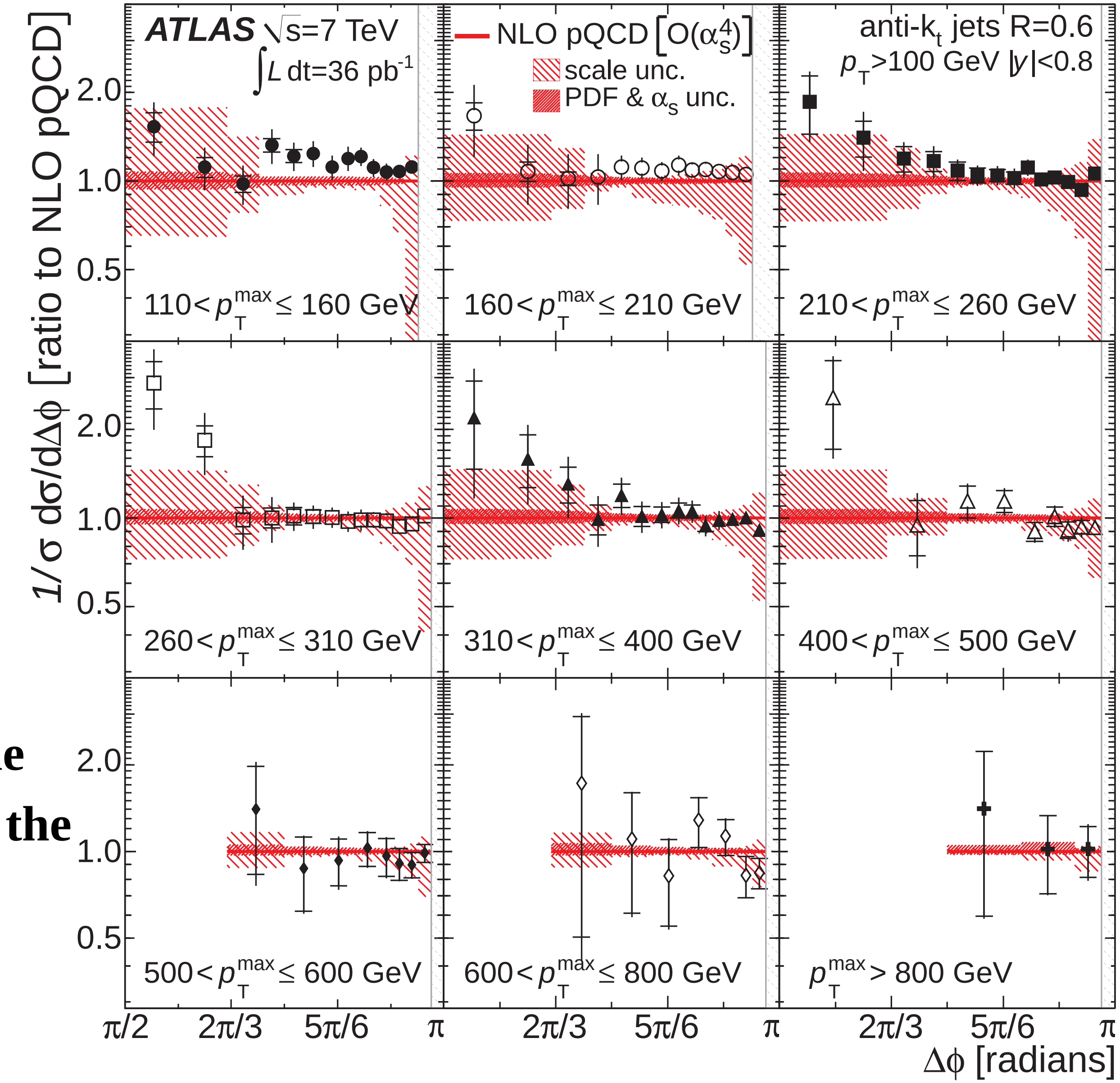

Dijet azimuthal decorrelations

- Comparison to MC generators PYTHIA, HERWIG and SHERPA

$\rightarrow$ the leading-logarithmic approximations in the parton shower lead to a good description of the data in $\Delta\phi \sim \pi$

$\rightarrow$ the measurements in $\pi/2 < \Delta\phi < 5\pi/6$ (multijets!) distinguish between the generators

- SHERPA (with up to $2 \rightarrow 6$) performs well!

- PYTHIA and HERWIG (having been tuned to previous ATLAS measurements) also describe the data

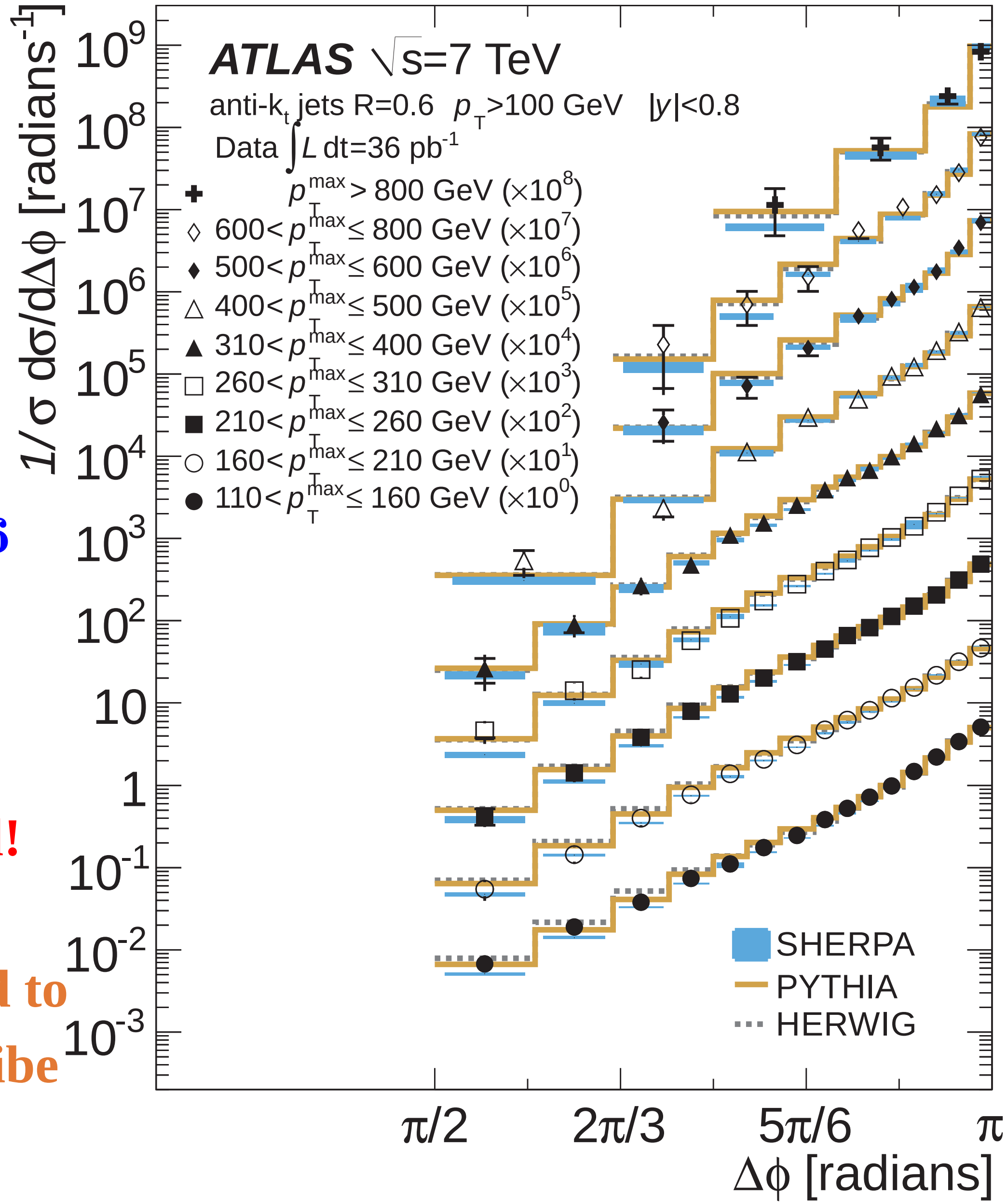

Dijet azimuthal decorrelations

- **Comparison to MC generators PYTHIA, HERWIG and SHERPA**

→ the leading-logarithmic approximations in the parton shower lead to a good description of the data in $\Delta\phi \sim \pi$

→ the measurements in $\pi/2 < \Delta\phi < 5\pi/6$ (multijets!) distinguish between the generators

- **SHERPA (with up to $2 \to 6$) performs well!**

- **PYTHIA and HERWIG (having been tuned to previous ATLAS measurements) also describe the data**

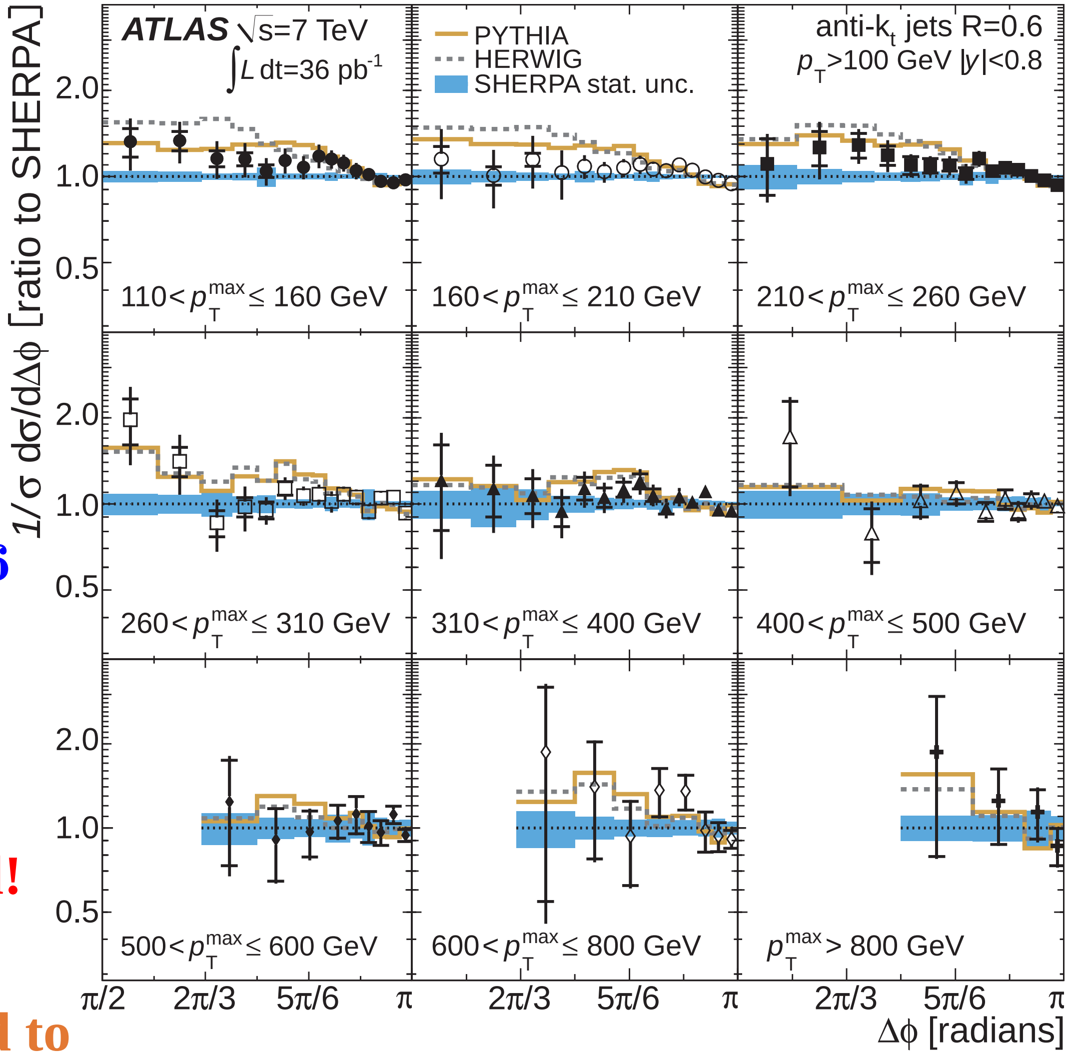

Looking inside jets

Looking inside jets produced in pp collisions at $\sqrt{s} = 7$ TeV

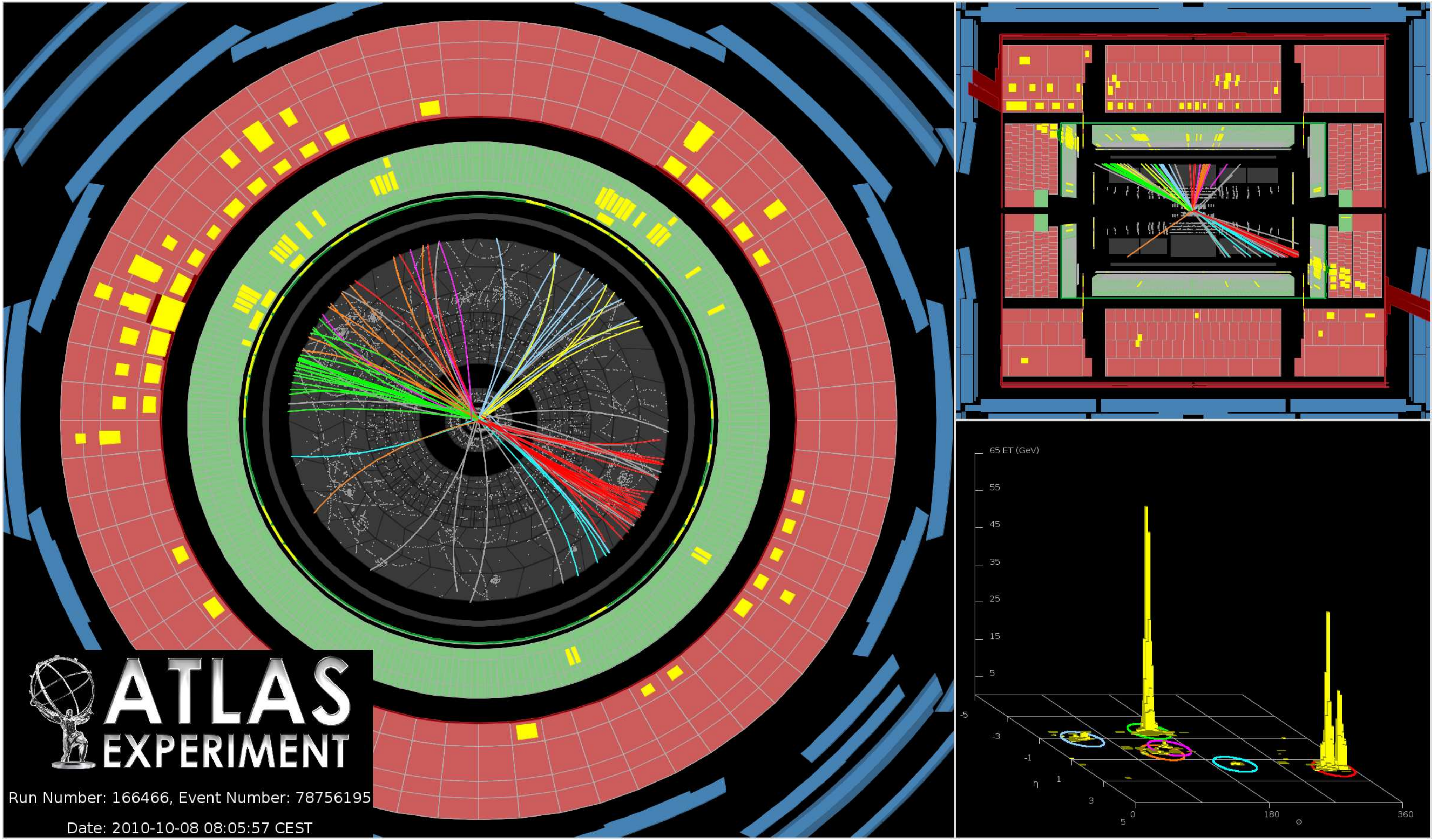

Looking inside jets produced in *pp* collisions

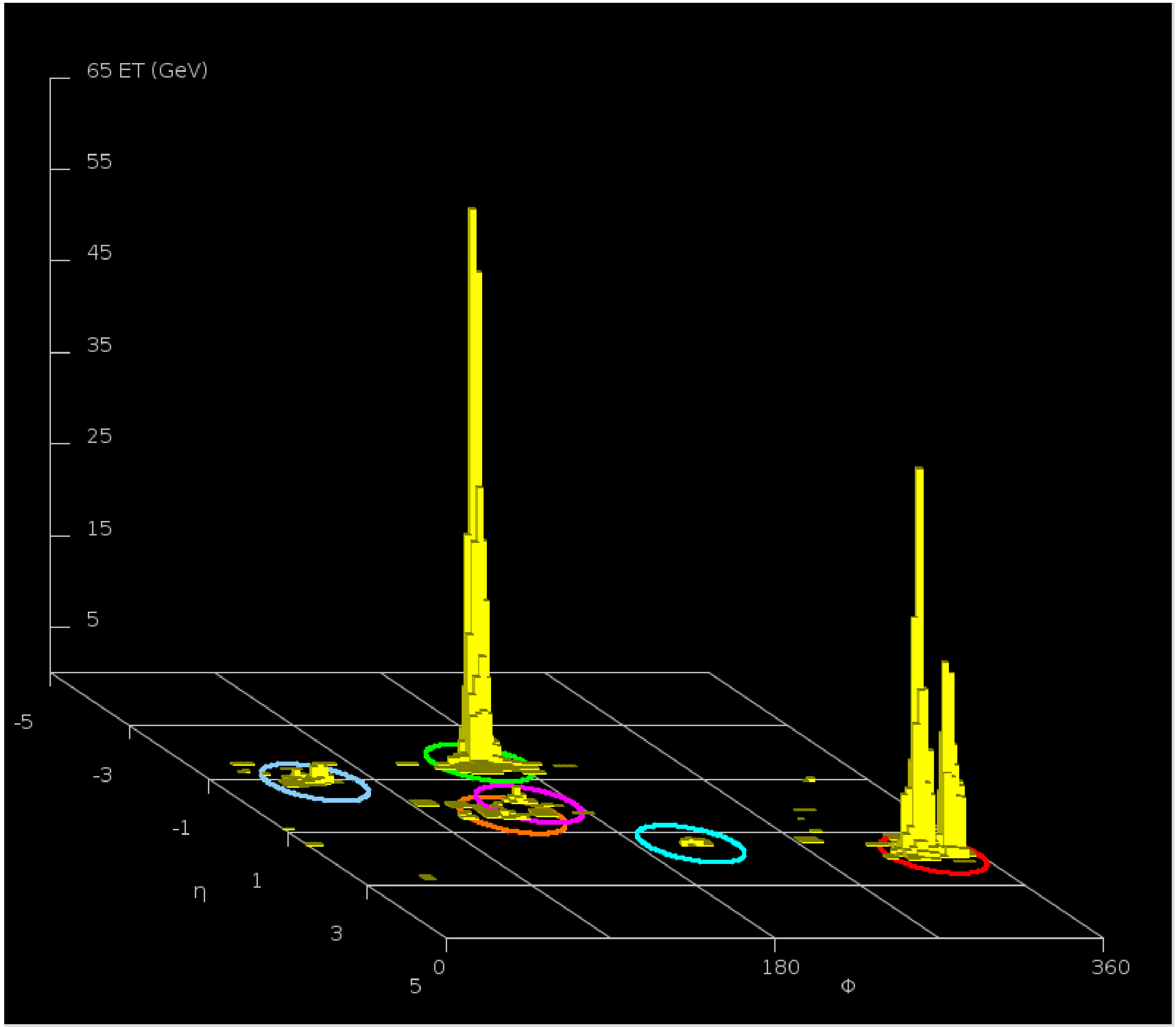

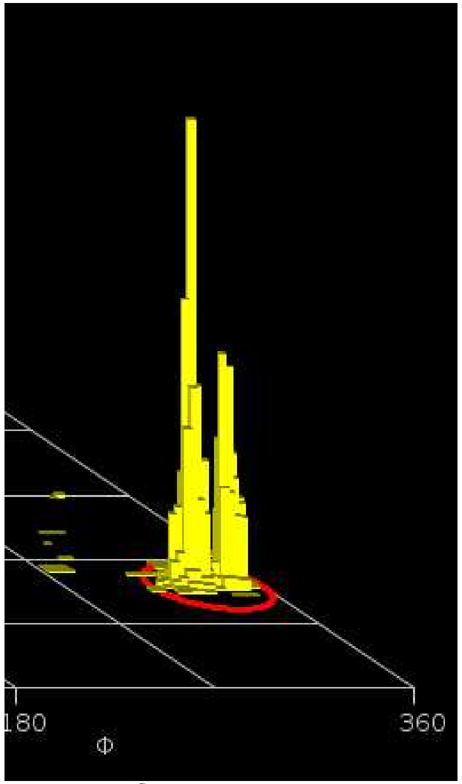

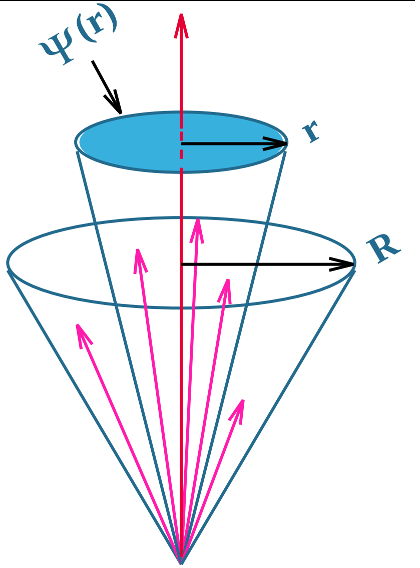

Looking inside jets produced in pp collisions

- **Integrated jet shape:**

$$\Psi(r) = \frac{1}{N_{jets}} \sum_{jets} \frac{p_T(0,r)}{p_T(0,R)}$$

Average fraction of the jet's transverse momentum that lies inside a circle in the y-ϕ plane of radius r concentric with the jet axis

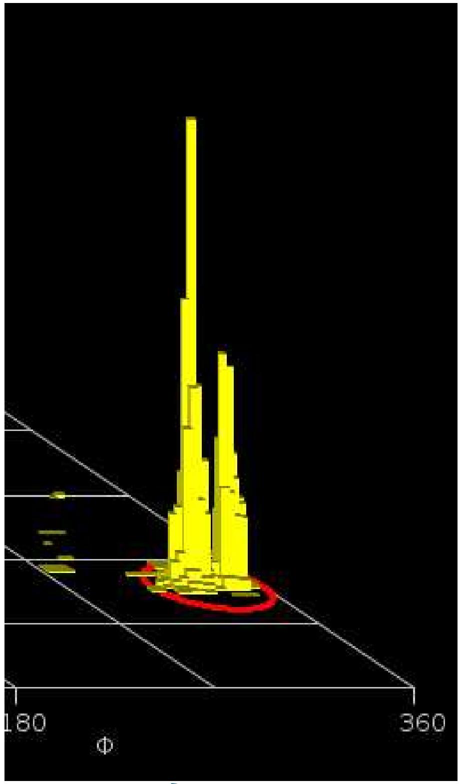

- **Differential jet shape:**

$$\rho(r) = \frac{1}{\Delta r N_{jets}} \sum_{jets} \frac{p_T(r-\Delta r/2, r+\Delta r/2)}{p_T(0,R)}$$

Average fraction of the jet's transverse momentum that lies inside an annulus of inner (outer) radius $r - \Delta r/2$ ($r + \Delta r/2$) concentric with the jet axis

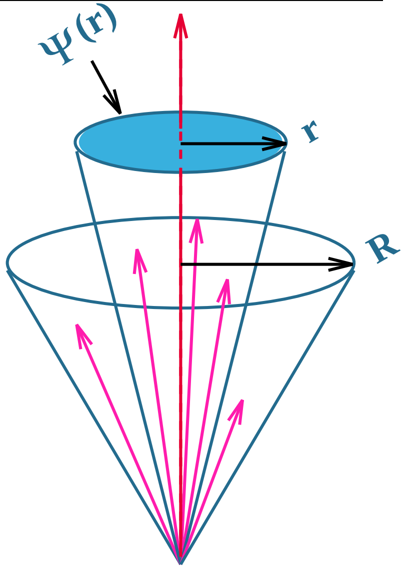

Looking inside jets produced in pp collisions

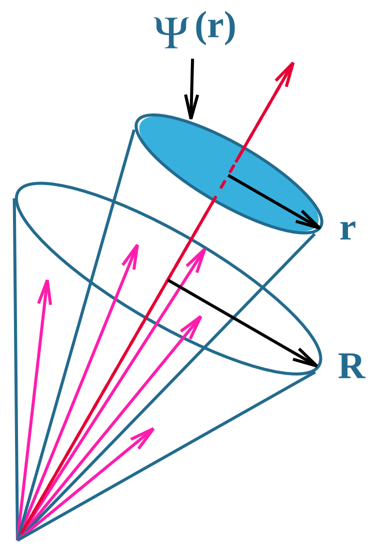

- Information about the transition parton→jet
- At sufficiently high p_T the jet shape is calculable in pQCD

→ multiple parton emissions from the primary parton

  - QCD predicts that gluon jets are broader than quark jets

  $\Rightarrow \Psi_{QUARKS}(r) > \Psi_{GLUONS}(r)$

  - QCD predicts that jets from bottom quarks are broader than jets from $u, d, s, c \Rightarrow \Psi_{u,d,s,c}(r) > \Psi_b(r)$

- At lower p_T non-perturbative effects play a role

  → hadronization and underlying-event effects

- Measurements of jet shapes allow

  → tuning of models for soft contributions

  → tests of pQCD calculations

- Among others, jet shapes are being investigated vigorously to search for new physics → highly boosted particles decaying into multiple (close-by) jets

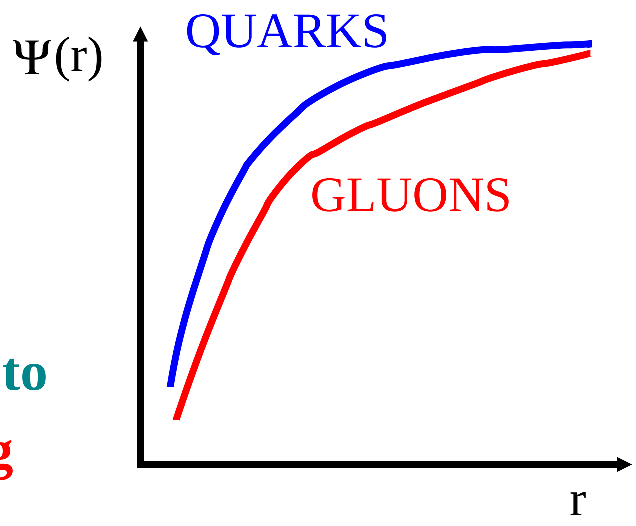

Jet shapes in pp collisions at $\sqrt{s} = 7$ TeV

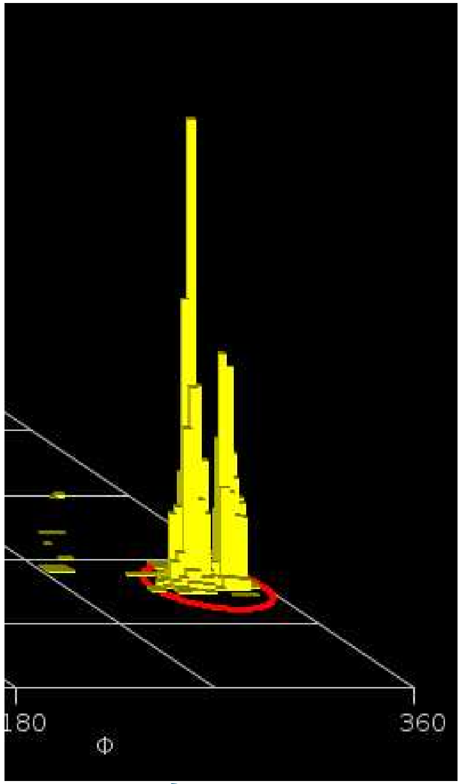

- Measurement of jet shapes, $\rho(r)$ and $\Psi(r)$, for jets with $30 < p_T < 600$ GeV and $|y| < 2.8$ (anti-k_T algorithm with $R = 0.6$) using $\mathcal{L} = 3$ pb^{-1}
- Events with at least one jet with $p_T > 30$ GeV and $|y| < 2.8$ and exactly one primary vertex (to suppress pileup!)
- Reconstruction of the jet shape using calorimeter topological clusters $\longrightarrow$ corrected to particle level using MC simulations
  - ρ-correction factors between 0.95 and 1.1 as r increases
- Systematic uncertainties ($\rho(r)$):
  - $\longrightarrow$ absolute jet energy scale of individual clusters (3-15%)
  - $\longrightarrow$ model of the calorimeter showers in MC (1-4%)
  - $\longrightarrow$ remaining JES uncertainty (3-5%)
  - $\longrightarrow$ model of parton shower, hadronization, UE in MC (2-10%)
  - $\longrightarrow$ no significant dependence on $\mathcal{L}_{inst} \Rightarrow$ pileup effects negligible
- Cross checks using tracks or calorimeter towers (0.1×0.1 in $y \times \phi$)

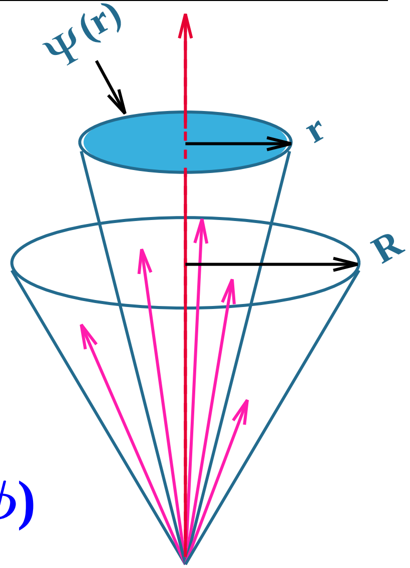

Jet shapes in pp collisions at $\sqrt{s} = 7$ TeV

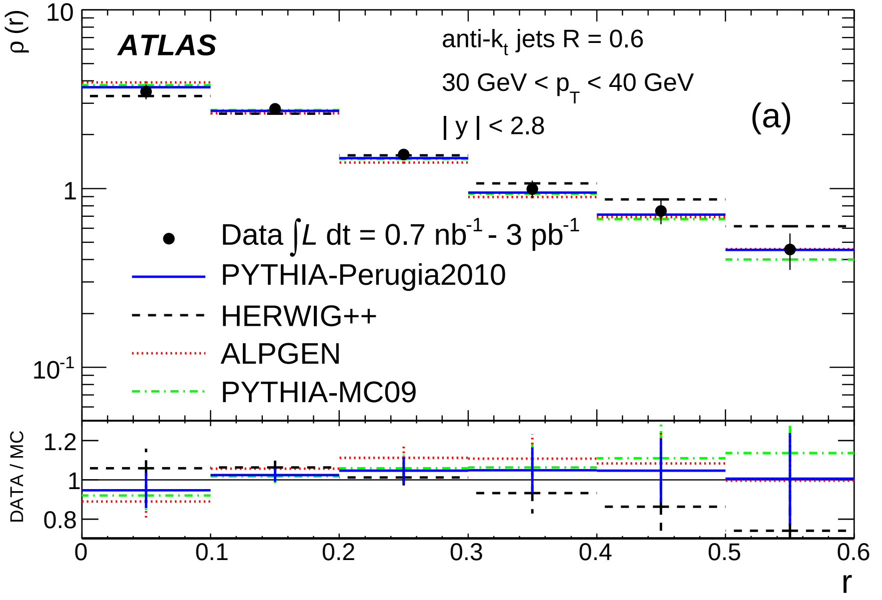

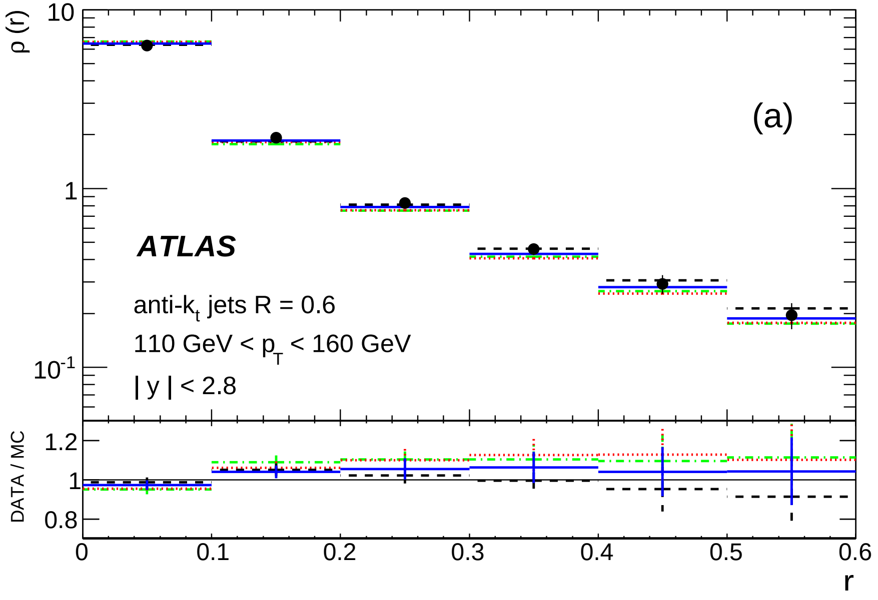

- Dominant peak at small $r \to$ most of the momentum is concentrated close to the jet axis
- At low p_T^{jet} more than 80% of the transverse momentum within $r = 0.3$; this fraction increases up to 95% at very high p_T^{jet}

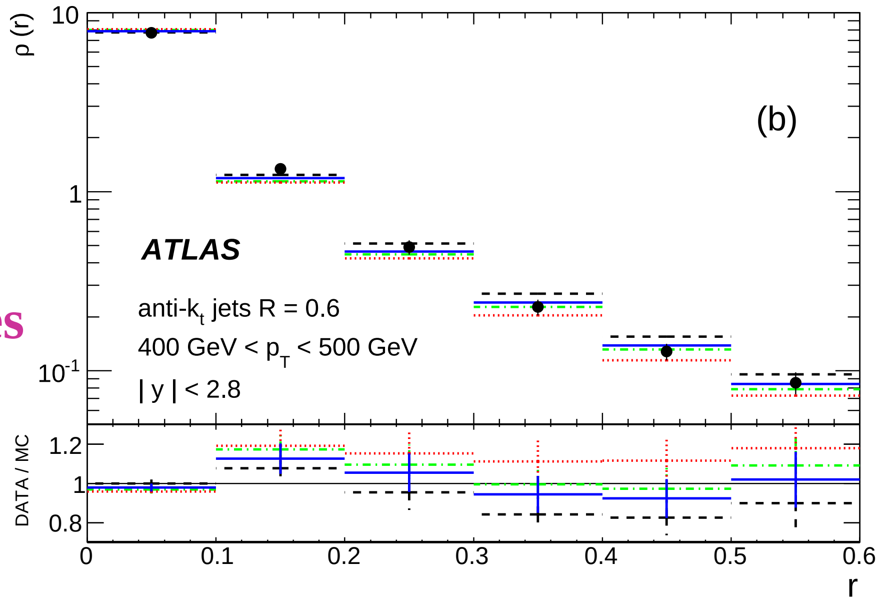

$\Rightarrow$ Jets become narrower as p_T^{jet} increases

Jet shapes in pp collisions at $\sqrt{s} = 7$ TeV

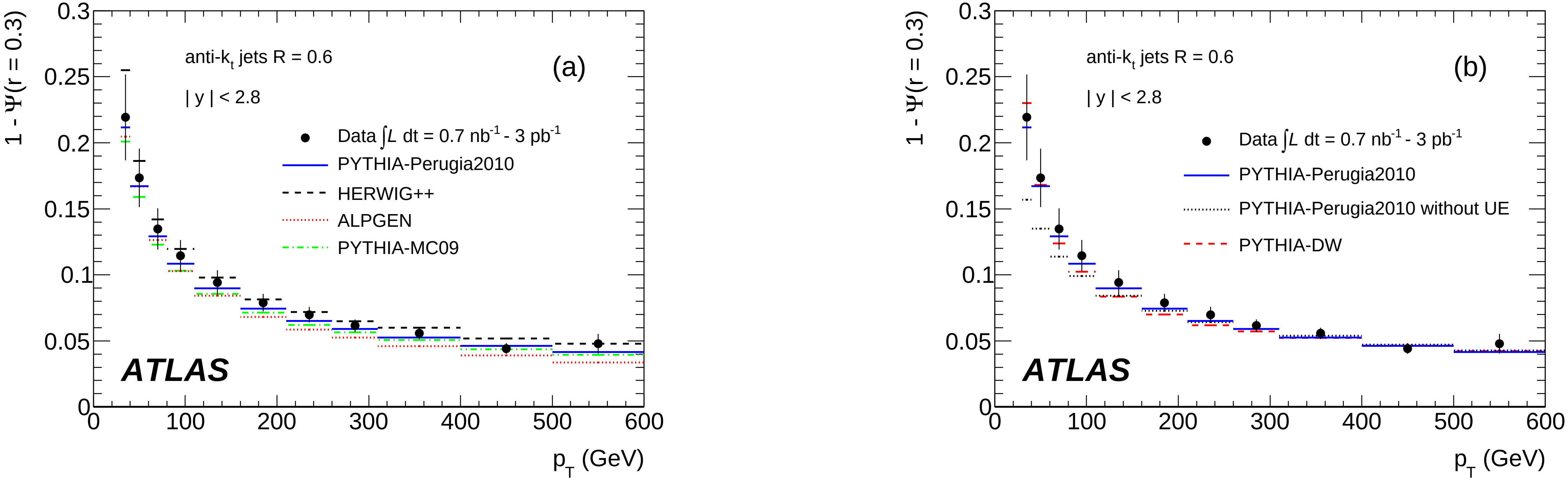

⇒ Jets become narrower as p_T^{jet} increases

- **PYTHIA-Perugia2010 gives a reasonable description of the data**
- **HERWIG++ predicts broader jets at low and high p_T^{jet}**
- **ALPGEN is similar to PYTHIA-Perugia2010 at low p_T^{jet}, but jets are narrower than in the data at high p_T^{jet}**
- **PYTHIA-Perugia2010 without underlying event → jets too narrow at low p_T^{jet} ⇒ sensitivity of the jet shape in $p_T^{jet} < 160$ GeV to underlying event effects (tuning!)**

Jet shapes in pp collisions at $\sqrt{s} = 7$ TeV

- **Comparison to the predictions of PYTHIA-Perugia2010 for quark- and gluon-initiated jets (by matching particle-level jets in y-ϕ to the final state partons in the QCD $2 \rightarrow 2$ hard process):**

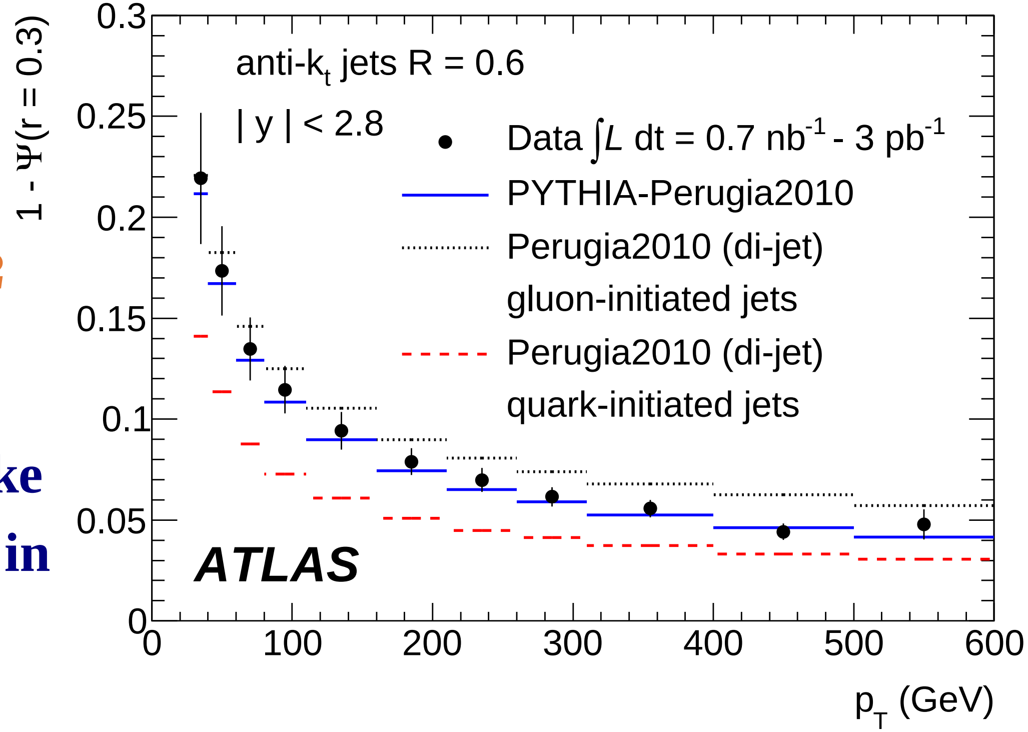

$\rightarrow$ **The measured jets at low p_T^{jet} are gluon like as expected from the dominance of gluons in the final state**

$\rightarrow$ **At high p_T^{jet} (smaller impact of the underlying event) the trend observed in the data is mainly attributed to a changing admixture of quark- and gluon-initiated jets (convoluted with the effects of the running coupling constant)**

$\Rightarrow$ **All in all, potential of the jet shape measurements to constrain the current phenomenological models for soft gluon radiation, underlying event and fragmentation**

Shapes of b-jets and light jets in *pp* collisions

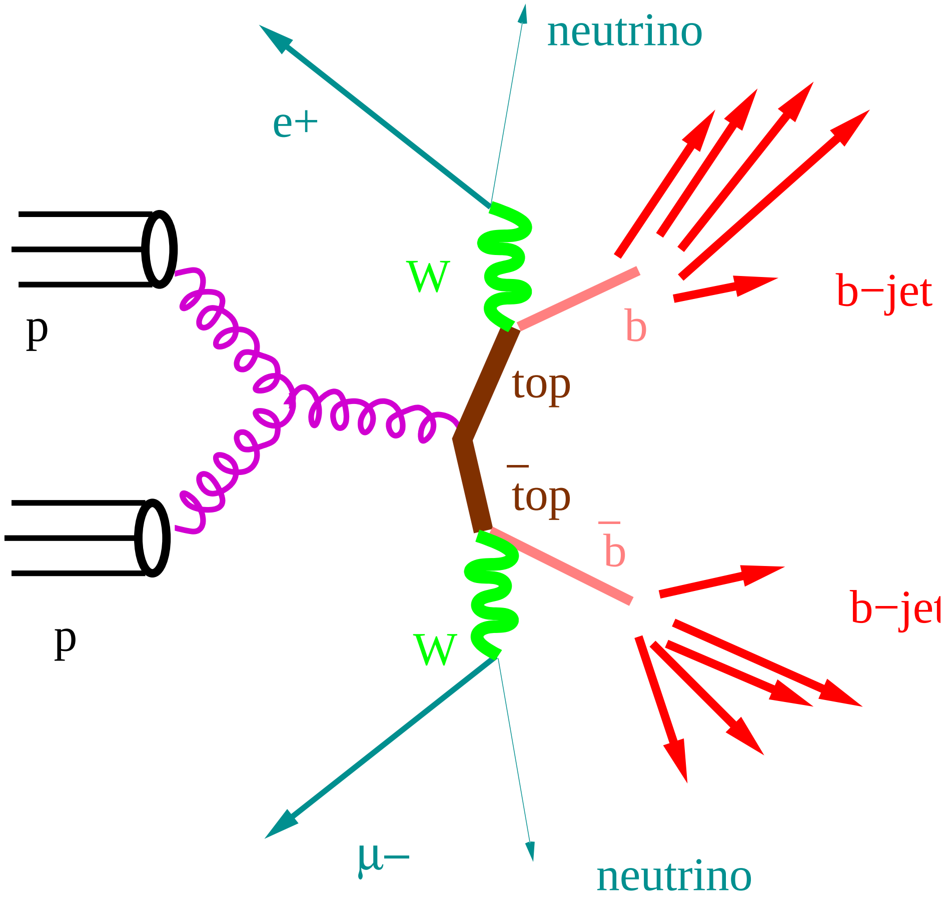

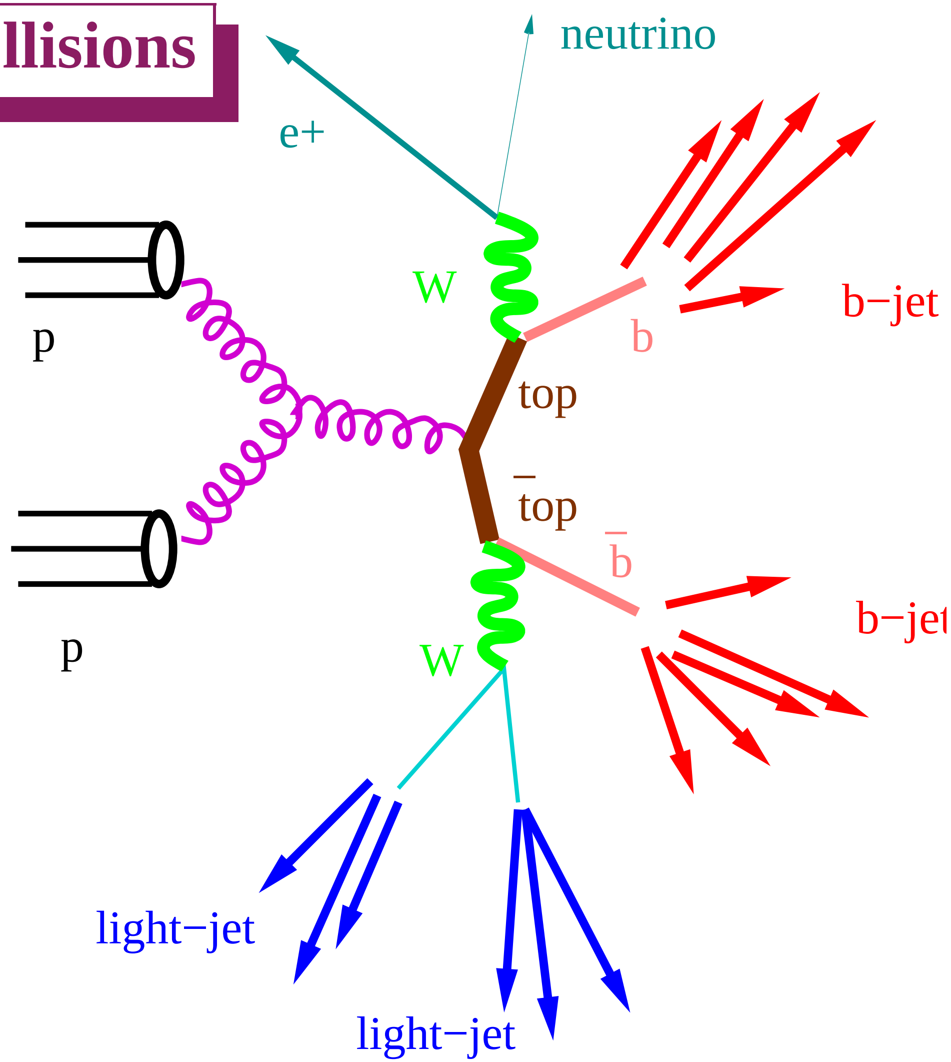

- **Dilepton channel of $t\bar{t}$ production: very pure source of b-jets**
- **Single-lepton channel of $t\bar{t}$ production:**

$\rightarrow$ source of b-jets (from top decays) and light (u, d, c, s) jets (from W decays)

Shapes of b-jets and light jets in pp collisions

- Anti-k_T algorithm with $R = 0.4$:
  $p_t^{jet} > 25$ GeV and $|\eta^{jet}| < 2.5$
- Charged leptons: $p_t^{e,\mu} > 25$ (20) GeV
- Dilepton sample: two isolated charged leptons (ee, $\mu\mu$, $e\mu$) E_T^{miss}; at least two jets and at least one b-tagged jet
- Single-lepton sample: one isolated charged lepton (e, μ) E_T^{miss}; at least four jets and at least one b-tagged jet
- Jet shapes: $p_T^{jet} > 30$ GeV and $\Delta R_{jj} > 0.8$
- b-jet sample: b-tagged jets
- Light-quark jet sample: pair of (non-b-tagged) jets with m_{jj} closest to m_W
- Single-lepton sample: purity of b-jets $\rightarrow$ 89%
  purity of light-jets $\rightarrow$ 66%
- Dilepton sample: purity of b-jets $\rightarrow$ 99%

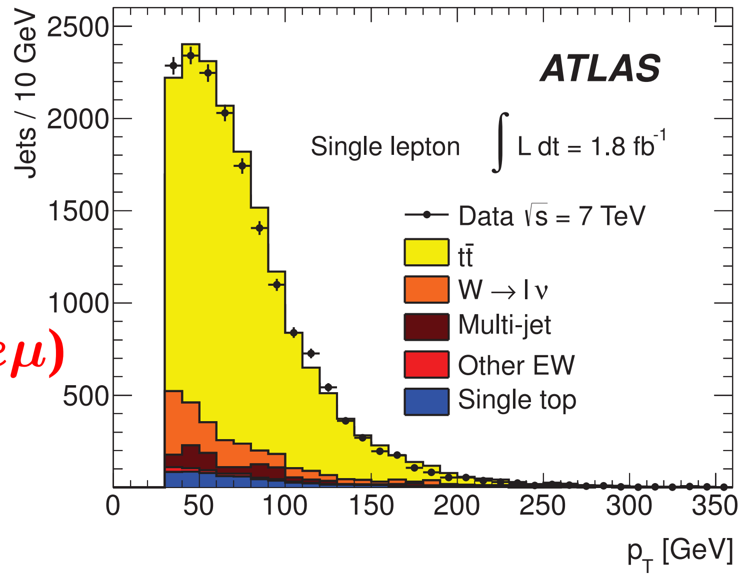

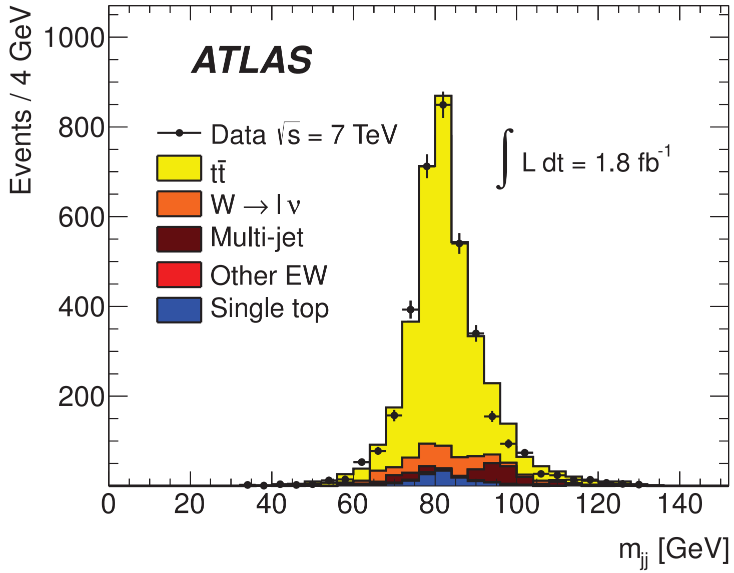

Shapes of b-jets and light jets in pp collisions at $\sqrt{s} = 7$ TeV

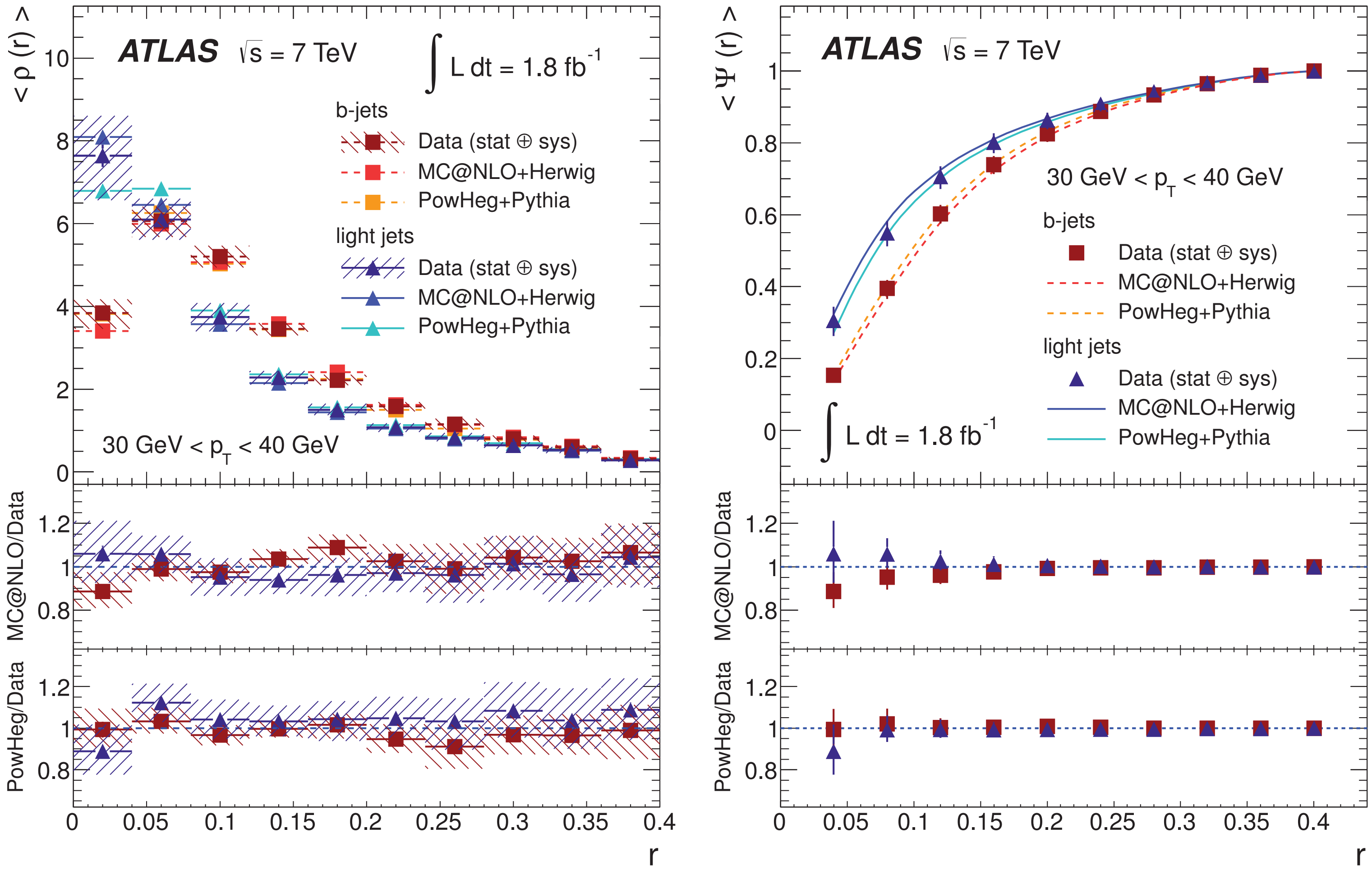

$30 < p_T^{jet} < 40$ GeV

⇒ *b*-jets are broader than light jets

- MC predictions (MC@NLO+HERWIG and POWHEG+PYTHIA) with NLO matrix elements plus parton shower give a good description of both measurements

Shapes of b-jets and light jets in pp collisions at $\sqrt{s} = 7$ TeV

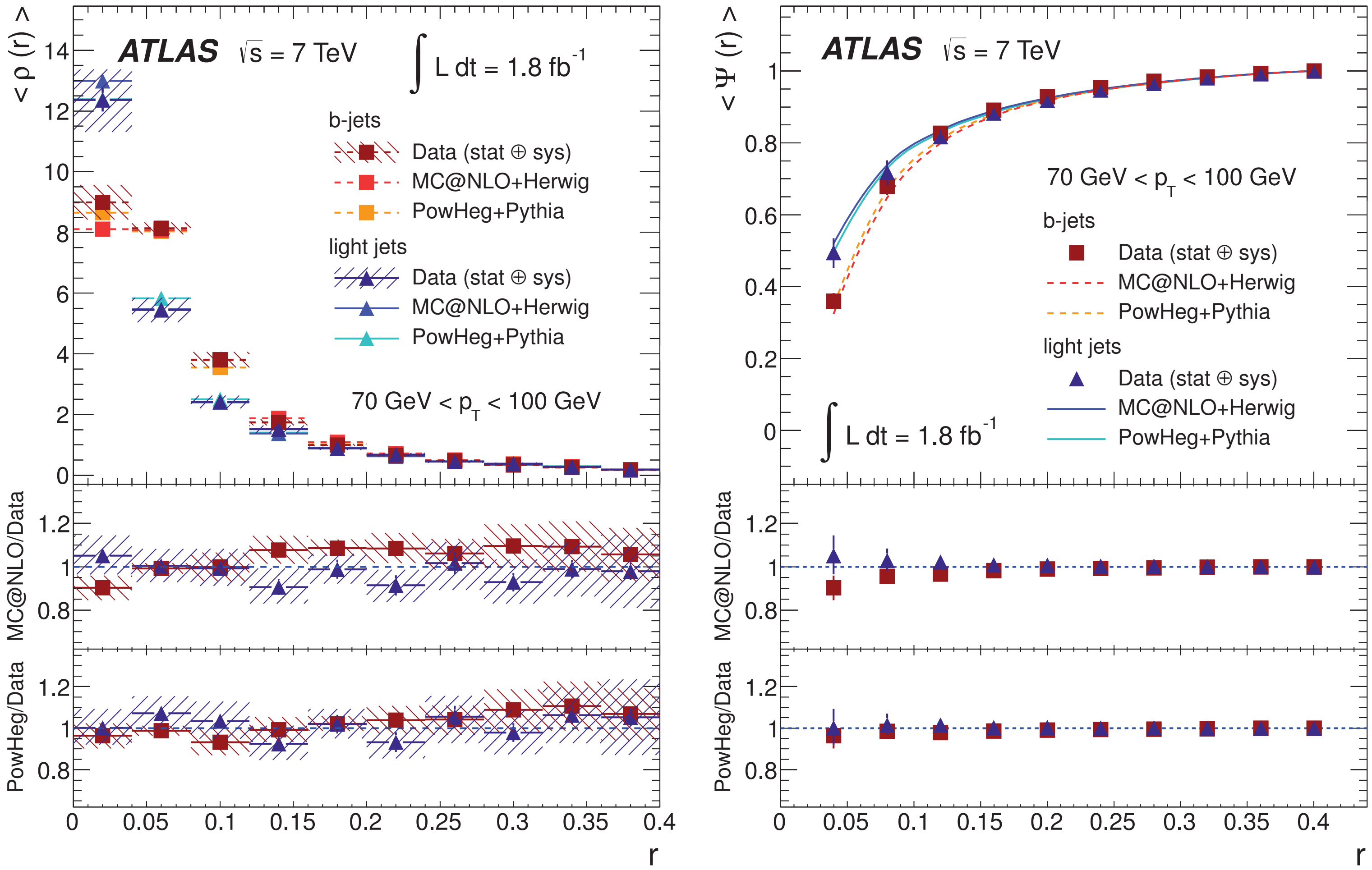

$70 < p_T^{jet} < 100$ GeV

⇒ ***b*-jets are broader than light jets**

- **MC predictions (MC@NLO+HERWIG and POWHEG+PYTHIA) with NLO matrix elements plus parton shower give a good description of both measurements**

Photons

Photon production in pp collisions at LHC

- **Photon production in pp collisions allows**
  $\rightarrow$ tests of perturbative QCD
  $\rightarrow$ experimental information on the proton PDFs

- **Possibilities to study inclusive production of photons or in association with jets**

- **Prompt photons represent a cleaner probe of the hard interaction**

- **Diphoton production is of special interest as the major background to $H \rightarrow \gamma\gamma$**

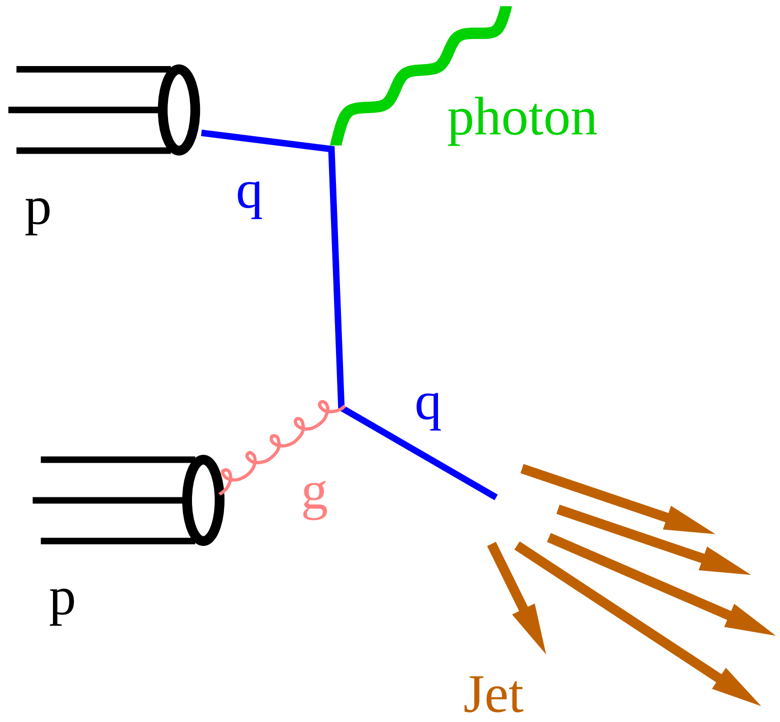

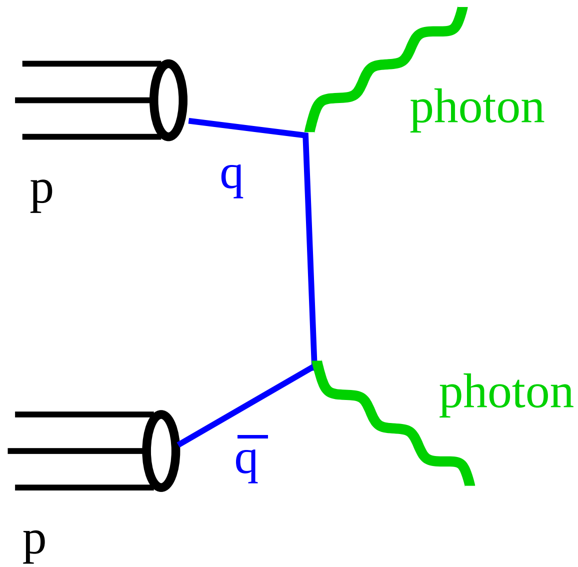

Other sources of photons

- Quarks and gluons are sources of photons

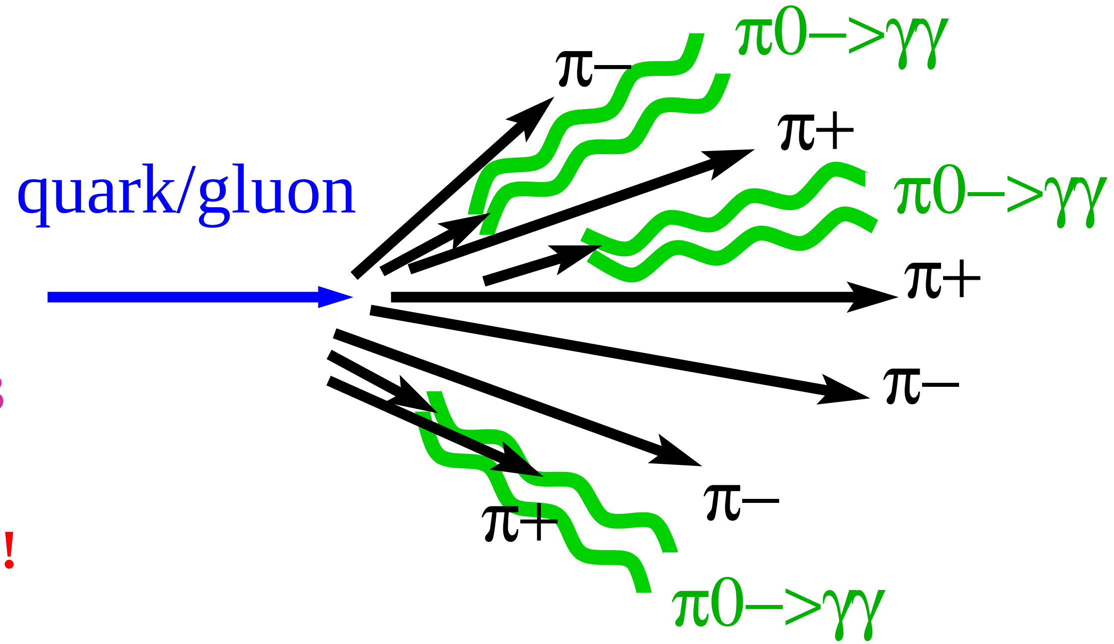

→ Quarks and gluons fragment mostly into pions and, by isospin symmetry, $1/3$ are π^0's, which decay into two photons
⇒ γ's are produced copiously inside jets!

→ Quarks have electric charge and radiate photons
⇒ fragmentation function $D^{\gamma}_{q/g}(z, \mu_f)$

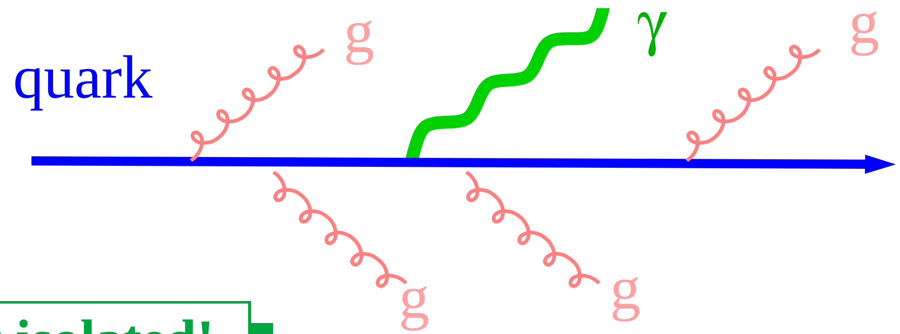

⇒ Distinct feature: photons inside jets, i.e. not isolated!

Photon isolation

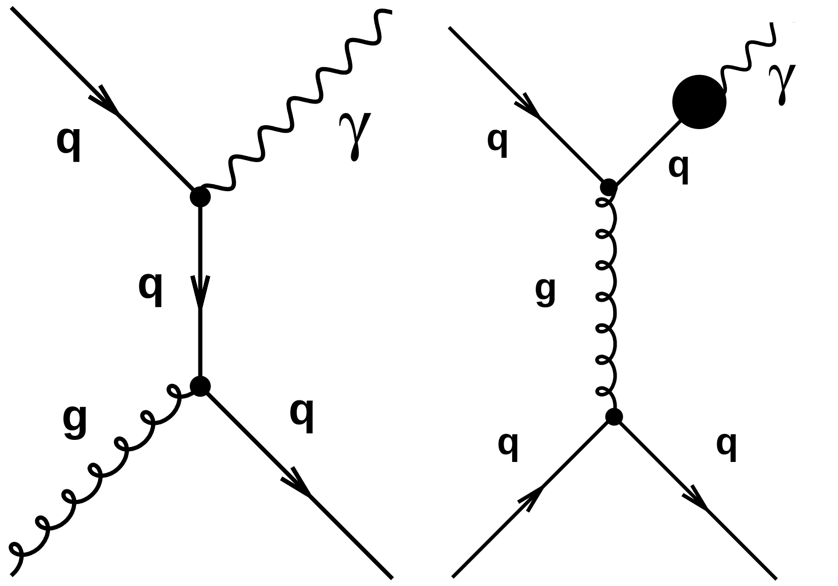

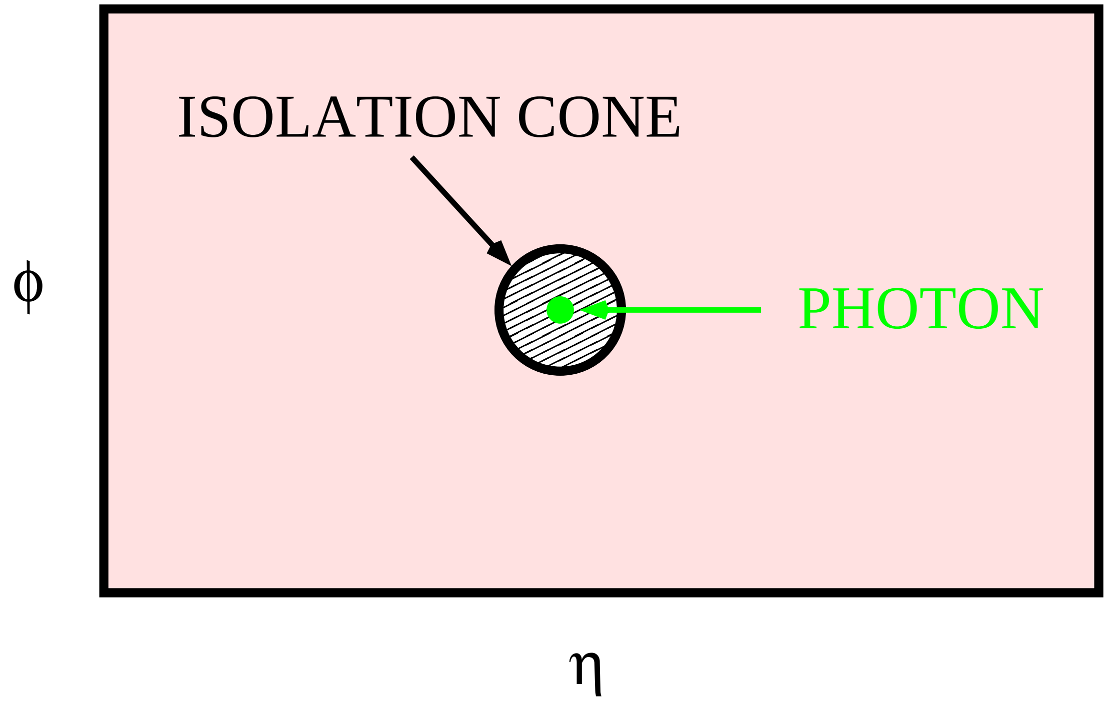

- It is essential to require the photon to be isolated. It is achieved by requiring $E_T^{iso} \equiv \sum_i E_T^i < E_T^{max}$ with the sum over the particles (except the photon!) inside a cone of radius R centered on the photon in the $\eta - \phi$ plane

- The isolation requirement suppresses the contribution of photons inside jets: π^0 (as well as other neutral mesons) decays and the fragmentation contribution

Photons with the ATLAS detector

Photon reconstruction in the ATLAS LAr Calorimeter

• Layout of the ATLAS electromagnetic calorimeter (Lead-liquid Argon)

$\rightarrow$ barrel section, $|\eta| < 1.475$

$\rightarrow$ two end-cap sections, $1.375 < |\eta| < 3.2$

$\rightarrow$ three longitudinal layers

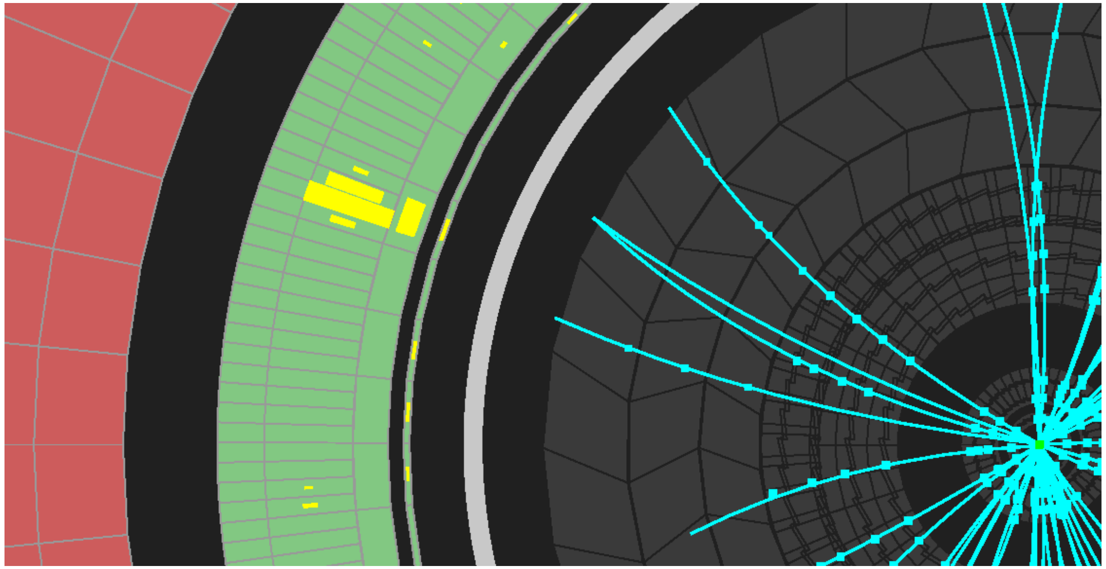

— First layer: high granularity in η direction, width 0.003-0.006 (except for $1.4 < |\eta| < 1.5$ and $|\eta| > 2.4$)

— Second layer: collects most of the energy, granularity 0.025×0.025 in $\eta \times \phi$

— Third layer: used to correct for leakage

• Cluster of EM cells without matching track:

$\rightarrow$ "unconverted" photon candidate

• Cluster of EM cells matched to pairs of tracks (from reconstructed conversion vertices in the inner detector)

$\rightarrow$ "converted" photon candidate

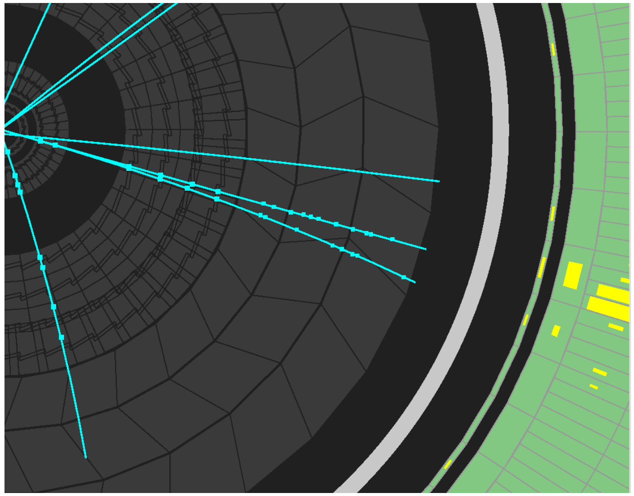

Photon identification in the ATLAS LAr Calorimeter

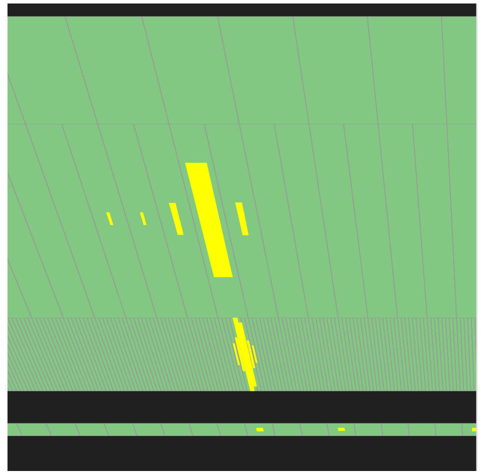

- **To discriminate signal vs background:** shape variables from the lateral and longitudinal energy profiles of the shower in the calorimeters; "loose" and "tight" identification criteria.
- "Loose" identification criteria:

$\rightarrow$ leakage $R_{had} = E_T^{had}/E_T$ (1st layer hadronic calorimeter)

$\rightarrow$ $R_\eta = E^{S2}_{3\times 7}/E^{S2}_{7\times 7}$; $S2$=second layer

$\rightarrow$ RMS width of the shower in η direction in $S2$

- "Tight" identification criteria:

$\rightarrow$ $R_\phi = E^{S2}_{3\times 3}/E^{S2}_{3\times 7}$

and shower shapes in the first layer (to discriminate single-photon showers from overlapping nearby showers, such as $\pi^0 \rightarrow \gamma\gamma$)

$\rightarrow$ e.g. asymmetry between the 1st and 2nd maxima in the energy profile along η ($S1$)

- Estimated efficiencies: 97% for "loose" and 85% for "tight" photons with $E_T > 20$ GeV

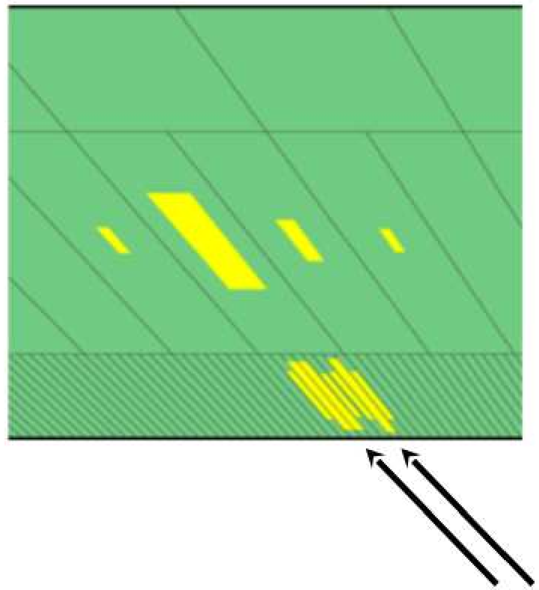

$\pi^0 \rightarrow \gamma\gamma$

Photon isolation in ATLAS

- $E_T^{iso}(R = 0.4)$ computed using the calorimeter cells (EM and HAD) in a cone $R = 0.4$, but excluding the contributions from 3×5 EM cells around photon

- The leakage of the photon energy outside that region is subtracted (few %)

- The underlying event and pileup contribute to E_T^{iso}!

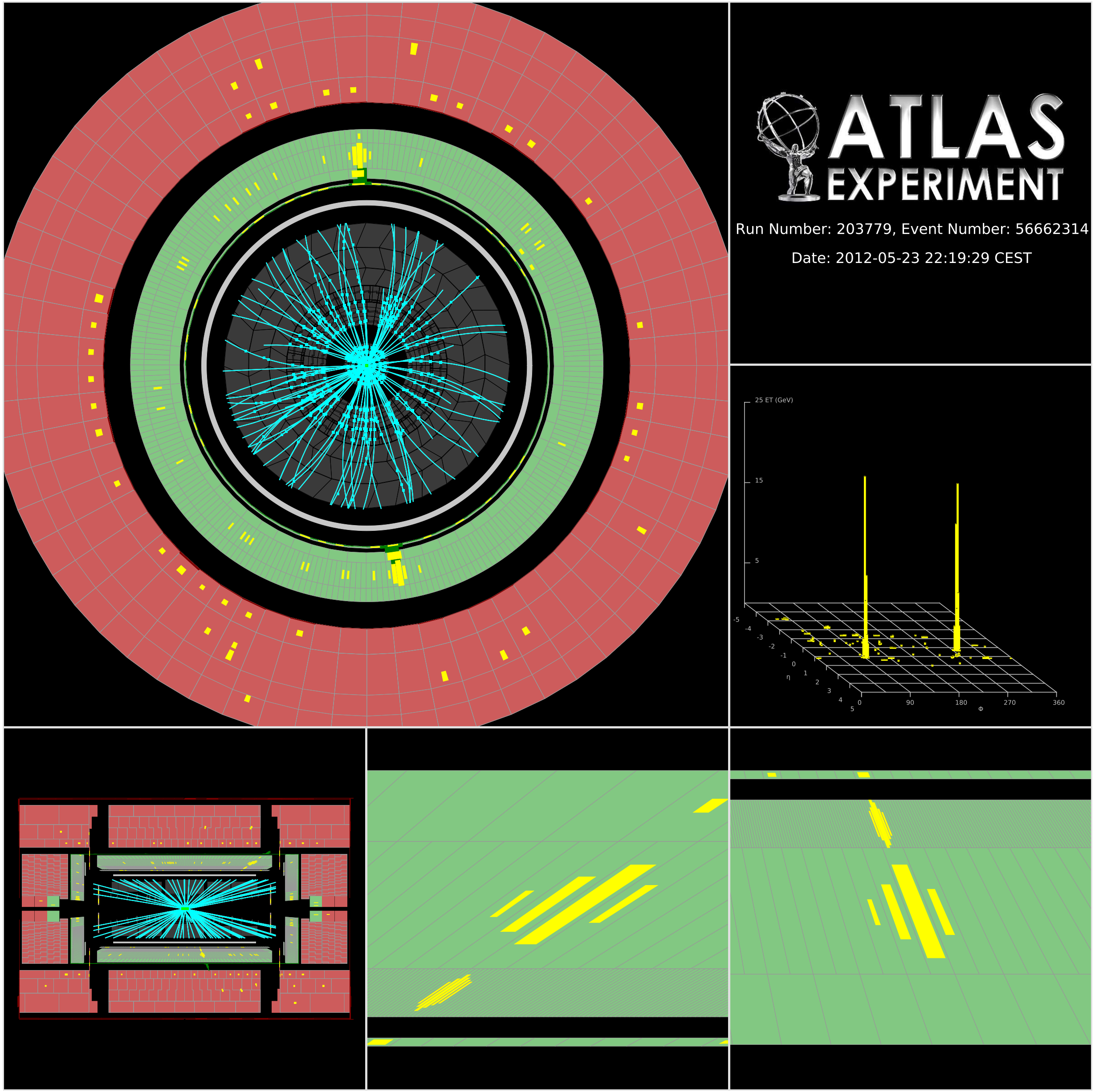

Photon isolation in ATLAS

- E_T^{iso} is corrected by subtracting the estimated contributions from the underlying event and pileup; the correction is computed on an event-by-event basis (to avoid the large fluctuations) using the jet-area method (M. Cacciari et al.)
  $\Rightarrow$ ambient transverse-energy density
  540 MeV (in $R = 0.4$ cone) for events with at least one photon candidate with $E_T > 15$ GeV and exactly one PV (+170 MeV for each extra PV)
- After the correction the E_T^{iso} distribution is centered at zero with a width of 1.5 GeV in simulated signal events
- A photon candidate is considered isolated if $E_T^{iso} < 3$ GeV
- Residual background still expected

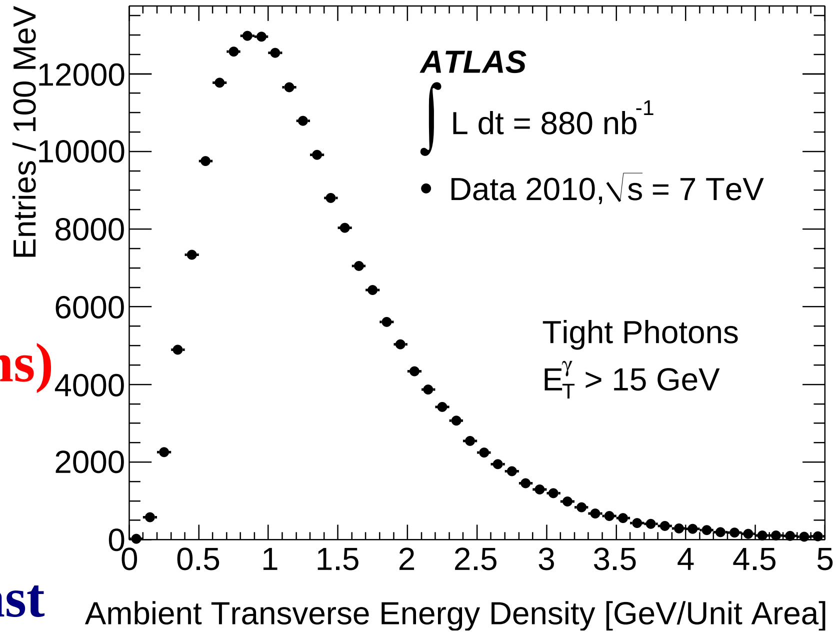

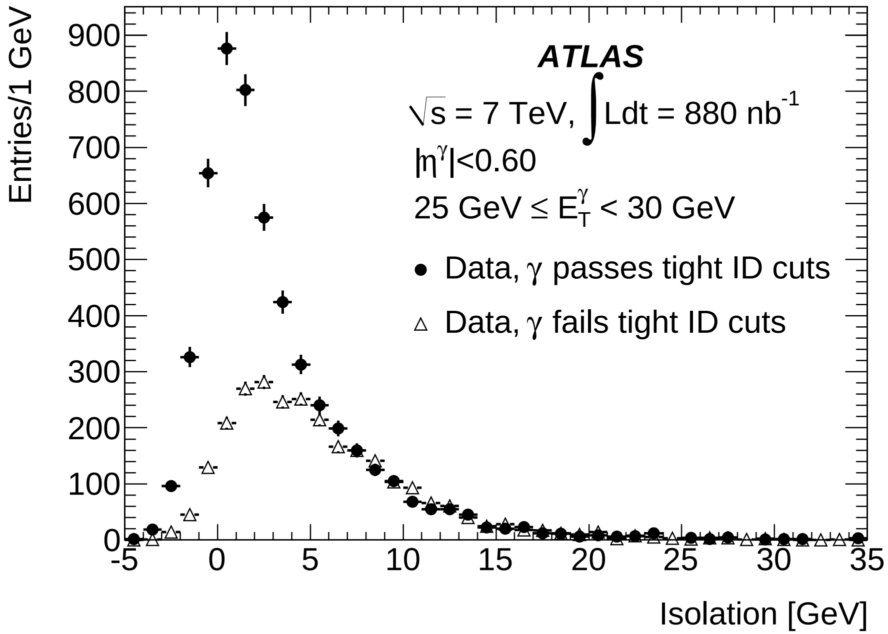

Background subtraction

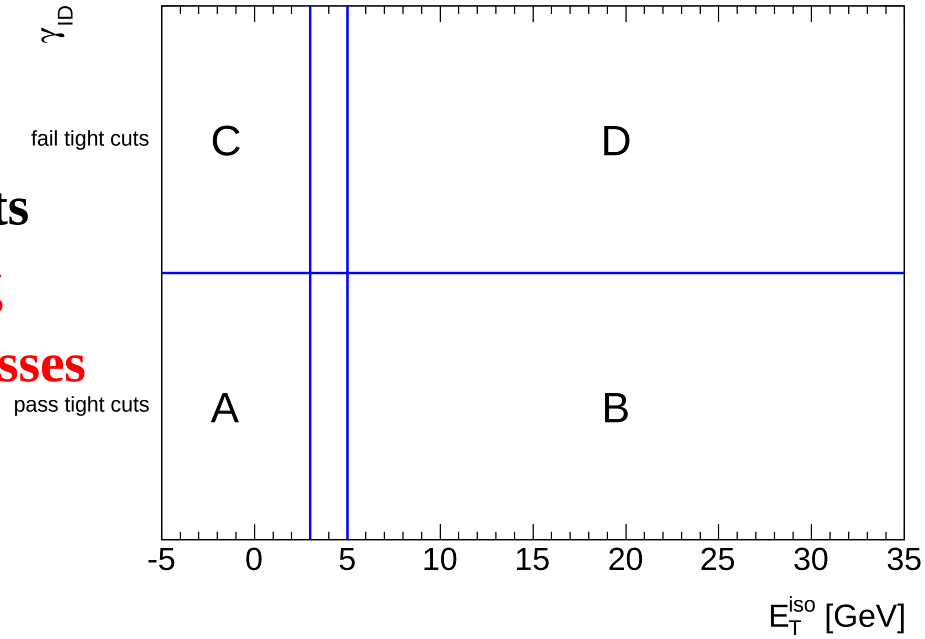

- **Residual background still expected even after the tight identification and isolation requirements**
- **A data-driven method necessary to avoid relying on detailed simulations of the background processes**
- **The two-dimensional sideband method:**

→ photon identification γ_{ID} vs E_T^{iso} plane

→ four regions are defined

— region A (signal): tight and isolated photons ($E_T^{iso} < 3$ GeV)

— region B (bkg): tight and non-isolated photons ($E_T^{iso} > 5$ GeV)

— region C (bkg): non-tight and isolated photons ($E_T^{iso} < 3$ GeV)

— region D (bkg): non-tight and non-isolated photons ($E_T^{iso} > 5$ GeV)

- **It is assumed that for background events there is no correlation between γ_{ID} and E_T^{iso}**

$$\frac{N_A^{bkg}}{N_B^{bkg}} = \frac{N_C^{bkg}}{N_D^{bkg}} \qquad \Rightarrow N_A^{sig} = N_A - N_B^{bkg}\frac{N_C^{bkg}}{N_D^{bkg}}$$

further assuming that signal contamination is small in B, C and D

Background subtraction

- The effects of the small signal contaminations can be accounted for

$$\frac{N_A^{bkg}}{N_B^{bkg}} = \frac{N_C^{bkg}}{N_D^{bkg}} \quad \Rightarrow \frac{N_A - N_A^{sig}}{N_B - \epsilon_B N_A^{sig}} = \frac{N_C - \epsilon_C N_A^{sig}}{N_D - \epsilon_D N_A^{sig}}$$

where the leakage fractions (ϵ_K, $K = B, C, D$) are estimated using MC samples of signal processes, $\epsilon_K \equiv N_K^{sig}/N_A^{sig}$

- Purity of the sample as a function of E_T^γ for different ranges in $|\eta^\gamma|$
$\rightarrow$ purity $\gtrsim 90\%$ for $E_T^\gamma > 40$ GeV

- Results cross-checked using another method based on isolation template fits
$\rightarrow$ good agreement

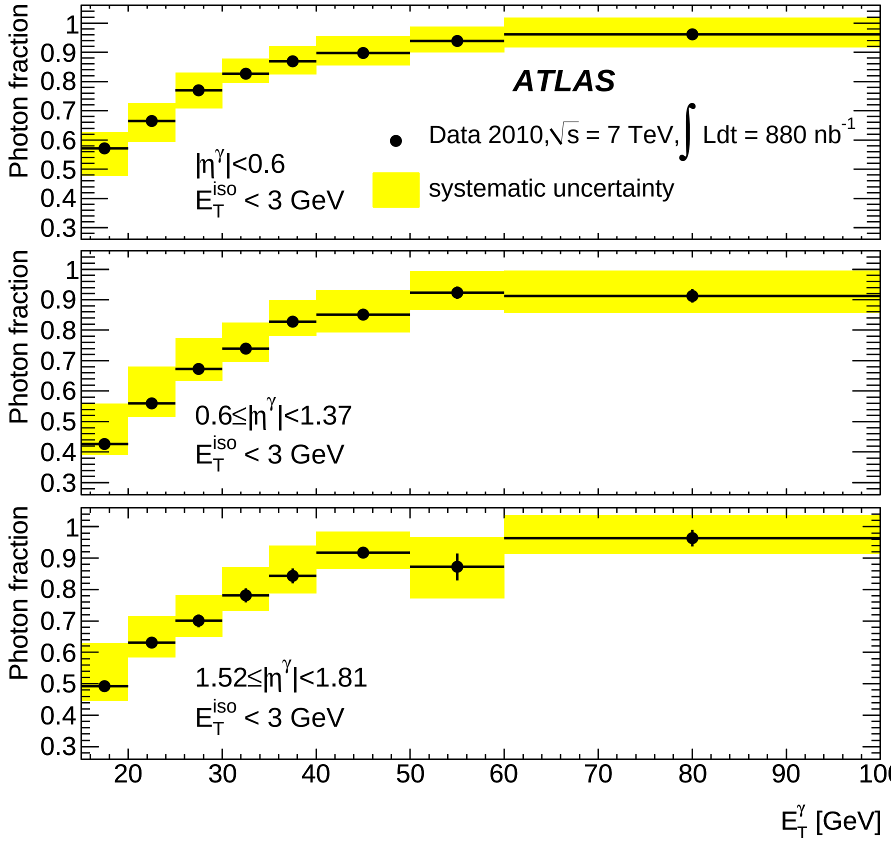

Inclusive photon production

NLO QCD calculations for inclusive photon production

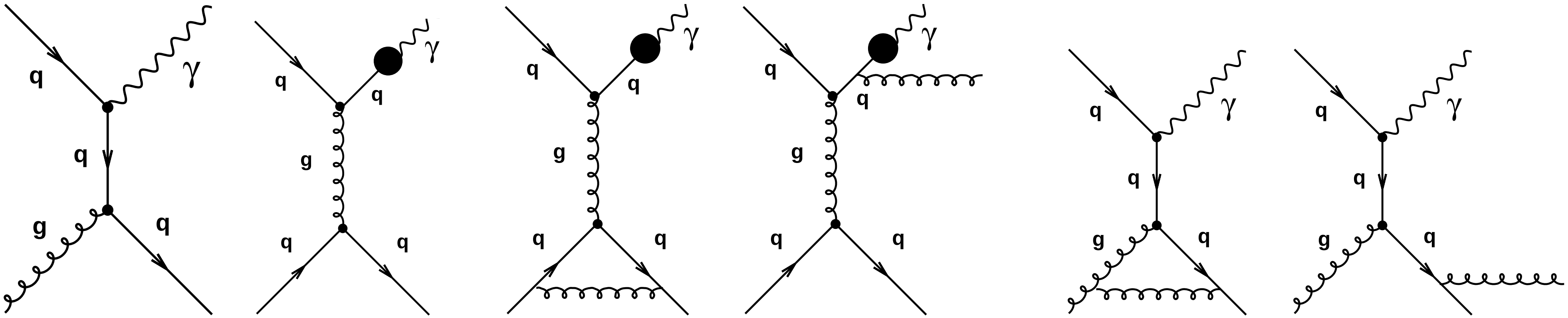

$$\sigma_{pp\to\gamma+X} = \sum_{i,j,a} \int_0^1 dx_1\, f_{i/p}(x_1,\mu_F^2) \int_0^1 dx_2\, f_{j/p}(x_2,\mu_F^2)\ \hat{\sigma}_{ij\to\gamma a} +$$

$$\sum_{i,j,a,b} \int_{z_{min}}^1 dz\, D_a^\gamma(z,\mu_f^2) \int_0^1 dx_1\, f_{i/p}(x_1,\mu_F^2) \int_0^1 dx_2\, f_{j/p}(x_2,\mu_F^2)\ \hat{\sigma}_{ij\to ab}$$

- The calculations includes NLO corrections for both direct-photon and fragmentation contributions; beware the components are not distinguishable beyond LO
- The calculations implement the photon isolation requirement at "parton" level: E_T^{iso} calculated with the (few) final-state partons in the perturbative QCD calculation

NLO QCD calculations for inclusive photon production

$$\sigma_{pp\to\gamma+X} = \sum_{i,j,a} \int_0^1 dx_1\, f_{i/p}(x_1,\mu_F^2) \int_0^1 dx_2\, f_{j/p}(x_2,\mu_F^2)\ \hat{\sigma}_{ij\to\gamma a} +$$

$$\sum_{i,j,a,b} \int_{z_{min}}^1 dz\, D_a^\gamma(z,\mu_f^2) \int_0^1 dx_1\, f_{i/p}(x_1,\mu_F^2) \int_0^1 dx_2\, f_{j/p}(x_2,\mu_F^2)\ \hat{\sigma}_{ij\to ab}$$

- $\mu_R = \mu_F = \mu_f = E_T^\gamma$
- proton PDF set → CTEQ6.6, CT10, MSTW2008
- fragmentation function → BFG set II

→ Corrections for hadronisation and underlying event needed

- Theoretical uncertainties:

→ higher-order terms (beyond NLO); estimated by varying μ_R, μ_F, μ_f

→ PDF-induced uncertainties; estimated using set of PDF eigenvectors

→ uncertainty on α_s; estimated taking into account correlation with PDF

→ uncertainty on non-perturbative correction; estimated with different MC and tunes

Corrections for non-perturbative effects; photon isolation

- The measurements are corrected for detector effects to the "particle" level
  $\rightarrow$ to isolated photons, where E_T^{iso} is calculated using all the final-state particles and the jet-area method is also applied ($\Rightarrow E_T^{iso*}$)
  This is performed using MC simulations

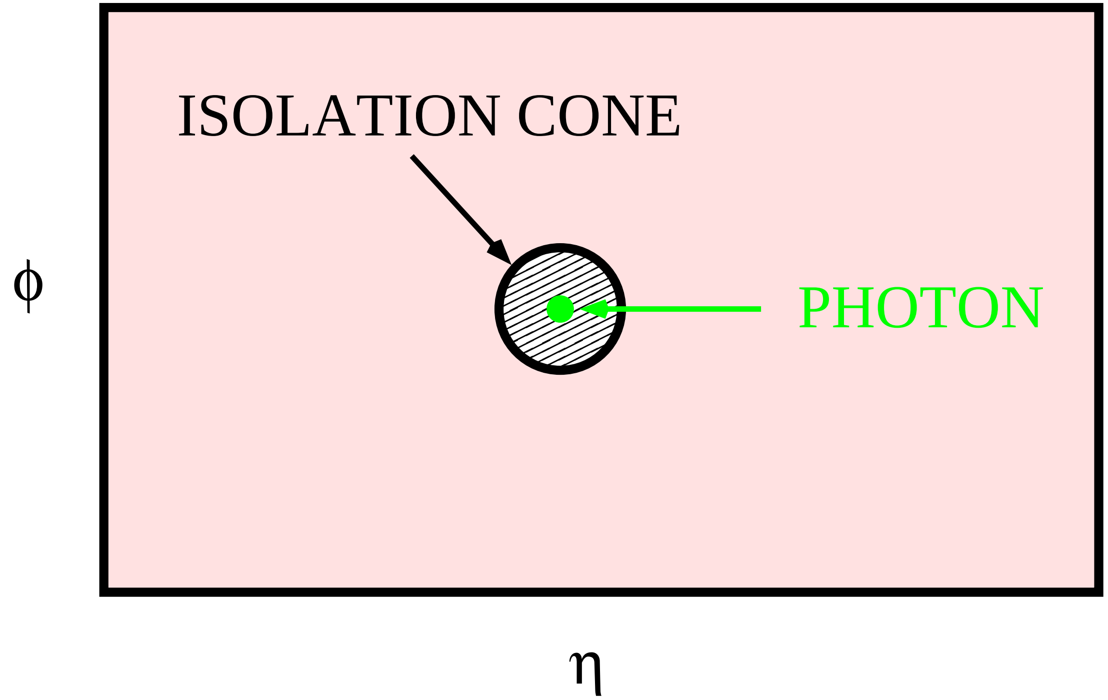

- Corrections for non-perturbative effects (hadronisation and underlying event)

$$C_{NP} = \frac{\sigma_{\gamma+\mathrm{x}}(\mathrm{MC, particle-level, UE})}{\sigma_{\gamma+\mathrm{x}}(\mathrm{MC, parton-level, no\ UE})}$$

$\rightarrow$ Less dependence on the modelling of the final state by having used the jet-area method to subtract the "extra" transverse energy contribution to E_T^{iso}

Inclusive isolated-photon production in pp collisions at $\sqrt{s} = 7$ TeV

$|\eta^\gamma| < 0.6$ $\quad$ $0.6 < |\eta^\gamma| < 1.37$ $\quad$ $1.81 < |\eta^\gamma| < 2.37$

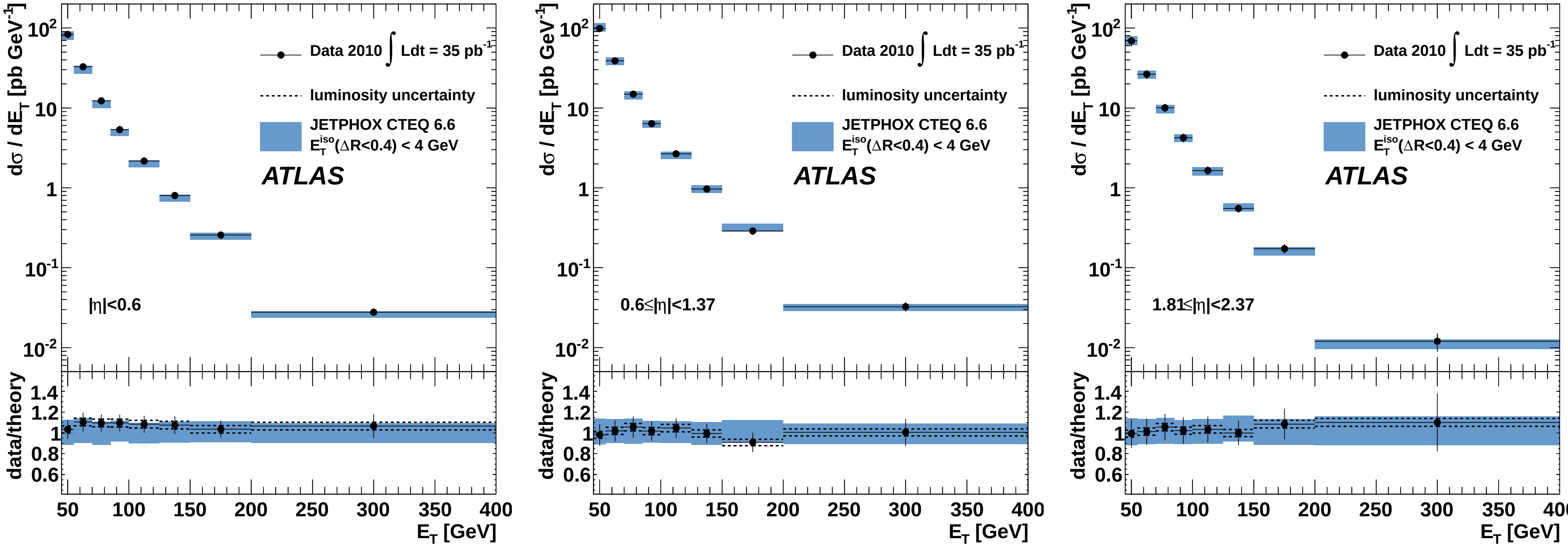

- **Measurement of $d\sigma/dE_T^\gamma$ for $25 < E_T^\gamma < 400$ GeV and different ranges in η^γ using $\mathcal{L} = 35\ \mathrm{pb}^{-1}$ of pp collision data at $\sqrt{s} = 7$ TeV**
- **Good description of the data by NLO QCD calculations (corrected for NP effects) in the new energy range opened by the LHC**

Impact of inclusive isolated photon measurements at LHC on PDFs

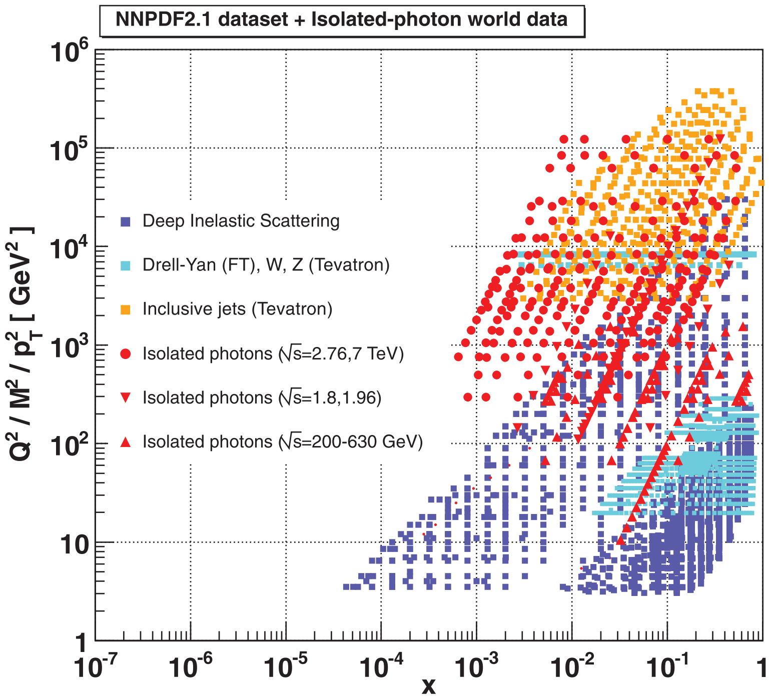

- Analysis by D. d'Enterria and J. Rojo (NPB860,2012,311)
- Study of the impact on the gluon density of existing isolated-photon measurements from a variety of experiments, from $\sqrt{s} = 200$ GeV up to 7 TeV
  - $\rightarrow$ those at LHC are the more constraining datasets
  - $\rightarrow$ reduction of gluon uncertainty up to 20%
  - $\rightarrow$ localised in the range $x \approx 0.002$ to 0.05

$\Rightarrow$ improved predictions for low mass Higgs production in gluon fusion, PDF-induced uncertainty decreased by 20%

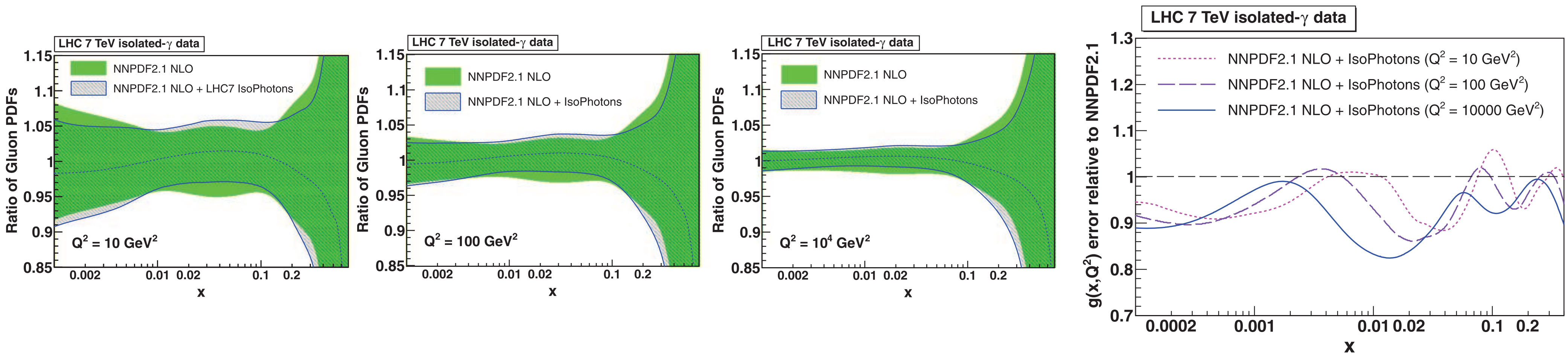

Inclusive isolated-photon production with 2011 data

$E_T^\gamma > 100$ GeV

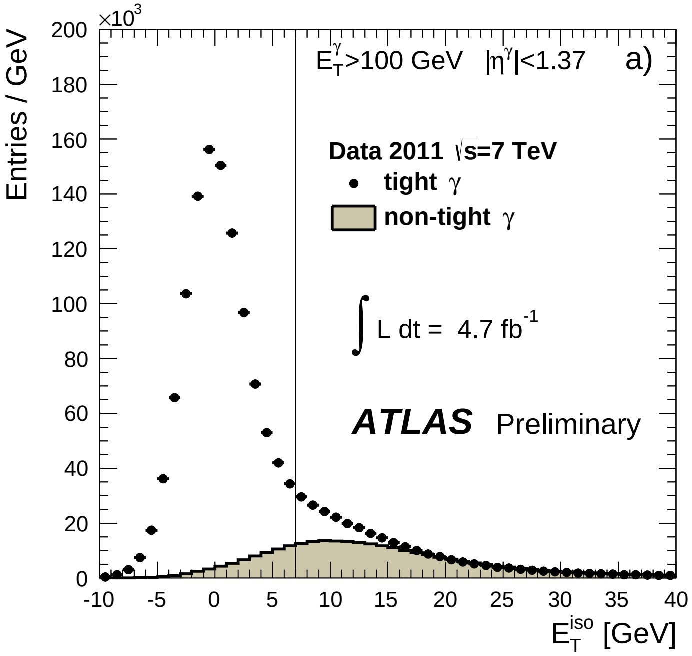

$500 < E_T^\gamma < 600$ GeV

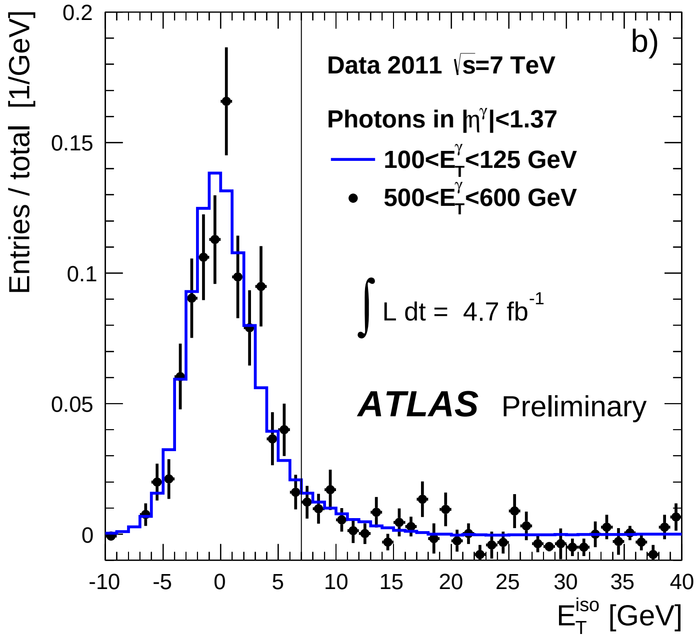

Signal purity

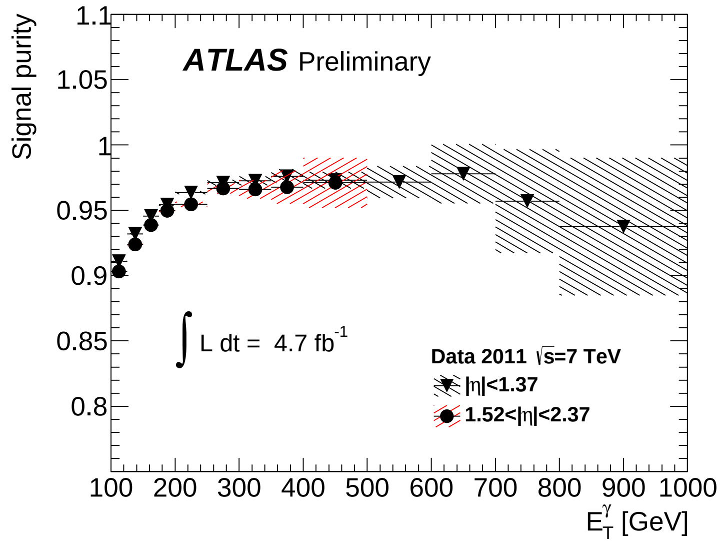

- **Measurement of inclusive isolated-photon production for $E_T^\gamma > 100$ GeV using $\underline{\mathcal{L} = 4.7\ \text{fb}^{-1}}$ of pp collision data at $\sqrt{s} = 7$ TeV (higher pileup during 2011)**
- **Photon isolation requirement $E_T^{iso} < 7$ GeV in order to optimize the signal purity and the photon reconstruction efficiency at high E_T^γ**

Inclusive isolated-photon production with 2011 data

$E_T^\gamma > 100$ GeV $\quad |\eta^\gamma| < 1.37 \quad 1.52 < |\eta^\gamma| < 2.37$

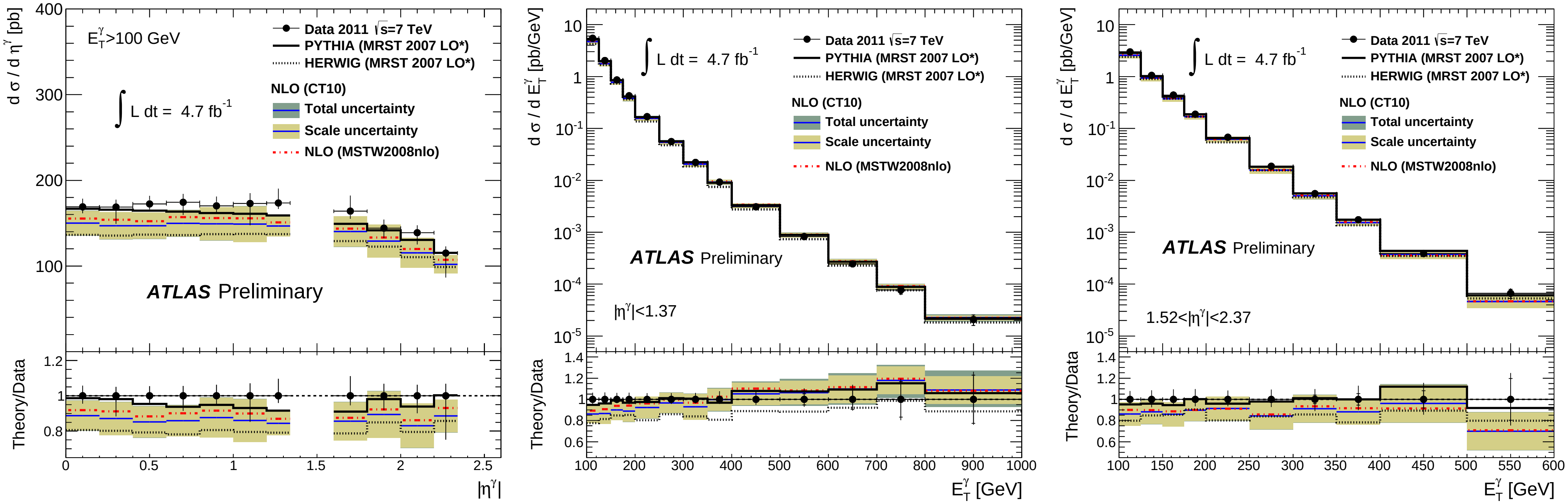

- **Measurement of $d\sigma/dE_T^\gamma$ and $d\sigma/d|\eta^\gamma|$ for $E_T^\gamma > 100$ GeV and different ranges in η^γ using $\mathcal{L} = 4.7$ fb^{-1} of pp collision data at $\sqrt{s} = 7$ TeV; $E_T^{iso*} < 7$ GeV**

- **Good description of the data by NLO QCD calculations up to ~ 1 TeV**
- **Tendency in the data to be above NLO QCD at low E_T^γ**

Photon+jet production

γ + jet production in pp collisions at $\sqrt{s} = 7$ TeV

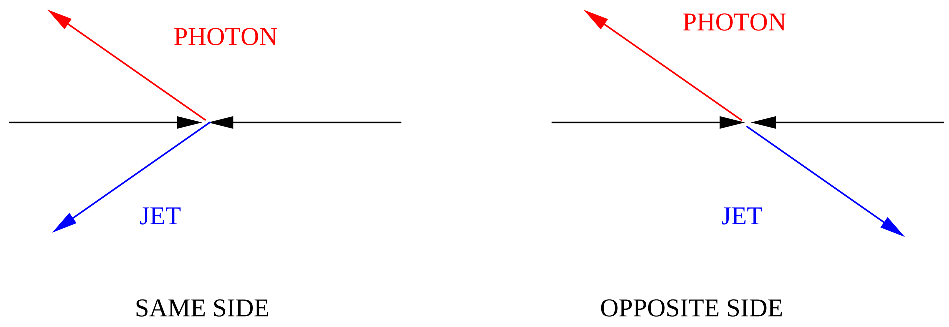

- Further experimental information can be extracted from photon production data by measuring the recoiling jet and
- Measuring γ + jet for different angular configurations (same side vs opposite side) and different ranges in $|y^{\rm jet}|$

  $\Rightarrow$ allows the separation of contributions from different x values

  $x_1 = E_T^\gamma(e^{+\eta^\gamma} + e^{+y^{\rm jet}})/\sqrt{s}$ $\quad x_2 = E_T^\gamma(e^{-\eta^\gamma} + e^{-y^{\rm jet}})/\sqrt{s}$

  $\Rightarrow$ allows the comparison with theory in regions where fragmentation contributions are different: fragmentation contribution in OS is 20-50% higher than in SS
- Measurement of $d\sigma/dE_T^\gamma$ in the phase-space region defined by $E_T^\gamma > 25$ GeV, $|\eta^\gamma| < 1.37$, $p_T^{\rm jet} > 20$ GeV and three ranges in $y^{\rm jet}$: $|y^{\rm jet}| < 1.2$, $1.2 < |y^{\rm jet}| < 2.8$ and $2.8 < |y^{\rm jet}| < 4.4$ (leading jet, reconstructed using the anti-k_t algorithm with $R = 0.4$), both for OS and SS; $E_T^{\rm iso*} < 4$ GeV and $\Delta R_{\gamma j} > 1$
- The measurements cover the region $x \gtrsim 10^{-3}$ and $625 < Q^2 < 1.6 \cdot 10^5$ GeV^2

Systematic experimental uncertainties

- Distorted material: simulation of the detector geometry (photon conversions and EM showers); 1-23% depending on E_T^γ and $|y^{\rm jet}|$
- Photon simulation: PYTHIA vs HERWIG; direct-photon vs photons radiated off quarks; 4-16% depending on E_T^γ and $|y^{\rm jet}|$
- Photon energy scale and resolution: negligible
- Jet energy scale: mostly 1st bin E_T^γ; 3-7% (9-20%) for central/forward (very forward) jets
- Tightness control region: using a different set of background identification criteria; 5% (12%) for central (forward) jets and decreasing with E_T^γ
- Trigger efficiency: 0.6% (0.4%) for $E_T^\gamma < 45$ GeV (> 45 GeV)
- Luminosity uncertainty: 3.4%

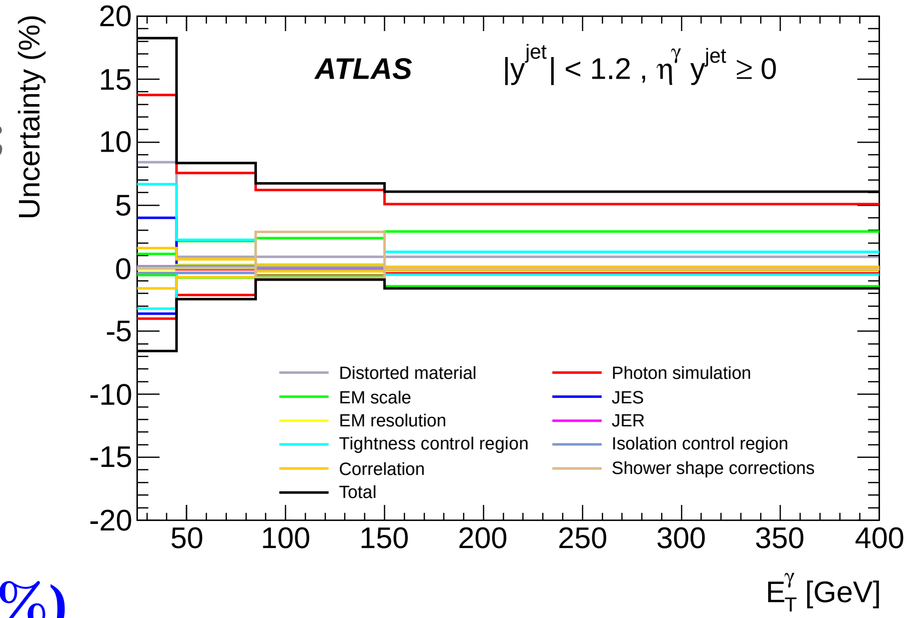

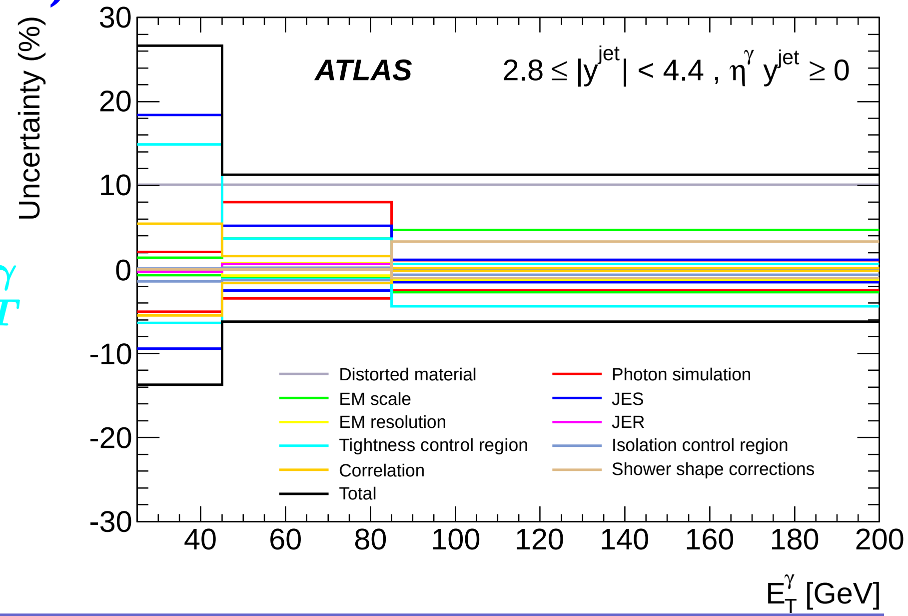

NLO QCD calculations and non-perturbative effects

- NLO QCD calculations of γ + jet production
  - $\rightarrow \mu_R = \mu_F = \mu_f = E_T^\gamma$
  - $\rightarrow$ CT10 proton PDFs
  - $\rightarrow$ NLO photon fragmentation function (BFG set II)
  - $\rightarrow$ photon-isolation requirement at parton level E_T^{iso}(partons)< 4 GeV
- Corrections for non-perturbative effects (hadronisation and underlying event) using PYTHIA (AMBT1 and Perugia2010 tunes) and HERWIG (UE7000-2 tune)
- Theoretical uncertainties

$\rightarrow$ terms beyond NLO (variations of μ_R, μ_F, μ_f)

$\rightarrow$ PDF-induced uncertainties

$\rightarrow$ correspondence parton/particle-level isolation

$\rightarrow$ non-perturbative correction

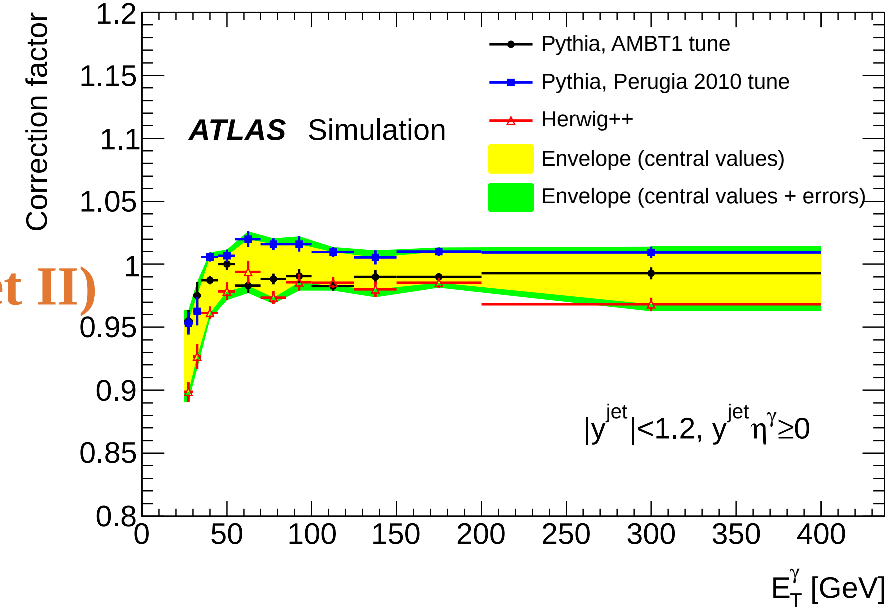

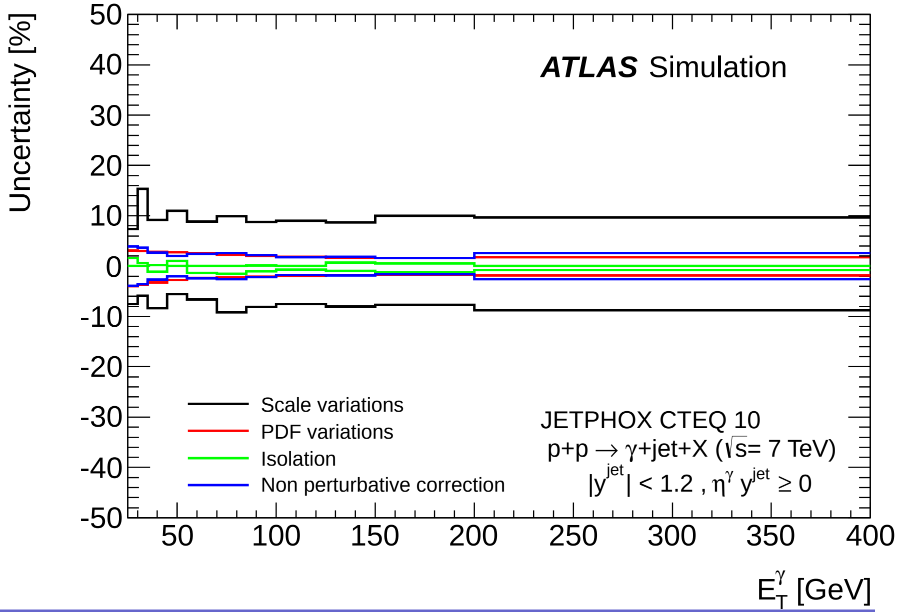

γ + jet production: same side, $\eta^\gamma \cdot y^{\rm jet} \geq 0$

$|y^{\rm jet}| < 1.2$ $\quad$ $1.2 < |y^{\rm jet}| < 2.8$ $\quad$ $2.8 < |y^{\rm jet}| < 4.4$

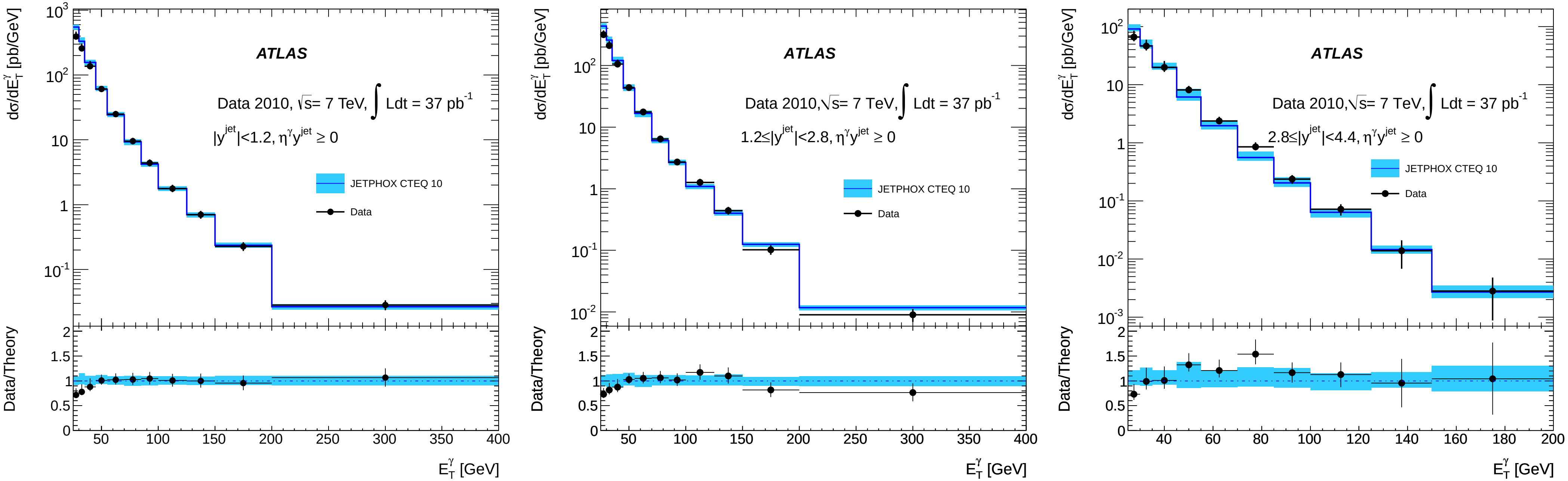

- **NLO QCD calculations corrected for non-perturbative effects are in fair agreement with the measurements within the uncertainties except for $E_T^\gamma < 45$ GeV**

- **Data consistently lower than the calculations for $E_T^\gamma < 45$ GeV**
  $\rightarrow$ Inadequacy of the NLO QCD calculations at low E_T^γ? higher-order effects?

$\gamma + \text{jet}$ production: opposite side, $\eta^{\gamma} \cdot y^{\text{jet}} < 0$

$|y^{\text{jet}}| < 1.2$ | $1.2 < |y^{\text{jet}}| < 2.8$ | $2.8 < |y^{\text{jet}}| < 4.4$

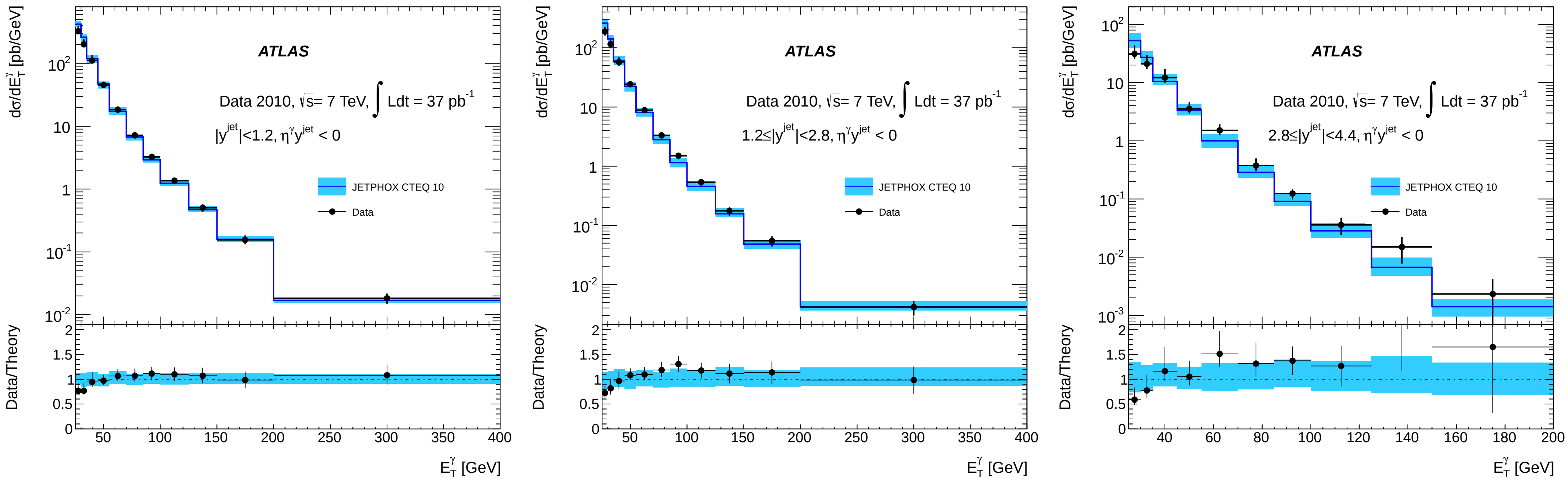

- NLO QCD calculations corrected for non-perturbative effects are in fair agreement with the measurements within the uncertainties except for $E_T^{\gamma} < 45$ GeV
- Data consistently lower than the calculations for $E_T^{\gamma} < 45$ GeV

  $\rightarrow$ Inadequacy of the NLO QCD calculations at low E_T^{γ}? higher-order effects?

- The data have the potential to contribute to the determination of the proton PDFs

Dynamics of $\gamma +$ jet production in pp collisions at $\sqrt{s} = 7$ TeV

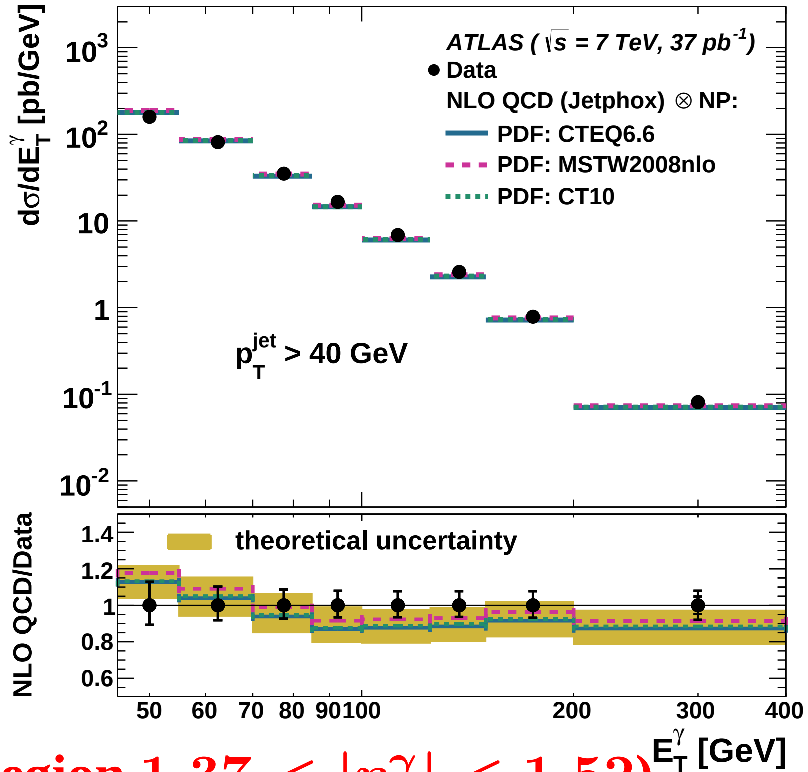

- Study of the $\gamma +$ jet dynamics by measuring the differential cross sections as functions of
  $\rightarrow$ Photon: E_T^γ
  $\rightarrow$ Jet: $p_T^{\rm jet}$, $y^{\rm jet}$
  $\rightarrow$ Photon+Jet: $\Delta\phi^{\gamma j}$, $m^{\gamma j}$, $\cos\theta^{\gamma j}$
  where $\cos\theta^{\gamma j} = \tanh\frac{1}{2}(y^{\rm jet} - \eta^\gamma)$
  $\theta^{\gamma j} =$ scattering angle in centre-of-mass frame for $2 \rightarrow 2$ hard collinear scattering
- Measurements in the phase-space region defined by: $E_T^\gamma > 45$ GeV, $|\eta^\gamma| < 2.37$ (excluding the region $1.37 < |\eta^\gamma| < 1.52$)
  $p_T^{jet} > 40$ GeV, $|y^{\rm jet}| < 2.37$ for the leading jet (anti-k_t algorithm with $R = 0.6$)
  $E_T^{\rm iso*} < 4$ GeV and $\Delta R_{\gamma j} > 1$
- Comparison to NLO QCD calculation (JETPHOX) corrected for non-perturbative effects
- Small experimental and theoretical uncertainties: $\sim 10\%$
- Good description of the measured $d\sigma/dE_T^\gamma$ by the NLO QCD calculations

Dynamics of $\gamma + $ jet production in pp collisions

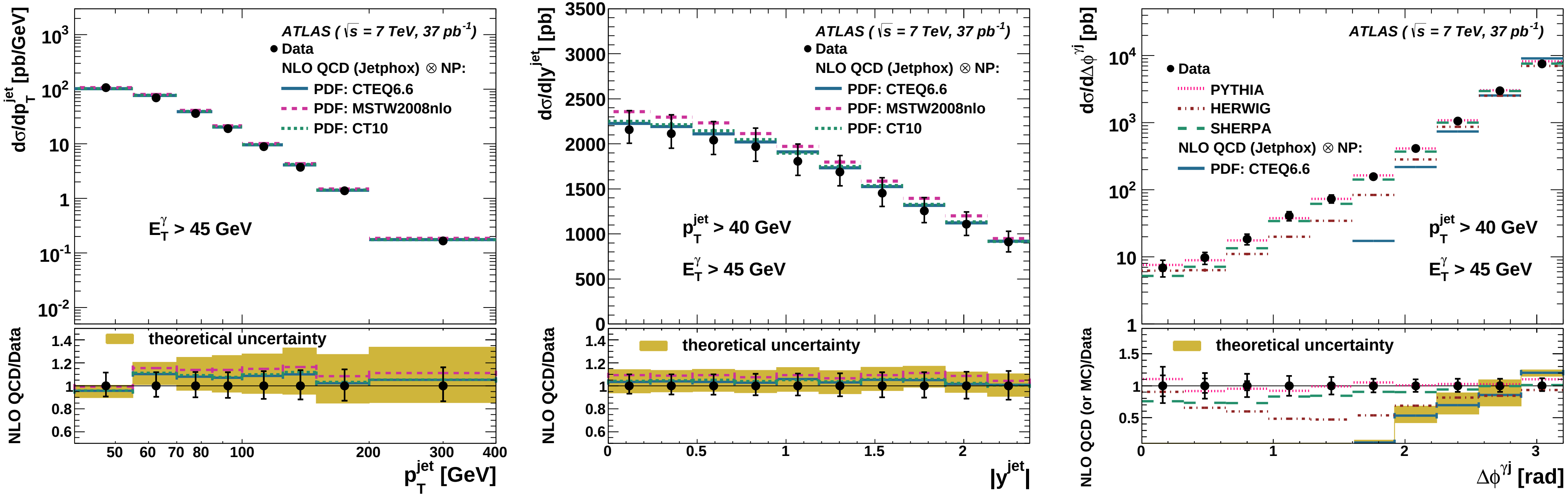

- Good description of the measured $d\sigma/dp_T^{\rm jet}$ and $d\sigma/d|y^{\rm jet}|$ by the NLO QCD calculations both in normalisation and shape
- Not unexpectedly, NLO QCD calculations fail to describe $d\sigma/d\Delta\phi^{\gamma j}$: with up to three final-state particles, the photon and the leading jet cannot be in the same hemisphere in the transverse plane $\Rightarrow \Delta\phi^{\gamma j} \geq \pi/2$
- PYTHIA and SHERPA MC models give a good description of $d\sigma/d\Delta\phi^{\gamma j}$

Selection of unbiased region to measure the $m^{\gamma j}$ and $\theta^{\gamma j}$ distributions

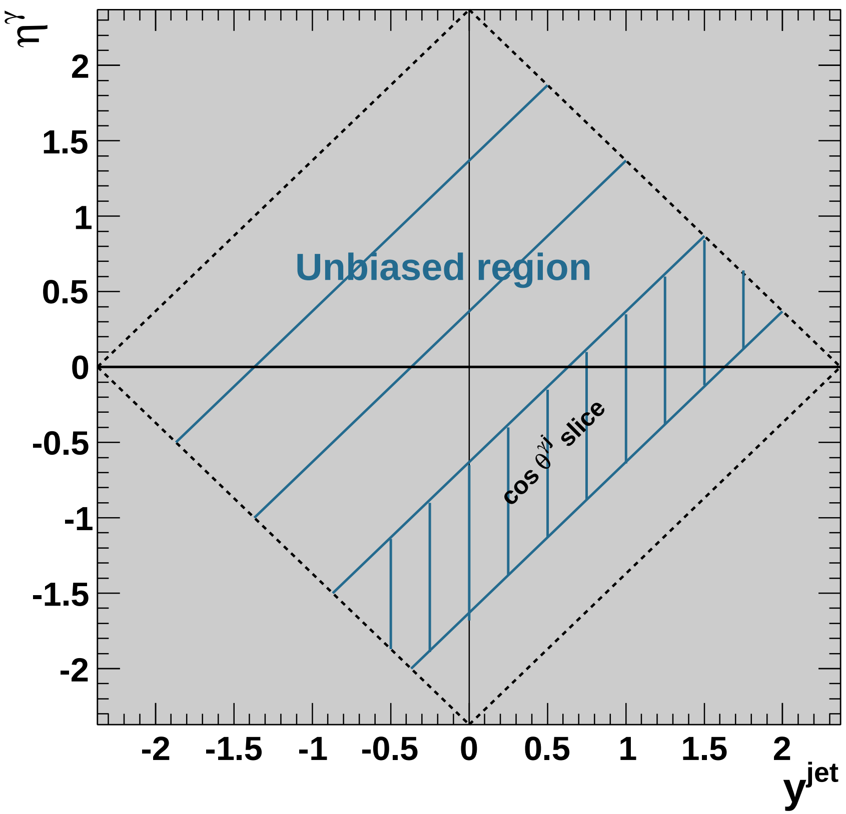

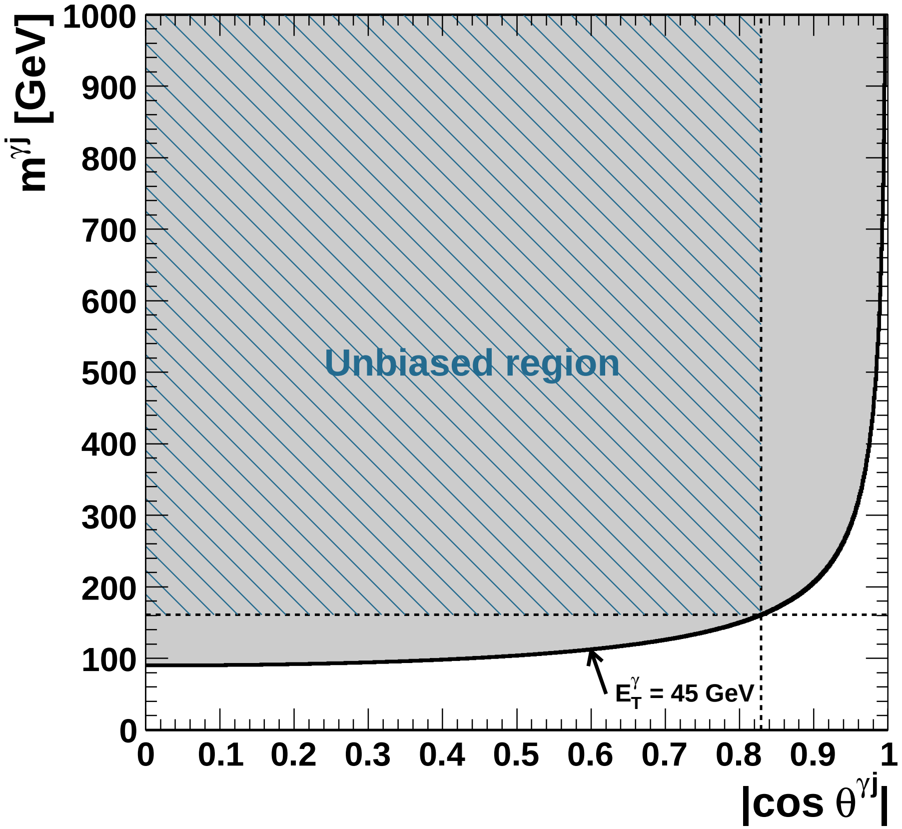

$$|\eta^{\gamma} + y^{jet}| < 2.37 \quad , \quad |\cos\theta^{\gamma j}| < 0.83 \quad , \quad m^{\gamma j} > 161 \text{ GeV}$$

- First two requirements: avoiding the bias induced by cuts on η^{γ} and y^{jet}; slices of $\cos\theta^{\gamma j}$ have the same length along the $\eta^{\gamma} + y^{jet}$ axis
- Third requirement: avoiding the bias due to $E_T^{\gamma} > 45$ GeV in $(|\cos\theta^{\gamma j}|, m^{\gamma j})$ plane

Dynamics of $\gamma + $ jet production in pp collisions

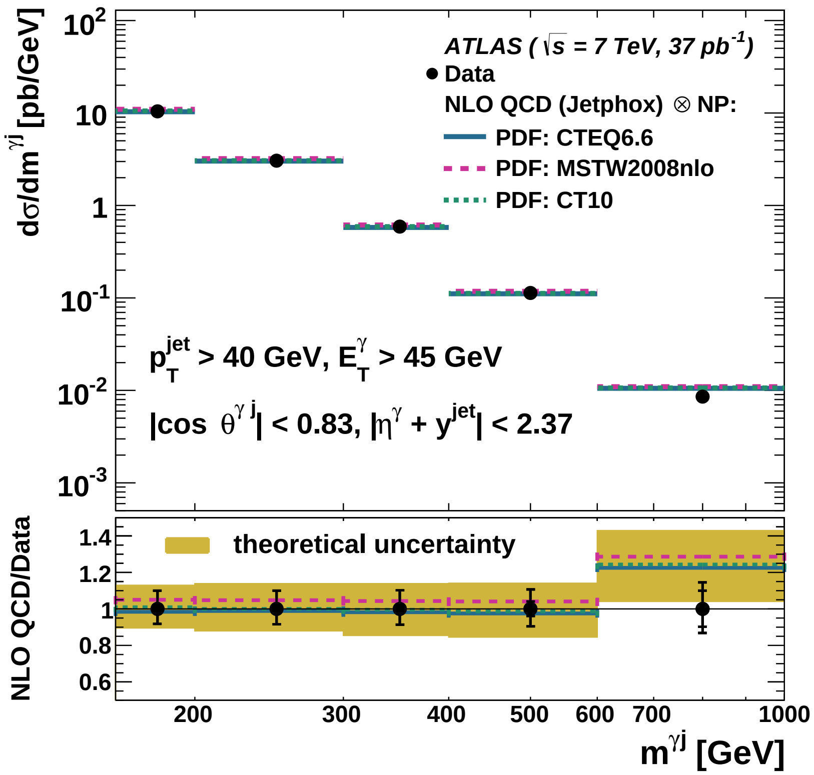

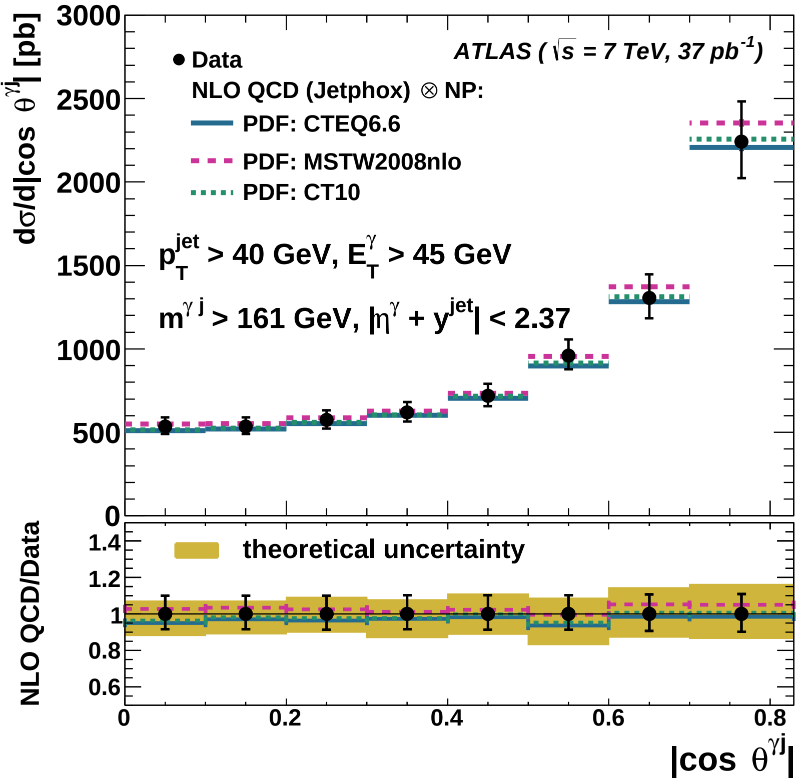

- In the selected (unbiased) region the angular distribution increases as $|\cos\theta^{\gamma j}|$ increases
- Good description of the data by the NLO QCD calculations within the (small) experimental and theoretical uncertainties $\Rightarrow$ validation of the description of the dynamics of $\gamma +$ jet production in pp collisions at $\mathcal{O}(\alpha_{em}\alpha_s^2)$

Dynamics of γ + jet production in pp collisions

- Angular distribution $d\sigma/d|\cos\theta^{\gamma j}|$ sensitive to the spin of the exchanged (virtual) particle: quark(1/2) vs gluon(1)

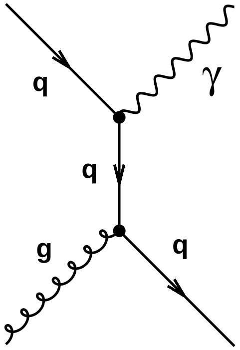

direct-photon process

$$d\sigma/d|\cos\theta^{\gamma j}| \sim (1 - |\cos\theta^{\gamma j}|)^{-1}$$

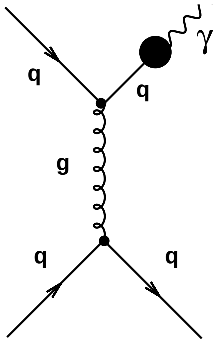

fragmentation process

$$d\sigma/d|\cos\theta^{\gamma j}| \sim (1 - |\cos\theta^{\gamma j}|)^{-2}$$

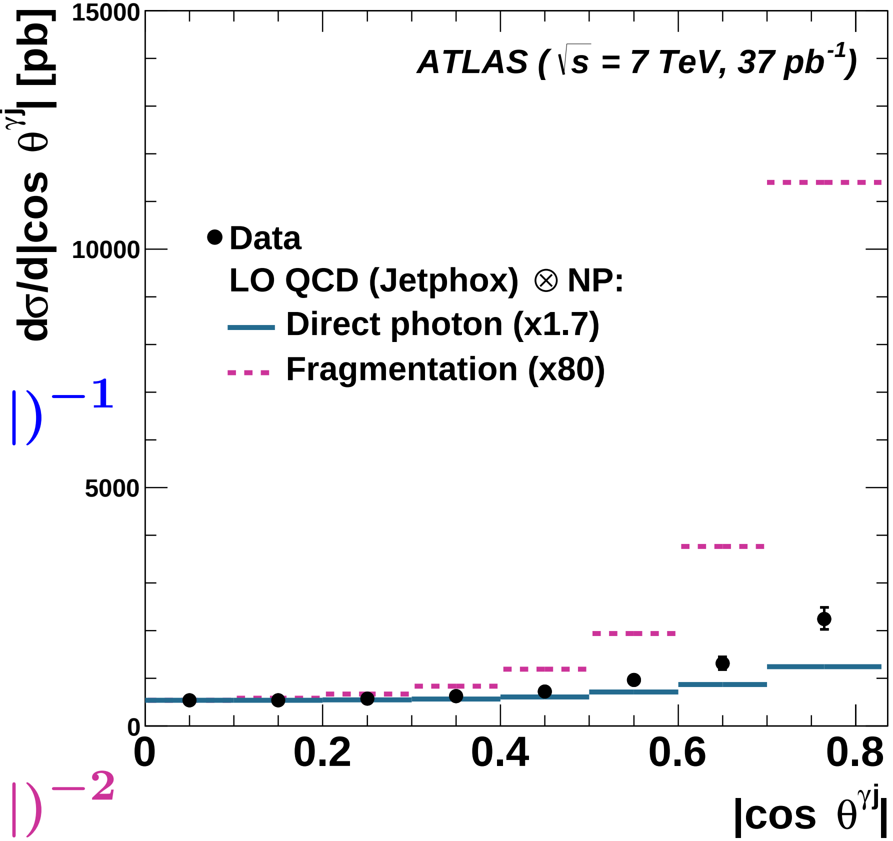

- Measured angular distribution closer to that of direct-photon processes than fragm.

$\Rightarrow$ consistent with the dominance of processes in which a virtual quark is exchanged

Understanding the $\gamma + \text{jet}$ background to $H \to \gamma\gamma$

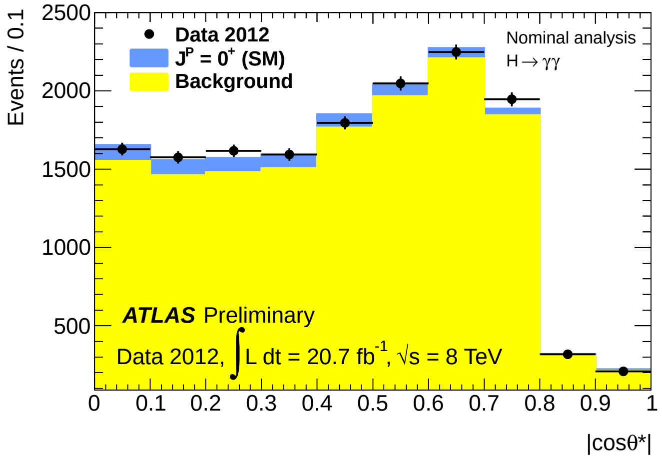

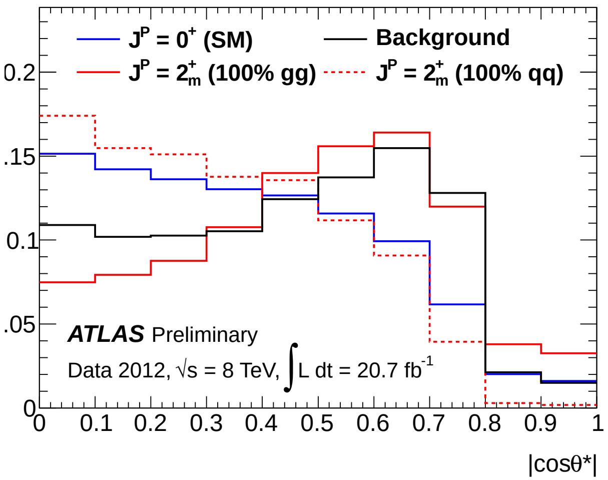

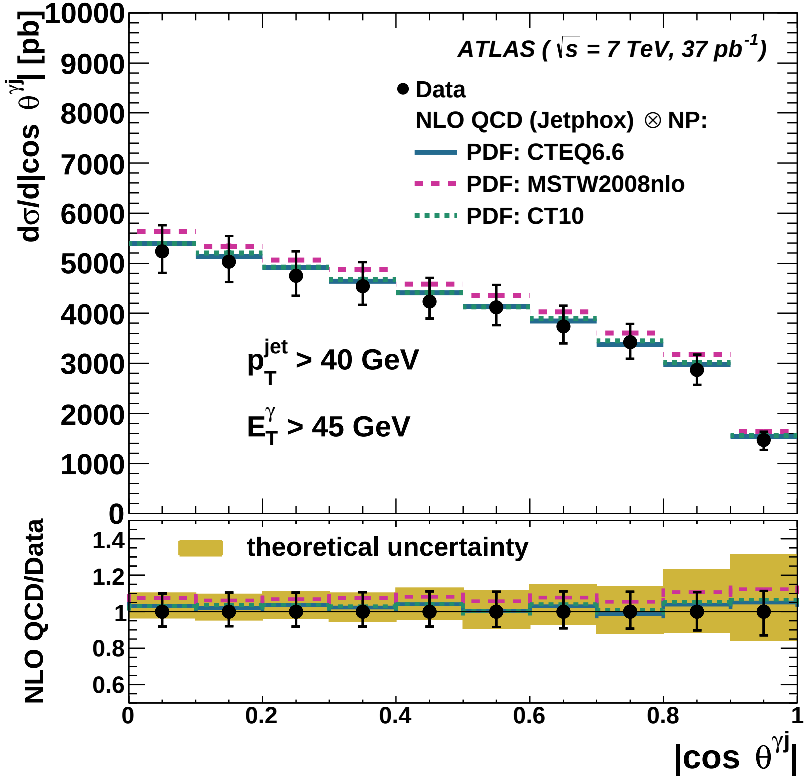

- $\gamma + \text{jet}$ production is the 2nd largest source of background to $H \to \gamma\gamma$
- $\cos\theta^*$ distribution used to determine the spin of the Higgs-like particle discovered in 2012
- Measurement of $d\sigma/d|\cos\theta^{\gamma j}|$ without additional requirements (no cut on $m^{\gamma j}$!)
- Good description of the measurement by NLO QCD calculations

  $\Rightarrow$ precise understanding of this background both in normalization and shape in terms of the Standard Model

Photon pair production

Isolated-photon pair production in *pp* collisions

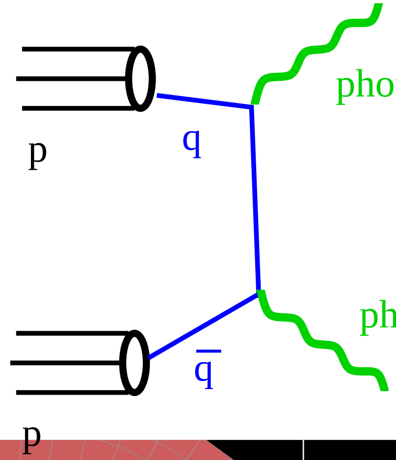

- Measurements of the process $pp \to \gamma\gamma + \mathrm{X}$ with the aim of testing pQCD and understanding the irreducible background to new physics processes involving photons or $H \to \gamma\gamma$
- Measurement of differential cross sections as functions of

$\to$ diphoton invariant mass, $m_{\gamma\gamma}$

$\to$ diphoton transverse momentum, $p_{T,\gamma\gamma}$

$\to$ azimuthal separation in LAB frame, $\Delta\phi_{\gamma\gamma}$

$\to$ cosine of the polar angle of highest-E_T photon in the Collins-Soper diphoton rest frame, $\cos\theta^*_{\gamma\gamma}$

in the phase-space region defined by: $E_T^{\gamma 1,2} > 25(22)$ GeV, $|\eta^\gamma| < 2.37$ (excluding the region $1.37 < |\eta^\gamma| < 1.52$), $\Delta R_{\gamma\gamma} > 0.4$ and $E_T^{iso*} < 4$ GeV using $\underline{\mathcal{L} = 4.9\ \mathrm{fb}^{-1}}$

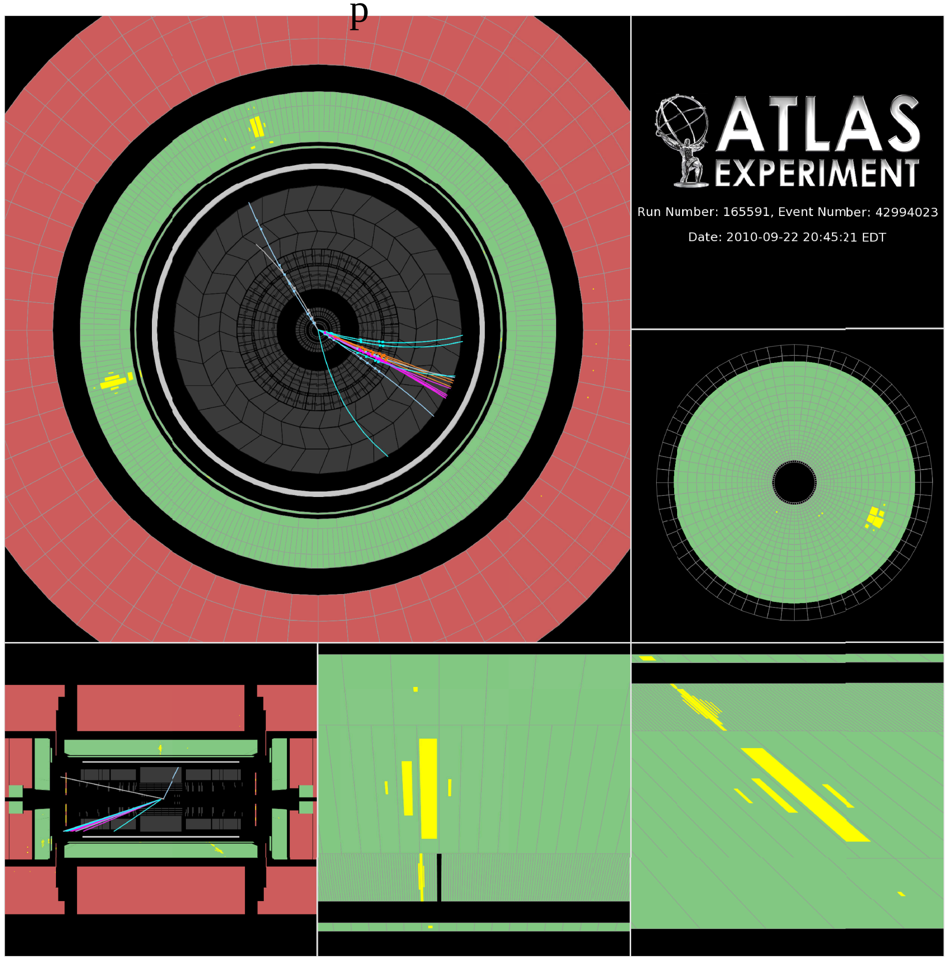

Isolated-photon pair production in pp collisions at $\sqrt{s} = 7$ TeV

- **Comparison to theoretical calculations**
- **Fixed-order QCD calculations (NP corrected)**
  - $\rightarrow$ **2γNNLO program; NNLO calculation of direct-photon contribution (no fragm.)**
  - $\rightarrow$ **DIPHOX program; NLO calculation of direct-photon and fragmentation contributions; box diagram $gg \rightarrow \gamma\gamma$ (at NLO) included using GAMMA2MC**
- **Matrix-elements plus parton shower calculations**
  - $\rightarrow$ **PYTHIA (2 $\rightarrow$ 2 + PS)**
  - $\rightarrow$ **SHERPA (2 $\rightarrow$ 2(3, 4) + PS)**
- **The contribution from $H \rightarrow \gamma\gamma$ is neglected (1%)**

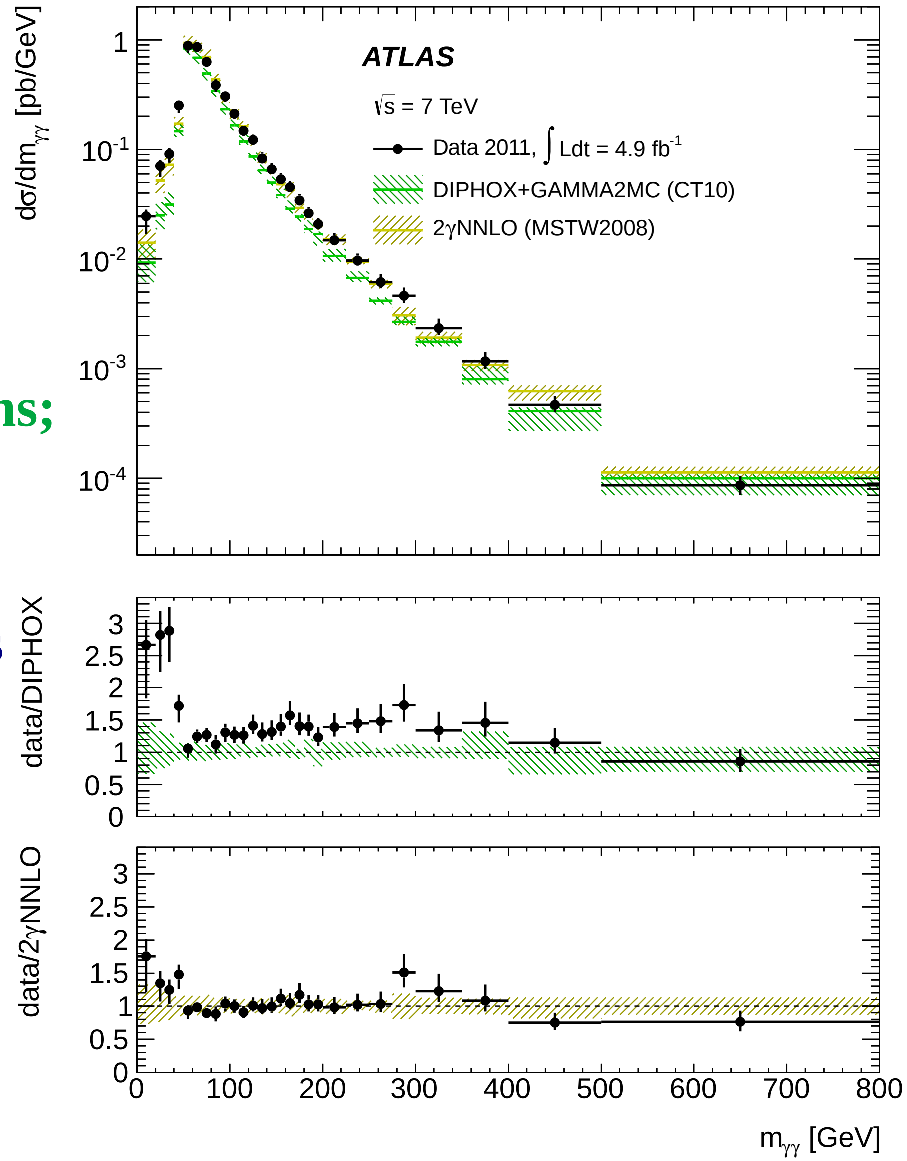

Isolated-photon pair production in pp collisions at $\sqrt{s} = 7$ TeV

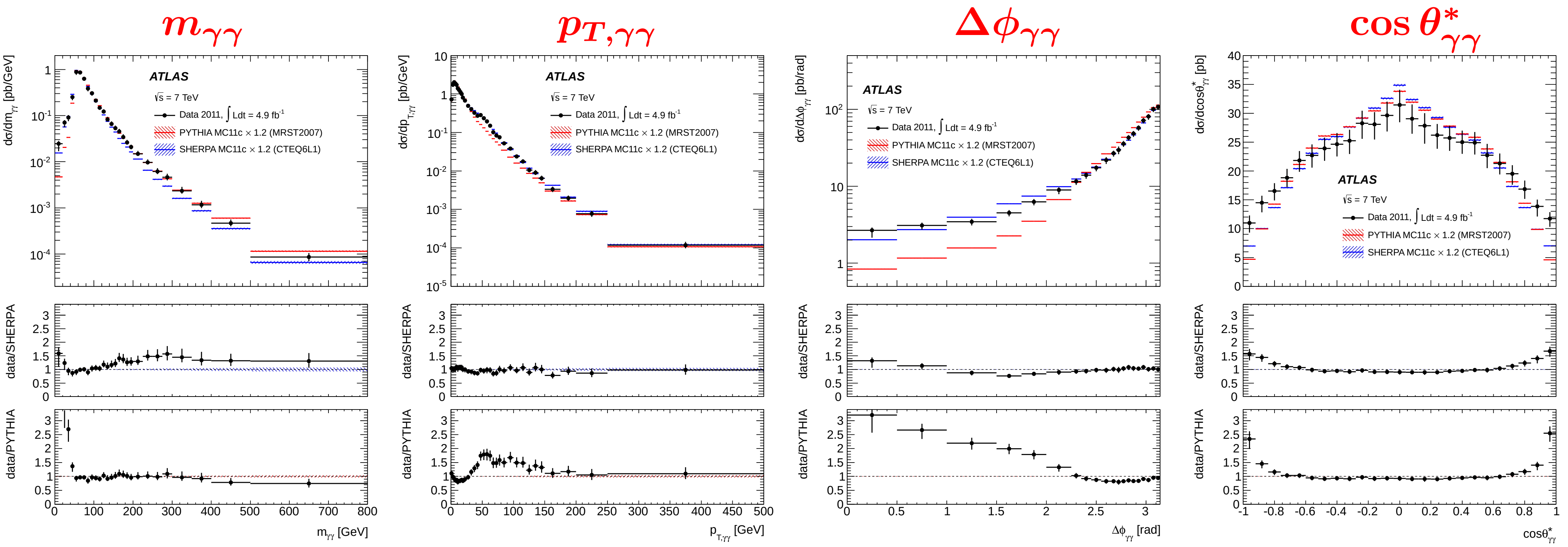

- **Comparison to matrix-elements plus parton shower calculations of PYTHIA and SHERPA**
  - **$\rightarrow$ MC normalisations rescaled by 1.2 to compare shapes**
  - **$\rightarrow$ $\Delta\phi_{\gamma\gamma} \sim \pi$ and low $p_{T,\gamma\gamma}$ (soft gluon resummation important): both MCs do well**
  - **$\rightarrow$ low $\Delta\phi_{\gamma\gamma}$ and low $m_{\gamma\gamma}$: PYTHIA fails**
  - **$\rightarrow$ SHERPA performs well except for high $m_{\gamma\gamma}$**

Isolated-photon pair production in pp collisions at $\sqrt{s} = 7$ TeV

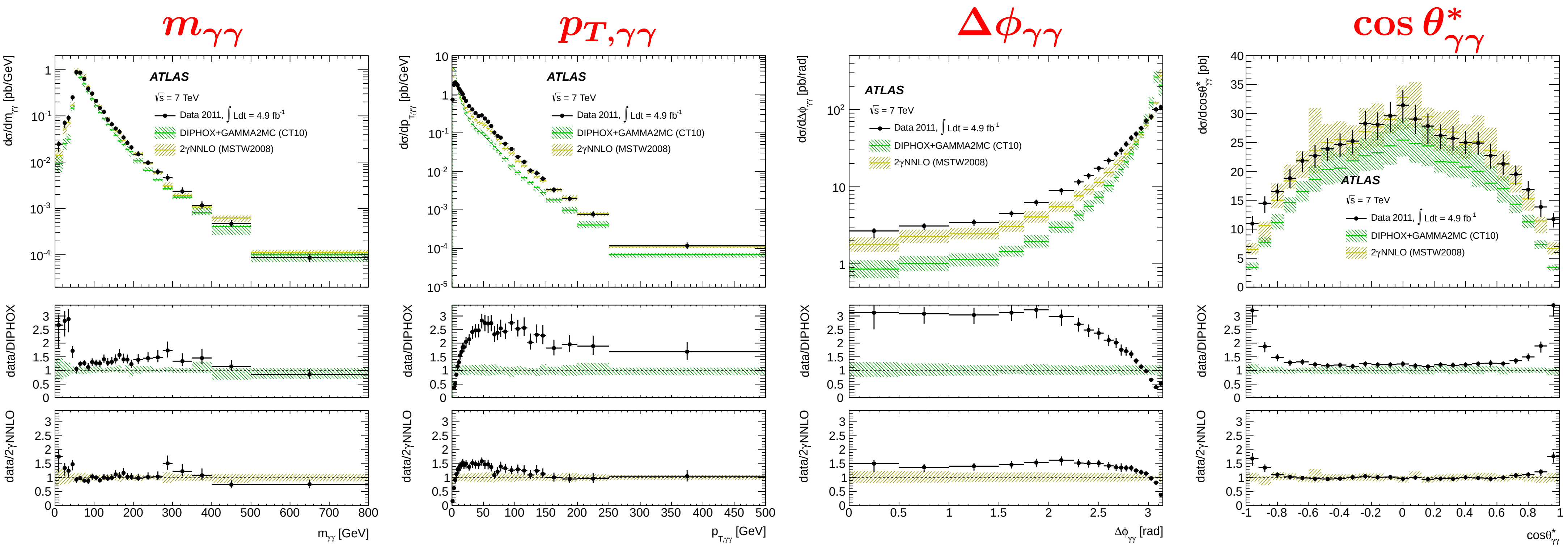

- **Comparison to fixed-order calculations of 2γNNLO and DIPHOX+GAMMA2MC**
  - → no re-scaling of the normalisations! (absolute predictions)
  - → $\Delta\phi_{\gamma\gamma} \sim \pi$ and low $p_{T,\gamma\gamma}$ (soft gluon resummation important): both fail
  - → DIPHOX+GAMMA2MC predictions underestimate the data
  - → inclusion of h.o. (2γNNLO) improves dramatically the description of the data

2012 data

Even more data (with more pile-up) being analysed!

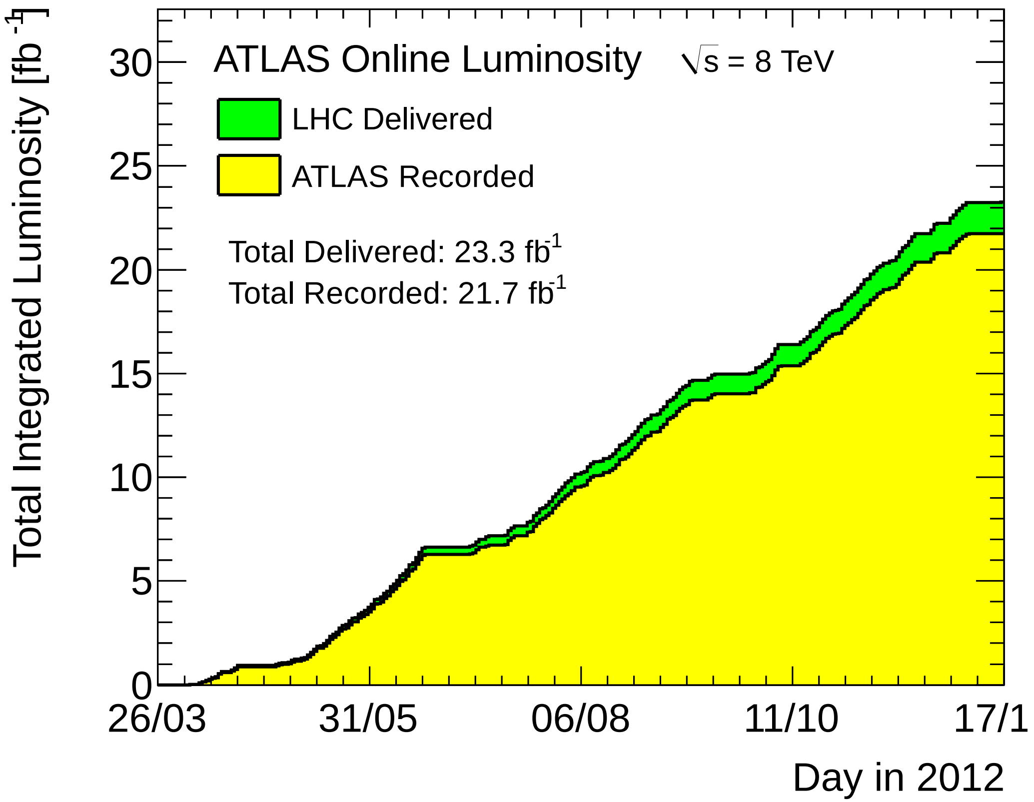

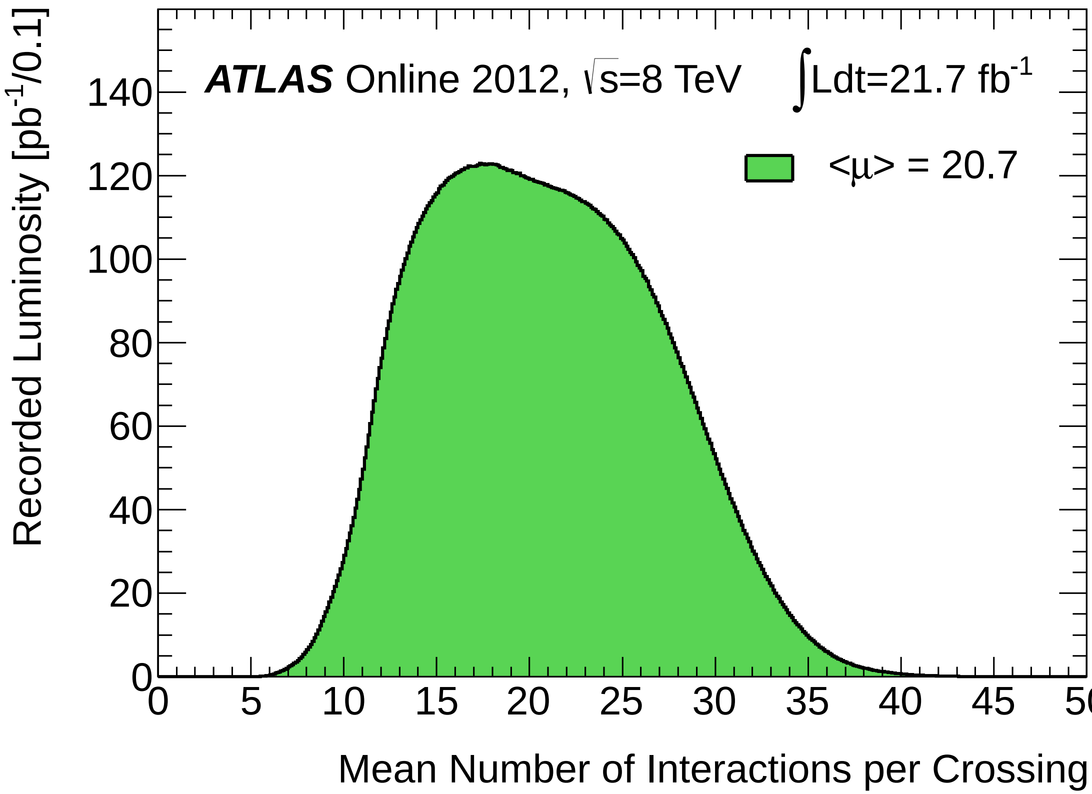

- An integrated luminosity of ~ 20 fb^{-1} of pp collisions at $\sqrt{s} = 8$ TeV

$\rightarrow$ **Mean number of interactions per crossing $\langle\mu\rangle = 20.7$ (harsh environment!)**

$\Rightarrow$ **Exploration of the high tails in jet p_T and dijet (multijet) invariant mass**

Even more data (with more pile-up) being analysed!

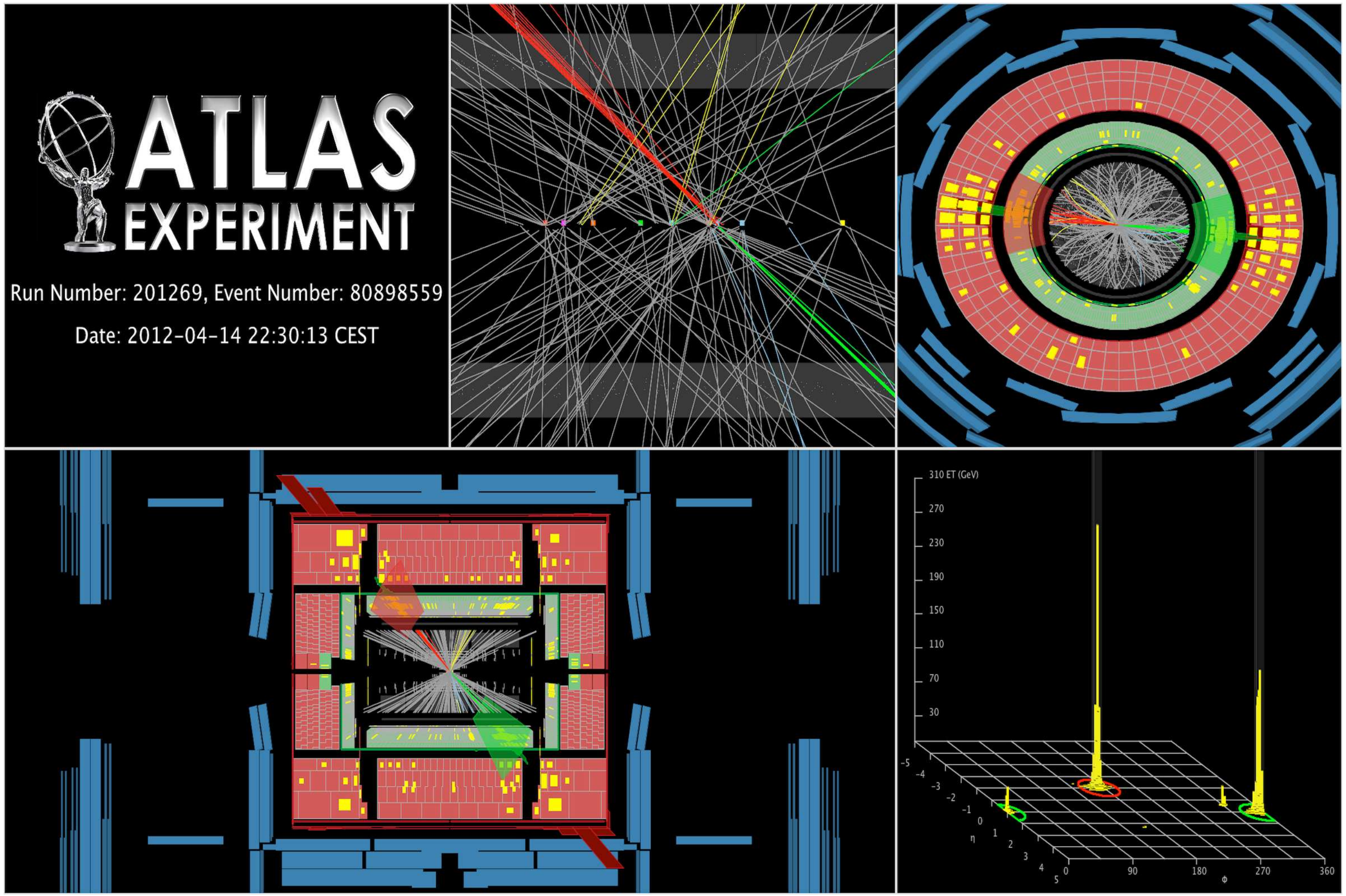

- A high-mass central dijet event collected in 2012: $m_{12} = 4.23$ TeV
  1st jet: $p_T = 1.36$ TeV, $\eta = -1.02$; 2nd jet: $p_T = 1.29$ TeV, $\eta = 1.06$

Summary of jet measurements in *pp* collisions at the LHC

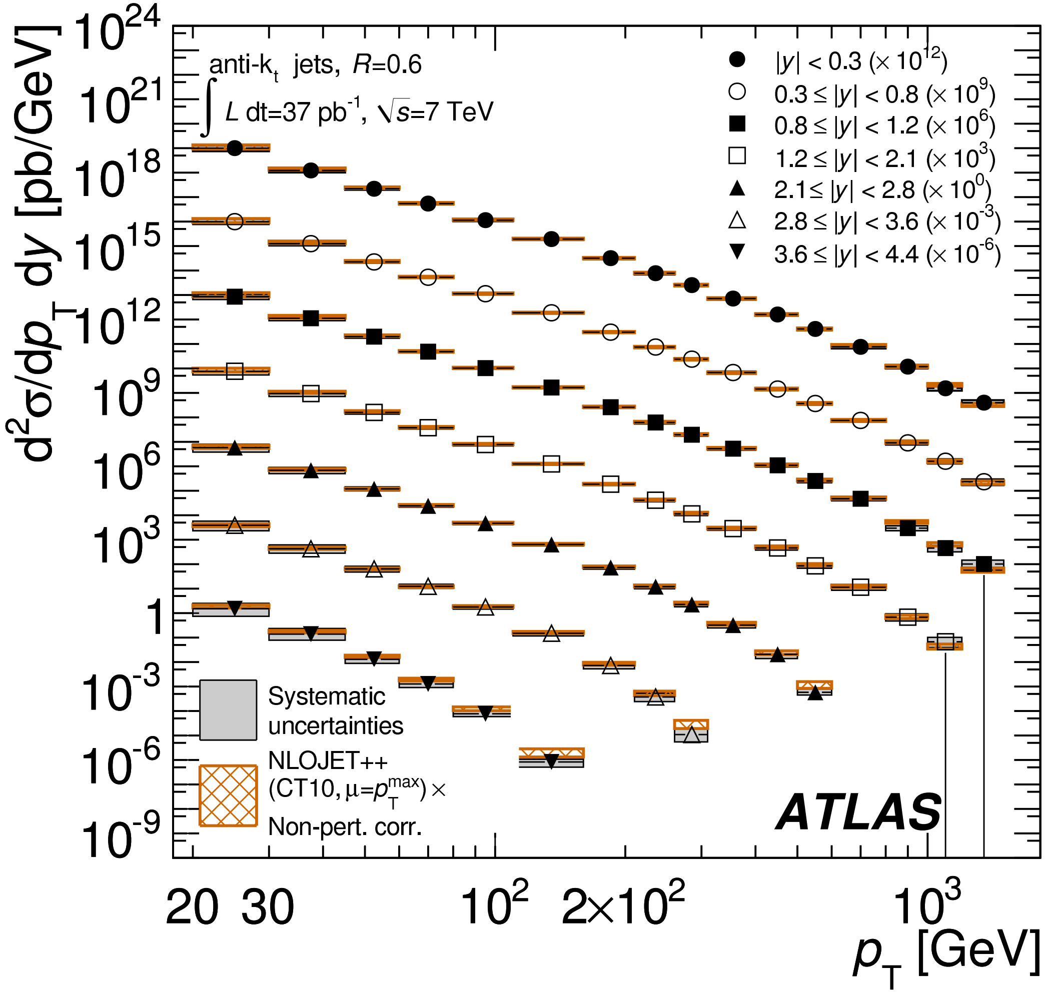

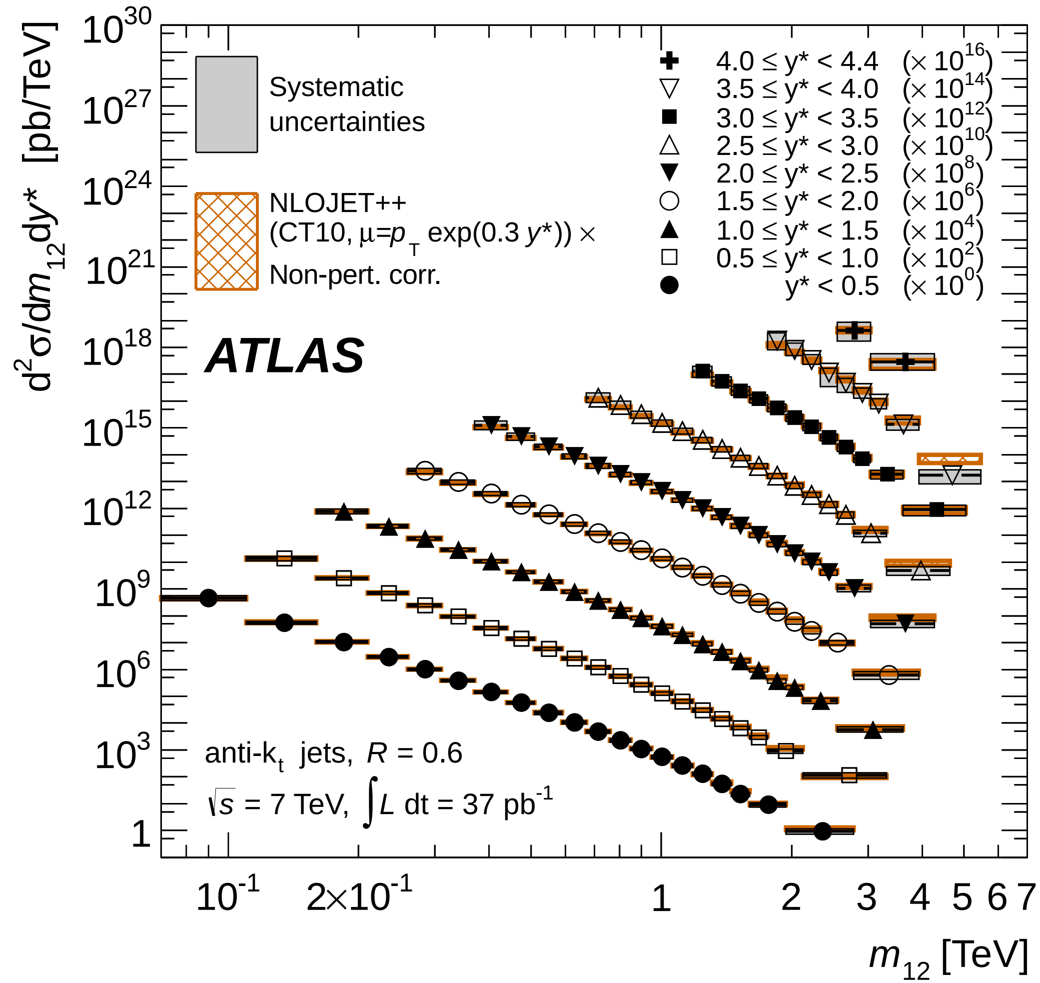

- Exploration of jet dynamics in pp collisions up to $p_T \sim 1.5$ TeV and dijet mass ~ 5 TeV
- Wealth of measurements: inclusive jet, dijet, multijet, jet substructure, ...
- Perturbative QCD succeeds in describing the data; determinations of α_s at the TeV scale!

But this is not yet the end

- **The "jet" saga continues**
  - → $\mathcal{L} \sim 20$ fb^{-1} of 2012 data
  - → forthcoming LHC runs at $\sqrt{s} = 13(14)$ TeV